

GRASSMANNIAN ORIGIN
OF
SCATTERING AMPLITUDES

JAROSLAV TRNKA

A DISSERTATION PRESENTED
TO THE FACULTY OF
PRINCETON UNIVERSITY IN
CANDIDACY FOR THE DEGREE
OF DOCTOR OF PHILOSOPHY

RECOMMENDED FOR ACCEPTANCE
BY THE DEPARTMENT OF PHYSICS
ADVISOR: NIMA ARKANI-HAMED

SEPTEMBER 2013

© Copyright by Jaroslav Trnka, 2013.
All Rights Reserved.

ABSTRACT

Quantum field theory (QFT) is our central theoretical framework to describe the microscopic world, arising from the union of quantum mechanics and special relativity. Since QFTs play such a central role in our understanding of Nature, a deeper study of their physical properties is one of the most exciting directions of research in theoretical physics. This has led to the discovery of many important theoretical concepts, such as supersymmetry and string theory. One of the most prominent physical observable in any QFT is the *scattering amplitude*, which describes scattering processes of elementary particles. Theoretical progress in understanding and computing scattering amplitudes has accelerated in last few years with the discovery of amazing new mathematical structures in a close cousin of QCD, known as $\mathcal{N}=4$ Super-Yang-Mills theory (SYM).

In the first chapter we study integrands of loop amplitudes in planar $\mathcal{N} = 4$ SYM and show their astonishing simplicity when written in terms of special set of chiral integrals. In chapter two we show how to reconstruct the multi-loop integrand recursively starting from tree-level amplitudes. This approach makes the long-hidden Yangian symmetry of the theory completely manifest and provides a Lagrangian-independent approach for determining the integrand at any loop order. In chapter three we demonstrate that the problem of calculating of scattering amplitudes in planar $\mathcal{N} = 4$ SYM can be completely reformulated in a new framework in terms of on-shell diagrams and integrals over the positive Grassmannian $G_+(k, n)$. Remarkably, the building blocks for amplitudes play a fundamental role in an active area of research in mathematics spanning algebraic geometry to combinatorics. In chapter four we sketch the argument that the amplitude itself is represented by a single geometrical object defined purely using a new striking property – *positivity* – and all physical concepts like unitarity and locality emerge as derived concepts, each having a sharp geometric interpretation.

ACKNOWLEDGEMENTS

I am grateful to the many people whose help and support have made this thesis possible. First and foremost, I would like to thank my advisor and collaborator, Nima Arkani-Hamed. He is such a great person in all aspects that it is hard to say in words how important role he played during my stay in Princeton. I admire his broad and deep knowledge of theoretical physics and absolute honesty in all aspects of life. Nima showed me how to do great science and I will always draw inspiration from years I had the humble honor to work with Nima.

I would like to thank Freddy Cachazo who has been a second advisor to me, and I am very proud of considering myself also his student. I admire his original ideas, accurate thinking and vast knowledge of quantum field theory which I benefited from during our collaboration. He is an excellent teacher and I am grateful to him for sharing his wisdom with me. I will always look up to Freddy as a brilliant physicist and a great man.

I am also thankful to Jacob Bourjaily who was my older buddy in our collaboration at Princeton. I enjoyed very much our collaboration as well as midnight discussions about our work and science in general. His remarkable knowledge of history of physics and mathematics and his mastery in MATHEMATICA have always fascinated me.

I would also like to thank also my other collaborators, Simon Caron-Huot, Alexander Goncharov and Alexander Postnikov for their important contributions to the results described in this dissertation.

It is not possible to do justice to all the people from whom I have learned so much during my time at Princeton, but I am especially indebted to many fruitful conversations about scattering amplitudes with Tim Adamo, Matthew Bullimore, James Drummond, Johannes Henn, Andrew Hodges, Lionel Mason, David McGady, Dave Skinner, and Edward Witten, and

many others. I would also like to thank Igor Klebanov, Herman Verlinde, Edward Groth for serving on my thesis committee.

It is a pleasure to thank Pierre Deligne, Bob MacPherson, and Mark Goresky for several months of intensive discussions on mathematics underlying the newly discovered structures in scattering amplitudes.

Finally, I would like to express my heartfelt thanks to my friends, my family and especially to my wife and son for their love and support.

Thanks to the Institute for Advanced Study for the hospitality. This dissertation was supported in part by NSF Grant PHY-0756966.

Contents

| | |
|--|-----------|
| Abstract | iii |
| Acknowledgements | iv |
| Introduction | 1 |
| 1 Local Integrals for Planar Scattering Amplitudes | 9 |
| 1.1 Invitation to Local Loop Integrals and Integrands | 9 |
| 1.2 Foundations | 12 |
| I. Loop Integrals | 16 |
| II. The Loop <i>Integrand</i> | 23 |
| III. Leading Singularities | 26 |
| 1.3 Chiral Integrals with Unit Leading Singularities | 42 |
| I. Integrals with Unit Leading Singularities, or <i>Pure</i> Integrals . . | 42 |
| II. Chiral Integrals | 46 |
| III. Evaluation of Pure Integrals | 48 |
| IV. Example: 1-Loop MHV Amplitudes | 49 |
| 1.4 Finite Integrals | 50 |
| 1.5 Multiloop Amplitudes | 55 |
| I. A New Form for the MHV 1-Loop Integrand | 56 |
| II. The 1-Loop NMHV Integrand, Revisited | 59 |
| III. The 2-Loop MHV Amplitude and Its Logarithm | 62 |
| IV. All 2-Loop NMHV Amplitudes | 66 |
| V. All 3-Loop MHV Amplitudes | 68 |
| 2 Recursion Relations for the Loop Integrand | 70 |
| 2.1 The Loop <i>Integrand</i> for $\mathcal{N} = 4$ SYM Amplitudes | 70 |
| I. Grassmannian Duality for Leading Singularities | 70 |
| II. The Planar Integrand | 72 |

| | | |
|----------|--|------------|
| III. | Recursion Relations for All Loop Amplitudes | 73 |
| 2.2 | Canonical Operations on Yangian Invariants | 75 |
| I. | Adding Particles | 76 |
| II. | Removing Particles | 77 |
| III. | Fusing Invariants | 78 |
| IV. | Leading Singularities are Yangian Invariant | 79 |
| V. | The BCFW Bridge | 80 |
| 2.3 | Loops From Hidden Entanglement | 83 |
| 2.4 | Recursion Relations For All Loop Amplitudes | 86 |
| I. | Single-Cuts and the Forward-Limit | 88 |
| II. | BCFW For All Loop Amplitudes | 90 |
| III. | Simple Examples | 90 |
| IV. | Unitarity as a Residue Theorem | 93 |
| 2.5 | Final remarks | 95 |
| I. | Origin of Loops | 95 |
| II. | Simplicity of Integrals and IR-Anomalies | 97 |
| III. | Other Planar Theories | 100 |
| 3 | Scattering Amplitudes and Positive Grassmannian | 101 |
| 3.1 | Overview of the chapter | 101 |
| 3.2 | On-Shell Diagrams | 104 |
| I. | On-Shell Building Blocks: the Three-Particle Amplitudes | 104 |
| II. | Gluing Three-Particle Amplitudes Into On-Shell Diagrams | 106 |
| III. | The BCFW “Bridge” | 108 |
| IV. | On-Shell Recursion for All-Loop Amplitudes | 109 |
| V. | Physical Equivalences Among On-Shell Diagrams | 112 |
| 3.3 | Permutations and Scattering Amplitudes | 118 |
| I. | Combinatorial Descriptions of Scattering Processes | 118 |
| II. | The BCFW-Bridge Construction of Representative Graphs | 123 |
| 3.4 | From On-Shell Diagrams to the Grassmannian | 128 |
| I. | The Grassmannian of k -Planes in n Dimensions, $G(k, n)$ | 128 |

| | | |
|------|---|-----|
| II. | Grassmannian Description of Kinematical Data: the 2-Planes λ and $\widetilde{\lambda}$ | 130 |
| III. | Grassmannian Representation of On-Shell Diagrams | 132 |
| IV. | Amalgamation of On-Shell Graphs | 136 |
| V. | “Boundary Measurements” and Canonical Coordinates | 139 |
| VI. | Coordinate Transformations Induced by Moves and Reduction | 143 |
| VII. | Relation to Composite Leading Singularities | 147 |
| 3.5 | Configurations of Vectors and the Positive Grassmannian | 151 |
| I. | The Geometry and Combinatorics of the Positroid Stratification | 151 |
| II. | Canonical Coordinates and the Equivalence of Permutation Labels | 158 |
| III. | Positroid Cells and the Positive Part of the Grassmannian | 161 |
| IV. | Canonically Positive Coordinates for Positroids | 166 |
| 3.6 | Boundary Configurations, Graphs, and Permutations | 169 |
| I. | Physical Singularities and Positroid Boundaries | 169 |
| II. | Boundary Configuration Combinatorics in the Positroid Stratification | 170 |
| III. | (Combinatorial) Polytopes in the Grassmannian | 172 |
| IV. | Approaching Boundaries in Canonical Coordinates | 174 |
| 3.7 | The Invariant Top-Form and the Positroid Stratification | 176 |
| I. | Proving Equivalence with the Canonical Positroid Measure | 178 |
| 3.8 | (Super) Conformal and Dual Conformal Invariance | 180 |
| I. | The Grassmannian Geometry of Momentum Conservation | 181 |
| II. | Twistor Space and the Super-Conformal Invariance of On-Shell Forms | 182 |
| III. | Momentum-Twistors and Dual Super-Conformal Invariance | 184 |
| 3.9 | Positive Diffeomorphisms and Yangian Invariance | 190 |
| 3.10 | Combinatorics of Kinematical Support for On-Shell Forms | 194 |
| I. | Kinematical Support of NMHV Yangian-Invariants | 195 |
| II. | Kinematical Support for One-Dimensional Kinematics | 196 |
| III. | General Combinatorial Test of Kinematical Support | 197 |
| 3.11 | The Geometric Origin of Identities Among Yangian-Invariants | 200 |

| | | |
|----------|--|------------|
| I. | Homological Identities in the Grassmannian | 201 |
| 3.12 | The Yang-Baxter Relation and ABJM Theories | 206 |
| I. | The On-Shell Avatar of the Yang-Baxter Relation | 206 |
| II. | ABJM Theories | 208 |
| 3.13 | On-Shell Diagrams with $\mathcal{N} < 4$ Supersymmetries | 215 |
| 3.14 | On-Shell Representations of Scattering Amplitudes | 220 |
| I. | (Diagrammatic) Proof of the BCFW Recursion Relations | 221 |
| II. | The Structure of (Tree-)Amplitudes in the Grassmannian | 225 |
| III. | Canonical Coordinates for Loop Integrands | 230 |
| IV. | The Transcendentality of Loop Amplitudes | 239 |
| 3.15 | Outlook | 244 |
| 4 | Locality and Unitarity from Positivity | 249 |
| 4.1 | Introduction and summary | 249 |
| 4.2 | MHV amplitudes at all loop orders | 257 |
| I. | One-loop amplitudes | 257 |
| II. | Two-loop amplitudes | 259 |
| III. | Generalization to all loop orders | 264 |
| 4.3 | N^k MHV one-loop amplitudes | 266 |
| I. | NMHV amplitudes | 267 |
| 4.4 | General conjecture for the integrand | 270 |
| A | All 2-Loop NMHV Amplitude Integrands | 272 |
| B | All 3-Loop MHV Amplitude Integrands | 274 |
| | Bibliography | 278 |

Introduction

The traditional formulation of quantum field theory—encoded in its very name—is built on the two pillars of *locality* and *unitarity* [1]. The standard apparatus of Lagrangians and path integrals allows us to make these two fundamental principles manifest. This approach, however, requires the introduction of a large amount of unphysical redundancy in our description of physical processes. Even for the simplest case of scalar field theories, there is the freedom to perform field-redefinitions. Starting with massless particles of spin-one or higher, we are forced to introduce even larger, gauge redundancies, [1].

Over the past few decades, there has been a growing realization that these redundancies hide amazing physical and mathematical structures lurking within the heart of quantum field theory. This has been seen dramatically at strong coupling in gauge/gauge (see, e.g., [2–4]) and gauge/gravity dualities, [5]. The past decade has uncovered further remarkable new structures in field theory even at weak coupling, seen in the properties of scattering amplitudes in gauge theories and gravity (for reviews, see [6–11]). The study of scattering amplitudes is fundamental to our understanding of field theory, and fueled its early development in the hands of Feynman, Dyson and Schwinger among others. It is therefore surprising to see that even here, by committing so strongly to particular, gauge-redundant descriptions of the physics, the usual formalism is completely blind to astonishingly simple and beautiful properties of the gauge-invariant physical observables of the theory.

Recent Progress in Scattering Amplitudes

The dawn of the new era of scattering amplitudes goes back to 1985 when Park and Taylor found a surprisingly simple formula for the tree-level scattering process of six gluons. Although the original Feynman diagram expression spanned six pages of algebra the final result was written on a single line. Soon afterwards they found

a generalization for n gluons (MHV Parke-Taylor amplitude) which showed the same remarkable simplicity, totally hidden in the standard calculation, which first appeared at six points.

This motivated many people to develop new alternative methods for calculations both tree-level and loop amplitudes. In this context, the scattering amplitude is not taken as a sum of Feynman diagrams but rather a function of physical data characterizing asymptotic scattering states which must satisfy a lot of non-trivial properties like correct factorization. These constraints are extremely strong and in most cases determine the amplitude completely. Bern, Dixon and Kosower, among others, developed unitarity-based methods in early 1990's, e.g. [12] which lead to many new theoretical predictions for QCD processes that were impossible to obtain using the standard Feynman diagrams approach. When searching for new physics at LHC it is crucial to have accurate SM predictions (usually called background). The potential new discoveries will have just mild effect, therefore it is crucial to know the higher order corrections to the background such that it can be distinguished from new physics. The unitarity methods, recursion relations and others provide a very powerful computational tool which is a part of the main computer codes for LHC calculations (e.g. Sherpa, BlackHat).

In 2003 Witten discovered that scattering amplitudes in Yang-Mills theory have remarkable geometrical properties when formulated in terms of twistor variables rather than momenta [13]. Two year later Britto, Cachazo, Feng and Witten (BCFW) found new on-shell recursion relations for tree-level amplitudes of gluons [14]. They are based on a remarkably simple idea combining the properties of analytic functions and contour integrations together with the physical concept of unitarity. Later these relations were applied to gravity and for the large class of other theories that satisfy certain analytic properties.

Many of the recent developments have been driven by an intensive exploration of $\mathcal{N} = 4$ supersymmetric Yang-Mills (SYM) in the planar limit, [11, 15]. Recently, it was made a connection to remarkable new structures in algebraic geometry, associated with contour integrals over the Grassmannian $G(k, n)$, [16–19]. This makes both the *conformal* and long-hidden *dual conformal* invariance of the theory (which together close into the infinite-dimensional Yangian symmetry) completely manifest, [20]. It is

remarkable that a single function of external kinematical variables can be interpreted as a scattering amplitude in one space-time, and as a Wilson-loop in another (for a review, see [11]). Each of these descriptions makes a commitment to locality in its own space-time, making it impossible to see the dual picture. By contrast, the Grassmannian picture makes no mention of locality or unitarity, and does not commit to any gauge-redundant description of the physics, allowing it to manifest *all* the symmetries of the theory.

There has also been extraordinary progress in determining the amplitude itself beyond the integrand, using the technology of symbols of transcendental functions to powerfully constrain and control the polylogarithms occurring in the final results, [21, 22]. While a global picture is still missing, a huge amount of data has been generated. The symbol for all 2-loop MHV amplitudes has been determined, [23] (see also [24]), and a handful of 2-loop NMHV and 3-loop MHV symbols have been found, [25–27]. Remarkable strategies have also been presented to bootstrap amplitudes to very high loop-orders, [28–32]. Many of these ideas have a strong resonance with the explosion of progress in the last decade using integrability to find exact results in planar $\mathcal{N}=4$ SYM, starting with the spectacular solution of the spectral problem for anomalous dimensions, [15, 33].

Despite the fact that planar $\mathcal{N} = 4$ SYM is not directly realized in Nature, it is and has been a fruitful laboratory for testing new ideas in field theory. On one hand we can think about it as a toy model for gauge theories because of enormous amount of symmetry, in particular infinite dimensional Yangian symmetry and its connection to integrability. On the other hand it is a highly nontrivial theory at all and it contains many of the salient features of generic quantum field theories, that are relevant to our world, especially QCD. The ultimate goal of our program is to reformulate the quantum field theory completely in a way that makes all symmetries and properties of physical observables manifest. This very ambitious program. Necessarily, the first step is to provide such a reformulation for the simplest case: planar $\mathcal{N} = 4$ SYM theory. As we will see in this thesis, specifically in chapters 3 and 4, this new formulation does not rely on the space-time physics at all. Scattering amplitudes naturally want to live in the Grassmannian (and its generalization) rather than space-time. Unlike the case for space-time descriptions, the Grassmannian make

all the symmetries manifest. Further, as we will explore, the fundamental principle in the Grassmannian formulation of S-matrix is *positivity*, rather than locality and unitarity known from the local quantum field theory.

There are many open problems even within our toy model: exploring this new space from point of view of algebraic geometry, as well as using there new insights to explicitly solve for particular amplitudes. But conceptually the problem of the reformulation of planar $\mathcal{N} = 4$ SYM is solved and chapter 4 provides a short report on it. The big question is how to generalize these ideas for other cases. There are several parallel directions: going beyond planar limit, turning on masses for particles or considering no supersymmetry. There is an interesting question if these discoveries are limited just to on-shell scattering amplitudes or the same structure can be expected to appear in other observables like correlation functions and form-factors. All these big questions are left for future work.

Overview of the thesis

The thesis contains four parts which show the essential progress we have made in last three years in understanding scattering amplitudes in planar $\mathcal{N} = 4$ SYM, together with some extensions to other planar theories. See also other papers on this topic by the author of this thesis [19, 34–37] that are not included here, and presentations at various conferences.¹

The first chapter is based on the paper,

N. Arkani-Hamed, J. Bourjaily, F. Cachazo, J. Trnka, *Local Integrals for Planar Scattering Amplitudes*, **JHEP** **1206**, 125 (2012)

In it, we provide a method how to reconstruct the integrand of multi-loop scattering amplitudes using integrals with special properties – chiral integrals with unit leading singularities. The method of writing the integrand in terms of scalar and tensor integrals rather than a sum of Feynman diagrams has been studied over the

¹Exact Results in Gauge/Gravity dualities, Perimeter Institute, Canada, 09/2011; Amplitudes 2011, Michigan, 11/2011; Amplitudes 2012, Hamburg, 03/2012; Scattering Amplitude, Trento, 07/2012; Geometry of Scattering Amplitudes, Banff, 08/2012; Amplitudes and Periods, Paris, 12/2012; Amplitudes 2013, Munich, 04/2013

past two decades in the context of both planar $\mathcal{N} = 4$ SYM and pure QCD. We show that the method of *leading singularities* provides a powerful tool to find the integral building blocks that are most suitable for scattering amplitudes. As a result, we are able to determine the integrand for certain 2-loop and 3-loop amplitudes for any number of external legs which would not be accessible using any other method.

The second chapter is devoted to the discovery of loop recursion relations in,

N. Arkani-Hamed, J. Bourjaily, F. Cachazo, S. Caron-Huot, J. Trnka, *The All-Loop Integrand For Scattering Amplitudes in Planar $N=4$ SYM*, **JHEP** **1101**, 041 (2011).

Here, we generalize BCFW recursion relations [14], originally found in the context of tree-level amplitudes to the integrand of loop amplitudes in planar $\mathcal{N} = 4$ SYM. The construction is done in momentum twistor space, a space which naturally encodes momentum conservation and the cyclic symmetry of planar amplitudes. Higher-loop amplitudes are then systematically and efficiently built-up, recursively from lower-loop amplitudes. There is a huge conceptual difference between the construction of amplitudes in chapter 1 and chapter 2. While in chapter 1 we expanded the integrand in terms of a very special set of local tensor integrals, the pieces in loop recursion relations have non-local poles. This is a feature familiar from the tree-level recursion relations where the non-local poles were also present. On the other hand this formulation makes all symmetries of the amplitude manifest term-by-term, including the infinite dimensional Yangian symmetry which is invisible in the standard formulation.

The first two chapters serve as an entree to the main result of the thesis which is a content of chapter 3 where we present a completely new formalism for on-shell scattering amplitudes. This work was done in a joint collaboration with two mathematicians,

N. Arkani-Hamed, J. Bourjaily, F. Cachazo, A. Goncharov, A. Postnikov, J. Trnka, *Scattering Amplitudes and Positive Grassmannian*, arXiv:1212.5605 [hep-th], to appear in *Cambridge University Press*

The main result is the detailed description of the connection between on-shell scattering amplitudes on one side and the fundamental object in algebraic geometry - the Grassmannian $G(k, n)$, on the other. We will derive this connection starting

physically from first principles. This will lead us into direct contact with several beautiful and active areas of current research in mathematics [38–46]. The past few decades have seen vigorous interactions between physics and mathematics in a wide variety of areas, but what is going on here involves *new* areas of mathematics that have only very recently played any role in physics, involving simple but deep ideas ranging from combinatorics to algebraic geometry. It is both startling and exciting that such elementary mathematical notions are found at the heart of the physics of scattering amplitudes. This new way of thinking about scattering amplitudes involves many novel physical and mathematical ideas.

The crucial role in the story is played by on-shell three point amplitudes. We glue them together and build *on-shell diagrams* which are physical gauge invariant objects and serve as building blocks for on-shell scattering amplitudes. The particular recipe that determines which diagrams to consider when calculating particular amplitude is provided by recursion relations which have a very natural interpretation in this language. Surprisingly, the same diagrams (called *plabic graphs*) play a crucial role in recent studies of positive Grassmannians and permutations. In this approach all symmetries are completely manifest. Furthermore, there is one more conceptual point: for the first time on-shell scattering amplitudes are written in terms of fully on-shell objects. Unlike in the representation of Feynman diagrams or tensor integral expansion which are intrinsically off-shell, on-shell diagrams have all internal lines on-shell and there is no need to access off-shell physics.

In chapter 3 we mostly work in planar $\mathcal{N} = 4$ SYM but the concept of on-shell diagrams and their connection to positive Grassmannian is completely universal for any planar theory. The advantage of $\mathcal{N} = 4$ SYM is the simplicity of the *form* that comes with each on-shell diagram and our ability to explicitly construct the amplitude using recursion relations. However, the framework can be used for any other theory including QCD and gravity.

The last chapter is a brief invitation to the work in progress,

N. Arkani-Hamed, J. Trnka, *Locality and Unitarity from Positivity, to appear*

In the new framework described in chapter 3, amplitudes are represented by sums of on-shell diagrams given by recursion relations. Some time ago we conjectured [37]

that amplitudes can be intrinsically defined as special geometrical objects and any representation (recursion relations, local integrals) can be understood as a triangulation. We developed this idea for the simple examples of NMHV tree amplitudes where the full amplitude was a volume of a polytope (known as cyclic polytope to mathematicians) in the projective space \mathbb{P}^3 but we could not find a generalization to other amplitudes for more than two years.

However, this conjecture indeed generally does have a concrete realization! We sketch a solution for planar $\mathcal{N} = 4$ SYM in chapter 4 of this thesis, more detailed explanation will appear in the paper. Any tree-level amplitude corresponds to the positive region in the Grassmannian $G(k, k+4)$ and any expansion in terms of on-shell diagrams provides a triangulation of this space in terms of elementary regions which are cells in $G_+(k, n)$. This positive space is defined as a union of two *positive* worlds: *internal* positive Grassmannian and *external* positive kinematical data. We show that this remarkable object has exactly the same properties as the tree-level amplitude in $\mathcal{N} = 4$ SYM. We also present a generalization to the integrand of any loop amplitude, which corresponds to the positive region of a generalized Grassmannian (such structure is currently unknown to mathematicians).

This definition of scattering amplitudes relies only on the positive structure of the internal Grassmannian and external kinematical data. All symmetries and physical properties (like locality and unitarity) are derived concepts. This finishes (at least conceptually) the first goal of the program: the complete reformulation of planar $\mathcal{N} = 4$ SYM where the space-time description is replaced by a new mathematical structure.

Before starting our journey let us first define notation used in the field of scattering amplitudes which might be not so familiar to other physicists.

Notation: Encoding External Kinematical Data

We are interested in the scattering amplitude for n massless particles with momenta p_a and helicities h_a , for $a = 1, \dots, n$. Since the momenta are null, the (2×2) -matrix,

$$p_a^{\alpha\dot{\alpha}} \equiv p_a^\mu \sigma_\mu^{\alpha\dot{\alpha}} = \begin{pmatrix} p_a^0 + p_a^3 & p_a^1 - ip_a^2 \\ p_a^1 + ip_a^2 & p_a^0 - p_a^3 \end{pmatrix}, \quad (0.1)$$

has vanishing determinant; and so $p^{\alpha\dot{\alpha}}$ has (at most) rank 1. We can therefore write

$$p_a^{\alpha\dot{\alpha}} = \lambda_a^\alpha \tilde{\lambda}_a^{\dot{\alpha}}, \quad (0.2)$$

where $\lambda, \tilde{\lambda}$ are referred to as *spinor helicity* variables [47–49]. If the momentum is real, we have $\tilde{\lambda}_a = \pm\lambda_a^*$; but in general, we will allow the momenta to be complex and consider $\lambda, \tilde{\lambda}$ as independent, complex variables.

The rescaling $\lambda_a \mapsto t_a \lambda_a, \tilde{\lambda}_a \mapsto t_a^{-1} \tilde{\lambda}_a$ leaves the momentum p_a invariant and represents the action of the *little group* (for more details see e.g. [1, 50]). All the information about the helicities h_a of particles involved in a scattering amplitude A_n is encoded by its weights under such rescaling:

$$A_n(t_a \lambda_a, t_a^{-1} \tilde{\lambda}_a; h_a) = t_a^{-2h_a} A_n(\lambda_a, \tilde{\lambda}_a; h_a). \quad (0.3)$$

Theories with maximal supersymmetry have the wonderful feature that particles of all helicities can be unified into a single super-multiplet, [13, 50–53]. For $\mathcal{N} = 4$ SYM, we can group all the helicity states into a single *Grassmann coherent state* labeled by Grassmann (anti-commuting) parameters $\tilde{\eta}^I$ for $I = 1, \dots, 4$:

$$|\tilde{\eta}\rangle \equiv | +1 \rangle + \tilde{\eta}^I | +\frac{1}{2} \rangle_I + \frac{1}{2!} \tilde{\eta}^I \tilde{\eta}^J | 0 \rangle_{IJ} + \frac{1}{3!} \epsilon_{IJKL} \tilde{\eta}^I \tilde{\eta}^J \tilde{\eta}^K | -\frac{1}{2} \rangle^L + \frac{1}{4!} \epsilon_{IJKL} \tilde{\eta}^I \tilde{\eta}^J \tilde{\eta}^K \tilde{\eta}^L | -1 \rangle.$$

The complete amplitude, denoted $\mathcal{A}_n(\lambda_a, \tilde{\lambda}_a, \tilde{\eta}_a)$, is then a polynomial in the $\tilde{\eta}$'s. It is convenient to expand this according to,

$$\mathcal{A}_n(\lambda_a, \tilde{\lambda}_a, \tilde{\eta}_a) = \sum_k \mathcal{A}_n^{(k)}(\lambda_a, \tilde{\lambda}_a, \tilde{\eta}_a), \quad (0.4)$$

where $\mathcal{A}_n^{(k)}$ is a polynomial of degree $4k$ in the $\tilde{\eta}$'s. Under the little group, $\tilde{\eta}$ transforms like $\tilde{\lambda}$, so $\tilde{\eta}_a \mapsto t_a^{-1} \tilde{\eta}_a$; with this, the “super-amplitude” $\mathcal{A}_n^{(k)}$ transforms uniformly according to:

$$\mathcal{A}_n^{(k)}(t_a \lambda_a, t_a^{-1} \tilde{\lambda}_a, t_a^{-1} \tilde{\eta}_a) = t_a^{-2} \mathcal{A}_n^{(k)}(\lambda_a, \tilde{\lambda}_a, \tilde{\eta}_a). \quad (0.5)$$

The $\mathcal{A}_n^{(k)}$ super-amplitude contains among its components those amplitudes which involve k ‘negative helicity’ ($h_a = -1$) and $(n - k)$ ‘positive-helicity’ ($h_a = +1$) gluons—particles for which $h_a = \pm 1$. $\mathcal{A}_n^{(k)}$ is often referred to as an “ $\mathcal{N}^{(k-2)}$ MHV amplitude”, where ‘MHV’ stands for ‘maximal helicity violating’ and ‘ \mathcal{N} ’ denotes ‘next-to’— $\mathcal{A}_n^{(k=2)}$ are considered ‘MHV’ because $\mathcal{A}_n^{(k<2)}$ have vanishing kinematical support.

Chapter 1 *Local Integrals for Planar Scattering Amplitudes*

1.1 Invitation to Local Loop Integrals and Integrands

In this chapter we report on a remarkable simplicity of the loop integrands *when expressed in a manifestly local way*. This is surprising, since the enormous complexity of Feynman diagrams is inexorably tied to locality, while by contrast, the great simplicity of BCFW recursion (discussed in the next chapter) is inexorably tied to the presence of non-local poles. What we are finding is a *new* local form of the integrand—certainly not following from Feynman diagrams!—which is even simpler than the forms obtained from BCFW recursion.

This great simplicity is apparent only when the integrand is written in momentum-twistor space, using a special set of objects that are almost completely *chiral*, and have *unit leading singularities*. For instance, all 2-loop MHV amplitudes are given as a sum over a single type of object,

$$\mathcal{A}_{\text{MHV}}^{2\text{-loop}} = \frac{1}{2} \sum_{i < j < k < l < i} \text{Diagram} \quad (1.1.1)$$

We will describe these objects in much more detail in the body of this Chapter; here, it suffices to say that these are simple double-pentagon integrals with a special tensor-numerator structure which is indicated by the wavy lines, and that the notation ‘ $i < j < \dots < k < i$ ’ in the summand should be understood as the sum of all cyclically-ordered sets of labels i, j, \dots, k for each $i \in \{1, \dots, n\}$.

All 2-loop NMHV amplitudes are also associated with similar integrands; indeed, the n -point NMHV scattering amplitude’s integrand is simply given by,

$$\begin{aligned}
\mathcal{A}_{\text{NMHV}}^{2\text{-loop}} = & \sum_{\substack{i < j < l < m < k < i \\ i < j < k < l < m < i \\ i \leq l < m \leq j < k < i}} \text{Diagram 1} + \frac{1}{2} \sum_{i < j < k < l < i} \text{Diagram 2} \\
& \times [i, j, j+1, k, k+1] \times \left\{ \begin{aligned} & \mathcal{A}_{\text{NMHV}}^{\text{tree}}(j, \dots, k; l, \dots, i) \\ & + \mathcal{A}_{\text{NMHV}}^{\text{tree}}(i, \dots, j) \\ & + \mathcal{A}_{\text{NMHV}}^{\text{tree}}(k, \dots, l) \end{aligned} \right\}
\end{aligned} \tag{1.1.2}$$

Here, $[i j k l m]$ denotes the familiar dual-superconformal invariant of five particles,

$$[i j k l m] \equiv \frac{\delta^{0|4} (\langle j k l m \rangle \eta_i + \langle k l m i \rangle \eta_j + \langle l m i j \rangle \eta_k + \langle m i j k \rangle \eta_l + \langle i j k l \rangle \eta_m)}{\langle i j k l \rangle \langle j k l m \rangle \langle k l m i \rangle \langle l m i j \rangle \langle m i j k \rangle}. \tag{1.1.3}$$

Finally, all 3-loop MHV amplitude integrands are given by a sum over the same types of objects,

$$\begin{aligned}
\mathcal{A}_{\text{MHV}}^{3\text{-loop}} = & \frac{1}{3} \sum_{\substack{i_1 \leq i_2 < j_1 \leq \\ \leq j_2 < k_1 \leq k_2 < i_1}} \text{Diagram 3} + \frac{1}{2} \sum_{\substack{i_1 \leq j_1 < k_1 < \\ < k_2 \leq j_2 < i_2 < i_1}} \text{Diagram 4}
\end{aligned}$$

As we will see, these extremely simple expressions are very closely related to the leading singularity structure of the theory. The reason for the dramatic simplicity of these results is that there, each integrand was straightforwardly expanded in terms of a fixed basis of chiral integrals with unit leading singularities, while here we are tailoring the objects that appear directly to the amplitude. The structures are motivated by matching a particularly simple set of leading singularities of the theory; this is made possible only by using chiral integrands with unit leading singularities, which is why these objects play such a crucial role in the story. What is remarkable is that matching only a small subset of leading singularities in this way suffices to determine the full result. Of course, we confirm this not by laboriously matching all leading singularities,

but rather by directly checking the conjectured local forms against what we obtain from the all-loop recursion relation.

We do not yet have a satisfactory understanding for the origin of this amazing simplicity. Certainly, these expressions differ from the BCFW form (discussed in the next chapter) in that they are not term-by-term Yangian invariant. This suggests the existence of a deeper theory for the integrand that will directly produce these new local forms, allowing a more direct understanding of the emergence of local spacetime physics. We strongly suspect that it is *this* formulation that will also help explain the amazing simplicity [37] seen in the *integrals* yielding the physical amplitudes, and also form the point of contact with the remarkable integrable structures of $\mathcal{N} = 4$ SYM—Y-systems and Yang-Yang equations—seen at strong coupling and also in some collinear limits [54–56].

We close this invitation with an outline for the rest of the chapter. We begin with a pedagogical introduction to some of the foundations of the subject in section 1.2 starting with a review of momentum-twistors and some of the associated projective geometry in \mathbb{CP}^3 . We also discuss how planar loop integrals are written in momentum-twistor space; while our focus in this Chapter is on $\mathcal{N} = 4$ SYM, we expect that the momentum-twistor representation of loop amplitudes will be extremely useful for *any* planar theory. We discuss the way that momentum-twistors make integral reduction trivial, and illustrate this by showing how the 1-loop integrand can be reduced to a sum over pentagon integrals. Finally we discuss leading singularities at 1-loop and beyond in momentum-twistor language. The standard exercise of determining quadruple-cuts in momentum space is mapped in momentum-twistor language to a simple, beautiful and classic problem in enumerative geometry first posed by Schubert in the 1870’s, and we discuss the solution of these “Schubert problems” in detail.

In section 1.3 we introduce chiral integrals with unit leading singularities which play a central role in our story. We illustrate how they work starting with the simplest case of 1-loop MHV amplitudes.

In section 1.4, we discuss another feature of chiral integrals with unit leading singularities—generic integrals of this form are manifestly infrared finite, and can be used to express finite objects related to scattering amplitudes, such as the ratio function [57].

In section 1.5, we discuss multi-loop amplitudes. We describe our heuristic strategy for using leading singularities to tailor momentum-twistor integrals to the amplitude, and show how this works for the 1-loop MHV amplitude, reproducing one of the local forms first derived using the polytope picture []. We also discuss the 1-loop NMHV amplitudes in the same way. We then extend these methods to two loops and beyond, and show how to “glue” the 1-loop expressions together to produce natural conjectures for all 2- and 3-loop MHV amplitudes, as well all 2-loop NMHV amplitudes. These conjectures are verified by comparing with the integrand derived from the all-loop recursion relation.

1.2 Foundations

In theories with massless particles, a well-known and convenient way of trivializing the constraint $p_a^2 = 0$ for each particle is to introduce a pair of spinors $\lambda^{(a)}$ and $\tilde{\lambda}^{(a)}$, replacing $p_a^\mu \mapsto (p_a)_{\underline{\alpha}\dot{\alpha}} \equiv p_a^\mu (\sigma_\mu)_{\underline{\alpha}\dot{\alpha}} \equiv \lambda_{\underline{\alpha}}^{(a)} \tilde{\lambda}_{\dot{\alpha}}^{(a)}$. Of course, this map is not invertible, as any rescaling $\{\lambda, \tilde{\lambda}\} \rightarrow \{t\lambda, t^{-1}\tilde{\lambda}\}$ leaves p invariant. This reflects that these variables come with a new source of redundancy; in the case of particles with spin, this redundancy is quite welcomed as it allows the construction of functions that transform with fixed projective weights as S-matrix elements under Lorentz transformations. This is all well-known under the name of the *spinor-helicity formalism* [?, 47–49, 58].

Amplitudes are supported on momenta that satisfy momentum conservation. Clearly, it would be convenient to find variables where this constraint, $\sum_a p_a = 0$, is trivial. In planar theories, where color ordering is available, there is a natural way to achieve this, by choosing instead to express the external momenta in terms of what are known as dual-space coordinates, writing $p_a \equiv x_a - x_{a-1}$, [59].

To see the role played by planarity, consider the standard decomposition of scattering amplitudes according to the overall color structure, keeping only the leading color part:

$$A_n = \text{Tr}(T^{a_1} T^{a_2} \dots T^{a_n}) \mathcal{A}_n(1, 2, \dots, n) + \text{permutations}; \quad (1.2.4)$$

here, each *partial amplitude* $\mathcal{A}_n(1, 2, \dots, n)$ can be expanded in perturbation theory, and we denote the L -loop contribution by $\mathcal{A}_n^{L\text{-loop}}$. Partial amplitudes are computed by summing over Feynman diagrams with a given color-ordering structure.

In this chapter we only consider the planar sector of the theory, and therefore $\mathcal{A}_n^{L\text{-loop}}$ will always refer to the leading-color, partial amplitude in the planar limit.

Restricted to a particular partial amplitude, say, $\mathcal{A}_n(1, 2, \dots, n)$, each momenta can be expressed as the difference of two “spacetime” points. More precisely, we make the identification $p_a \equiv x_a - x_{a-1}$, with $p_1 = x_1 - x_n$. It is clear that momenta obtained in this way automatically satisfy $\sum_a p_a = 0$ —and the redundancy introduced in this case is a translation $x_a \rightarrow x_a + y$ by any fixed vector y .

Now, the only poles that can occur in $\mathcal{A}_n(1, 2, \dots, n)$ are of the form $\sum_{m=a}^b p_m$, *i.e.*, only the sum over consecutive momenta can appear. In the dual variables these become $\sum_{m=a+1}^b p_m = x_a - x_b$. The same kind of simplifications happen in planar Feynman diagrams to all orders in perturbation theory as we will describe.

Now we have the variables $\{\lambda, \tilde{\lambda}\}$ which make the null condition trivial while ignoring momentum conservation, while the dual-space variables do the opposite. It is perfectly natural to wonder if there exists any way to combine these two constructions which makes both the null-condition and momentum conservation trivial. It turns out that such a set of variables does exist: they are known as *momentum-twistors* and were introduced by Hodges in [60].

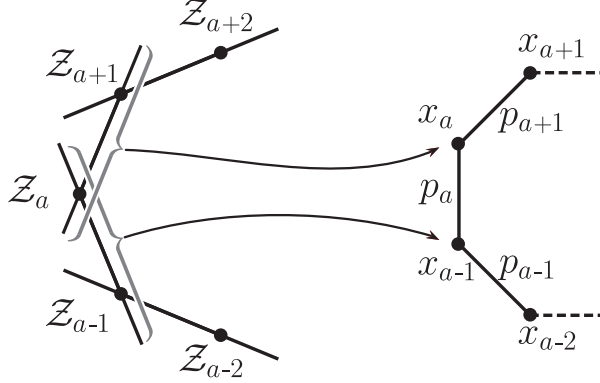
The standard twistor construction developed in the 1960’s [61] starts by making a connection between points in an auxiliary space—twistor-space—and null rays in spacetime. Likewise, a complex line in twistor space is related to a point in spacetime. The key formula is called the *incidence relation*, according to which a point x in spacetime corresponds to set of twistors $Z = (\lambda, \mu)$ which satisfy

$$\mu_{\dot{\alpha}} = x_{\alpha\dot{\alpha}} \lambda^{\alpha}. \tag{1.2.5}$$

Twistors satisfying this relation form a projective line in \mathbb{CP}^3 . Even though Z has the components of a point in \mathbb{C}^4 , the incidence relation cannot distinguish Z from tZ , and therefore the space is projectivized.

In order to specify a line in twistor space—and therefore a point in spacetime—all that is needed is a pair of twistors, say Z_A and Z_B , that belong to the line. Given the twistors, the line or spacetime point is found by solving the four equations coming from imposing the incidence relation for Z_A and Z_B with x . It is easy to check that

Figure 1.1: Defining the connections between momentum-twistors, dual-coordinates, and cyclically-ordered external four-momenta



the solution is,

$$x_{\underline{\alpha}\underline{\dot{\alpha}}} = \frac{\lambda_{A,\underline{\alpha}}\mu_{B,\underline{\dot{\alpha}}}}{\langle \lambda_A \lambda_B \rangle} + \frac{\lambda_{B,\underline{\alpha}}\mu_{A,\underline{\dot{\alpha}}}}{\langle \lambda_B \lambda_A \rangle}. \quad (1.2.6)$$

(Here, we have made use of the familiar Lorentz-invariant contraction of two spinors $\langle \lambda_A \lambda_B \rangle \equiv \epsilon_{\underline{\alpha}\underline{\beta}}\lambda_A^\alpha\lambda_B^\beta$).

Hodges' construction starts with any set of n twistors $\{Z_1, \dots, Z_n\}$. Using the association $x_a \leftrightarrow (Z_a, Z_{a+1})$, n spacetime points are defined. Quite nicely, it is trivial that $p_a^2 = (x_a - x_{a-1})^2 = 0$ because the corresponding lines, or (\mathbb{CP}^1 s), intersect. This is illustrated in Figure 1.1.

Given the importance of this latter fact, it is worth giving it a slightly more detailed discussion than we have so far. If two lines in twistor-space intersect, *i.e.* share a twistor Z_{int} , then the corresponding spacetime points, say x and y , associated with the lines are null-separated. To see this, take the difference of the incidence relations for Z_{int} ,

$$\mu_{\underline{\dot{\alpha}}}^{\text{int}} = x_{\underline{\alpha}\underline{\dot{\alpha}}}\lambda_{\text{int}}^\alpha, \quad \mu_{\underline{\dot{\alpha}}}^{\text{int}} = y_{\underline{\alpha}\underline{\dot{\alpha}}}\lambda_{\text{int}}^\alpha,$$

to get

$$(x - y)_{\underline{\alpha}\underline{\dot{\alpha}}}\lambda_{\text{int}}^\alpha = 0;$$

which means that the 2×2 -matrix $(x - y)$ has a non-vanishing null eigenvector, *i.e.* $\lambda_{\text{int}}^\alpha$, and therefore the determinant of $(x - y)$ vanishes. But the determinant is proportional to $(x - y)^2$ when x and y are taken as vectors; and therefore x and y are null separated.

As useful background for the rest of the Chapter let us discuss the null-separation condition, which is a conformally invariant statement, in twistor space. Consider

again two generic spacetime points x and y and choose two representatives of the lines associated to them in twistor space, say, (Z_A, Z_B) and (Z_C, Z_D) . Treating each twistor as a vector in \mathbb{C}^4 there is a natural SL_4 (conformal) invariant that can be constructed. This is done by contracting all four twistors with the completely antisymmetric tensor ϵ_{IJKL} to produce

$$\langle Z_A Z_B Z_C Z_D \rangle = \epsilon_{IJKL} Z_A^I Z_B^J Z_C^K Z_D^L. \quad (1.2.7)$$

Clearly, this conformally-invariant quantity must encode information about how x and y are causally related. The Lorentz invariant separation $(x - y)^2$ is not conformally-invariant because it is not a cross ratio. However, the way to relate the two quantities is simple

$$(x - y)^2 = \frac{\langle Z_A Z_B Z_C Z_D \rangle}{\langle \lambda_A \lambda_B \rangle \langle \lambda_C \lambda_D \rangle}. \quad (1.2.8)$$

This relation is consistent with our earlier finding that if the points x and y are null-separated, then the twistors Z_A, Z_B, Z_C and Z_D , are coplanar as points in \mathbb{CP}^3 . In other words, the two complex lines intersect.

When twistors are used to produce a configuration of points in spacetime which are pairwise null separated and then used to build momenta, the corresponding twistor space is called *momentum-twistor space* [60].

This twistor construction is in fact slightly more involved when one is interested in *real* slices of spacetime. In our discussion so far, we have been assuming that momenta are complex and hence the dual spacetime is complexified. This is useful for *e.g.* defining the usual unitarity cuts of loop amplitudes. In this chapter, the complex version suffices and we refer the interested reader to [60, 62].

A related construction is called dual momentum twistor space. Here ‘dual’ refers to the usual geometric—‘Poincaré’—dual of a space. In other words, the dual space is the space of planes in \mathbb{CP}^3 . Points in the new space which is also a \mathbb{CP}^3 are denoted by W_I . The construction maps points to planes and lines to lines. In Hodges’ construction [60], there is a natural definition of dual points associated to the planes defined by consecutive lines of the polygon in momentum twistor space.

The construction defines a dual polygon by introducing dual momentum twistors

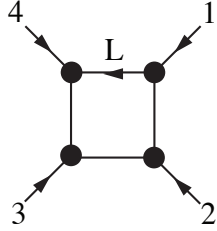
W_a defined by

$$(W_a)_I = \frac{\epsilon_{IJKL} Z_{a-1}^J Z_a^K Z_{a+1}^L}{\langle \lambda_{a-1} \lambda_a \rangle \langle \lambda_a \lambda_{a+1} \rangle}. \quad (1.2.9)$$

This definition is made so that W_a contains $\tilde{\lambda}_a$ as two of its components.

I. Loop Integrals

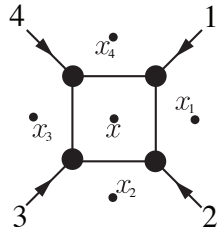
The focus of this chapter is loop integrands and integrals. Here too, it is well known that in planar theories, loop integrals are very naturally expressed in terms of dual spacetime coordinates. Consider a very simple 1-loop integral, known as a zero mass integral,



The diagram shows a square loop with four vertices. External momenta are labeled 1, 2, 3, and 4, each with an arrow pointing outwards from a vertex. The top-left edge of the loop is labeled with the letter 'L' and an arrow pointing to the right, indicating the direction of the loop's internal momentum.

$$= \int d^4 L \frac{N}{L^2 (L - p_1)^2 (L - p_1 - p_2)^2 (L - p_1 - p_2 - p_3)^2} \quad (1.2.10)$$

where the external momentum at each of the four vertices is null (hence the name) and $N = (p_1 + p_2)^2 (p_2 + p_3)^2$ is a convenient normalization factor. Momentum conservation gives $p_4 = -p_1 - p_2 - p_3$; and introducing the dual-coordinates $p_a = x_a - x_{a-1}$, it is easy to see that the unique choice of L that makes translation invariance (in x -space) manifest is $L = x - x_4$. The integral becomes [59]



The diagram shows a square loop with four vertices. External momenta are labeled 1, 2, 3, and 4, each with an arrow pointing outwards from a vertex. The vertices are labeled with dual coordinates x_1, x_2, x_3, x_4 . A central point is labeled x .

$$= \int d^4 x \frac{N}{(x - x_1)^2 (x - x_2)^2 (x - x_3)^2 (x - x_4)^2}, \quad (1.2.11)$$

where $N = (x_1 - x_3)^2 (x_2 - x_4)^2$. Imposing translation-invariance gives rise to the same integral in x -space regardless of the original definition of L in the loop diagram. In other words, a different propagator could have been chosen to be L and the form (1.2.11) would still be the same. This uniqueness plays a crucial role in the definition of the integrand of the theory.

Integrating over all points x in spacetime is the same as integrating over all \mathbb{CP}^1 's in \mathbb{CP}^3 . As before, each line in twistor space can be represented by a pair of twistors

$x \leftrightarrow (Z_A, Z_B)$. Clearly, any $GL_2(\mathbb{C})$ transformation on the A, B “indices” leaves the line invariant. Therefore the integral over spacetime is the same as the integral over the pairs (Z_A, Z_B) modulo GL_2 . This is nothing but the Grassmannian $G(2, 4)$ which can be parameterized by a 2×4 matrix

$$\begin{pmatrix} Z_A^1 & Z_A^2 & Z_A^3 & Z_A^4 \\ Z_B^1 & Z_B^2 & Z_B^3 & Z_B^4 \end{pmatrix} = \begin{pmatrix} \lambda_A^1 & \lambda_A^2 & \mu_A^1 & \mu_A^2 \\ \lambda_B^1 & \lambda_B^2 & \mu_B^1 & \mu_B^2 \end{pmatrix}. \quad (1.2.12)$$

We can immediately write a measure which is GL_2 -invariant by integrating over all Z_A 's and Z_B 's together with a combination of 2×2 minors of the matrix (1.2.12) with total weight -4 . It turns out that the precise measure that corresponds to a d^4x integration is

$$\int d^4x \Leftrightarrow \int \frac{d^4Z_A d^4Z_B}{\text{vol}(GL_2) \times \langle \lambda_A \lambda_B \rangle^4}, \quad (1.2.13)$$

where $\langle \lambda_A \lambda_B \rangle$ is the $(1\ 2)$ minor of (1.2.12)—the determinant of the first two columns of the 2×4 matrix (1.2.12). In the twistor literature this is written as $\langle \lambda_A \lambda_B \rangle = \langle Z_A Z_B I_\infty \rangle$ where $(I_\infty)^{KL}$ is the infinity twistor which is block diagonal with the only nonzero diagonal element equal to ϵ_{ab} . I_∞ is called the infinity twistor because it corresponds to a choice of the point at infinity in spacetime and therefore a line in twistor space. Its presence therefore breaks conformal invariance. This is not surprising as the measure d^4x ‘knows about’ the metric in spacetime.

Since the integration over lines will appear in many different contexts in this chapter we introduce a special notation for it. Let's define

$$\int_{(AB)} \Leftrightarrow \int \frac{d^4Z_A d^4Z_B}{\text{vol}(GL_2)}. \quad (1.2.14)$$

The reason we have not included the factor $\langle \lambda_A \lambda_B \rangle^4$ in the definition is that in this chapter we mostly deal with $\mathcal{N} = 4$ SYM and in its integrand factors with infinity twistors cancel.

Going back to the loop integral in x -space (1.2.11), one can introduce the four momentum twistors in Hodges' construction $\{Z_1, Z_2, Z_3, Z_4\}$ to describe the external particles. Using the relation between the Lorentz invariant separations and momentum twistor invariants in (1.2.8), the integral (1.2.11) becomes

$$\int_{(AB)} \frac{\langle 1234 \rangle^2}{\langle AB\ 12 \rangle \langle AB\ 23 \rangle \langle AB\ 34 \rangle \langle AB\ 41 \rangle}. \quad (1.2.15)$$

where $\langle ijkl \rangle$ stands for the determinant of the 4×4 matrix with columns given by four twistors Z_i, Z_j, Z_j, Z_k defined in (1.2.7).

One of the remarkable facts about (1.2.15) is that all factors involving the infinity twistor have disappeared. This means that the integral is formally conformal invariant under the conformal group that acts on the dual spacetime. This is why it is said to be *dual conformally invariant* (DCI).

Clearly, if we had started with a triangle integral then the factor $\langle Z_1 I Z_2 \rangle = \langle \lambda_1 \lambda_2 \rangle$ would not have canceled and would have remained with power one in the denominator as if it were a propagator. Indeed, this viewpoint trivializes the surprising connections made in the past between the explicit form of triangle and box integrals. In other words, one can think of a triangle integral as a box where one of the points is at infinity.

Once again, a careful definition of the contour which should correspond to only points in a real slice of complexified spacetime is not needed in this chapter. It suffices to say that on the physical contour, the integrals can have infrared divergences (IR). This is the reason why we said that the integral was ‘formally’ DCI. We postpone a more detailed discussion of IR-divergences to section 1.4.

The purpose of this section is to show how momentum twistors are the most natural set of variables to work with loop amplitudes in planar theories. In order to do this we will first show how many familiar results can be translated into momentum twistors. Not infrequently, momentum twistors will completely clarify physics points which have been misunderstood in the literature.

Integral Reduction at 1-Loop Level

In a general theory, 1-loop integral reduction techniques allow scattering amplitudes to be expressed as linear combinations of a basic set of scalar integrals¹. The integrals have the topology of bubbles, triangles or boxes.

Let us start this section by translating each of the integrals in the standard basis into momentum twistor language. Their corresponding form in momentum twistor

¹This is true in theories with no rational terms or in general theories for what is known as the cut-constructible part of them. See [7] for more details. In $\mathcal{N} = 4$ SYM rational terms are absent. This is why we do not elaborate more on this point.

space is

$$\begin{aligned}
I_{\text{Box}} &= \int_{(AB)} \frac{\langle i \ i+1 \rangle \langle j \ j+1 \rangle \langle k \ k+1 \rangle \langle l \ l+1 \rangle}{\langle AB \ i \ i+1 \rangle \langle AB \ j \ j+1 \rangle \langle AB \ k \ k+1 \rangle \langle AB \ l \ l+1 \rangle}; \\
I_{\text{Triangle}} &= \int_{(AB)} \frac{1}{\langle AB \rangle} \frac{\langle i \ i+1 \rangle \langle j \ j+1 \rangle \langle k \ k+1 \rangle}{\langle AB \ i \ i+1 \rangle \langle AB \ j \ j+1 \rangle \langle AB \ k \ k+1 \rangle}; \\
I_{\text{Bubble}} &= \int_{(AB)} \frac{1}{\langle AB \rangle^2} \frac{\langle i \ i+1 \rangle \langle j \ j+1 \rangle}{\langle AB \ i \ i+1 \rangle \langle AB \ j \ j+1 \rangle}.
\end{aligned} \tag{1.2.16}$$

Note that here we have translated the plain scalar integrals without any normalization factors. Once again, only boxes are dual conformal invariant except for an overall factor which only depends on the external data. This factor involving 2-brackets and hence the infinity twistor can always be removed by a proper normalization as done in the zero-mass example (1.2.15). Scalar boxes in momentum twistor space have also been recently studied in [62, 63].

A well known fact about $\mathcal{N} = 4$ SYM is that at 1-loop level, bubbles and triangles are absent and all one needs are scalar box integrals. However, as we will see, this point of view is not the most natural one and actually turns out to be misleading.

In order to understand this point, one needs to review the reduction procedures used to reach this conclusion. Before doing that let us mention some useful facts about momentum twistors.

In loop integrals, combinations of momentum twistors of the form $Z_A^{[I} Z_B^{J]}$ make an appearance in every expression (where the brackets mean that the indices are anti-symmetrized), reflecting the fact that it is the *line* (AB) that is being integrated-over, and not the individual twistors Z_A and Z_B .

These two-index objects are a class of more general ones called bitwistors. A generic bitwistor is a rank-two antisymmetric tensor Y^{IJ} . Given two bitwistors, Y and \tilde{Y} , the conformally-invariant inner-product is given by $\langle Y \ \tilde{Y} \rangle = \epsilon_{IJKL} Y^{IJ} \tilde{Y}^{KL}$. A bitwistor which can be written in terms of two twistors as $Z_A^{[I} Z_B^{J]}$ is called *simple*.

It is easy to show that a bitwistor is simple if and only if $Y^2 = 0$ with the product defined as above.

The reason for discussing bitwistors is that they provide a very natural integral reduction procedure. The procedure can be applied to integrals at any loop order but in this section we concentrate on only 1-loop integrals. The procedure we are about to present is in part the momentum twistor analog of the one introduced by van-Neerven and Vermaseren in [64].

At 1-loop one starts with general Feynman integrals of the form

$$T_{\mu_1 \dots \mu_m} \int d^4 L \frac{L^{\mu_1} \dots L^{\mu_m}}{\prod_{i=1}^n (L - P_i)^2} \quad (1.2.17)$$

where the tensor T is made out of polarization vectors, momenta of external particles and the spacetime metric.

By Lorentz invariance, it is clear that one can decompose integrals of this type as linear combinations of momentum twistor tensor integrals of the form

$$\int_{(AB)} \frac{1}{\langle AB I_\infty \rangle^{4-(n-m)}} \frac{\langle AB Y_1 \rangle \langle AB Y_2 \rangle \dots \langle AB Y_m \rangle}{\langle AB 12 \rangle \langle AB 23 \rangle \dots \langle AB n-1 n \rangle \langle AB n 1 \rangle} \quad (1.2.18)$$

where Y_a are generic bitwistors.

The reduction procedure relies on the fact that a generic bitwistor has six degrees of freedom and can therefore be expanded in a basis of any six independent bitwistors. To reduce the integrals in (1.2.18) simply choose any six of the bitwistors that appear in the denominator, say, $Z_1 Z_2, Z_2 Z_3, \dots, Z_6 Z_7$ and expand any of the bitwistors in the numerator as

$$(Y_j)^{IJ} = \alpha_1 Z_1^I Z_2^J + \alpha_2 Z_2^I Z_3^J + \dots + \alpha_6 Z_6^I Z_7^J. \quad (1.2.19)$$

The coefficients can be found by contracting with enough bitwistors to get six independent equations. More explicitly, one can consider equations of the form

$$\langle Z_2 Z_3 Y_j \rangle = \alpha_4 \langle 2345 \rangle + \alpha_5 \langle 2356 \rangle + \alpha_6 \langle 2367 \rangle.$$

and solve for the α 's. Once this is done, the factor $\langle AB Y_j \rangle$ becomes a linear-combination of factors in the denominator, thus reducing the degree of the denominator and numerator by one.

The integral in (1.2.18) is for a general quantum field theory with a planar sector. One can continue with the integral procedure in this case but it will take us too far away from the main line of this Chapter. Therefore we concentrate directly on $\mathcal{N} = 4$ SYM. In $\mathcal{N} = 4$ SYM it has been known since the 1990's [12] that all integrals satisfy $n - m = 4$. In modern language, this means that the integrals are dual conformally-invariant as discussed in the simple example of the all massless box integral (1.2.15).

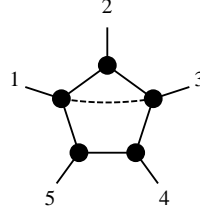
Iterating the reduction procedure, we can write the any amplitude as a sum over pentagons and boxes. But as far as we have seen, the reduction procedure we have described so far does not reduce the pentagons any further. Notice that the pentagons we have described here are not *scalar* pentagons, but *tensor* pentagons—and they are *manifestly* DCI. However, one is always free to choose a basis of bitwistors including $Y = I_\infty$ to obtain scalar pentagons, but only at the cost of manifest dual conformal invariance.

But doesn't the reduction procedure of van-Neerven and Vermaseren, when applied to $\mathcal{N} = 4$ SYM, allow for a reduction all the way down to only scalar boxes? One might wonder why our analysis so far does not generate this familiar 'box-expansion'. The answer is that the reduction to box-integrals is *not valid at the level of the integrand*—only the reduction to boxes *and pentagons* (scalar or otherwise) is valid at the level of the integrand. In order to obtain the all-too familiar box-expansion, it is necessary to parity-symmetrize the integrand—a step that is only justified when integrated on a parity-invariant contour, and one which does violence to the highly *chiral* loop-integrands of a quantum field theory such as $\mathcal{N} = 4$ SYM.

Here, we should briefly clarify a point which has been unnecessarily confused in the literature on $\mathcal{N} = 4$. Because *integrand*-level reduction must terminate with boxes *and* pentagons, and box-integrals are both manifestly parity-even and DCI while *scalar* pentagons—which have a factor of $\langle AB I_\infty \rangle$ in the numerator—are not DCI, the corrections to the box-expansion needed to match the full integrand of $\mathcal{N} = 4$ were first expressed in terms of parity-odd combinations of scalar pentagons. This led some researchers to suppose that there was some connection between DCI and parity. There is of course no such connection: as evidenced by the extension of BCFW to all-loop orders, the full $\mathcal{N} = 4$ loop-integrand is DCI.

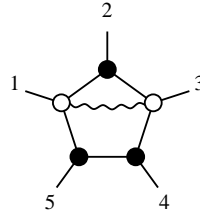
Especially for theories such as $\mathcal{N} = 4$ which are DCI, one should strictly avoid

parity-symmetrization at one-loop or higher. Although scalar pentagon integrals are quite familiar, *chiral* pentagons are slightly novel—although they have already played an important role in the literature (see e.g. [65,66]). The first appearance of pentagon integrals occurs for five particles, and there are essentially two possibilities that arise:



$$\int_{(AB)} \frac{\langle AB Y \rangle \times \langle 2345 \rangle \langle 4512 \rangle}{\langle AB 12 \rangle \langle AB 23 \rangle \langle AB 34 \rangle \langle AB 45 \rangle \langle AB 51 \rangle}, \quad (1.2.20)$$

where $\langle 2345 \rangle \langle 4512 \rangle$ in the numerator is for normalization² and the bitwistor Y is simply $Z_1 Z_3$ (this is indicated by the dashed-line in the associated figure); and,



$$\int_{(AB)} \frac{\langle AB \tilde{Y} \rangle \times \langle 3451 \rangle}{\langle AB 12 \rangle \langle AB 23 \rangle \langle AB 34 \rangle \langle AB 45 \rangle \langle AB 51 \rangle}, \quad (1.2.21)$$

where the factor $\langle 3451 \rangle$ in the numerator is for normalization, and the bitwistor $\tilde{Y} \equiv '(512) \cap (234)'$ is the line in twistor-space which lies along the intersection of the planes spanned by twistors (Z_5, Z_1, Z_2) and (Z_2, Z_3, Z_4) —which is indicated in the figure by the ‘wavy-line’. As the first of many such examples, it is useful to write-out \tilde{Y} explicitly:

$$\begin{aligned} \tilde{Y} &\equiv (512) \cap (234) = Z_5 Z_1 \langle 2234 \rangle + Z_1 Z_2 \langle 5234 \rangle + Z_2 Z_5 \langle 1234 \rangle, \\ &= 0 + Z_1 Z_2 \langle 5234 \rangle + Z_2 Z_5 \langle 1234 \rangle, \end{aligned} \quad (1.2.22)$$

where we have used the fact that $\langle 2234 \rangle = 0$. (The translation between statements such as ‘the line along the intersection of two planes’ and explicit representative formulae such as the above will be explained in more detail below; here, we merely quote the result in a way from which we hope it will be easy to guess the general case.)

These two integrals are examples of a very important class of integrals that we call *chiral integrals with unit leading singularities*, or *pure* integrals. In each case, the

²We will see that this normalization follows from the requirement that the integral have *unit leading-singularities*, and its sign is fixed by parity relative to the ‘wavy-line’ pentagon drawn below it. In fact, as we will describe in section 1.3, the dashed-line in the figure dictates both the bitwistor $Y \equiv Z_1 Z_3$ and the normalization of the integral.

bitwistor appearing in the numerator (together with the integrand’s normalization) is completely specified by the dashed- or wavy-line in the corresponding figure. We will explain many of the important features of these integrals together with the way their graphical representations in more detail in section 1.3. It is worth noting in passing, however, that the two integrals are parity conjugates of one another, and special bitwistors Y and \tilde{Y} represent the two lines in twistor-space which simultaneously intersect the four lines (51), (12), (23), and (34); this means that $\langle Y 51 \rangle = \langle Y 12 \rangle = \langle Y 23 \rangle = \langle Y 34 \rangle = 0$, and similarly for \tilde{Y} . Because of this, they represent the two isolated points in (AB) -space for which these four propagators go on-shell.

Before moving-on to discuss loop integrands, we should emphasize that because the primary focus of this chapter is the loop *integrand*—the sum of all the Feynman diagrams, as a rational function—there is nothing to say about the regulation of IR-divergent integrals such as the zero-mass box integral and the pentagons integrals given above. The only *integrals* we will evaluate explicitly are all *manifestly* finite (in a precise sense which will be described in section 1.4), and hence are well-defined without any regulator. However, it is important to mention that IR-divergent integrals can also easily be regulated and evaluated. In fact, the most natural way to add a regulator is also a very physical one, given by moving out on the Coulomb branch [67] of the theory.

II. The Loop *Integrand*

A simple but far-reaching consequence of writing each Feynman integral in a loop amplitude using the dual variables is that one can meaningfully combine all integrals appearing in a particular amplitude under the same integral sign. This leads to the concept of *the* loop *integrand* [65]. We stress again that planarity and the use of dual variables plays a crucial role in making this possible—for a general theory, there is no natural origin of loop momentum space and therefore no canonical way of combining all Feynman diagrams under a common loop integral.

It is easy to characterize the structure of the n particle 1-loop integrand for $\mathcal{N} = 4$ SYM using momentum-twistor space integrals. All the terms in the integrand can be combined defining a universal denominator containing all n physical propagators of the form $\langle AB a a+1 \rangle$. If a particular Feynman diagram has fewer propagators, then

the numerator is chosen so as to cancel the extra propagators. The loop amplitude is given as an an integral over a single rational function,

$$\mathcal{A}_n = \int_{(AB)} \frac{\sum_i c_i \langle AB Y_1^i \rangle \langle AB Y_2^i \rangle \dots \langle AB Y_{n-4}^i \rangle}{\langle AB 12 \rangle \langle AB 23 \rangle \dots \langle AB n-1 n \rangle \langle AB n 1 \rangle} \quad (1.2.23)$$

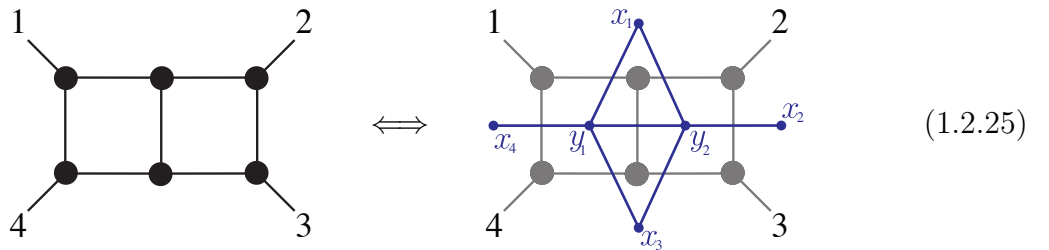
where \mathcal{A}_n is the full 1-loop partial amplitude. This formula is already written using the simplifications that arise in $\mathcal{N} = 4$ SYM, in other words, it is manifestly DCI. However, the integrand exists in any planar theory: for a theory which is not DCI, (1.2.23) would necessarily contain also terms with powers of $\langle AB I_\infty \rangle$.

At higher loops, say L loops, scattering amplitudes are given as linear combination of integrals of the form

$$\int \prod_{i=1}^L d^4 \ell_i \frac{\prod_{j=1}^L N(\ell_j)}{\prod_{k=1}^L P(\ell_k)} \times \frac{1}{R(\ell_1, \dots, \ell_L)}, \quad (1.2.24)$$

where N, P , and R are products of Lorentz invariants constructed out of Feynman propagators and which depend on the variables shown and on the external momenta. Written in this form, there is clearly a large amount of redundancy in the definitions of the internal loop momenta.

Since we are dealing with only planar integrals, for each Feynman diagram there exists a dual diagram (the standard dual graph of a planar graph). Consider for example the following four-point two-loop integral:



Using x_i to denote the dual coordinates of the external momenta and y_i to denote the internal points, one can write any planar L -loop integral in dual coordinates. There is, however, one slight subtlety in using such a prescription to uniquely define ‘the’ integrand: while the definition of the external points x_i is unique, the labeling of the internal points is not (when $L > 1$). But the solution to this problem is very simple: we are always free to completely symmetrize the integrand with respect to all $L!$ permutations of the internal loop-variable labels. Although we will often

write multi-loop integrands in some particular representative choice of the labels for internal propagators, complete-symmetrization over all permutations of indices is always implied (including a factor of $1/L!$ from this symmetrization).

Consider for example the simplest two-loop integral, given above in (1.2.25). Written in dual-coordinates, the integral would be given by

$$\int \frac{d^4 y_1 d^4 y_2}{2} \frac{((x_1 - x_3)^2)^2 (x_2 - x_4)^2}{(y_1 - x_3)^2 (y_1 - x_4)^2 (y_1 - x_1)^2 (y_2 - x_1)^2 (y_2 - x_2)^2 (y_2 - x_3)^2 (y_1 - y_2)^2} + (y_1 \leftrightarrow y_2),$$

—where the numerator was chosen in order to make the integral dual-conformally invariant, and the factor of $1/2$ in the measure reflects the complete-symmetrization.

Of course, as we will see repeatedly throughout this chapter, (multi-)loop integrands are much more naturally expressed in terms of momentum-twistor variables. To translate the integral (1.2.25) in momentum-twistor variables, we need to associate a pair of twistors to each of the two loop variables. This we can do by making the association

$$y_1 \leftrightarrow (Z_A, Z_B) \quad \text{and} \quad y_2 \leftrightarrow (Z_C, Z_D). \quad (1.2.26)$$

Using this notation and the translation of propagators in terms of momentum twistors given in (1.2.8) one finds

$$\int_{(AB, CD)} \frac{\langle 1234 \rangle^2 \langle 2341 \rangle}{\langle AB 41 \rangle \langle AB 12 \rangle \langle AB 23 \rangle \langle CD 23 \rangle \langle CD 34 \rangle \langle CD 41 \rangle \langle ABCD \rangle},$$

where ‘ (AB, CD) ’ implies that the integration measure carries with it a factor of $1/2$ from the symmetrization of $(AB) \leftrightarrow (CD)$. We should mention here that for 3-loops, we will use (Z_E, Z_F) to denote the line corresponding to y_3 —but of course, a convention such as that of associating (Z_{A_m}, Z_{B_m}) with y_m would be increasingly preferable at high-loop order.

Before we leave the topic of *the* loop-integrand in general, we should mention that the form of the integrand obtained via BCFW as described in Chapter 2 makes it completely manifest that the loop-integrands in $\mathcal{N} = 4$ enjoy the full Yangian symmetry of the theory. (Of course, the choice of an integration contour which introduces IR-divergences, such as the physical contour, breaks this symmetry.)

However, just as with the BCFW recursion relations at tree level, the formulae obtained from the recursion do not enjoy manifest locality or manifest cyclic invariance.

The restriction that we impose throughout this work, however, is that loop-integrand be expanded in a way which makes use of only planar, local propagators. As we have stressed a number of times, we will find amazingly simple, manifestly cyclically symmetric and local expressions for multi-loop amplitudes, that are significantly simpler and more beautiful than other in the literature.

The local formulae presented in this chapter are very closely related to and influenced by the concept of the *leading singularities* of scattering amplitudes, which we proceed to presently describe.

III. Leading Singularities

Definition

The concept of leading singularities was introduced in the 1960's in the context of massive scalar theories [68]. More recently, in 2004, the same concept was modified to accommodate massless particles and this was exploited for Yang-Mills in [69]. The original definition of 'leading-singularity' refers to a discontinuity of a scattering amplitude across a singularity of the highest possible co-dimension. At 1-loop, for example, leading singularity discontinuities are computed using a generalization of a unitarity cut, but where four propagators are cut instead of two. Using \mathcal{A}_i for $i = 1, \dots, 4$ to denote the four partial amplitudes, each with their associated momentum-conserving δ -function, one has what can be called leading-singularity discontinuity,

$$\begin{aligned}
 &= \int \prod_{r=1}^4 d^4 \tilde{\eta}_r d^4 \ell_r \delta(\ell_r^2) \mathcal{A}_1(\{\ell_1, \tilde{\eta}_1\}, \{-\ell_2, \tilde{\eta}_2\}, \dots) \times \mathcal{A}_2(\{\ell_2, \tilde{\eta}_2\}, \{-\ell_3, \tilde{\eta}_3\}, \dots) \\
 &\quad \times \mathcal{A}_3(\{\ell_3, \tilde{\eta}_3\}, \{-\ell_4, \tilde{\eta}_4\}, \dots) \times \mathcal{A}_4(\{\ell_4, \tilde{\eta}_4\}, \{-\ell_1, \tilde{\eta}_1\}, \dots).
 \end{aligned}$$

Here, the integrations over the internal loop momenta are there only to remind us that we are to sum-over all solutions to the conditions imposed by the δ -functions,

and the integral over the Grassmann coordinate $\tilde{\eta}_i$ of each internal particle ℓ_i is there to remind us that we are to sum-over the exchange of all possible internal particles—which in the case of $\mathcal{N} = 4$ means the full super-multiplet.³

This point of view of leading-singularities has been very useful and allows a complete determination of 1-loop amplitudes in $\mathcal{N} = 4$ and in $\mathcal{N} = 8$ supergravity amplitudes when thought of as linear combinations of scalar box integrals with rational coefficients. The rational coefficients can be computed using the notion of generalized unitarity. Clearly, the notion of discontinuities is not related to the existence of an integrand and this is the reason it works in $\mathcal{N} = 8$, supergravity where an analog of ‘the integrand’—which requires a way to combine integrals with different cyclic orderings—has not yet been found.

As mentioned in our discussion of reduction procedures in $\mathcal{N} = 4$ SYM, the expansion in terms of boxes cannot give the physical integrand. The physical integrand is defined as that which coincides with the one from Feynman diagrams, prior any to reduction techniques, as rational functions—and, as we will see, the Feynman diagrams of $\mathcal{N} = 4$ in a given R -charge sector are *chiral*.

The importance of dealing with a specific rational function is that we can integrate it on *any* choice of contour we’d like—not just the real-contour which defines the Feynman integral. This allows us to define a more refined notion of a leading-singularity—the previous notion, motivated by generalized unitarity, is much coarser version of the one we will use now. In [70], this more refined notion was introduced, and it was used to match the full $\mathcal{N} = 4$ integrand for several 1-loop and 2-loop examples. However, in [70] the deep reason for why the idea was working, *i.e.*, the existence of the integrand, was not appreciated.

Whether written in ordinary momentum space, using dual-coordinates, or using momentum-twistors, loop integrals can be thought of as complex contour integrals on \mathbb{C}^4 with the choice of contour corresponding to \mathbb{R}^4 —the real-slice. However, this choice of contour is known to break many of the symmetries of the theory, and is littered with IR-divergences, etc. that can be the source of confusion. From various

³Here, we are using an on-shell superspace formalism which allows us to talk about all particles in the same super-multiplet as a single 1-particle state. We assume familiarity with this concept, but for careful definitions, more references and applications see [50].

viewpoints, the most natural contours would instead be those which compute the *residues* of the integrand. These are always finite, are often vanishing, and make manifest the full Yangian symmetry of the theory. We refer the reader to [71] for a mathematical definition of residues in several complex variables; here we hope the reader will find the definitions a natural generalization of the one-dimensional residues with which everyone is familiar.

Let us present the definition using x variables first. Consider a contour of integrations with the topology of a $T^4 = (S^1)^4$. In order to compute a particular residue one has to choose four propagators $(x - x_{a_i})^2$, with $i = 1, \dots, 4$ and integrate over the T^4 , defined by $|(x - x_{a_i})| = \epsilon_i$ where ϵ_i are small positive real numbers near one of the solutions. The circles, S^1 are parametrized by the phases and are given a particular orientation.

The definition of a multidimensional residue is very natural if one defines variables $u_i = (x - x_{a_i})^2$. Performing the change of variables the integral becomes

$$\int \prod_{i=1}^4 \frac{du_i}{u_i} \times \frac{1}{J} \times \{\text{The rest of the integrand}\} \quad (1.2.28)$$

where now the contour becomes small circles around $u_i = 0$. J is the Jacobian of the change of variables. The residue is then the Jacobian times the rest of the integrand evaluated at $u_i = 0$. The Jacobian

$$J = \det \left(\frac{\partial(u_1, u_2, u_3, u_4)}{\partial(x_1, x_2, x_3, x_4)} \right), \quad (1.2.29)$$

is clearly antisymmetric in the order of the columns. Different orderings can differ by a sign and this is related to the orientation of the contour. These signs are important

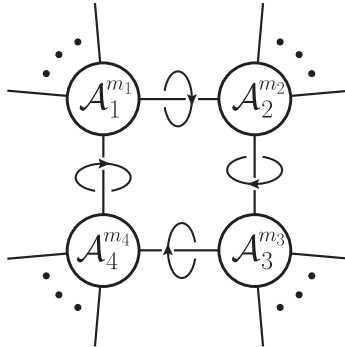


Figure 1.2: A ‘quad-cut’ one-loop leading-singularity viewed as a T^4 contour-integral which ‘encircles’ the point in \mathbb{C}^4 where four-propagators are made on-shell.

when discussing the generalization of residue theorems to the multidimensional case, which will play an important role momentarily.

From now on we call each individual residue a *leading-singularity*. As before, these are given by the product of four on-shell tree amplitudes as shown in Figure 1.2. The reason for the appearance of the tree amplitudes is that the residue of the poles is computed where the four propagators vanish and therefore internal particles can be taken on-shell.

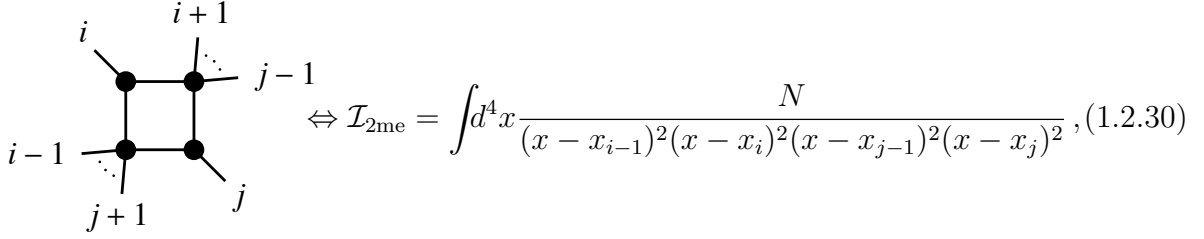
Leading singularities at higher loop-level can also be defined as residues of a complex, multidimensional integral over \mathbb{C}^{4L} where L is the loop order. This means that in order to define a residue one has to define a T^{4L} torus as a contour of integration. Naïvely, residues can only be defined for integrals with at least $4L$ propagators. However, noticing that propagators are quadratic in the loop-momentum, one can define *composite leading singularities* which involve less than $4L$ propagators as done in [16, 70, 72], using the self-intersection of curves defined by the on-shell condition to define isolated points in \mathbb{C}^4 about which the T^{4L} contour should ‘encircle.’

We will not discuss composite leading singularities in detail here simply because we will present evidence that when a special set of integrals, we call *chiral integrals with unit leading-singularities*, are used, matching non-composite leading-singularities appears to suffice to fix the entire amplitude. Moreover, we will see that only a very small subset of non-composite leading-singularities need to be considered to accomplish this.

Chirality of Leading Singularities

It turns out that for nonsingular external momenta, there are exactly two solutions to the equations $(x - x_{a_i})^2 = 0$, with $i = 1, \dots, 4$, and therefore two residues of each choice of four propagators. (This has a beautiful geometric interpretation in momentum twistors as we will see shortly.) This means that for an n -particle amplitude, there are $2\binom{n}{4}$ (non-composite) one-loop leading-singularities.

Consider any box integral, say, an integral with two massless legs and two massive, known as the ‘two-mass-easy’ integral:



$$\Leftrightarrow \mathcal{I}_{2\text{me}} = \int d^4x \frac{N}{(x-x_{i-1})^2(x-x_i)^2(x-x_{j-1})^2(x-x_j)^2}, \quad (1.2.30)$$

where N is just some normalization that need not concern us presently. The equations

$$(x-x_{i-1})^2 = (x-x_i)^2 = (x-x_{j-1})^2 = (x-x_j)^2 = 0$$

have two solutions, and therefore a residue can be computed for each such point separately. We'll soon see that these two solutions are easily found and differentiated when written with momentum-twistor variables; but for now, let us suppose the two solutions have been found, and denote the corresponding contours T_1^4 and T_2^4 .

A very important tool that will make an appearance many times is multidimensional analogue of Cauchy's theorem, called the *Global Residue Theorem* (GRT). The GRT states that—given a suitable condition at infinity—the sum over all the residues of a given rational function vanishes (see chapter 6 of [71]). This means, in the present case, that

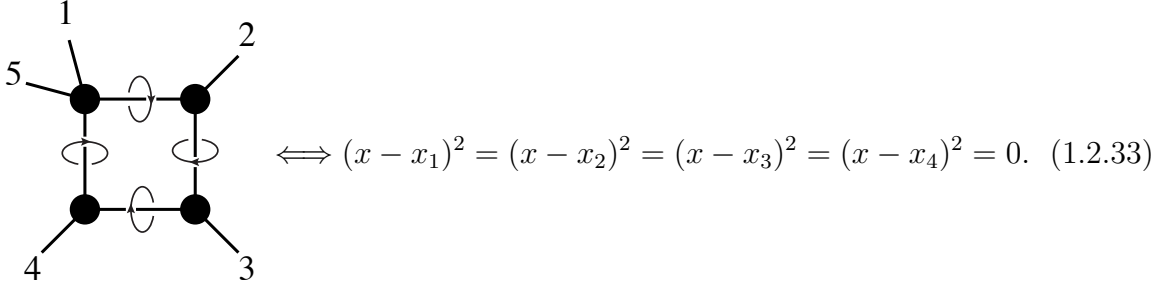
$$\text{res}_{T_1^4}(\mathcal{I}_{2\text{me}}) + \text{res}_{T_2^4}(\mathcal{I}_{2\text{me}}) = 0 \quad (1.2.31)$$

Moreover, we can choose the normalization N is such that, say $\text{res}_{T_1^4}(\mathcal{I}_{2\text{me}}) = 1$. Such a choice is possible for all box integrals, following from the simple fact that all box-integrals—having only four propagators—must have residues which are proportional equal and opposite. We refer to this fact by saying that scalar box integrals are *not chiral*. The use of the word chiral is justified by the fact that the locations of the leading singularities, as points in \mathbb{C}^4 , are mapped into each other by parity—which is just complex conjugation. And so the corresponding contours are mapped into each other up to orientation by parity. If use $(T_1^4)^*$ to denote the parity conjugate contour of T_1^4 , then $\text{res}_{(T_1^4)^*} = -\text{res}_{T_2^4}$ and the GRT implies that

$$\text{res}_{T_1^4}(\mathcal{I}_{2\text{me}}) = \text{res}_{(T_1^4)^*}(\mathcal{I}_{2\text{me}}). \quad (1.2.32)$$

Let us now consider the leading-singularities of the one-loop integrands of $\mathcal{N} = 4$ Yang-Mills. We'll see that, as scattering amplitudes of $\mathcal{N} = 4$ in a given R -charge

sector are chiral, so are the one-loop leading-singularities of field theory! In other words, the two residues associated with the two solutions of cutting four-propagators are *not* the same. Let us see this in an example. The simplest possible example is the five-particle MHV amplitude⁴. Let us consider taking the leading singularities of the field-theory integrand which encircles the point in \mathbb{C}^4 where the following four propagators go on-shell:



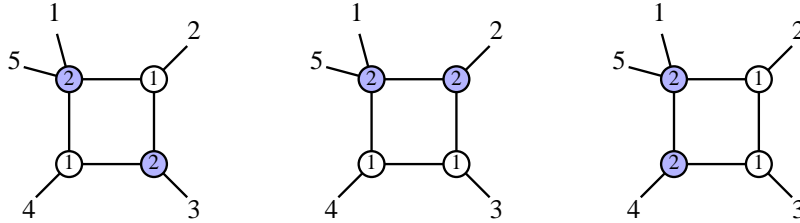
$$\iff (x - x_1)^2 = (x - x_2)^2 = (x - x_3)^2 = (x - x_4)^2 = 0. \quad (1.2.33)$$

It was noticed already in [69] that on one solution $\mathcal{N} = 4$ SYM gives the tree amplitude, A_5^{tree} , while it vanishes on the second.

The vanishing of leading singularities can be understood from pure supersymmetry. Consider an amplitude in the R -charge sector m . Recall the N^{m-2} MHV classification of amplitudes in $\mathcal{N} = 4$: under a rescaling of all $\tilde{\eta}_a$ variables by $t\tilde{\eta}_a$, an N^{m-2} MHV amplitude picks up a factor of t^{4m} . From the definition of leading singularities as the product of tree amplitudes connected by internal on-shell states we see that every internal line contributes (-1) to the R -charge counting coming from the integration over $\tilde{\eta}$ variables. At 1-loop, we have four tree-amplitudes and four propagators. If the R -charge of each tree-amplitude is m_i (see Figure 1.2), then the R -charge of the leading singularity is $m_1 + m_2 + m_3 + m_4 - 4$.

Returning to the five-particle example, because we are interested in a one-loop MHV amplitude, all its leading-singularities must have $m = 2$. The four-particle vertex (in the upper-left of the figure above) can only have $m_1 = 2$ and therefore the three-particle vertices have to satisfy $m_2 + m_3 + m_4 = 4$. Since the possible values for m for a three-particle amplitude are 1 and 2, two vertices must have $m = 1$ and one must have $m = 2$. This leaves only the possibilities shown below:

⁴The only DCI object for four-particles is the zero-mass box integral. This is why both leading singularities are equal to the tree amplitude.



Of these three possible leading-singularities of field theory, it turns out that the first one is equal to the five-point MHV tree-amplitude, and the latter two vanish for generic external momenta. In fact, whenever one is considering a leading singularity which involves 3-particle vertices, some very simple and powerful rules prove very useful: 1. any leading singularity involving adjacent three-particle vertices with the same R -charge will vanish for generic external momenta (momentum conservation in this case, requires that the external particles attached to these vertices must be collinear); and 2. leading singularities involving three-particle amplitudes are almost always *chiral*—the only exception being the four-particle amplitude.

In the case of the five particle example under consideration, we see that the residue from the contour encircling one of the two solutions to the quad-cut equations in (1.2.33) is equal to $\mathcal{A}_{5,\text{MHV}}^{\text{tree}}$, while the conjugate contour integral vanishes. We will explore this in more detail once we introduce the geometric point of view.

Dual Formulation of Leading Singularities

In the rest of the Chapter, we will make much use of the fact that leading-singularities satisfy many relations. These relations can be seen as resulting from residue theorems of the integrals which compute them. As a final comment before exploring the connection between leading singularities and the classic enumerative problems in the projective geometry of momentum twistor space let us briefly introduce the Grassmannian formulation.

In [16], leading singularities were proposed as completely IR-finite quantities that were likely to contain all the information needed to compute the S-Matrix of $\mathcal{N} = 4$ SYM. Moreover, it was conjectured that all leading singularities of the theory, which can be obtained to arbitrarily higher loop order, are computed by a contour integral over a Grassmannian manifold⁵ $G(m, n)$ called $\mathcal{L}_{m,n}$. Here m determines the R -charge sector of the theory under consideration.

⁵The Grassmannian $G(m, n)$, a natural generalization of ordinary projective space, is the space of

The integral was first presented in twistor space

$$\mathcal{L}_{m,n}(\mathcal{W}_a) = \int \frac{d^{nm} C_{\alpha a}}{\text{vol}(GL_m)} \frac{\prod_{\alpha=1}^m \delta^{4|4} (\sum_{a=1}^n C_{\alpha a} \mathcal{W}_a)}{(1\ 2 \cdots m)(2\ 3 \cdots m+1) \cdots (n\ 1 \cdots m-1)}. \quad (1.2.34)$$

In this presentation, residues of this integral are manifestly superconformal invariant (that is, superconformally-invariant in ordinary spacetime). Here we have introduced the concept of dual super twistor space $W = (\tilde{\lambda}, \mu, \tilde{\eta})$. This particular space will not play a significant role in this work, so we refer the interested reader to [16, 73] for more details.

This formula can be transformed to momentum-space and then to momentum-twistor space. Very remarkably, the formula in momentum-twistor space also turns out to be an integral over a Grassmannian, with the MHV-tree-amplitude arising as the Jacobian from the change of variables. Specifically,

$$\mathcal{L}_{m,n}|_{\text{momentum-space}}(\lambda, \tilde{\lambda}, \tilde{\eta}) = \mathcal{L}_{2,n} \times \mathcal{R}_{k,n}, \quad (1.2.35)$$

where $k = m - 2$ and

$$\mathcal{R}_{k,n}(\mathcal{Z}_a) = \int \frac{d^{nk} D_{\alpha a}}{\text{vol}(GL_k)} \frac{\prod_{\alpha=1}^k \delta^{4|4} (\sum_{a=1}^n D_{\alpha a} \mathcal{Z}_a)}{(1\ 2 \cdots k)(2\ 3 \cdots k+1) \cdots (n\ 1 \cdots k-1)}. \quad (1.2.36)$$

This representation in momentum twistor space makes *dual* superconformal invariance manifest [17, 18]. With some more effort one can prove that residues of this formula are also invariant under level one generators of the Yangian of the dual superconformal algebra and hence invariant under the whole Yangian [74]. The level one generators are nothing but the superconformal generators when passed through $\mathcal{L}_{2,n}$.

It has now been proven that all leading singularities are Yangian invariant and that all Yangian invariants are residues of the integral (1.2.36). From the physical point of view the problem has been solved. It might also be interesting to go further and prove that all residues of (1.2.36) correspond to some leading singularity but we will not discuss this issue any further.

Momentum Twistors and Schubert Problems

Statements like the number of solutions to setting four propagators to zero is two are non-obvious from the dual space x point of view. In terms of momentum twistors, m -dimensional planes in n -dimensions. Each point in $G(m, n)$ can be represented by the m n -vectors which span the plane, modulo a GL_m redundancy.

this statement turns out to be a simple, classic problem of the enumerative geometry of \mathbb{CP}^3 , solved by Schubert in the 1870's [75, 76].

Recall that an n -particle 1-loop amplitude can be written as

$$\mathcal{A}_n = \int_{(AB)} \frac{\sum_i c_i \langle AB Y_1^i \rangle \langle AB Y_2^i \rangle \cdots \langle AB Y_{n-4}^i \rangle}{\langle AB 12 \rangle \langle AB 23 \rangle \cdots \langle AB n-1 n \rangle \langle AB n 1 \rangle}. \quad (1.2.37)$$

Each one-loop leading-singularity is associated with a *point* in the space of loop-momenta for which some choice of four propagators simultaneously become on-shell,

$$\begin{array}{c} i \quad i+1 \\ \bullet \quad \bullet \\ \vdots \quad \vdots \\ l+1 \text{---} \bullet \text{---} \bullet \text{---} j \\ \vdots \quad \vdots \\ l \text{---} \bullet \text{---} \bullet \text{---} j+1 \\ \vdots \quad \vdots \\ k+1 \quad k \end{array} \iff \langle AB i i+1 \rangle = \langle AB j j+1 \rangle = \langle AB k k+1 \rangle = \langle AB l l+1 \rangle = 0;$$

Because the loop momentum is represented in momentum-twistors as the *line* (AB) , the solution to these four equations should correspond to a particular configuration for the line (AB) . We will see that for all leading-singularities which involve a three-particle vertex (a ‘massless leg’), the two solutions to four equations above are cleanly distinguished geometrically, allowing for a richly-chiral description of the integrand.

Before describing the full problem of putting four propagators on-shell, let us briefly consider the geometric significance of having a single factor, say $\langle AB i i+1 \rangle$, vanish. Recall that the four-bracket $\langle \cdots \rangle$ is nothing but the determinant of the 4×4 matrix of components of its four momentum-twistor arguments (viewed as elements of \mathbb{C}^4). As such, $\langle AB i i+1 \rangle = 0$ if and only if the vectors Z_A, Z_B, Z_i, Z_{i+1} are *not* linearly independent, implying the existence of some linear relation among the four twistors of the form $\alpha_A Z_A + \alpha_B Z_B + \alpha_i Z_i + \alpha_{i+1} Z_{i+1} = 0$. Trivially rearranging we see that

$$\alpha_A Z_A + \alpha_B Z_B = -(\alpha_i Z_i + \alpha_{i+1} Z_{i+1}), \quad (1.2.38)$$

which we may read as saying there is a point on the line spanned by Z_A, Z_B —namely $(\alpha_A Z_A + \alpha_B Z_B)$ —which lies along the line spanned by Z_i, Z_{i+1} . Which is to say, the lines (AB) and $(Z_i Z_{i+1})$ *intersect*; and because two intersecting lines describe a plane, we say that the four points Z_A, Z_B, Z_i, Z_{i+1} are *coplanar*.

Therefore, the problem of finding the particular lines (AB) for which four propagators simultaneously vanish is equivalent to finding the set of lines in \mathbb{CP}^3 which

simultaneously intersect four given lines (which are presumed fixed by the external data). The number of solutions to this problem is one of the classic examples of the enumerative geometry developed by Schubert in the 1870's. For this reason we call these problems *Schubert problems*.

The answer to the number of lines which intersect a given four turns out to be remarkably robust: provided the four lines are sufficiently generic, there are always 2 solutions, and an infinite number otherwise.⁶ (An example of a *non-generic* configuration would be one for which three or more of the lines were coplanar; these are never found for generic external momenta.)

Schubert derived the number of such solutions with an argument that is deceptively simple. The idea is to consider a particular configuration where it is easy to count the number of solutions. Schubert intuited that the answers to such enumerative questions should be topological in nature, and therefore should not depend on the particular configuration in question. Therefore, one can analyze the most convenient possible configuration (for which the number of solutions is not infinite) and the answer found for that case, should be the answer in general. Said another way, the number of solutions to a given Schubert problem should not change when a particular special configuration is smoothly moved into a more general position.

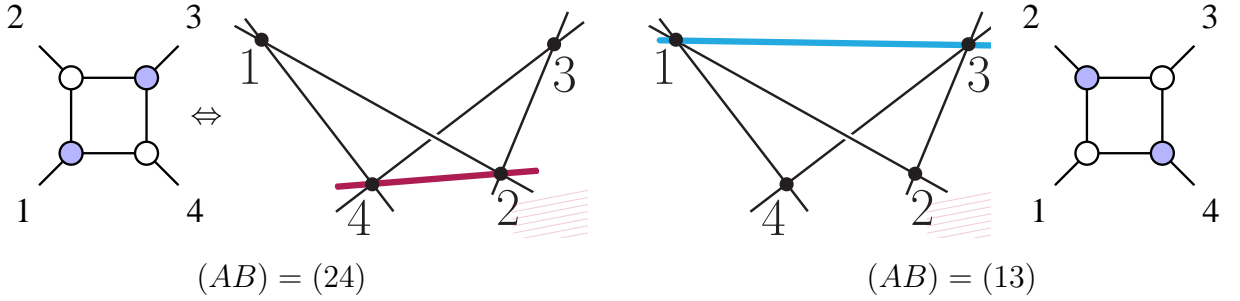
Perhaps the easiest configuration for which we can count the number of solutions to the Schubert problem of finding the lines (AB) that intersect four given lines in $\mathbb{C}\mathbb{P}^3$ is the *zero-mass* configuration; it is so-called because it is the configuration which corresponds to the box integral with *zero* of its four corners massive,

$$\begin{array}{c} 2 \qquad 3 \\ \diagdown \quad \diagup \\ \bullet \quad \bullet \\ \diagup \quad \diagdown \\ 1 \qquad 4 \end{array} \iff \int_{(AB)} \frac{\langle 1234 \rangle \langle 2341 \rangle}{\langle AB 12 \rangle \langle AB 23 \rangle \langle AB 34 \rangle \langle AB 41 \rangle},$$

which is an integral we have seen before. Explicitly, we would like to find all the lines (AB) which intersect all the four lines (12) , (23) , (34) , and (41) . This problem

⁶To be precise, we must count solutions with multiplicity; however, for a generic set of lines in the problem, the 2 solutions will always be distinct.

is indeed easy to solve, and the two solutions are drawn below.



Clearly, because $(12) \cap (23) \supset Z_2$ and $(34) \cap (41) \supset Z_4$, the line $(AB) = (24)$ intersects all four lines, as desired; this is drawn in red above. The same argument also applies to the second solution, the line $(AB) = (13)$, drawn in blue above. Also in this figure, we have indicated which leading-singularities have non-vanishing support on the corresponding (complex) point in the space of loop-momenta which corresponds to the particular line (AB) . As explained above, each three-particle MHV ($m = 2$)—colored blue in the figure above—or $\overline{\text{MHV}}$ ($m = 1$)—colored white—vertex of a leading singularity vanishes for every leading-singularity, and so which of the 2 three-particle amplitudes is non-vanishing for this value of the loop-momentum determines the chirality of the contour.

As a convenient way to gain some intuition about momentum-twistor geometry that will prove useful in the rest of this chapter and to establish some of the notation that will be ubiquitous throughout, we will study each of the 1-loop Schubert problems in turn.

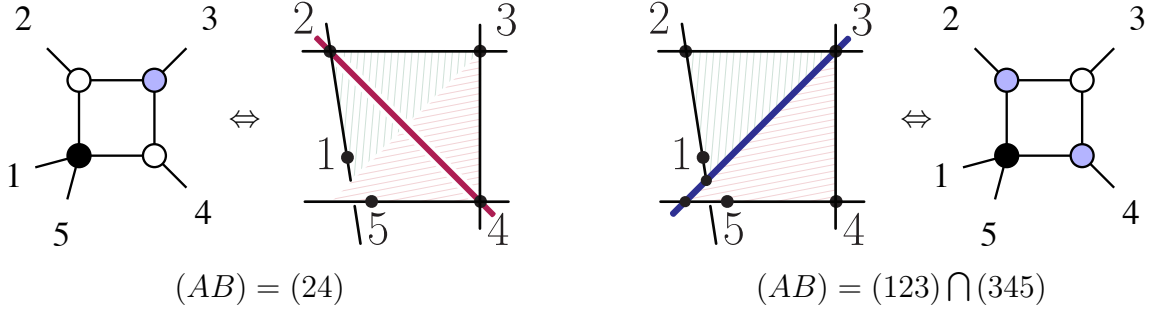
One-Mass Schubert Problem:

A ‘one-mass’ 1-loop leading singularity is one for which three of the four legs are massless, and is associated with the following archetypical box-integral:

$$\begin{array}{c} 2 \\ \diagdown \quad \diagup \\ \bullet \quad \bullet \\ | \quad | \\ \bullet \quad \bullet \\ \diagup \quad \diagdown \\ 1 \quad 4 \\ \quad \quad 5 \end{array} \iff \int_{(AB)} \frac{\langle 12 \ 34 \rangle \langle 23 \ 45 \rangle}{\langle AB \ 12 \rangle \langle AB \ 23 \rangle \langle AB \ 34 \rangle \langle AB \ 45 \rangle} . \quad (1.2.39)$$

In momentum-twistor space, the leading-singularities of this integral are associated with the lines (AB) which intersect the four lines (12) , (23) , (34) , and (45) . Considering the configuration of lines, it is not hard to find the two configurations which

solve this Schubert problem:



As before, because $(12) \cap (23) \supset Z_2$ and $(34) \cap (45) \supset Z_4$, the line $(AB) = (24)$ intersects all four lines. The second solution, however, is new. This solution is drawn in blue in the figure above, and represents the line of the intersection of the planes spanned by $(Z_1, Z_2, Z_3) \equiv (123)$ and $(Z_3, Z_4, Z_5) \equiv (345)$. Although geometrically clear, it is worthwhile to recall that any generic line in the plane (123) will intersect the lines (12) , (23) , and (31) , and any generic line in the plane (345) will intersect the lines (34) , (45) , and (53) . Therefore, the line $(AB) = (123) \cap (345)$ will intersect all four lines, as required.

Similar to the case discussed in the context of the pentagon with a ‘wavy-line’ numerator (1.2.21), the line $(123) \cap (345)$ can easily be expanded in terms of ordinary bitwistors as: $(23)\langle 1\ 345 \rangle + (31)\langle 2\ 345 \rangle$. This follows from a more general rule which review presently.

On the Intersection of Planes in Twistor-Space

In general, the intersection of the planes $(abc) \cap (def)$ is can be canonically expanded in either of the following ways:

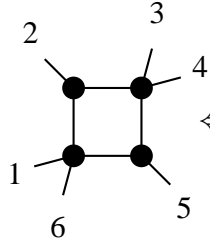
$$\begin{aligned}
 (abc) \cap (def) &= Z_a Z_b \langle c d e f \rangle + Z_b Z_c \langle a d e f \rangle + Z_c Z_a \langle b d e f \rangle; \\
 &= \langle a b c d \rangle Z_e Z_f + \langle a b c f \rangle Z_d Z_e + \langle a b c e \rangle Z_f Z_d.
 \end{aligned}
 \tag{1.2.40}$$

Alternatively, when expanding a four-bracket of the form $\langle xy (abc) \cap (def) \rangle$, the manifest dependence on the two planes can be preserved at the cost of breaking the manifest dependence on the line (xy) , as follows:

$$\langle xy (abc) \cap (def) \rangle = \langle x abc \rangle \langle y def \rangle - \langle y abc \rangle \langle x def \rangle.
 \tag{1.2.41}$$

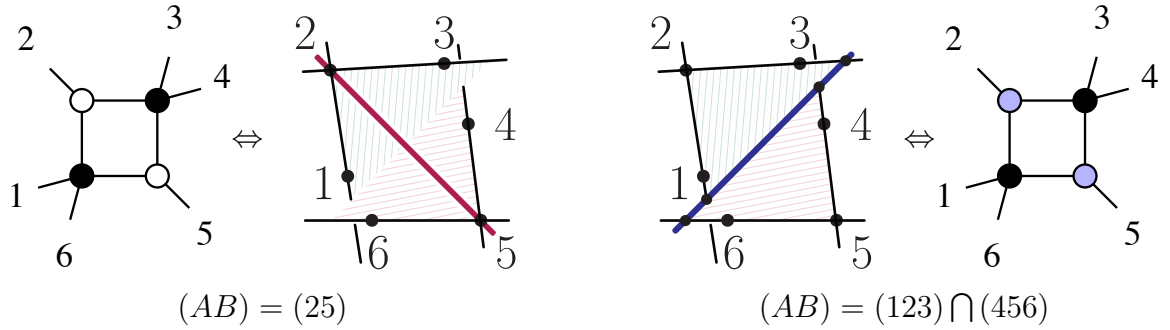
Two-Mass-Easy Schubert Problem

The two-mass-easy Schubert problem is associated with the following one-loop archetypical box-integral,



$$\int_{(AB)} \frac{\langle 1235 \rangle \langle 2345 \rangle}{\langle AB12 \rangle \langle AB23 \rangle \langle AB45 \rangle \langle AB56 \rangle}, \quad (1.2.42)$$

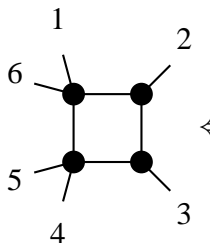
which has leading singularities supported on the configuration (AB) which intersect all four of the lines (12) , (23) , (45) , and (56) . The two solutions are essentially the same as for the one-mass Schubert problem, and are illustrated in the Figure below:



Once again, there is a very easy solution, in this case the line $(AB) = (25)$ which obviously intersects the four lines. And using the same reasoning as in the one-mass Schubert problem, it is easy to see that the second solution is simply the intersection of the planes $(123) \cap (456)$.

Two-Mass-Hard Schubert Problem

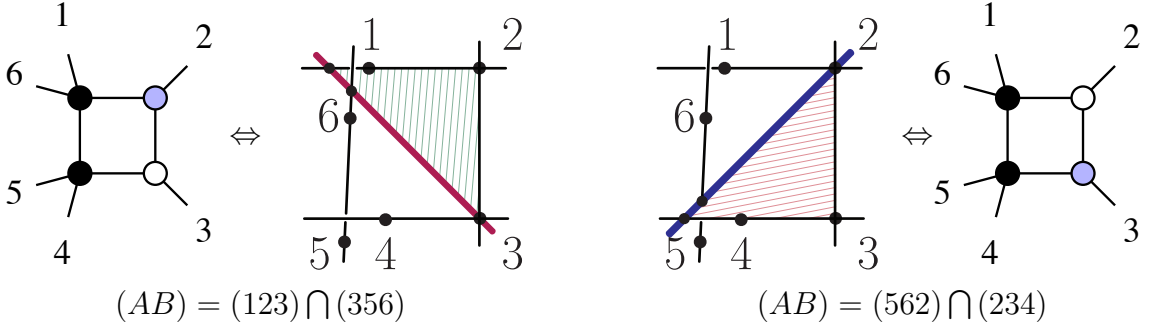
The two-mass-hard Schubert problem differs from the two-mass easy problem in that the two massless corners are adjacent—making the Schubert problem slightly less ‘easy’ (which at least partially justifies the name). It is associated with the following archetypical one-loop integral,



$$\int_{(AB)} \frac{\langle 1234 \rangle \langle 2356 \rangle}{\langle AB12 \rangle \langle AB23 \rangle \langle AB34 \rangle \langle AB56 \rangle}, \quad (1.2.43)$$

and has leading singularities supported where the line (AB) intersects the four lines

(12), (23), (34), and (56). The two solutions are shown in the Figure below:



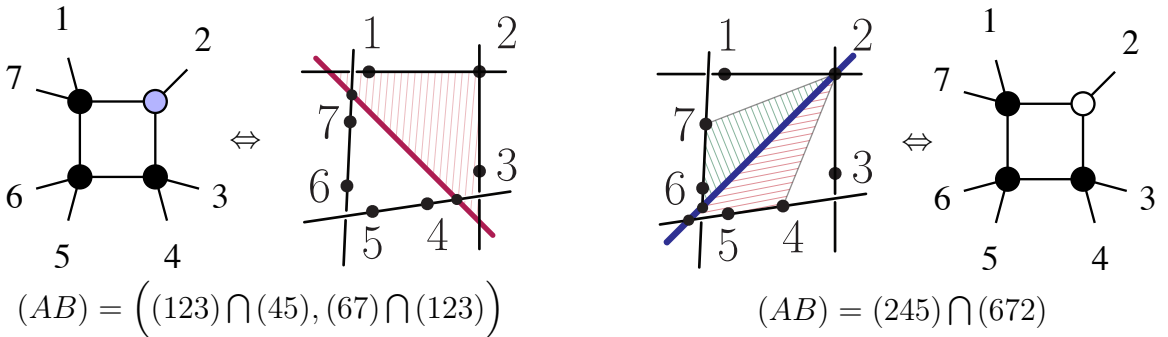
Let us briefly discuss the first of the two solutions. Here, the line $(AB) = (123) \cap (356)$ intersects the lines (23), (34) trivially because $Z_3 \subset (123) \cap (356)$, and it intersects the lines (12) and (56) because any generic line in the plane (123) intersects (12), and any generic line in the plane (356) intersects (56).

Three-Mass Schubert Problem

The last Schubert problem that involves a massless corner is known as the ‘three-mass’ problem, and is associated with the following archetypical one-loop integral:

$$\begin{array}{c} 1 \\ 7 \\ 6 \\ 5 \\ 4 \\ 3 \\ 2 \end{array} \begin{array}{c} \bullet \\ \bullet \\ \bullet \\ \bullet \\ \bullet \\ \bullet \\ \bullet \end{array} \Leftrightarrow \int_{(AB)} \frac{\langle 1(245) \cap (672) 3 \rangle}{\langle AB 12 \rangle \langle AB 23 \rangle \langle AB 34 \rangle \langle AB 45 \rangle} . \quad (1.2.44)$$

This integral is the most general one which involves a massless corner, and supports leading singularities where the line (AB) intersects the four lines (12), (23), (45), and (67). The two solutions are indicated in the Figure below.



Here, the notation ‘ $(ab) \cap (cde)$ ’ has been used to indicate the *point* in twistor-space where the line (ab) intersects the plane (cde) . We will discuss the expansion of such

geometrically-defined objects more generally at the end of this subsection; for now, let us merely quote the result:

$$(ab) \cap (cde) \equiv Z_a \langle bcde \rangle + Z_b \langle cdea \rangle = - \left(Z_c \langle deab \rangle + Z_d \langle eabc \rangle + Z_e \langle abcd \rangle \right);$$

and similarly,

$$(cde) \cap (ab) \equiv Z_c \langle deab \rangle + Z_d \langle eabc \rangle + Z_e \langle abcd \rangle = - \left(Z_a \langle bcde \rangle + Z_b \langle cdea \rangle \right);$$

so that $(ab) \cap (cde) = -(cde) \cap (ab)$.

On Schouten-Identities and Projective Geometry

Perhaps the single most useful identity for momentum-twistor geometry is known as ‘the five-term identity:’ any arbitrary set of five twistors $\{Z_a, Z_b, Z_c, Z_d, Z_e\}$ will satisfy the following identity,

$$Z_a \langle bcde \rangle + Z_b \langle cdea \rangle + Z_c \langle deab \rangle + Z_d \langle eabc \rangle + Z_e \langle abcd \rangle = 0. \quad (1.2.45)$$

This identity merely reflects the general solution to a homogeneous, linear system of equations in four-variables, and as such, has analogues in any number of dimensions. For example, in two dimensions, we have that for any $\{\lambda_a, \lambda_b, \lambda_c\} \subset \mathbb{C}^2$, there is an identity

$$\lambda_a \langle bc \rangle + \lambda_b \langle ca \rangle + \lambda_c \langle ab \rangle = 0, \quad (1.2.46)$$

where we have naturally extended the definition of ‘ $\langle \cdot \cdot \rangle$ ’ to be the determinant of the components of the corresponding two-vectors. This two-dimensional identity represents the general solution to a homogeneous, linear system of equations in 2 unknowns, and by contracting it with a fourth two-vector λ_d , we obtain the familiar ‘Schouten identity:’

$$\langle da \rangle \langle bc \rangle + \langle db \rangle \langle ca \rangle + \langle dc \rangle \langle ab \rangle = 0. \quad (1.2.47)$$

This familiar identity of course has an analogue descending from equation (1.2.45). By contracting equation (1.2.45) with any arbitrary plane (fgh) , we find the following 5-term identity which we will therefore call ‘a Schouten identity:’

$$\langle fgha \rangle \langle bcde \rangle + \langle fghb \rangle \langle cdea \rangle + \langle fghc \rangle \langle deab \rangle + \langle fghd \rangle \langle eabc \rangle + \langle fgh e \rangle \langle abcd \rangle = 0.$$

In addition to being quite useful for simplifying formulae, equation (1.2.45) can be trivially re-arranged to yield the solutions to some of the most often-encountered problems in momentum-twistor geometry:

1. the expansion of any arbitrary twistor Z_a into a basis composed of any four linearly-independent twistors $\{Z_b, Z_c, Z_d, Z_e\}$:

$$Z_a\langle bcde \rangle = -\left(Z_b\langle cdea \rangle + Z_c\langle deab \rangle + Z_d\langle eabc \rangle + Z_e\langle abcd \rangle\right);$$

2. the point along the line (ab) which intersects the plane (cde) :

$$(ab) \cap (cde) \equiv Z_a\langle bcde \rangle + Z_b\langle cdea \rangle = -\left(Z_c\langle deab \rangle + Z_d\langle eabc \rangle + Z_e\langle abcd \rangle\right);$$

3. the point on the plane (abc) which intersects the line (de) :

$$(abc) \cap (de) \equiv Z_a\langle bcde \rangle + Z_b\langle cdea \rangle + Z_c\langle deab \rangle = -\left(Z_d\langle eabc \rangle + Z_e\langle abcd \rangle\right);$$

and so-on.

Matching All Leading Singularities

We close this introductory section to momentum twistor integrals and leading singularities with a physical point. We have seen that the leading singularities of $\mathcal{N} = 4$ SYM are chiral while those of scalar boxes are non-chiral. This means that if we want to construct the integrand of the theory it is impossible to do it using scalar boxes. Momentum twistors already give the solution to this problem. Since leading singularities are Yangian invariant and in particular dual conformal invariant (DCI), one should use the reduction procedure to go down to tensor pentagons and boxes and not any further. Even going down to scalar pentagons would be doing something brutal to the manifestly DCI structure of the amplitudes.

In the rest of the Chapter, we will find that by using a special class of integrals known as *chiral unit leading singularity* integrals, the full integrand of scattering amplitudes can be reproduced yielding to stunningly simple forms.

1.3 Chiral Integrals with Unit Leading Singularities

In the previous section we showed that the usual constructions of, say, one-loop amplitudes in $\mathcal{N} = 4$ SYM as a linear combination of scalar boxes cannot possibly be the physical integrand. Of course, the answer obtained from scalar boxes gives the same integrals as the one originally defined from Feynman diagrams. However, as we will see, insisting in obtaining the physical integral leads to stunningly simple formulas for one and higher loop amplitudes. These new formulas are possible thanks to the use of a new suit of integrals with very special properties. These are *chiral integrals with unit leading singularities*.

I. Integrals with Unit Leading Singularities, or *Pure Integrals*

Let us start by given a definition of integrals with unit leading singularities. As we will see, it is appropriate to call these *pure integrals*.

Consider a particular DCI L -loop integral and compute all possible residues. If all non-vanishing residues are the same up to a sign then the integral can be normalized so that all residues are ± 1 or 0. When this is done, the integral is said to have *unit leading singularities* or to be a *pure integral*.

We already encountered examples of pure integrals in the previous section. The zero mass box (1.2.15), the general scalar box (1.2.16) (properly normalized), and the pentagon integrals in (1.2.20) and (1.2.21).

Using the global residue theorem, we proved in section 2 that boxes are pure integrals. However, it is not obvious that the pentagons in (1.2.20) and (1.2.21) satisfy the requirement.

Consider first pentagons of the first class

$$\int_{(AB)} \frac{\langle AB 13 \rangle N}{\langle AB 12 \rangle \langle AB 23 \rangle \langle AB 34 \rangle \langle AB 45 \rangle \langle AB 51 \rangle} \quad (1.3.48)$$

where $N = \langle 12 45 \rangle \langle 23 45 \rangle$.

In order to see that all non-vanishing leading singularities are equal up to a sign let us use a global residue theorem. In section 2 we gave a very imprecise definition of the global residue theorem (GRT) which was enough for the purposes of that section.

Here we have to be more precise. The GRT states that given a choice of a map $f : \mathbb{C}^4 \rightarrow \mathbb{C}^4$ made from polynomial factors in the denominator, the sum over all the residues associated with the zeroes of the map vanishes.

In the present case, consider the map given by $f = (f_1, f_2, f_3, f_4)$ where

$$f_1 = \langle AB 12 \rangle, f_2 = \langle AB 23 \rangle, f_3 = \langle AB 34 \rangle, f_4 = \langle AB 45 \rangle \langle AB 51 \rangle.$$

It is easy to see that the map f has four zeroes (see section 2 for more details). The GRT assures that the sum over the four residues vanishes. How can we prove that residues are equal if the GRT only gives relations among four residues?

The answer has to do with our choice of numerator. Consider the value of $\langle AB 13 \rangle$ on the four zeroes. Each zero is a line which is the solution to some Schubert problem⁷. The four solutions are the lines (24) , $(123) \cap (345)$, (13) and $(512) \cap (234)$ (see the end of the section or section 2 for the notation). It is a simple exercise to show that $\langle AB 13 \rangle$ vanishes on the second and third solutions and it is non zero on the first and fourth. This means that the GRT implies that two leading singularities are equal and opposite in sign. The first is one of the two solutions to $\langle AB 12 \rangle = \langle AB 23 \rangle = \langle AB 34 \rangle = \langle AB 45 \rangle = 0$ while the fourth is one of the two solutions to $\langle AB 12 \rangle = \langle AB 23 \rangle = \langle AB 34 \rangle = \langle AB 51 \rangle = 0$. Let us denote these non-vanishing residues by $r_{(12),(23),(34),(45)}$ and $r_{(12),(23),(34),(51)}$ respectively. Therefore the GRT states that

$$(0 + r_{(12),(23),(34),(45)}) + (r_{(12),(23),(34),(51)} + 0) = 0$$

which implies the equality of the residues up a sign.

The pentagon integral as 10 leading singularities. This means that more work is needed to show that it has unit leading singularity. Consider a GRT associated to the map

$$f_1 = \langle AB 12 \rangle \langle AB 51 \rangle, f_2 = \langle AB 23 \rangle, f_3 = \langle AB 34 \rangle, f_4 = \langle AB 45 \rangle.$$

Once again, there are four zeroes of this map. Two of them are shared with the map we constructed before, *i.e.*, (24) and $(123) \cap (345)$. The two new solutions are (35)

⁷A Schubert problem was defined in section 2 as the projective geometry problem of finding lines that intersect four given lines which can be in special configurations called one-mass, two-mass-easy, two-mass-hard, and three-mass, as well as in generic positions which we call four-mass configurations.

and $(234) \cap (451)$. As before, the numerator vanishes on $(123) \cap (345)$. Very nicely, it also vanishes on (35) . We can denote by $r_{(12),(23),(34),(45)}$ and $r_{(51),(23),(34),(45)}$ the corresponding non-zero residues. Therefore the GRT gives

$$(0 + r_{(12),(23),(34),(45)}) + (r_{(51),(23),(34),(45)} + 0) = 0$$

This means that the GRT sets equal the non vanishing leading singularity in $\langle AB 51 \rangle = \langle AB 23 \rangle = \langle AB 34 \rangle = \langle AB 45 \rangle = 0$ with the ones we found before.

This procedure can be continued three more times by shifting the labels in the map by one. We leave it as an exercise for the reader to verify that in every case, the numerator vanishes on one solution implying that the GRT sets all non-zero leading singularities to be the same.

In order to compute the normalization and also to show how the GRT makes obvious statements that require computations to be verified, even in this trivial case, let us compute explicitly the two residues in the first GRT discussed above.

Consider the ones in the first step. In other words, let's evaluate the residue on the solution (24) to the system $\langle AB 12 \rangle = \langle AB 23 \rangle = \langle AB 34 \rangle = \langle AB 45 \rangle = 0$. The residue is given by

$$N \frac{\langle 2413 \rangle}{\langle 2451 \rangle \langle \langle 1234 \rangle \langle 2345 \rangle \rangle} \quad (1.3.49)$$

Here the terms in parenthesis are the Jacobian in the residue computation. A geometric way to see that the Jacobian has to contain the factors $\langle 1234 \rangle$ and $\langle 2345 \rangle$ is that on the special configurations where either one of them vanishes, the number of solutions to the Schubert problem becomes infinite. For example, consider the configuration where $\langle 1234 \rangle = 0$. In this case, any line on the plane (123) which passes through Z_4 solves the Schubert problem. Using the scaling of each momentum twistor, the Jacobian must be what we found.

In order to have a properly normalized integral we require (1.3.49) to be equal to one. This means that $N = \langle 5124 \rangle \langle 2345 \rangle$ which is the factor first given in section 2 in (1.2.20).

Consider now the residue coming the second Schubert problem, $\langle AB 12 \rangle = \langle AB 23 \rangle = \langle AB 34 \rangle = \langle AB 51 \rangle = 0$. The non-zero residue is associated with the solution $(512) \cap (234)$. This is a one-mass Schubert problem and one explicit form of Z_A

and Z_B was given in section 2. Let us use $Z_A = Z_2$ and $Z_B = -\langle 1234 \rangle Z_5 + \langle 5234 \rangle Z_1$ and compute the residue. The Jacobian is the same as before but with labels shifted back by one. The residue is then

$$N \frac{\langle 1234 \rangle \langle 2513 \rangle}{\langle 2345 \rangle \langle 5124 \rangle (\langle 1234 \rangle \langle 2513 \rangle)}. \quad (1.3.50)$$

Using the normalization derived above this quantity equals one as expected.

In section 2 we also presented a second pentagon integral which differs from the first one only in the choice of numerator. We leave it as an exercise for the reader to repeat the analysis done here and show that with the new numerator this is a pure integral⁸. Let us rewrite the integral here with the numerator given in geometric form

$$\int_{(AB)} \tilde{N} \frac{\langle AB (512) \cap (234) \rangle}{\langle AB 12 \rangle \langle AB 23 \rangle \langle AB 34 \rangle \langle AB 45 \rangle \langle AB 51 \rangle}. \quad (1.3.51)$$

Now it should be obvious that the comment made in section 2 is true. The special numerators are made from lines, (13) and $(512) \cap (234)$, which are the two solutions to a Schubert problem.

In section 4 we study a less trivial example; a hexagon integral where the special choice of numerator also allows the use of the GRT to show that all non-vanishing residues are equal. In the hexagon case, checking the statement that all residues are equal algebraically requires many applications of 4-bracket Schouten identities.

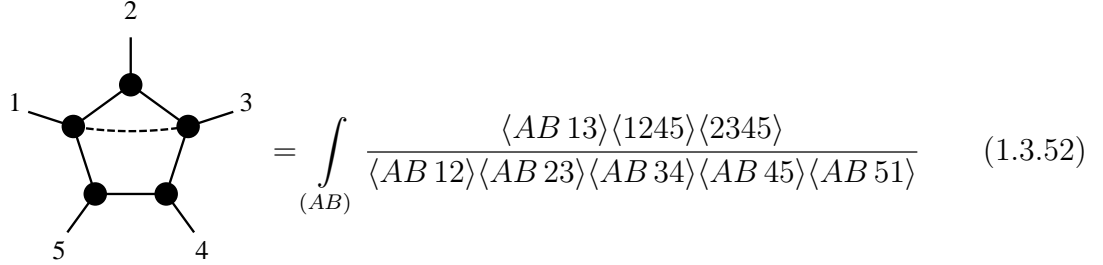
Basic Diagrammatic Notation

We find it convenient to introduce a diagrammatic representation for numerators. Note that with our definition of dual variables $p_a = x_a - x_{a-1}$ and of momentum twistors $x_a \leftrightarrow (Z_a, Z_{a+1})$, there is a natural diagrammatic relation between loop integrals and momentum twistor configurations. Consider a general one-loop amplitude as a polygon with n -sides. Attached to each vertex there is some momentum p_a . In momentum twistor space, we also have an n -sided polygon and attached to each vertex there is a momentum twistor Z_a . Following the intuitive correspondence between the two diagrams we are led to denote denominators (propagators) as lines connecting

⁸Of course, one could simply translate the whole problem into dual momentum twistor space to find exactly the same integral as before. However, it is still an instructive exercise to do it in momentum twistor space.

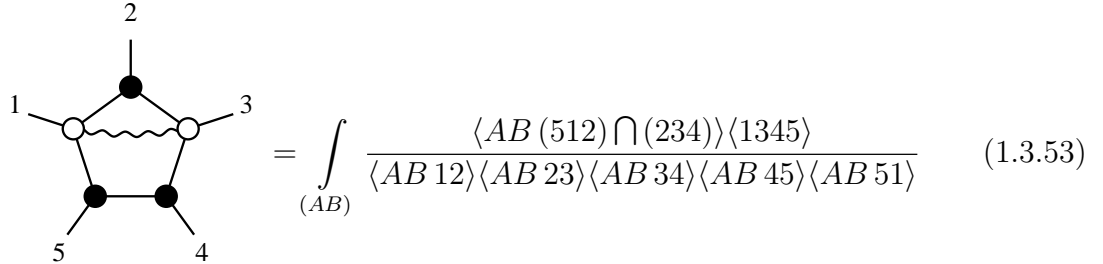
points depending on their geometric configuration. These are denoted by solid lines. In order to distinguish numerators, we also introduce dashed and wavy lines.

Dashed lines: Numerators which correspond to factors of the form $\langle AB ef \rangle$, where (ef) represents a line in momentum twistor space specified by two momentum twistors Z_e and Z_f is represented by a dashed line connecting points e and f as in



$$= \int_{(AB)} \frac{\langle AB 13 \rangle \langle 1245 \rangle \langle 2345 \rangle}{\langle AB 12 \rangle \langle AB 23 \rangle \langle AB 34 \rangle \langle AB 45 \rangle \langle AB 51 \rangle} \quad (1.3.52)$$

Wavy lines: We also allow points to represent dual twistors. In this case the second class of numerators constructed as intersection of planes can also be represented by a line connecting two points. In order to distinguish this from the previous case we use wavy lines. In the example where the numerator corresponds to the line $(512) \cap (234)$ or in dual twistors terminology to the point $(13)_W$, one has



$$= \int_{(AB)} \frac{\langle AB (512) \cap (234) \rangle \langle 1345 \rangle}{\langle AB 12 \rangle \langle AB 23 \rangle \langle AB 34 \rangle \langle AB 45 \rangle \langle AB 51 \rangle} \quad (1.3.53)$$

II. Chiral Integrals

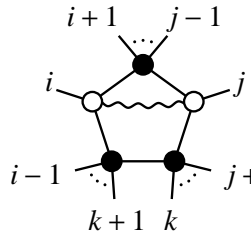
From the discussion of the pentagons, it is clear that there is a striking difference between a pentagon with a special numerator and plain scalar box integrals. Even though both kind of objects can be made pure integrals, each Schubert problem in the case of the pentagon has a single non-vanishing residue while in the boxes both solutions give rise to a residue.

When an integral has the property that the residues associated to at least one of its Schubert problems are not the same, we say that the integral is *chiral*. The reason for the terminology comes from the fact that the two contours associated to a given

Schubert problem are exchanged under parity (see section 2 for more details). This means that one can have chiral, pure, or chiral and pure integrals.

At one-loop, one can have an even more especial class of integrals. When an integral has a numerator where at most one of the solutions to each Schubert problem gives a non-zero residue then we say that the integral is *completely chiral*.

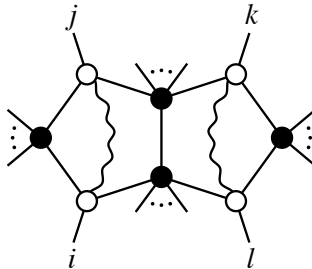
Let us give two more examples in this section. The first is the most general class of chiral pure pentagon integrals. This is an integral where only two of the five legs needs to be massless. Moreover, it is clear that in order to write a special numerator the two massless legs cannot be adjacent. The claim is that the following family of integrals is (completely) chiral and pure.



$$= \int_{(AB)} \frac{\langle AB(i-1 i i+1) \cap (j-1 j j+1) \rangle \langle i j k k+1 \rangle}{\langle AB i-1 i \rangle \langle AB i i+1 \rangle \langle AB j-1 j \rangle \langle AB j j+1 \rangle \langle AB k k+1 \rangle} \quad (1.3.54)$$

In this case, the GRT can also be applied to show that all residues are the same. In order to show that the normalization gives unit leading singularities, identities of the form discussed at the end of this section are needed.

Next, let us give a six-point two-loop example. Consider the following integral



$$= \left\{ \frac{\langle AB(i-1 i i+1) \cap (j-1 j j+1) \rangle \langle i j k l \rangle}{\langle AB i-1 i \rangle \langle AB i i+1 \rangle \langle AB j-1 j \rangle \langle AB j j+1 \rangle \langle AB C D \rangle} \times \frac{\langle C D (k-1 k k+1) \cap (l-1 l l+1) \rangle}{\langle C D k-1 k \rangle \langle C D k k+1 \rangle \langle C D l-1 l \rangle \langle C D l l+1 \rangle} \right\}$$

This integral has the structure of two of the general pentagon integrals joined by the all massive edge. Consider a residue of the full integral over \mathbb{C}^8 which computes a residue of the pentagon on the left. The contour integral in Z_A and Z_B is the same as before except that the normalization is different and therefore the residue is not equal to one. The residue must then be the ration of the two normalizations, *i.e.*, $\langle i j k l \rangle / \langle i j C D \rangle$. Plugging this in the integral over Z_C and Z_D we now find a properly normalized integral and therefore the remaining part of residue computation gives one.

One might be tempted at this point to think that all completely chiral integrals are pure. In section 4, we describe in detail the example of a hexagon with a wavy line and a dashed line in the numerator. This integral is in fact completely chiral but it is not pure.

III. Evaluation of Pure Integrals

Evaluating integrals explicitly can be very hard and many techniques have been developed for this purpose. At one-loop, all integrals appearing in the standard reduction techniques are known analytically. At higher loops, very few examples have been evaluated analytically. Many of our chiral pure integrals turn out to be completely IR finite and therefore their evaluation can be made directly four dimensions without any regulators.

Consider the family of pentagon integrals discussed above. The evaluation of the integrals for generic j and k gives

$$\begin{aligned}
I_5(i, j, k) &= \int_{(AB)} \frac{\langle AB (i-1 i i+1) \cap (j-1 j j+1) \rangle \langle i j k k+1 \rangle}{\langle AB i-1 i \rangle \langle AB i i+1 \rangle \langle AB j-1 j \rangle \langle AB j j+1 \rangle \langle AB k k+1 \rangle}, \quad (1.3.55) \\
&= \log(u_{j,k,i-1,j-1}) \log(u_{k,i-1,i,j}) + \text{Li}_2(1 - u_{j,k,i-1,j-1}) + \text{Li}_2(1 - u_{k,i-1,i,j}) \\
&\quad - \text{Li}_2(1 - u_{j,k,i,j-1}) - \text{Li}_2(1 - u_{i,j-1,k,i-1}) + \text{Li}_2(1 - u_{i,j-1,j,i-1})
\end{aligned}$$

where

$$u_{i,j,k,l} \equiv \frac{\langle i i+1 j j+1 \rangle \langle k k+1 l l+1 \rangle}{\langle l l+1 j j+1 \rangle \langle k k+1 i i+1 \rangle} \quad (1.3.56)$$

For special values of j and k the integral becomes IR-divergent and a regulator is needed. We postpone this discussion to section 4.

The reason for presenting the explicit form of the pentagon integrals is to note a general fact about pure integrals: The explicit evaluation of the integrals must be a linear combination of functions known as iterated integrals, such as polylogarithms, all with coefficient one.

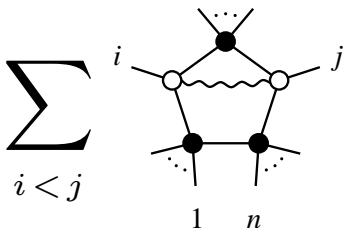
It is striking that the coefficients do not depend on kinematic invariants but this is a consequence of having unit leading singularities. This is the motivation for the terminology: pure integrals. Roughly speaking, the coefficients of the different polylogarithms are the leading singularities of the integrals. Having a pure integral ensures that no coefficient can depend on kinematical invariants.

Once again, the hexagon with a wavy and a dashed line in the numerator given in section 4 will be an example of a completely chiral and IR finite integral which is not pure and its evaluation gives products of logarithms with different coefficients that depend on kinematic invariants.

IV. Example: 1-Loop MHV Amplitudes

Up until now we have been studying integrals individually. This is a good point to actually use them to determine the full physical integral of the simplest set of amplitudes. These are one-loop MHV amplitudes. Historically, one-loop MHV amplitudes were the very first set of amplitudes to be computed for all n as a linear combination of scalar box integrals [12]. It was found that the answer is very simple; an overall prefactor, proportional to the tree-level amplitude, and a sum over all one-mass and two-mass-easy box integrals with coefficient one, when properly normalized. In our modern terminology, the normalization was such that only pure integrals appear. It was realized that this form of the amplitude was not equivalent to the Feynman diagram amplitude as an expansion in the dimensional regularization parameter but it differs from it only at $\mathcal{O}(\epsilon)$. In our language this is nothing but the fact that an expansion in terms of box integrals cannot possibly reproduce the physical integrand of the theory as stressed a number of times already.

Now that we have a set of chiral pure integrals, the natural question is how much more complicated the amplitude will look like if written in a form that matches the physical integrand. It turns out that the full integrand is stunningly simple

$$\mathcal{A}_{\text{MHV}}^{1\text{-loop}} = \sum_{i < j} \langle ABn1 \rangle \quad (1.3.57)$$


where the propagator $\langle ABn1 \rangle$ is present in all terms. Note that not all integrals in the sum are chiral pure integrals. There are boundary terms which are box integrals. Consider for example $j = i + 1$. In this case the numerator cancels one of the propagators leaving us with the box. We give no derivation for this formula here and

postpone a more detailed discussion to section 6. A final comment, even though the line $(n1)$ seems especial, the amplitude is cyclic as it should be!

1.4 Finite Integrals

We have seen that the chiral integrals with unit leading singularities, naturally written in momentum-twistor space, provide a natural basis of objects to express the loop integrand. In this section we will see that they have another beautiful property—most such integrals are manifestly infrared finite.

Let us begin by illustrating with a simple example. Consider a general 1-loop integral for 6 particles, which we can write as

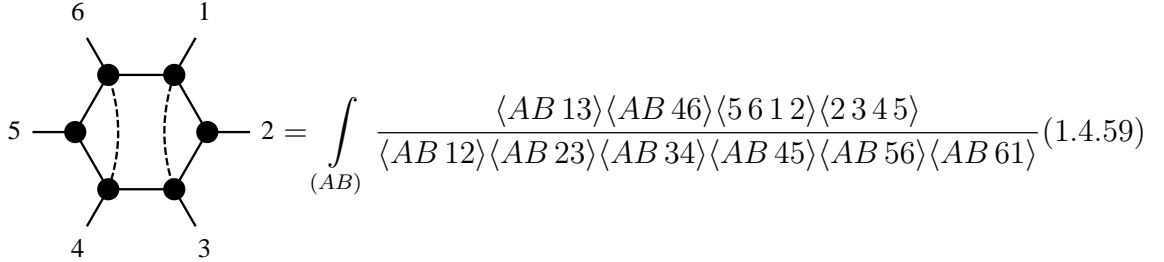
$$\int_{(AB)} \frac{\langle AB X \rangle \langle AB Y \rangle}{\langle AB 12 \rangle \langle AB 23 \rangle \cdots \langle AB 61 \rangle}. \quad (1.4.58)$$

Here X, Y are generic bitwistors. Of course, like almost all generic integrals with massless external legs, this integral is infrared divergent. Recall that the infrared divergences arise when the loop momentum l become collinear to a massless external momentum p_a , *i.e.* when $l \cdot p_a \rightarrow 0$. The extra soft logarithmic divergence can be thought of as an even more special case of this situation, where the loop momentum becomes collinear to two consecutive momenta so that $l \cdot p_a, l \cdot p_{a+1} \rightarrow 0$. In the dual co-ordinate space, the collinear divergence arises when the loop integration point x approaches one of the edges of the Wilson loop, connecting x_a with x_{a+1} , and of course the extra soft divergence occurs when x gets close to both the lines $(x_{a-1} x_a)$ as well as $(x_a x_{a+1})$, that is when it is close to the point x_a itself. But again the IR-divergence is fundamentally a collinear one, with the soft divergence being thought of as “double-collinear”.

We can finally describe these IR-divergent regions in momentum-twistor language. The collinear divergence associated with $l \cdot p_a \rightarrow 0$ corresponds to the region where the line (AB) in momentum twistor space, associated to the loop integration point, passes through Z_a while lying in the plane $(Z_{a-1} Z_a Z_{a+1})$. Note that this region is quite nicely parity invariant. Recall that in momentum-twistor variables, parity is just the poincare duality, and exchanges the point Z_a^I with the plane $W_{aI} = (Z_{a-1} Z_a Z_{a+1})_I$

naturally paired with Z_a . Thus, the condition is that the line $(AB)^{IJ}$ passes through Z_a^I , and also that the dual line $(AB)_{IJ}$ passes through W_{aI} .

While a generic integral will indeed be IR-divergent, we see a simple way of getting completely IR finite integrals. If the bitwistors X, Y are chosen to have a zero in all the dangerous IR-divergent configurations, then the integrals will be finite. This is very simple to achieve. For instance, let us choose $X = (13)$ and $Y = (46)$; we can write out the integral again as,



$$= \int_{(AB)} \frac{\langle AB 13 \rangle \langle AB 46 \rangle \langle 5 6 1 2 \rangle \langle 2 3 4 5 \rangle}{\langle AB 12 \rangle \langle AB 23 \rangle \langle AB 34 \rangle \langle AB 45 \rangle \langle AB 56 \rangle \langle AB 61 \rangle} \quad (1.4.59)$$

Let us check that the numerator has a zero in all the IR-divergent regions. Consider first collinearity with p_3 . We need to see what the numerator does when (AB) passes through Z_3 while lying in the plane (234) . However, the numerator factor $\langle AB 13 \rangle$ vanishes simply if (AB) passes through 1 or 3, regardless of whether or not it also happens to lie in the plane (234) . In this way, we can see that the collinear divergences with 1, 3, 4, 6 are all killed by the numerator. Next, consider what happens when (AB) passes through 2, lying in the plane (123) . Since (AB) lies in (123) , it necessarily intersects the line (13) , and therefore, $\langle AB 13 \rangle = 0$, regardless of whether or not (AB) also happens to pass through 2. A completely analogous argument holds for the collinear divergence associated with particle 5.

Thus we see that with this numerator, *all* the regions with collinear divergences are killed by the numerator factors, and the integral is completely IR-finite! There are other choices for X, Y that will do the same job; our argument above also holds if one or both of the numerator factors $(13), (46)$ were replaced by their parity-conjugates, $(612) \cap (234)$ and $(345) \cap (561)$, respectively—changing one or more of the dashed-lines in (1.4.59) to wavy-lines.

Now, these finite integrals are clearly chiral. And when the two numerators are of the same kind, they have, quite nicely and non-trivially, unit leading singularities. As usual, verifying by direct computation requires manipulating non-trivial sequences of 4-bracket Schouten identities, but the result follows much more transparently from

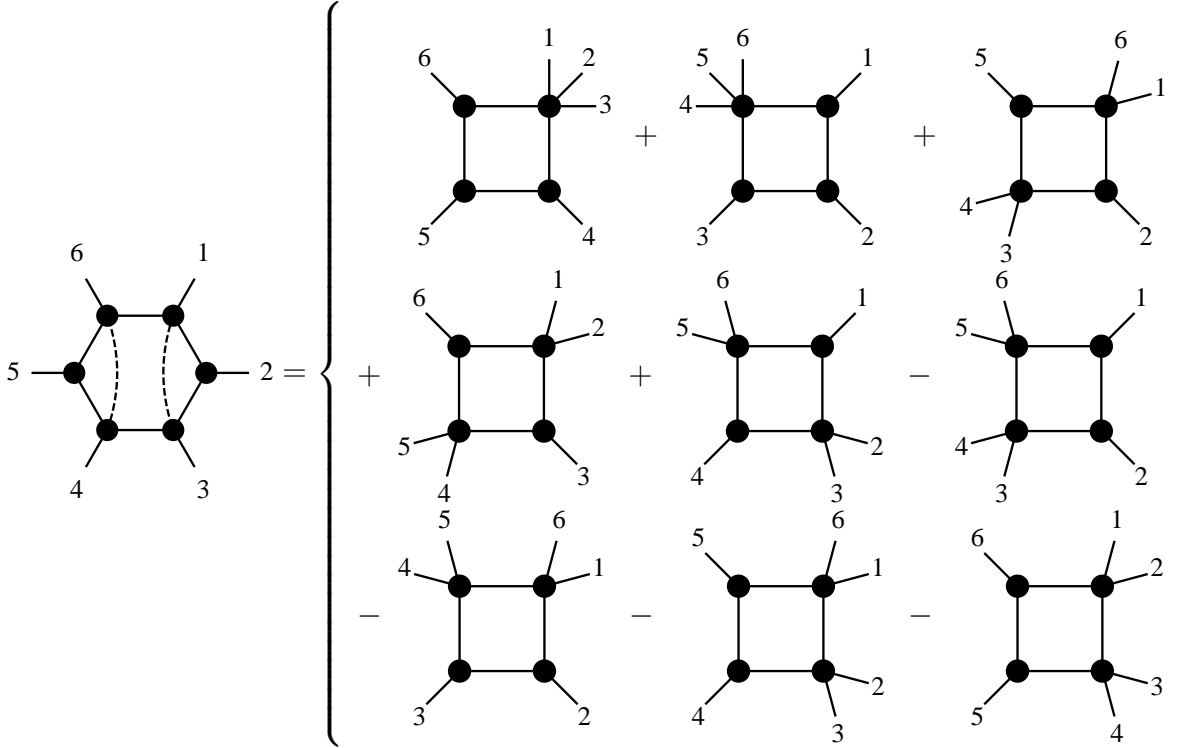
an application of the global residue theorem to this integral. Consider for instance the GRT following from choosing $f_1 = \langle AB 34 \rangle$, $f_2 = \langle AB 45 \rangle$, $f_3 = \langle AB 56 \rangle$ and $f_4 = \langle AB 61 \rangle \langle AB 12 \rangle \langle AB 23 \rangle$. We have three different Schubert problems to consider, with the lines (34), (45), (56) combined with (61), (12), (23). Consider first the Schubert problem with the four lines (34), (45), (56), (61). This is a one-mass configuration, and it is easy to see that the numerator kills the solution where (AB) is the line (46), only leaving the solution passing through 5. Let us call this non-vanishing residue $r_{(34),(45),(56),(61)}$. Similarly, for the Schubert problem with lines (34), (45), (56) and (12), the numerator kills the solution passing through 4 while leaving the one passing through 5; we can call this single non-vanishing residue $r_{(34),(45),(56),(12)}$. Finally, for the Schubert problem with lines (34), (45), (56), (23), we can see that *both* solutions—the line 35 as well the line passing through 4—are killed by the numerator, so both of these residues vanish. The GRT then tells us that

$$\begin{aligned} (0 + r_{(34),(45),(56),(61)}) + (0 + r_{(34),(45),(56),(12)}) + (0 + 0) &= 0 \\ \rightarrow r_{(34),(45),(56),(61)} &= -r_{(34),(45),(56),(12)} \end{aligned} \tag{1.4.60}$$

It is possible to repeat this argument for other GRT's, finding a sequence of 2-term identities relating *all* the non-vanishing residues, showing that the integral is not only chiral but has *unit* leading singularities. Thus, we see in this instance something that can be checked also to be true for all other residues: the integral is completely chiral; at most one of the two solutions to each Schubert problem are non-vanishing, and sometimes both vanish.

Given that this integral has unit leading singularities, it is instructive to expand it in terms of boxes, which will then also have unit coefficients. This simple, finite

momentum-twistor integral in fact expands into the sum of nine boxes:



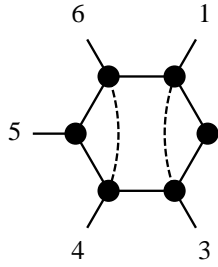
The seemingly complicated combinations of a large number of boxes have been encountered before in the computation of finite 1-loop objects, such as the NMHV ratio function [53, 57, 77, 78]—the ratio function for the full superamplitude is simply defined to be

$$\mathcal{R}_{n,k}^{1\text{-loop}} = \mathcal{A}_{n,k}^{1\text{-loop}} - \mathcal{A}_{n,k}^{\text{tree}} \cdot \mathcal{A}_{n,k=2}^{1\text{-loop}}. \quad (1.4.61)$$

Note that in the box expansion, every integral is individually IR-divergent, the IR-divergences only canceling in the sum. Moreover, the boxes themselves are not dual conformal invariant—again, only become dual conformal invariant in the sum. But since the hexagon in which we are interested is manifestly finite and dual conformal invariant⁹, we can evaluate it directly—for example, using Feynman parameterization

⁹In the literature on ratio functions, some authors have found what were claimed to be “finite” combinations of boxes that did *not* end up being dual-conformal invariant. In every case, the combinations of boxes in question were not honestly IR-finite: the divergences from different regions of the integration contour canceling between each-other. Such a cancellation is highly regulator-dependent, and is not very meaningful.

directly without any regularization. A straightforward computation shows,

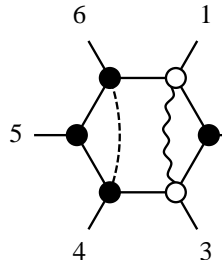


$$2 = \text{Li}_2(1-u_1) + \text{Li}_2(1-u_2) + \text{Li}_2(1-u_3) + \log(u_3)\log(u_1) - \frac{\pi^2}{3}, \quad (1.4.62)$$

where the u_i are the familiar six-point cross-ratios:

$$u_1 \equiv \frac{\langle 1234 \rangle \langle 4561 \rangle}{\langle 1245 \rangle \langle 3461 \rangle}, \quad u_2 \equiv \frac{\langle 2345 \rangle \langle 5612 \rangle}{\langle 2356 \rangle \langle 4512 \rangle}, \quad \text{and} \quad u_3 \equiv \frac{\langle 3456 \rangle \langle 6123 \rangle}{\langle 3461 \rangle \langle 5623 \rangle}. \quad (1.4.63)$$

It is easy to find examples of integrals which are finite and chiral, but which do not have unit leading singularities. For example, changing one the ‘dashed-line’ numerator factor $\langle AB13 \rangle$ in the integral above to a ‘wavy-line’ $\langle AB(612) \cap (234) \rangle$ will leave the integral finite and chiral, but spoil the equality of its leading singularities. Indeed, as it is also finite and dual-conformally invariant, the ‘mixed’ hexagon integral can also be evaluated without any regularization, and one finds that,



$$2 = \int_{(AB)} \frac{\langle AB(612) \cap (234) \rangle \langle AB46 \rangle}{\langle AB12 \rangle \langle AB23 \rangle \langle AB34 \rangle \langle AB45 \rangle \langle AB56 \rangle \langle AB61 \rangle}$$

$$= \left(\frac{\langle 1234 \rangle}{\langle 1345 \rangle \langle 1235 \rangle} \right) \log(u_1) \log(u_2) + \left(\frac{\langle 6134 \rangle}{\langle 1345 \rangle \langle 5613 \rangle} \right) \log(u_3) \log(u_1)$$

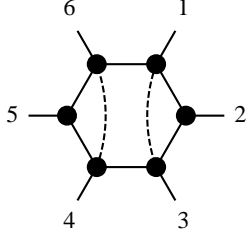
$$+ \left(\frac{\langle 6123 \rangle}{\langle 1235 \rangle \langle 3561 \rangle} \right) \log(u_2) \log(u_3).$$

In order for GRTs to yield the two-term identities necessary to guarantee that all the leading singularities are equal up-to a sign, the numerator must force vanishing residues for all but two Schubert problems. In the case of the ‘mixed-numerator’ hexagon integral, for example, GRTs can only be used to show that the coefficients of the logarithms sum to zero:

$$\left(\frac{\langle 1234 \rangle}{\langle 1345 \rangle \langle 1235 \rangle} \right) + \left(\frac{\langle 6134 \rangle}{\langle 1345 \rangle \langle 5613 \rangle} \right) + \left(\frac{\langle 6123 \rangle}{\langle 1235 \rangle \langle 3561 \rangle} \right) = 0. \quad (1.4.64)$$

It is clear that these chiral momentum-twistor integrals with unit leading singularities give us the simplest and most transparent way of talking about finite integrals.

Just as a trivial example, the 6-point NMHV ratio function, which is typically written in terms of all 15 six-point box-integrals, with many R -invariants as coefficients, is given simply by

$$\mathcal{R}_{\text{NMHV}}^{1\text{-loop}} \stackrel{\text{post-integration}}{=} (1 + g + g^2) \left\{ \begin{array}{c} \text{Diagram} \\ \times ([23456] - [34561] + [45612]) \end{array} \right\}, \quad (1.4.65)$$


where $g : i \mapsto i + 1$ acts on both the integrand and its coefficient. Also recall the definition of the R -invariants given in section 1,

$$[abcde] = \frac{\delta^{0|4}(\eta_a \langle bcde \rangle + \eta_b \langle cdea \rangle + \eta_c \langle deab \rangle + \eta_d \langle eabc \rangle + \eta_e \langle abcd \rangle)}{\langle abcd \rangle \langle bcde \rangle \langle cdea \rangle \langle deab \rangle \langle eabc \rangle}. \quad (1.4.66)$$

1.5 Multiloop Amplitudes

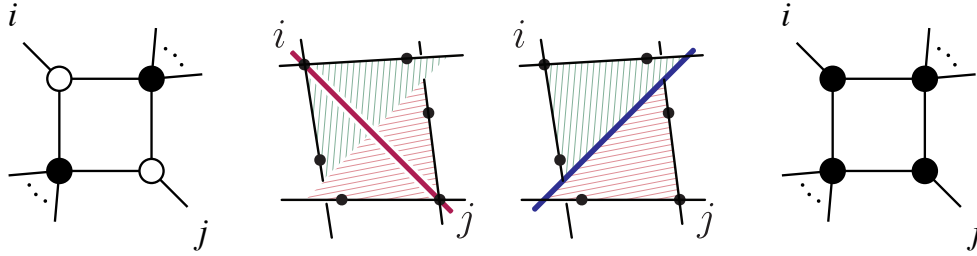
In this section, we introduce a new strategy for finding local representations of loop integrands. The idea is closely related to the leading singularity method, but the philosophy differs in some important ways. In particular we will *not* be guided by systematically trying to match all the leading singularities of the integrand. Instead, we will look at a simple subset of leading singularities defined for generic, large enough number of particles—no “composite” leading singularities will be considered. We will then find a natural set of pure integrals designed to match this subset of leading singularities. We will find that boldly summing over all such objects miraculously suffices to match the full integrand! In particular, while the pure integrals are motivated for a large-enough generic number of external particles, their degenerations nicely produce all the needed lower-point objects as well.

This method is heuristic—we do not yet have a deep understanding for why the miracles happen. However we have used this strategy successfully to find stunningly simple expressions for the integrands of all 2- and 3-loop MHV amplitudes as well as all 2-loop NMHV amplitudes, and have checked that the results are correct by comparing with the form obtained from the all-loop BCFW recursion discussed in the next chapter.

We will begin by illustrating this strategy by going back to 1-loop integrands, which will motivate structures for 1-loop integrands different from the ones we encountered in section 3. For the MHV integrand, this new form coincides with one of “polytope representations” discussed in [37]. We will then use this discussion as a springboard to our treatment of 2- and 3-loop integrands.

I. A New Form for the MHV 1-Loop Integrand

Let’s begin by going back to the MHV 1-loop integrand, and motivate a new form for it inspired by straightforwardly matching its leading singularities, associated with the familiar two-mass-easy colored diagrams



corresponding to cutting the propagators

$$\langle AB\ i-1\ i\rangle\langle AB\ i\ i+1\rangle\langle AB\ j-1\ j\rangle\langle AB\ j\ j+1\rangle \quad (1.5.67)$$

The amplitude has unit leading singularity for the first solution of the Schubert problem $(AB) = (ij)$, and vanishing leading singularity for the second solution where $(AB) = (i-1\ i\ i+1) \cap (j-1\ j\ j+1)$. We would like to build the integrand out of objects that have exactly this property. To beat a dead horse yet again—it is obvious that the two-mass-easy box does not do this job because it is not chiral. The easiest way to do this is to simply insert a factor in the numerator, $\langle AB\ (i-1\ i\ i+1) \cap (j-1\ j\ j+1)\rangle$, that kills the “wrong” leading singularity. For correct little-group weights, we add a factor $\langle AB\ X\rangle$ in the denominator, where X is an arbitrary bitwistor, and look at an object of the form

$$I_{i,j} = \frac{\langle AB\ (i-1\ i\ i+1) \cap (j-1\ j\ j+1)\rangle\langle X\ i\ j\rangle}{\langle AB\ i-1\ i\rangle\langle AB\ i\ i+1\rangle\langle AB\ j-1\ j\rangle\langle AB\ j\ j+1\rangle\langle AB\ X\rangle} \quad (1.5.68)$$

which is just the pentagon already familiar from section 2, where the local propagator $\langle AB\ n\ 1\rangle$ has been replaced by $\langle AB\ X\rangle$. We denote this graphically as

(1.5.69)

Note that there is in general no significance to the presence of the legs adjacent to X in this picture. We draw it in this way because in the special case where $X = (k, k+1)$, the legs adjacent to X are identified with $k, k+1$.

Now consider the Schubert problems associated with cutting four physical propagators. By construction this object has vanishing leading singularities on the “wrong” solution, and can easily be seen to have unit leading singularity on the “right” one. Summing over all the indices $i < j$ —with $|i - j| \geq 2$ corresponding to the two-mass easy colored graphs—produces an object matching all the physical leading singularities of the amplitude. Naïvely this should give us the integrand, but there is a catch: each term also has “spurious cuts” where $\langle AB X \rangle$ is one on the cut propagators. Indeed, the sum we just described does not match the integrand.

However some wonderful magic happens: the sum over *all* indices $i < j$, including a “boundary term” with $j = i+1$, which is not included in the sum over colored graphs, *does* reproduce the amplitude! We have

$$A_{\text{MHV}}^{1\text{-loop}} = \sum_{i < j} \frac{\langle AB (i-1, i, i+1) \cap (j-1, j, j+1) \rangle \langle X i j \rangle}{\langle AB X \rangle \langle AB i-1 i \rangle \langle AB i i+1 \rangle \langle AB j-1 j \rangle \langle AB j j+1 \rangle} \quad (1.5.70)$$

or written pictorially

$$\mathcal{A}_{\text{MHV}}^{1\text{-loop}} = \sum_{i < j < i} \left\{ \begin{array}{c} \text{Diagram (1.5.69)} \end{array} \right\} . \quad (1.5.71)$$

This form is manifestly cyclic but has spurious $\langle AB X \rangle$ poles term-by-term. The sum is however independent of X . If we choose X to correspond to one of the external point $X = (k, k+1)$, all the poles are manifestly physical but the formula is not manifestly cyclic invariant.

As mentioned above, this expression follows from a simple “polytope” interpretation described in [37]. The local formula given in [65] is obtained by choosing

$X = k k+1$, summing over all k and dividing by $1/n$. The similar expression in [79] corresponds to setting $X = I_\infty$ where I_∞ is infinity twistor.

Let us look at the “boundary term” where $j = i + 1$ in more detail—using $\langle i-1 i i+1 i+2 \rangle \langle AB i i+1 \rangle = \langle AB (i-1 i i+1) \cap (i i+1 i+2) \rangle$, we can see that it is just a (spurious) box

$$\frac{\langle i-1 i i+1 i+2 \rangle \langle X i i+1 \rangle}{\langle AB X \rangle \langle AB i-1 i \rangle \langle AB i i+1 \rangle \langle AB i+1 i+2 \rangle} \quad (1.5.72)$$

It is instructive to explicitly understand the purpose of this boundary term in this simple example, since the same phenomenon will occur in all the rest of our examples in this section. Let us return to our most naïve ansatz, summing only over the pentagons associated with the colored graphs. Each of the spurious cuts involving $\langle AB X \rangle$, such as

$$\langle AB X \rangle \langle AB i-1 i \rangle \langle AB i i+1 \rangle \langle AB j-1 j \rangle \quad (1.5.73)$$

is shared by two pentagons e.g. $I_{i,j-1}$ and $I_{i,j}$. For generic terms in the sum, these cuts cancel against each other in pairs. However, in the limiting cases when $j = i+2$ (or $j = i-2$) the quad-cut is shared by $I_{i,i+2}$ and $I_{i-1,i+1}$ but there is no cancelation between them because the non-vanishing leading singularities occur for two different solutions of the Schubert problems. The spurious box of (1.5.72) precisely has non-vanishing leading singularities for these two Schubert problems and completes the cancelation of all $\langle AB X \rangle$ poles, ensuring the full sum is independent of X . It is quite remarkable that the “new” object needed to fix the leading singularities and match the amplitude is simply a degeneration of the pentagon itself.

In our remaining examples, we will not delve into understanding the details of how all leading singularities match. We will instead take a class of leading singularities as a guide for the local integrals to consider, and sum over all the relevant objects, including boundary terms that do not directly correspond to any of the leading singularity pictures that motivated the construction of the objects to begin with. These formulae are then verified by comparing with the integrand as computed by BCFW recursion.

Let us finally note a very pretty property of equation (1.5.70): for generic X , all the pentagons in the double sum are manifestly manifestly IR finite. This ceases to be true if we make the special choice like $X = (12)$, since the diagrams with $i = 2$ or $j = n$ have an additional massless corner which is not controlled by the numerator.

$$\begin{array}{ccc}
 \begin{array}{c} 4 \quad i-1 \\ \vdots \\ \text{---} \\ \vdots \\ 3 \quad i \\ \vdots \\ 2 \quad \vdots \quad X \quad \vdots \quad i+1 \end{array} & \xrightarrow{X = (12)} & \begin{array}{c} 4 \quad i-1 \\ \vdots \\ \text{---} \\ \vdots \\ 3 \quad i \\ \vdots \\ 2 \quad \vdots \quad 1 \quad \vdots \quad i+1 \end{array}
 \end{array} \tag{1.5.74}$$

II. The 1-Loop NMHV Integrand, Revisited

We proceed to use the same strategy to determine a local expression for the NMHV 1-loop integrand, which will yield a quite different form than we obtained in section 3. We again start with the colored graphs for leading singularities. There are two of them for NMHV amplitudes:

$$\begin{array}{ccc}
 \begin{array}{c} \vdots \\ \text{---} \\ \text{---} \\ \text{---} \\ \vdots \\ j \end{array} & \text{and} & \begin{array}{c} \vdots \\ \text{---} \\ \text{---} \\ \text{---} \\ \vdots \\ j+1 \end{array}
 \end{array} \tag{1.5.75}$$

Unlike the MHV case where the non-vanishing leading singularities were “1”, here the non-vanishing leading singularities are the R -invariants. The goal is to find objects with non-vanishing support on the same Schubert problems as the amplitude, and decorate these with the appropriate R -invariants to get a nice ansatz for the integrand.

The first colored graph correspond to 2-mass easy Schubert problems and have the same structure as the MHV case. The leading singularity is just the tree-level amplitude appearing in the upper-left corner of the figure, $\mathcal{A}_{\text{NMHV}}^{\text{tree}}(j, j+1, \dots, i-1, i)$. Thus we expect to have objects in the integrand of the form

$$\sum_{i < j < i} \left\{ \begin{array}{c} \vdots \\ \text{---} \\ \text{---} \\ \text{---} \\ \vdots \\ j \end{array} \times \mathcal{A}_{\text{NMHV}}^{\text{tree}}(j, j+1, \dots, i-1, i) \right\} \tag{1.5.76}$$

Finding an object matching the physical leading singularities of the second class

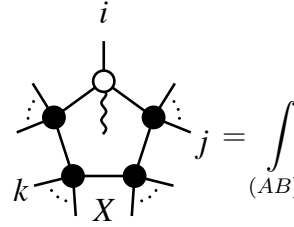
of colored diagrams is a more interesting exercise. The cut propogators are

$$\langle AB i-1 i \rangle \langle AB i i+1 \rangle \langle AB j j+1 \rangle \langle AB k k+1 \rangle \quad (1.5.77)$$

The leading singularities vanish for the solution

$(AB) = (i-1 i i+1) \cap (j j+1)(i-1 i i+1) \cap (k k+1)$, while for $(AB) = (i j j+1) \cap (i k k+1)$ the leading singularity is $[i, j, j+1, k, k+1]$.

Let us consider objects of the form

$$I_{i,j,k} \equiv \int_{(AB)} \frac{N(i, j, k)}{\langle AB X \rangle \langle AB i-1 i \rangle \langle AB i i+1 \rangle \langle AB j j+1 \rangle \langle AB k k+1 \rangle}$$


We are searching for a numerator supported on the same leading singularities as the amplitude. In addition it should also have unit leading singularity on all other spurious quad-cuts. The reason is that the spurious cuts must cancel in a sum over terms; since the integrals are multiplied by different R -invariants, the only way this can happen is through residue theorem 6-term identities between the R -invariants. For instance the spurious quad-cut

$$\langle AB X \rangle \langle AB i i+1 \rangle \langle AB j j+1 \rangle \langle AB k k+1 \rangle \quad (1.5.78)$$

is shared by six different integrals $I_{i,j,k}$, $I_{i+1;j,k}$, $I_{j;i,k}$, $I_{j+1;i,k}$, $I_{k;i,j}$ and $I_{k+1;i,j}$ that are multiplied by six different residues. There is a 6-term identity relating them

$$[i, j, j+1, k, k+1] + [i+1, j, j+1, k, k+1] + [j, i, i+1, k, k+1] \\ + [j+1, i, i+1, k, k+1] + [k, i, i+1, j, j+1] + [k+1, i, i+1, j, j+1] = 0$$

which can only possibly be of help in canceling spurious cuts if the integrands they multiply have support on the same Schubert problems, with unit leading singularities.

There is one final guiding principle for determining the structure of the numerator $N(i, j, k)$. The topologies occurring in (1.5.76) are the same as for the MHV amplitude, while the second class of integrals is “purely” NMHV-like. Since IR-divergences are universal, it would be nice if the IR-divergences could be completely isolated in the MHV-like topology. We should then try to choose the numerator $N(i, j, k)$ to be

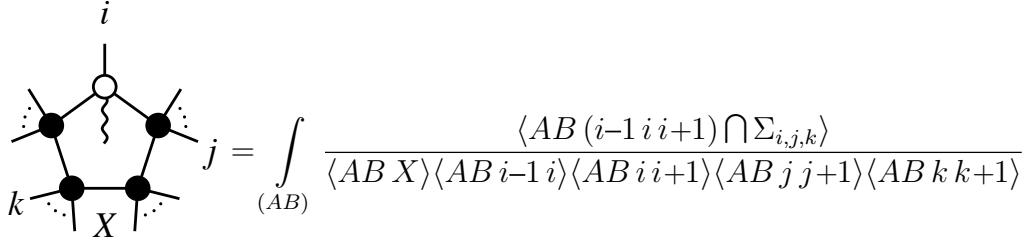
strictly finite. It would be nice if these integrals could be chosen to be manifestly finite. The only divergence in (1.5.78) can come from the Z_i -corner, *i.e.* the region when (AB) crosses point Z_i and lies in the plane $(i-1\ i\ i+1)$. In order to control this region the numerator should be of the form $N = \langle AB\ (i-1\ i\ i+1) \cap (\dots) \rangle$. Combined with the unit leading singularity constraint, the form of the numerator is fixed completely:

$$N(i, j, k) \equiv \langle AB\ (i-1\ i\ i+1) \cap \Sigma_{i,j,k} \rangle \quad (1.5.79)$$

with $\Sigma_{i,j,k}$ a special plane defined according to

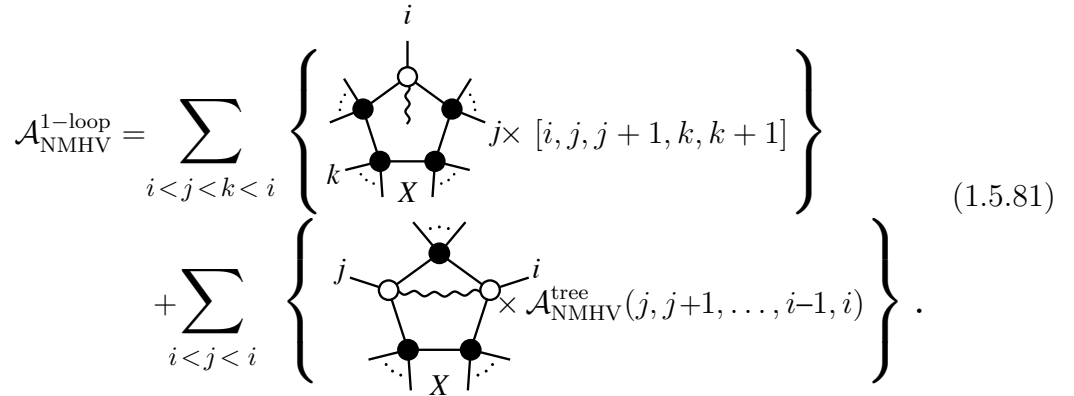
$$\Sigma_{i,j,k} \equiv \frac{1}{2} [(j\ j+1\ (i\ k\ k+1) \cap X) - (k\ k+1\ (i\ j\ j+1) \cap X)] \quad (1.5.80)$$

This is in fact the only choice we could have made consistent with little group weights and the desire to treat the j, k indices symmetrically. We will denote this by,



$$\text{Diagram} = \int_{(AB)} \frac{\langle AB\ (i-1\ i\ i+1) \cap \Sigma_{i,j,k} \rangle}{\langle AB\ X \rangle \langle AB\ i-1\ i \rangle \langle AB\ i\ i+1 \rangle \langle AB\ j\ j+1 \rangle \langle AB\ k\ k+1 \rangle}$$

With these objects in hand, we once again brazenly sum over all ranges of indices, including “boundary” terms with $j = i \pm 1$ not directly associated with colored graphs for leading singularities. The same magic happens as we saw in the MHV case—this sum agrees with the 1-loop NMHV amplitude as computed by BCFW recursion, and we find,



$$\mathcal{A}_{\text{NMHV}}^{1\text{-loop}} = \sum_{i < j < k < i} \left\{ \text{Graph} \times [i, j, j+1, k, k+1] \right\} + \sum_{i < j < i} \left\{ \text{Graph} \times \mathcal{A}_{\text{NMHV}}^{\text{tree}}(j, j+1, \dots, i-1, i) \right\}. \quad (1.5.81)$$

Note also that as in the MHV case, the only IR-divergent integrals are in the boundary terms. The (generically) finite integrals for $I_{i,j,k}$ are given by

$$I_{i,j,k} = -\text{Li}_2(1 - u_1) - \text{Li}_2(1 - u_2) + \text{Li}_2(1 - u_3) + \log(u_4) \log(u_5)$$

where the cross ratios are defined as:

$$u_1 \equiv \frac{\langle i i+1 j j+1 \rangle \langle X i-1 i \rangle}{\langle i i+1 X \rangle \langle j j+1 i-1 i \rangle}, \quad u_2 \equiv \frac{\langle i i+1 X \rangle \langle k k+1 i-1 i \rangle}{\langle i i+1 k k+1 \rangle \langle X i-1 i \rangle}, \quad u_3 \equiv \frac{\langle i i+1 j j+1 \rangle \langle k k+1 i-1 i \rangle}{\langle i i+1 k k+1 \rangle \langle j j+1 i-1 i \rangle},$$

$$u_4 \equiv \frac{\langle X k k+1 \rangle \langle i-1 i j j+1 \rangle}{\langle X i-1 i \rangle \langle k k+1 j j+1 \rangle}, \quad u_5 \equiv \frac{\langle j j+1 X \rangle \langle k k+1 i i+1 \rangle}{\langle j j+1 k k+1 \rangle \langle X i i+1 \rangle},$$

Finally, let us examine the 1-loop NMHV ratio function

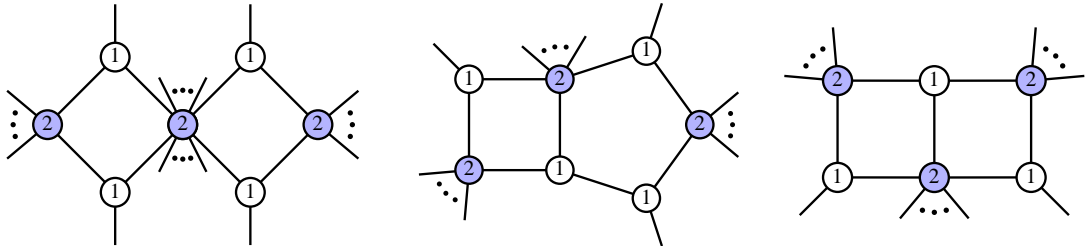
$$\mathcal{R}_{\text{NMHV}}^{1\text{-loop}} = \mathcal{A}_{\text{NMHV}}^{1\text{-loop}} - \mathcal{A}_{\text{MHV}}^{1\text{-loop}} \cdot \mathcal{A}_{\text{NMHV}}^{\text{tree}} \quad (1.5.82)$$

Comparing the expressions (1.5.70) and (1.5.81) we can see that the ratio function has the same form as NMHV amplitude, except that in the first sum we have $\mathcal{A}_{\text{NMHV}}^{\text{tree}}(i, i+1, \dots, j-1, j) - \mathcal{A}_{\text{NMHV}}^{\text{tree}}$ instead of just $\mathcal{A}_{\text{NMHV}}^{\text{tree}}(i, i+1, \dots, j-1, j)$. The manifest finiteness is obvious. The only divergent integrals are in the boundary term $j = i-1$, but their coefficient is given by $\mathcal{A}_{\text{NMHV}}^{\text{tree}}(i, i+1, \dots, j-1, j) - \mathcal{A}_{\text{NMHV}}^{\text{tree}}(1, \dots, n) = \mathcal{A}_{\text{NMHV}}^{\text{tree}}(i, i+1, \dots, i-2, i-1) - \mathcal{A}_{\text{NMHV}}^{\text{tree}}(1, \dots, n) = 0$. Therefore, the ratio function can be written only using manifestly finite integrals.

III. The 2-Loop MHV Amplitude and Its Logarithm

Now we turn to the 2-loop case. First we reproduce the MHV amplitude presented already in [65] and in addition we will write an expression for the log of the amplitude given in an interesting form in terms of non-planar diagrams.

We again start with the possible colored graphs,



$$(1.5.83)$$

There are more types of graphs in comparison to 1-loop where we had only boxes. In addition to two glued boxes (also referred to as “kissing boxes”) we have other

$$\mathcal{A}_{\text{MHV}}^{2\text{-loop}} = \frac{1}{2} \sum_{i < j < k < l < i} \text{Diagram} \quad (1.5.84)$$

The “boundary terms” in this case occur for for $j = i+1$ and/or $l = k+1$. In these cases the numerator exactly cancels one of the propagators, leaving us with:¹⁰

$$\text{Diagram 1} + \text{Diagram 2} + \text{Diagram 3} \quad (1.5.85)$$

Log of the Amplitude

Finally, we give an interesting new expression for the logarithm of the amplitude, using a non-planar sum of the same set of objects. At 2-loops, the log of the amplitude is

$$[\log \mathcal{A}]_{\text{MHV}}^{2\text{-loop}} = \left[\mathcal{A}_{\text{MHV}}^{2\text{-loop}} - \frac{1}{2} \left(\mathcal{A}_{\text{MHV}}^{1\text{-loop}} \right)^2 \right] \quad (1.5.86)$$

A beautiful expression for the log of the amplitude is made possible by the existence of a simple relation between the sum of 1-loop square and 2-loop diagrams:

$$\sum_{i < j} \text{Diagram AB} \times \sum_{k < l} \text{Diagram CD} = \sum_{\substack{i < j \\ k < l}} \text{Diagram} \quad (1.5.87)$$

The left-hand side is just $(\mathcal{A}_{\text{MHV}}^{1\text{-loop}})^2$ while the right-hand side contains not only the planar diagrams present in $\mathcal{A}_{\text{MHV}}^{2\text{-loop}}$ but also non-planar graphs when for example $i < k < j < l$. In fact, all planar graphs are equal to $2\mathcal{A}_{\text{MHV}}^{2\text{-loop}}$ while all non-planar graphs give us the log of the amplitude in the form

¹⁰This simplification was missed in Chapter [65], and the 2-loop MHV integrand was presented as a sum over three terms. We would like to thank Johannes Henn for pointing the simplification out to us.

$$[\log \mathcal{A}]_{\text{MHV}}^{2\text{-loop}} = - \sum_{i < k < j < l < i} \text{Diagram} \quad (1.5.88)$$

The formula found in [66] is the 4pt version of this expression.

Note that naïvely, all these integrals are IR finite because each individual 1-loop sub-integral is just a finite pentagon (which can not shrink to a box due to the restriction $j \neq i + 1$ and $l \neq k + 1$). However, the criteria for finiteness we described in section 4 applies to planar integrals, while the log contains non-planar terms which can be IR-divergent.

Let us focus on the piece of the integrand of the form

$$\frac{\langle ABX \rangle}{\langle ABi-1i \rangle \langle ABii+1 \rangle} \cdot \frac{1}{\langle ABCD \rangle} \cdot \frac{\langle CDY \rangle}{\langle CDj-1j \rangle \langle CDjj+1 \rangle} \quad (1.5.89)$$

Here X controls the IR-divergence of the region where the line (AB) intersects point Z_i and lies in the plane $(Z_{i-1}Z_iZ_{i+1})$, just as Y does for (CD) sector. However, if $i = j$ then (AB) and (CD) intersect in the point i and the propagator $\langle ABCD \rangle$ vanishes. Therefore, finiteness of the 1-loop sub-integrals is not enough. We need an extra condition that regulates this joint divergence. It is not hard to see that unless $\langle XY \rangle = 0$, a (mild) IR-divergence remains.

As a result, we can find that almost all integrals in (1.5.88) are finite except for the class of diagrams:

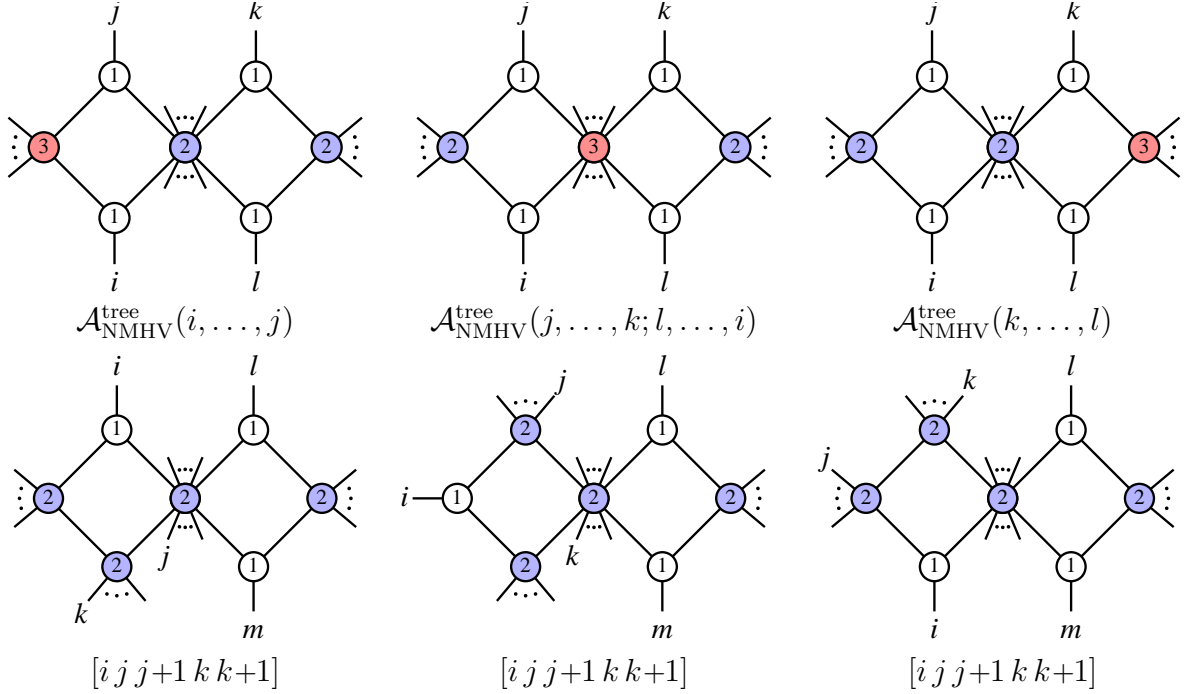
$$\text{Diagram} \quad (1.5.90)$$

In this case $X = (i-2i-1i) \cap (ii+1i+2)$ and $Y = (i-1ii+1) \cap (j-1jj+1)$, so $\langle XY \rangle \neq 0$. However the divergence is mild, as observed in the 4-point result of [66].

IV. All 2-Loop NMHV Amplitudes

We move on to present the integrand for all 2-loop NMHV amplitudes. Instead of a brute-force expansion into a basis of integrals, we follow the same strategy outlined above, obtaining results vastly simpler than those presented to date, which also generalize to all n .

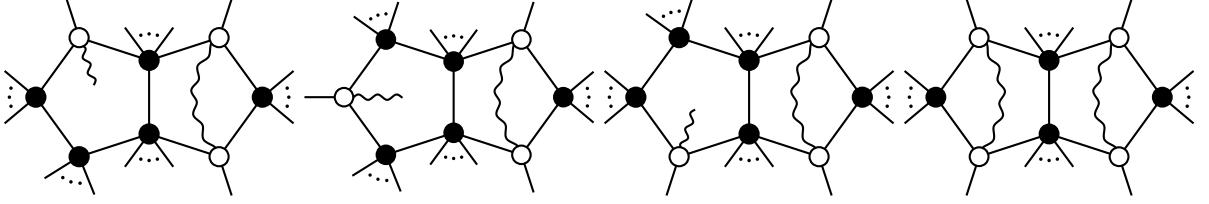
Let us first start by drawing the colored-graphs that contribute for general 2-loop NMHV amplitude that do not cut the internal propagator $\langle(ABCD)\rangle$.



Below each colored graph, we have indicated the leading singularity below each. Notice that the coefficient $\mathcal{A}_{\text{NMHV}}^{\text{tree}}(j, \dots, k; l, \dots, i)$ is the *same* function as an ordinary tree amplitude with particles labelled $(j, \dots, k; l, \dots, i)$ where k, l and i, j are both treated as if they were adjacently-labelled.

The idea is again to find a set of integrals that each individually have the same leading singularities as the amplitude on a given set of octa-cuts. The first step is to realize that the octa-cuts on the first line of (1.5.91) respectively looks like the product of NMHV 1-loop quad-cut \times MHV 1-loop quad-cut and MHV 1-loop quad-cuts \times MHV 1-loop quad-cuts. Therefore, one might think that the right integrals to start with look like the product of pentagons that appear in MHV and NMHV 1-loop amplitudes. This strategy worked perfectly in the MHV 2-loop case, where the

amplitude was literary made from double-pentagons whose origin was in the product of two MHV-like pentagons. So the natural objects to consider here are the same double-pentagons as in MHV 2-loop case and also other double-pentagons that look like NMHV 1-loop \times MHV 1-loop:



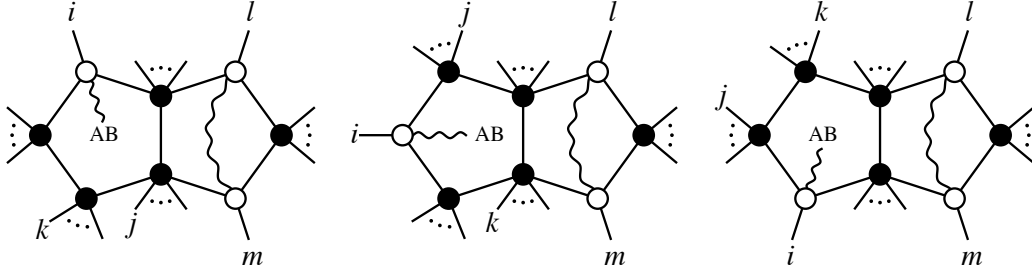
The numerators of the first three graphs have the same structure as the ones that appear in the NMHV 1-loop integrand. We provide the complete expressions in appendix A.

Note that first three diagrams are really represented just by single diagram with permuted indices. For instance, the second one can be obtained from the first one if we require $k > i$. So, it is non-planar version of the first graph in the same sense as we saw in the last subsection in the case of the log of MHV amplitude. We see that these four graphs are in one-to-one correspondence with the first four colored graphs in 1.5.91. If we cut all propagators except $\langle ABCD \rangle$ we get not only the same cuts as are in these colored graphs, but also the support on the correct Schubert problems. These integrals are definitely the right ones to start with. In order to get the correct field theory answer we have to multiply them by the leading singularities of corresponding octa-cuts which are

Now summing over all allowed indices we get,

$$\begin{aligned}
 & \sum_{\substack{\text{all allowed} \\ i,j,k,l,m}} \text{Diagram 1} + \frac{1}{2} \sum_{i < j < k < l < i} \text{Diagram 2} \\
 & \times [i, j, j+1, k, k+1] \\
 & \times \left\{ \begin{aligned} & \mathcal{A}_{\text{NMHV}}^{\text{tree}}(j, \dots, k; l, \dots, i) \\ & + \mathcal{A}_{\text{NMHV}}^{\text{tree}}(i, \dots, j) \\ & + \mathcal{A}_{\text{NMHV}}^{\text{tree}}(k, \dots, l) \end{aligned} \right\} \quad (1.5.91)
 \end{aligned}$$

where the first diagram really represents three as we mentioned earlier, namely, the complete set of cyclically ordered figures



The rest of the story proceeds in the by now familiar way. Simply carrying out the sum over the range of indices corresponding to the colored graphs does not give the right answer, however, a judicious choice for the range of summation adds the correct “boundary terms” to give exactly the right answer, and we finally obtain:

$$\begin{aligned}
 \mathcal{A}_{\text{NMHV}}^{2\text{-loop}} = & \sum_{\substack{i < j < l < m \leq k < i \\ i < j < k < l < m \leq i \\ i \leq l < m \leq j < k < i}} \text{Diagram 1} + \frac{1}{2} \sum_{i < j < k < l < i} \text{Diagram 2} \\
 & \times [i, j, j+1, k, k+1] \times \left\{ \begin{aligned} & \mathcal{A}_{\text{NMHV}}^{\text{tree}}(j, \dots, k; l, \dots, i) \\ & + \mathcal{A}_{\text{NMHV}}^{\text{tree}}(i, \dots, j) \\ & + \mathcal{A}_{\text{NMHV}}^{\text{tree}}(k, \dots, l) \end{aligned} \right\} \quad (1.5.92)
 \end{aligned}$$

These two terms represent the general 2-loop NMHV amplitude for any number of external particles. The explicit forms of the integrals in term of momentum-twistors are presented in appendix 1.

V. All 3-Loop MHV Amplitudes

Finally, we present the integrand for all 3-loop MHV amplitudes. These amplitudes were studied in the past, the 4pt formula for the integrand was given in [80] and the 5pt in [81]. However once again our new strategy will both yield vastly simpler expressions for these integrands and also generalize to all n .

We begin as always by drawing the colored graphs that contribute to general 3-loop amplitude. While there are a large number of them, our experience with the 2-loop NMHV calculation tells us that for the purpose of “translating” the graphs into

the integrals, one needs to focus on the colored graphs without internal propagators. There are just two of these:

$$(1.5.93)$$

The colored graphs suggest that the correct 3-loop integral must correspond to “gluing” together three 1-loop MHV integrals. But these can not be just pentagons because of number of internal propagators, we would also need hexagons. Fortunately, in the “polytope picture” of [37], the most natural form of MHV amplitude *is* written using hexagons. We leave the detailed exploration of this gluing procedure to future work. It suffices to say that we can indeed find objects which have support on the correct leading dodecacuts (1.5.93). Having identified them, the magic happens again: to get the full 3-loop amplitude, we need only to identify the correct ranges for the summations involved. As a result, we can write the general 3-loop MHV amplitude for any number of external particles as a sum of two structures,

$$\mathcal{A}_{\text{MHV}}^{3\text{-loop}} = \frac{1}{3} \sum_{\substack{i_1 \leq i_2 < j_1 \leq \\ \leq j_2 < k_1 \leq k_2 < i_1}} \text{[Graph 1]} + \frac{1}{2} \sum_{\substack{i_1 \leq j_1 < k_1 < \\ < k_2 \leq j_2 < i_2 < i_1}} \text{[Graph 2]}$$

The explicit formulas for these graphs with all numerator factors are given in the appendix B.

Chapter 2

Recursion Relations for the Loop Integrand

2.1 The Loop *Integrand* for $\mathcal{N} = 4$ SYM Amplitudes

The BCFW recursion relations [14, 50, 82, 83] presented extremely compact expressions for tree amplitudes using building blocks with both local and non-local poles. In a parallel development, an amazing hidden symmetry of planar $\mathcal{N} = 4$ SYM—dual conformal invariance—was noticed first in multi-loop perturbative calculations [59] and then at strong coupling [84], leading to a remarkable connection between null-polygonal Wilson loops and scattering amplitudes [57, 84–92]. It was quickly realized that the BCFW form of the tree amplitudes manifested both full superconformal and *dual* superconformal invariance, which together close into an infinite-dimensional Yangian symmetry algebra [93]. Understanding the role of this remarkable integrable structure in the full quantum theory, however, was clouded by the IR-divergences that appear to almost completely destroy the symmetry at loop-level, leaving only the anomalous action of the (Bosonic) dual conformal invariance [77, 78, 94, 95].

I. Grassmannian Duality for Leading Singularities

In [16], a strategy for making progress on these questions was suggested. The idea was to find objects closely associated with scattering amplitudes which are completely free of IR-divergences; the action of the symmetries would be expected to be manifest on such objects, and they would provide “data” that might be the output of a putative dual theory of the S-Matrix.

The leading singularities of scattering amplitudes are precisely objects of this sort. Thinking of loop amplitudes as multi-dimensional complex integrals, leading singularities arise from performing the integration not on the usual non-compact ‘contours’

over all real loop-momenta, but on compact contours ‘encircling’ isolated (and generally complex) poles in momentum space. As such, they are free of IR-divergences and well-defined at any loop order, yielding algebraic functions of the external momenta. Leading singularities were known to have strange inter-relationships and satisfy mysterious identities not evident in their field-theoretic definition. Morally they are also expected to be Yangian-invariant, although even this is not completely manifest¹. Thus leading singularities seem to be prime candidates for objects to be understood and computed by a dual theory.

Such a duality was proposed in [16], connecting leading singularities of color-stripped, n -particle N^k MHV scattering amplitudes in $\mathcal{N} = 4$ SYM to a simple contour integral over the Grassmannian $G(k, n)$:

$$\mathcal{Y}_{n,k}(\mathcal{Z}) = \frac{1}{\text{vol}(GL_k)} \int \frac{d^{k \times n} C_{\alpha a}}{(1 \cdots k)(2 \cdots k+1) \cdots (n \cdots k-1)} \prod_{\alpha=1}^k \delta^{4|4}(C_{\alpha a} \mathcal{Z}_a). \quad (2.1.1)$$

Here $a = 1, \dots, n$ labels the external particles, and \mathcal{Z}_a are variables in $\mathbb{CP}^{3|4}$. The original formulation of this object worked with twistor variables $\mathcal{W}_a = (W_a | \tilde{\eta}_a)$, and was given as $\mathcal{L}_{n,k+2}(\mathcal{W}) = \mathcal{Y}_{n,k+2}(\mathcal{W})$. This was quickly realized [18] to be completely equivalent to a second form in *momentum* twistor space [17], with $\mathcal{L}_{n,k+2}(\lambda, \tilde{\lambda}, \tilde{\eta}) = M_{\text{MHV}}^{\text{tree}} \times \mathcal{Y}_{n,k}(\mathcal{Z})$. Here the variables $\mathcal{Z}_a = (Z_a | \eta_a)$ are the ‘‘momentum-twistors’’ introduced by Hodges [60], which are the most natural variables with which to discuss *dual* superconformal invariance. Furthermore, these momentum twistors are simple algebraic functions of the external momenta, upon which scattering amplitudes conventionally depend².

Since the Grassmannian integral is invariant under both ordinary and dual superconformal transformations, it enjoys the full Yangian symmetry of the theory, as

¹Indeed we will give a proof of this basic fact in the next section.

²To quickly establish notation and conventions, the momentum of particle a is given by $p_a^\mu = x_{a+1}^\mu - x_a^\mu$, and the point x_a^μ in the dual co-ordinate space is associated with the line $(Z_{a-1} Z_a)$ in the corresponding momentum-twistor space. This designation ensures that the lines $(Z_{a-1} Z_a)$ and $(Z_a Z_{a+1})$ intersect, so that correspondingly, $x_{a+1}^\mu - x_a^\mu = p_a$ is null. (Bosonic) dual-conformal invariants are made with 4-brackets $\langle a b c d \rangle = \epsilon_{IJKL} Z_a^I Z_b^J Z_c^K Z_d^L$. An important special case is $\langle i-1 i j-1 j \rangle = \langle i-1 i \rangle \langle j-1 j \rangle (x_j - x_i)^2$; 2-brackets $\langle ij \rangle$ are computed using the upper-two components of Z_i, Z_j and cancel out in dual-conformal expressions. For more detail see [17, 18, 60].

has been proven more directly in [96]. In fact, it has been argued that these contour integrals in $G(k, n)$ generates *all* Yangian invariants.³ [74, 99].

Leading singularities are associated with residues of the Grassmannian integral. Residue theorems [71] imply many non-trivial and otherwise mysterious linear relations between leading singularities. These relations are associated with important physical properties such as locality and unitarity [16].

Further investigations [35] identified a new principle, the Grassmannian “particle interpretation”, which determines the correct contour of integration yielding the BCFW form of tree amplitudes [100]. Quite remarkably, a deformation of the integrand connects this formulation to twistor string theory [19, 35, 101]. Furthermore, another contour deformation produces the CSW expansion of tree amplitudes [34], making the emergence of local space-time a derived consequence from the more primitive Grassmannian starting point.

The Grassmannian integral and Yangian-invariance go hand-in-hand and are essentially synonymous; indeed, the Grassmannian integral is the most concrete way of thinking about Yangian invariants, since not only the symmetries but also the non-trivial relationship between different invariants are made manifest; even connections to non-manifestly Yangian-invariant but important physical objects (such as CSW terms) are made transparent.

Given these developments, we are encouraged to ask again: is there an analogous structure underlying not just the leading singularities but the full loop amplitudes? Does Yangian-invariance play a role? And if so, how can we see this through the thicket of IR-divergences that appear to remove almost all traces of these remarkable symmetries in the final amplitudes?

II. The Planar Integrand

Clearly, we need to focus again on finding well-defined objects associated with loop amplitudes. Fortunately, in *planar* theories, there is an extremely natural candidate: the loop *integrand* itself!

³The residues of $G(k, n)$ are Yangian-invariant for generic momenta away from collinear limits. See [97, 98] for important discussions of the fate of Yangian invariance in the presence of collinear singularities.

Now, in a general theory, the loop integrand is not obviously a well-defined object. Consider the case of 1-loop diagrams. Most trivially, in summing over Feynman diagrams, there is no canonical way of combining different 1-loop diagrams under the same integral sign, since there is no natural origin for the loop-momentum space. The situation is different in planar theories, however, and this ambiguity is absent. This is easy to see in the dual x -space co-ordinates [59]. The ambiguity in shifting the origin of loop momenta is nothing other than translations in x -space; but fixing the x_1, \dots, x_n of the external particles allows us to canonically combine all the diagrams. Alternatively, in a planar theory it is possible to unambiguously define the loop momentum common to all diagrams to be the one which flows from particle “1” to particle “2”.

At two-loops and above, we have a number of loop integration variables in the dual space x, y, \dots, z , and the well-defined loop integrand is completely symmetrized in these variables.

So the loop integrand is well-defined in the planar limit, and any dual theory should be able to compute it. All the symmetries of the theory should be manifest at the level of the integrand, only broken by IR-divergences in actually carrying out the integration—the symmetries of the theory are broken only by the choice of integration contour.

III. Recursion Relations for All Loop Amplitudes

Given that the integrand is a well-defined, rational function of the loop variables and the external momenta, we should be able to determine it using BCFW recursion relations in the familiar way⁴. At loop-level the poles have residues with different physical meaning. The first kind is the analog of tree-level poles and correspond to factorization channels. The second kind has no tree-level analog; these are single cuts whose residues are forward limits of lower-loop amplitudes. Forward limits are naïvely ill-defined operations but quite nicely they exist in any supersymmetric gauge theory, as was shown to one-loop level in [103]. There it was also argued that forward limits are well-defined to higher orders in perturbation theory in $\mathcal{N} = 4$ SYM. In

⁴We note that [102] have conjectured that the loop amplitudes can be determined by CSW rules, manifesting the superconformal invariance of the theory.

principle, this is all we need for computing the loop integrand in $\mathcal{N} = 4$ SYM to all orders in perturbation theory. However, our goal requires more than that. We would like to show that the integrand of the theory can be written in a form which makes all symmetries—the full Yangian—manifest. The Yangian-invariance of BCFW terms at tree-level becomes obvious once they are identified with residues of the Grassmannian integral, we would like to achieve the same at loop-level.

This is exactly what we will do in this chapter. We will give an explicit recursive construction of the all-loop integrand, in exact analogy to the BCFW recursion relations for tree amplitudes, making the full Yangian symmetry of the theory manifest.

The formulation also provides a new physical understanding of the meaning of loops, associated with simple operations for “removing” particles in a Yangian-invariant way. Loop amplitudes are associated with removing pairs of particles in an “entangled” way. We describe all these operations in momentum-twistor space, since this directly corresponds to familiar momentum-space loop integrals; presumably an ordinary twistor space description should also be possible.

As is familiar from the BCFW recursion relations at tree-level, the integrand is expressed as a sum over non-local terms, in a form very different than the familiar “rational function \times scalar integral” presentation that is common in the literature. Nonetheless, the Yangian-invariance guarantees that every term in the loop amplitude has Grassmannian residues as its leading singularities.

The integrands can of course be expressed in a manifestly-local form if desired, and are most naturally written in momentum-twistor space [62, 63]. As we will see, the most natural basis of local integrands in which to express the answer is not composed of the familiar scalar loop-integrals, but is instead made up of chiral tensor integrals with unit leading-singularities, which makes the physics and underlying structure much more transparent.

Of course the integrand is a well-defined rational function which is computed in four-dimensions without any regulators. The regularization needed to carry out the integrations is a very physical one, given by moving out on the Coulomb branch [67] of the theory. This can be beautifully implemented, both conceptually and in practice, with the momentum-twistor space representation of the integrand [62, 63].

Quite apart from the conceptual advantages of this way of thinking about loops,

our new formulation is also completely systematic and practical, taking the “art” out of the computation of multi-loop amplitudes in $\mathcal{N} = 4$ SYM. The result in this method served as a great source of data for the verification of the expressions for 2-loop and 3-loop amplitudes obtained in last chapter.

The structure of this chapter is following. In section 2.2, we describe a number of canonical operations on Yangian invariants—adding and removing particles, fusing invariants—that generate a variety of important physical objects in our story. In section 2.3 we describe the origin of Yangian-invariant loop integrals as arising from the “hidden entanglement” of pairs of removed particles. In section 2.4 we describe the main result of this Chapter: a generalization of the BCFW recursion relation to all loop amplitudes in the theory, and discuss some of its salient features through simple 1-loop examples.

2.2 Canonical Operations on Yangian Invariants

As a first step towards the construction of the all-loop integrand for $\mathcal{N} = 4$ SYM in manifestly Yangian form, we study simple operations that can map Yangian invariants $Y_{n,k}(\mathcal{Z}_1, \dots, \mathcal{Z}_n)$ to other Yangian invariants. In this discussion it will not matter whether the \mathcal{Z} 's represent variables in twistor-space or momentum-twistor space; we will simply be describing mathematical operations that mapping between invariants. Combining these operations in various ways yields many objects of physical significance. The same physical object will arise from different combinations of these operations in twistor-space vs. momentum-twistor space; we will content ourselves here by presenting mostly the momentum-twistor space representations.

As mentioned in the introduction, understanding these operations is not strictly necessary if we simply aim to find *a* formula for the integrand. The reason is that the BCFW recursion relations we introduce in section 2.4 can be developed independently for theories with less supersymmetry, which do not enjoy a Yangian symmetry. Our insistence in keeping the Yangian manifest however will pay off in two ways. The first is conceptual: the Yangian-invariant formulation will introduce a new physical picture for meaning of loops. The second is computational: the Yangian-invariant

formulation gives a powerful way to compute the novel “forward-limit” terms in the BCFW recursions in momentum-twistor space, using the Grassmannian language.

We will begin by discussing how to add and remove particles in a Yangian-invariant way. One motivation is an unusual feature of the Grassmannian integral—the space of integration depends on the number n of particles. It is natural to try and connect different n ’s by choosing a contour of integration that allows a “particle interpretation”, by which we mean simply that the variety defining the contour for the scattering amplitudes of $(n + 1)$ particles differs from the one for n particles only by specifying the extra constraints associated with the new particle [35]. Following this “add one particle at a time”-guideline completely specifies the contour for all tree amplitudes [19, 35], along the way exposing a remarkable connection with twistor string theory [?, 13, 101, 104, 105]. As we will see in this chapter, loops are associated with interesting “entangled” ways of *removing* particles from higher-point amplitudes. We will then move on to discuss how to “fuse” two invariants together. Using these operations we demonstrate the Yangian invariance of all leading singularities, and discuss the important special case of the “BCFW bridge” in some detail.

I. Adding Particles

Let us start with a general Yangian-invariant object

$$Y_{n,k}(\mathcal{Z}_1, \dots, \mathcal{Z}_n). \tag{2.2.2}$$

We will first describe operations that will add a particle to lower-point invariants to get higher-point invariants known as applying “inverse soft factors”, which are so named because taking the usual soft limit of the resulting object returns the original object. This can be done preserving k or increasing $k \mapsto k + 1$. We can discuss these in both twistor- and momentum-twistor space; for the purposes of this chapter we will describe these inverse-soft factor operations in momentum-twistor space.

The idea is that there are residues in $G(k, n)$ which are trivially related to residues in $G(k, n - 1)$ or $G(k - 1, n - 1)$. The k -preserving operation $Y_{n-1,k} \mapsto Y_{n,k}$ is particularly simple, being simply the identification

$$Y'_{n,k}(\mathcal{Z}_1, \dots, \mathcal{Z}_{n-1}, \mathcal{Z}_n) = Y_{n-1,k}(\mathcal{Z}_1, \dots, \mathcal{Z}_{n-1}); \tag{2.2.3}$$

that is, where we have simply added particle n as a label (but have not altered the functional form of Y in any way); thanks to the momentum-twistor variables, momentum conservation is automatically preserved. The k -increasing inverse soft factor is slightly more interesting. There is always a residue of $G(k, n)$ which has a C -matrix of the form

$$\begin{pmatrix} * & * & 0 & \cdots & 0 & * & * & 1 \\ * & \cdots & \cdots & \cdots & \cdots & \cdots & * & 0 \\ \vdots & \ddots & \ddots & \ddots & \ddots & \ddots & * & \vdots \end{pmatrix}. \quad (2.2.4)$$

Here, the non-zero elements in the top row, $* * * * 1$ correspond to particles $1, 2, (n-2), (n-1), n$, and we have generic non-zero entries in the lower $(k-1) \times (n-1)$ matrix. The corresponding residue is easily seen to be associated with

$$Y'_{n,k}(\dots, \mathcal{Z}_{n-1}, \mathcal{Z}_n, \mathcal{Z}_1, \dots) = [n-2 \ n-1 \ n \ 1 \ 2] \times Y_{n-1,k-1}(\dots, \widehat{\mathcal{Z}}_{n-1}, \widehat{\mathcal{Z}}_1, \dots) \quad (2.2.5)$$

where

$$[abcde] = \frac{\delta^{0|4}(\eta_a \langle bcde \rangle + \eta_b \langle cdea \rangle + \eta_c \langle deab \rangle + \eta_d \langle eabc \rangle + \eta_e \langle abcd \rangle)}{\langle abcd \rangle \langle bcde \rangle \langle cdea \rangle \langle deab \rangle \langle eabc \rangle} \quad (2.2.6)$$

is the basic ‘NMHV’-like R -invariant⁵ and the $\widehat{\mathcal{Z}}_{n-1,1}$ are deformed momentum twistor variables. The Bosonic components of the deformed twistors have a very nice interpretation: $\widehat{\mathcal{Z}}_1$ is simply the intersection of the line $(1 \ 2)$ with the plane $(n-2 \ n-1 \ n)$, which we indicate by writing $\widehat{\mathcal{Z}}_1 \equiv (n-2 \ n-1 \ n) \cap (1 \ 2)$; and $\widehat{\mathcal{Z}}_{n-1}$ is the intersection of the line $(n-2 \ n-1)$ with the plane $(1 \ 2 \ n)$, written $\widehat{\mathcal{Z}}_{n-1} \equiv (n-2 \ n-1) \cap (1 \ 2 \ n)$. Fully supersymmetrically, we have

$$\begin{aligned} \widehat{\mathcal{Z}}_1 &\equiv (n-2 \ n-1 \ n) \cap (1 \ 2) = \mathcal{Z}_1 \langle 2 \ n-2 \ n-1 \ n \rangle + \mathcal{Z}_2 \langle n-2 \ n-1 \ n \ 1 \rangle; \\ \widehat{\mathcal{Z}}_{n-1} &\equiv (n-2 \ n-1) \cap (n \ 1 \ 2) = \mathcal{Z}_{n-2} \langle n-1 \ n \ 1 \ 2 \rangle + \mathcal{Z}_{n-1} \langle n \ 1 \ 2 \ n-2 \rangle. \end{aligned} \quad (2.2.7)$$

II. Removing Particles

We can also remove particles to get lower-point Yangian invariants from higher-point ones. This turns out to be more interesting than the inverse-soft factor operation,

⁵When two sets of the twistors are consecutive, these “ R -invariants” are sometimes written $R_{r;s,t} \equiv [r \ s-1 \ s \ t-1 \ t]$. These invariants were first introduced in [57] in dual super-coordinate space.

though physically one might think it is even more straightforward. After all, we can remove a particle simply by taking its soft limit. However, while this is a well-defined operation on *e.g.* the full tree amplitude, it is *not* a well-defined operation on the individual residues (BCFW terms) in the tree amplitude. The reason is the presence of spurious poles: each term does not individually have the correct behavior in the soft limit.

Nonetheless, there *are* completely canonical and simple operations for removing particles in a Yangian-invariant way. One reduces $k \mapsto k - 1$, the other preserves k . The k -reducing operation removes particle n by integrating over its twistor coordinate

$$Y'_{n-1,k-1}(\mathcal{Z}_1, \dots, \mathcal{Z}_{n-1}) = \int d^{3|4} \mathcal{Z}_n Y_{n,k}(\mathcal{Z}_1, \dots, \mathcal{Z}_{n-1}, \mathcal{Z}_n). \quad (2.2.8)$$

This gives a Yangian-invariant for any closed contour of integration—meaning that under the Yangian generators for particles $1, \dots, n - 1$, this object transforms into a total derivative with respect to \mathcal{Z}_n . This statement can be trivially verified by directly examining the action of the level-zero and level-one Yangian generators on the integral. It is also very easy to verify directly from the Grassmannian integral. Note that depending on the contour that is chosen, a given higher-point invariant can in general map to several lower-point invariants.

The k -preserving operation “merges” particle n with one of its neighbors, $n - 1$ or 1 . For example,

$$Y'_{n-1,k}(\mathcal{Z}_1, \dots, \mathcal{Z}_{n-1}) = Y_{n,k}(\mathcal{Z}_1, \dots, \mathcal{Z}_{n-1}, \mathcal{Z}_n \mapsto \mathcal{Z}_{n-1}). \quad (2.2.9)$$

The Yangian-invariance of this operation is slightly less obvious to see by simply manipulating Yangian generators, but it can be verified easily from the Grassmannian formula.

We stress again that these operations are perfectly well-defined on *any* Yangian-invariant object, regardless of whether the standard soft-limits are well defined. Of course, they coincide with the soft limit when acting on *e.g.* the tree amplitude.

III. Fusing Invariants

Finally, we mention a completely trivial way of combining two Yangian invariants to produce a new invariant. Start with two invariants which are functions of a disjoint

set of particles, which we can label $Y_1(\mathcal{Z}_1, \dots, \mathcal{Z}_m)$ and $Y_2(\mathcal{Z}_{m+1}, \dots, \mathcal{Z}_n)$. Then, it is easy to see that the simple product

$$Y'(\mathcal{Z}_1, \dots, \mathcal{Z}_n) = Y_1(\mathcal{Z}_1, \dots, \mathcal{Z}_m) \times Y_2(\mathcal{Z}_{m+1}, \dots, \mathcal{Z}_n) \quad (2.2.10)$$

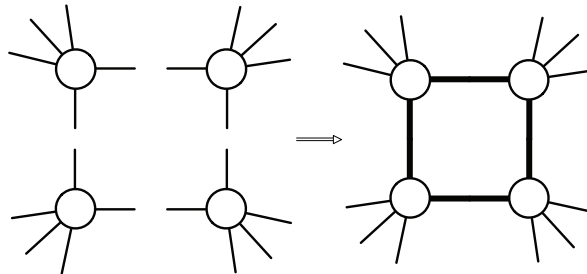
is also Yangian-invariant. Only the vanishing under the level-one generators requires a small comment. Note that the cross terms vanish because the corresponding level-zero generators commute and therefore the level-one generators cleanly splits into the smaller level-one generators.

IV. Leading Singularities are Yangian Invariant

Combining these operations builds new Yangian invariants from old ones; all of which have nice physical interpretations. An immediate consequence is a simple proof that all leading singularities are Yangian invariant. For this subsection only, we work in ordinary twistor space. Then we take any four Yangian invariants for disjoint sets of particles and we make a new invariant by taking the product of all of them,

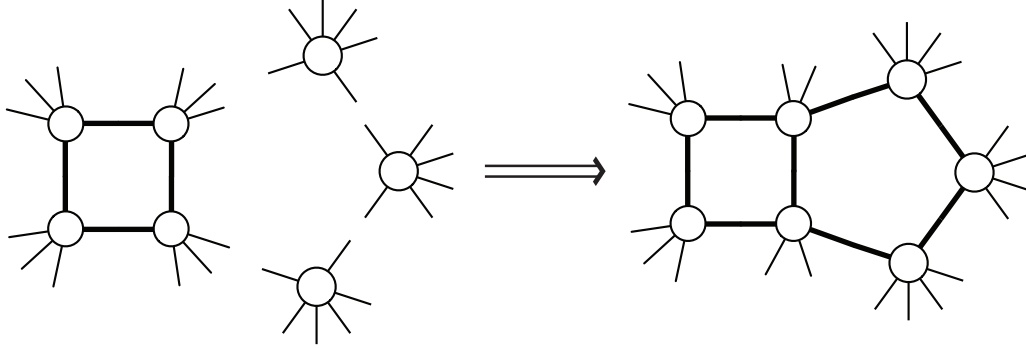
$$Y_1(\mathcal{W}_1, \dots, \mathcal{W}_m) Y_2(\mathcal{W}_{m+1}, \dots, \mathcal{W}_l) Y_3(\mathcal{W}_{l+1}, \dots, \mathcal{W}_p) Y_4(\mathcal{W}_{p+1}, \dots, \mathcal{W}_q).$$

We then “merge” m and $m+1$, l and $l+1$, p and $p+1$, and q with 1. We then integrate over m, l, p, q . This precisely yields the twistor-space expression for a “1-loop” leading singularity topology [106, 107].



In the figure, a thick black line denotes the merging of the two particles at the ends of the line, and integrating over the remaining variable. The generalization to all leading singularities is obvious; for instance, starting with the “1-loop” leading singularity we have already built, we can use the same merge and integrate operations to build

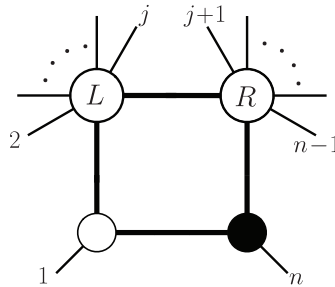
“2-loop” leading singularity topologies such as that shown below.



We conclude that all leading singularities are Yangian invariant. Given that all Yangian invariants are Grassmannian residues, this proves (in passing) the original conjecture in [16] that all leading singularities can be identified as residues of the Grassmannian integral.

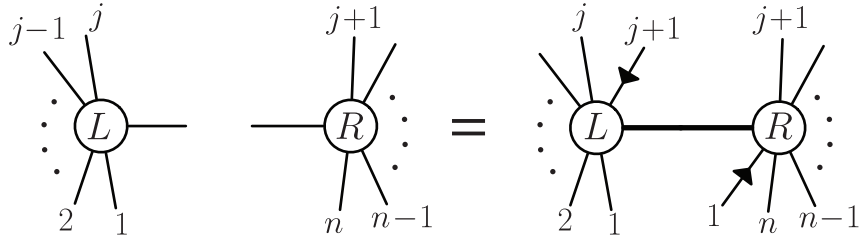
V. The BCFW Bridge

A particularly important way of putting together two Yangian invariants to make a third is the “BCFW bridge” [73, 83, 108], associated with the familiar “two-mass hard” leading singularities drawn below in twistor space [73, 108–110]:



Here, the open and dark circles respectively denote MHV and $\overline{\text{MHV}}$ three-particle amplitudes, respectively. We remark in passing that the inverse-soft factor operations mentioned above are special cases of the BCFW bridge where a given Yangian invariant is bridged with an $\overline{\text{MHV}}$ three-point vertex (for the k -preserving case) or an MHV three-point vertex (for the k -increasing case).

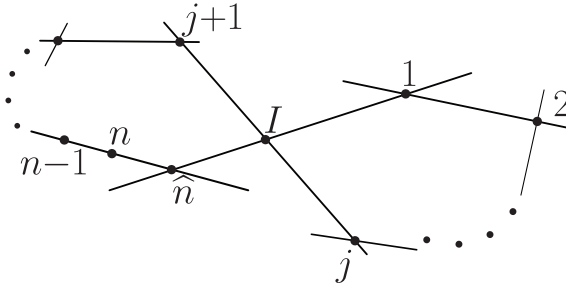
We will find it useful to also see the bridge expressed as a composition of our basic operations in momentum-twistor space, as



This is a pretty object since it uses all of our basic operations in an interesting way. In the figure, the solid arrows pointing inward indicate that particle-“1” is added as an k -increasing inverse soft factor on Y_L , and $j+1$ is added as a k -increasing inverse soft factor on Y_R . We are also using the merge operation to identify the repeated “1” and “ $j+1$ ” labels across the bridge. The internal line, which we label as \mathcal{Z}_I , is integrated over. The contour of integration is chosen to encircle the $\langle n-1 \ n \ 1 \ I \rangle$ -pole from the $[n-1 \ n \ 1 \ I \ j+1]$ -piece of the inverse-soft factor on Y_L , and the $\langle 1 \ I \ j+1 \ j \rangle$ - and $\langle I \ j+1 \ j \ j-1 \rangle$ -poles from the $[1 \ I \ j+1 \ j \ j-1]$ -piece of the inverse soft factor on Y_R . The deformation on \mathcal{Z}_n induced by the inverse-soft factor adding particle-1 on Y_L is of the form

$$\mathcal{Z}_n \mapsto \widehat{\mathcal{Z}}_n = \mathcal{Z}_n + z\mathcal{Z}_{n-1}, \quad \text{where} \quad \langle \widehat{\mathcal{Z}}_n Z_1 Z_j Z_{j+1} \rangle = 0. \quad (2.2.11)$$

This is the momentum-twistor space version of the BCFW deformation, which corresponds to deforming $\lambda_n, \widetilde{\lambda}_1$ in momentum-space. We remind ourselves of this deformation by placing the little arrow pointing from $n \mapsto n-1$ in the figure for the bridge. The momentum-twistor space geometry associated with this object is



which precisely corresponds to the expected BCFW deformation and the corresponding factorization channel.

We leave a detailed derivation of this picture to [?], but in fact the momentum-twistor structure of the BCFW bridge can be easily understood. Note that Y_L, Y_R

have k -charge k_L, k_R , while $Y_L \otimes Y_R$ has k -charge $k_L + k_R + 1$; given that the \mathcal{Z}_I decreases the k -charge by 1, we must start with Y_L and Y_R and get objects with k -charge $(k_L + 1)$ and $(k_R + 1)$ on the left and right. This can be canonically done by acting with k -increasing inverse soft factors; the added particle on Y_L must be adjacent to n in order to affect a deformation on \mathcal{Z}_n . Finally, the data associated with the “extra” particles introduced by the inverse soft factor must be removed in the only way possible, by using the merge operation. Explicitly, the final result for $Y_L \otimes_{\text{BCFW}} Y_R$ is

$$\left(Y_L \otimes_{\text{BCFW}} Y_R\right)(1, \dots, n) = [n-1 \ n \ 1 \ j \ j+1] \times Y_R(1, \dots, j, I) \times Y_L(I, j+1, \dots, n-1, \hat{n}) \quad (2.2.12)$$

with

$$\hat{n} = (n-1 \ n) \cap (j \ j+1 \ 1), \quad \text{and} \quad I = (j \ j+1) \cap (n-1 \ n \ 1). \quad (2.2.13)$$

Starting with the tree amplitude $M_{n,k,\text{tree}}$ ⁶, the BCFW deformation $\mathcal{Z}_n \mapsto \mathcal{Z}_n + z\mathcal{Z}_{n-1}$ can be used to recursively construct tree amplitudes in the familiar way: by writing,

$$M_{n,k,\text{tree}} = \oint \frac{dz}{z} \widehat{M}_{n,k,\text{tree}}(z), \quad (2.2.14)$$

it is clear that the desired amplitude $\widehat{M}_{n,k,\text{tree}}(z)$ is obtained by summing-over all the residues of the RHS *except* the pole at origin $z = 0$. Notice that there is a non-zero pole at infinity in this deformation: as $z \rightarrow \infty$, $\mathcal{Z}_n \rightarrow \mathcal{Z}_{n-1}$ projectively, and so the tree amplitude gets a contribution from $M_n(\mathcal{Z}_1, \dots, \mathcal{Z}_{n-1}, \mathcal{Z}_n) \rightarrow M_{n-1}(\mathcal{Z}_1, \dots, \mathcal{Z}_{n-1})$ ⁷. The pole at $z \rightarrow \infty$ corresponds to the term in the usual momentum-space BCFW formula using an $\overline{\text{MHV}}$ three-point vertex bridged with M_{n-1} , which simply acts as a k -preserving inverse-soft factor. The remaining physical poles are of

⁶We remind the reader that we are working in momentum-twistor space, so that what we are calling M_{tree} here is obtained after stripping off the MHV tree-amplitude factor from the full amplitude in momentum space.

⁷Note that $z \rightarrow \infty$ here does *not* correspond to going to infinity in the familiar momentum-space version of BCFW. The pole at infinity in ordinary momentum space here corresponds to a pole involving the infinity twistor $\langle \mathcal{Z}_n(z) \ I \ Z_1 \rangle = 0$. Of course we do not expect such a pole to arise in a dual-conformal invariant theory, not only at tree-level, but at all-loop order, as will be relevant to our subsequent discussion. A direct proof of this fact, not assuming dual conformal invariance, should follow from the “enhanced spin-lorentz symmetry” arguments of [108].

the form $\langle i \ i+1 \ j \ j+1 \rangle$. Under $\mathcal{Z}_n \mapsto \mathcal{Z}_n + z\mathcal{Z}_{n-1}$, we only access the poles where $\langle \mathcal{Z}_n(z)Z_1Z_jZ_{j+1} \rangle \rightarrow 0$, and the corresponding residues are computed by the BCFW bridge indicated above, with Y_L, Y_R being the lower-point tree amplitudes.

2.3 Loops From Hidden Entanglement

Let's imagine starting with some scattering amplitude or Grassmannian residue, and begin removing particles. The operation that decreases k in particular demands a choice for the contour of integration. If we remove particle \mathcal{Z}_A by integrating over it as $\int d^{3|4}\mathcal{Z}_A$, it is natural to choose a T^3 -contour of integration for the Bosonic $d^3\mathcal{Z}_A$ integral and compute a simple residue⁸.

We can then proceed to remove a subsequent particle either by merging, or performing further integrals $\int d^{3|4}\mathcal{Z}_B$ and so on. In this way we will simply proceed from higher-point Grassmannian residues to lower-point ones. In particular, if these operations are performed on a higher-point tree amplitude, we arrive at lower-point tree amplitudes, and don't encounter any new objects.

But we can imagine a more interesting way of removing not just one but a pair of particles. Consider removing particle A and subsequently removing the adjacent particle B . Instead of first integrating-out A and then B on separate T^3 's, let's consider an "entangled" contour of integration, which we will discover to yield, instead of lower-point Grassmannian residue, a loop integral.

Consider as a simple example removing two particles from the 6-particle $N^2\text{MHV} = \overline{\text{MHV}}$ tree amplitude, $M_{6,4,\ell=0}(1234AB)$. Performing the $d^{0|4}\eta_A, d^{0|4}\eta_B$ integrals is trivial, and this gives

$$\int d^3z_A d^3z_B \frac{\langle 1234 \rangle^3}{\langle 234z_A \rangle \langle 34z_A z_B \rangle \langle 4z_A z_B 1 \rangle \langle z_A z_B 12 \rangle \langle z_B 123 \rangle} \quad (2.3.15)$$

where we have chosen to label the Bosonic momentum twistors with lower-case z 's for later convenience. As we have claimed, on any closed contour, these integrals should

⁸Residues of rational functions in m complex variables are computed by choosing m polynomial factors f_i 's from the denominator and integrating along a particular T^m -contour, *i.e.* the product of m circles given as the solutions of $|f_i| = \epsilon$ with $\epsilon \ll 1$ and near a common zero of the f_i 's. See [71] for more details.

give a Yangian-invariant answer. Indeed, computing the z_B integral by residue on any contour leaves us with

$$\int d^3 z_A \frac{\langle 1234 \rangle^3}{\langle z_A 123 \rangle \langle z_A 234 \rangle \langle z_A 341 \rangle \langle z_A 412 \rangle} \quad (2.3.16)$$

and computing any of the simple residues of this remaining z_A integral gives 1, which is of course the only Yangian invariant for MHV amplitudes.

We will now see that starting with exactly the same integrand but choosing a different contour of integration yields, instead of “1”, the 4-particle 1-loop amplitude. Geometrically, the points z_A, z_B determine a line in momentum-twistor space, which is interpreted as a point in the dual x -space, or equivalently, a loop-integral’s four-momentum. We will first integrate over the positions of z_A, z_B on the line (AB) , and then integrate over all lines (AB) .

This contour can be described explicitly by parametrizing $z_{A,B}$ as

$$z_A = \begin{pmatrix} \lambda_A \\ x\lambda_A \end{pmatrix}, \quad z_B = \begin{pmatrix} \lambda_B \\ x\lambda_B \end{pmatrix} \quad (2.3.17)$$

where x will be the loop momentum. The measure is

$$d^3 z_A d^3 z_B = \langle \lambda_A d\lambda_A \rangle \langle \lambda_B d\lambda_B \rangle \langle \lambda_A \lambda_B \rangle^2 d^4 x. \quad (2.3.18)$$

The λ_A, λ_B integrals will be treated as contour integrals on $\mathbb{CP}^1 \times \mathbb{CP}^1$, while the x -integral will be over real points in the (dual) Minkowski space.

Using that $\langle z_A z_B j-1 j \rangle = \langle \lambda_A \lambda_B \rangle \langle j-1 j \rangle (x-x_j)^2$ our integral becomes

$$\int d^4 x \frac{x_{13}^2 x_{24}^2}{(x-x_1)^2 (x-x_2)^2 (x-x_4)^2} \int \frac{\langle 1234 \rangle \langle 23 \rangle \langle \lambda_A d\lambda_A \rangle \langle \lambda_B d\lambda_B \rangle}{\langle z_A 123 \rangle \langle 234 z_B \rangle \langle \lambda_A \lambda_B \rangle}. \quad (2.3.19)$$

The factor $\langle z_A 234 \rangle$ is linear in the projective variable λ_A while the factor $\langle 123 z_B \rangle$ is linear in λ_B . This implies that there is a unique way to perform the λ_A and λ_B integrals by contour integration, which gives us

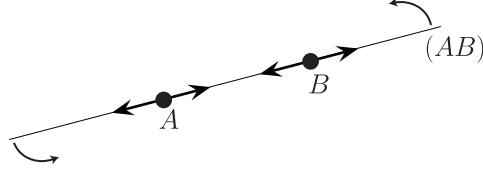
$$\int d^4 x \frac{x_{13}^2 x_{24}^2}{(x-x_1)^2 (x-x_2)^2 (x-x_3)^2 (x-x_4)^2}. \quad (2.3.20)$$

This is precisely the 1-loop MHV amplitude!

We have thus seen that, removing a pair of particles with this “entangled” contour of integration, where we first integrate over the position of two points along the line

joining them and then integrate over all lines, naturally produces objects that look like loop integrals.

There is a nicer way of characterizing this “entangled” contour that is also more convenient for doing calculations, let us describe it in detail. Given z_A, z_B , a general GL_2 -transformation on the 2-vector (z_A, z_B) moves A, B along the line (AB) . Thus, in integrating over $d^3 z_A d^3 z_B$, we’d like to “do the GL_2 -part of the integral first” to leave us with an integral that only depends on the line (AB) :



We can do this explicitly by writing

$$\begin{pmatrix} z_A \\ z_B \end{pmatrix} = \begin{pmatrix} c_A^{(A)} & c_A^{(B)} \\ c_B^{(A)} & c_B^{(B)} \end{pmatrix} \begin{pmatrix} Z_A \\ Z_B \end{pmatrix}; \quad (2.3.21)$$

then

$$d^3 z_A d^3 z_B = \langle c_A d c_A \rangle \langle c_B d c_B \rangle \langle c_A c_B \rangle^2 \left[\frac{d^4 Z_A d^4 Z_B}{\text{vol}(GL_2)} \right], \quad (2.3.22)$$

and our integral becomes—this time writing it out fully:

$$\int \left[\frac{d^4 Z_A d^4 Z_B}{\text{vol}(GL_2)} \right] \frac{\langle 1234 \rangle^3}{\langle AB 12 \rangle \langle AB 34 \rangle \langle AB 41 \rangle} \int \frac{\langle c_A d c_A \rangle \langle c_B d c_B \rangle}{\langle c_A c_B \rangle \langle c_A \psi_A \rangle \langle c_B \psi_B \rangle}, \quad (2.3.23)$$

where

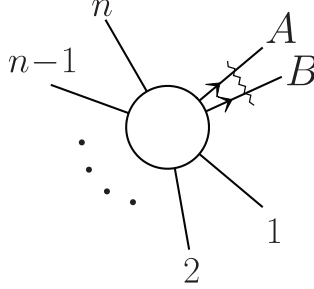
$$\psi_A = \begin{pmatrix} \langle A234 \rangle \\ \langle B234 \rangle \end{pmatrix}, \quad \psi_B = \begin{pmatrix} \langle A123 \rangle \\ \langle B123 \rangle \end{pmatrix}. \quad (2.3.24)$$

The c_A, c_B integral is naturally performed on a contour ‘encircling’ $c_A = \psi_A, c_B = \psi_B$, yielding $\frac{1}{\langle \psi_A \psi_B \rangle} = \frac{1}{\langle AB 23 \rangle \langle 1234 \rangle}$. More generally, if “234” and “123” in the definitions of ψ_A, ψ_B were to be replaced by arbitrary “ abc ” and “ xyz ”, $\langle \psi_A \psi_B \rangle = \langle Axyz \rangle \langle Babc \rangle - \langle Aabc \rangle \langle Bxyz \rangle \equiv \langle AB (abc) \cap (xyz) \rangle$ where $(abc) \cap (xyz)$ is the line corresponding to the intersection of the planes (abc) and (xyz) . We are then left with

$$\int \left[\frac{d^4 Z_A d^4 Z_B}{\text{vol}(GL_2)} \right] \frac{\langle 1234 \rangle^2}{\langle AB 12 \rangle \langle AB 23 \rangle \langle AB 34 \rangle \langle AB 41 \rangle}, \quad (2.3.25)$$

where the integration region is such that the line (AB) corresponds to a real point in the (dual) Minkowski space-time. We recognize this object as the 1-loop MHV amplitude, exactly as above.

We can clearly perform this operation starting with any Yangian invariant object $Y[\mathcal{Z}_A, \mathcal{Z}_B, \mathcal{Z}_1, \dots]$, which we will graphically denote as:



and write as

$$\int_{GL_2} Y[\dots, \mathcal{Z}_n, \mathcal{Z}_A, \mathcal{Z}_B, \mathcal{Z}_1, \dots] \quad (2.3.26)$$

This object is formally Yangian-invariant, in the precise sense that the integrand will transform into a total derivative under the action of the Yangian generators for the external particles. Of course, such integrals may have IR-divergences along some contours of integration, which is how Yangian-invariance is broken in practice.

The usual way of writing the loop amplitudes as “leading singularity \times scalar integral” ensures that the leading singularities of the individual terms are Yangian-invariant, but the factorized form seems very un-natural, and there is no obvious action of the symmetry generators on the integrand. By contrast, the loop integrals we have defined, as we will see, will not take the artificial “residue \times integral” form, but of course their leading singularities are automatically Grassmannian residues. The reason is that a leading singularity of the (AB) -integral can be computed as a simple residue of the underlying $d^{3|4}z_A d^{3|4}z_B$ integral, which is free of IR-divergences and guaranteed to be Yangian-invariant.

2.4 Recursion Relations For All Loop Amplitudes

Having familiarized ourselves with the basic operations on Yangian invariants, we are ready to discuss the recursion relations for loops in the most transparent way.

The loop integrand is a rational function of both the loop integration variables and the external kinematical variables. Just as the BCFW recursion relations allow us to compute a rational function from its poles under a simple deformation, the loop integrand can be determined in the same way. Consider the l -loop integrand $M_{n,k,\ell}$, and consider again the (supersymmetric) momentum-twistor deformation

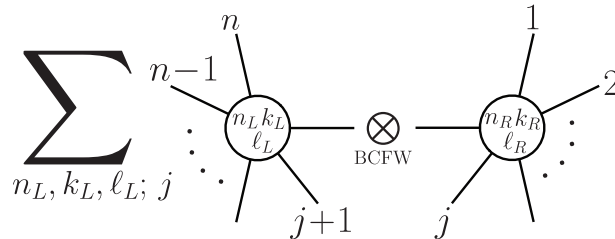
$$\mathcal{Z}_n \mapsto \mathcal{Z}_n + z\mathcal{Z}_{n-1}. \quad (2.4.27)$$

Then

$$M_{n,k,\ell} = \oint \frac{dz}{z} \widehat{M}_{n,k,\ell}(z) \quad (2.4.28)$$

and we sum over all the residues of the RHS away from the origin, all of which can be determined from lower-point/lower-loop amplitudes. This recursion relation can be derived in a large class of theories and is not directly tied to $\mathcal{N} = 4$ SYM or Yangian-invariance. However our experience with building Yangian-invariant objects will help us to understand (and compute) the terms in the recursion relations in a transparent way, and also easily recognize them as manifestly Yangian-invariant objects.

As in our discussion of the BCFW bridge at tree-level, the pole at infinity is simply the lower-point integrand with particle n removed. All the rest of the poles in z also have a simple interpretation: in general, all the poles arise either from $\langle Z_n(z) Z_1 Z_j Z_{j+1} \rangle \rightarrow 0$ or $\langle (AB)_q Z_n(z) Z_1 \rangle \rightarrow 0$, where $(AB)_q$ denotes the line in momentum twistor space associated with the q^{th} loop-variable. The first type of pole simply corresponds to factorization channels, and the corresponding residue is computed by the BCFW bridges between lower-loop/lower-point amplitudes:

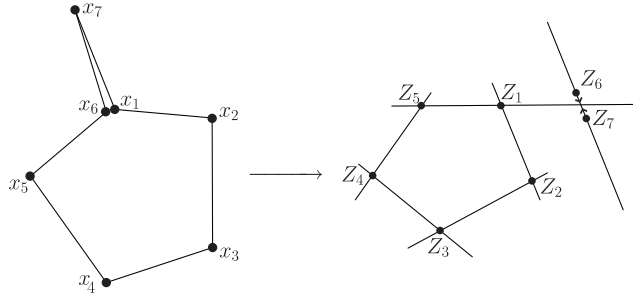


where $n_L + n_R = n + 2$, $k_L + k_R = k - 1$, $\ell_L + \ell_R = \ell$. Note that we treat all the poles (including the pole at infinity) on an equal footing by declaring the term with $j = 2$ to be given by the k -preserving inverse soft-factor acting on lower-point amplitude.

This is the most obvious generalization of the BCFW recursion relation from trees to loops, but it clearly can't be the whole story, since it would allow us to recursively reduce loop amplitudes to the 3-particle loop amplitude, which vanishes! Obviously, at loop-level, a “source” term is needed for the recursive formula.

I. Single-Cuts and the Forward-Limit

This source term is clearly provided by the second set of poles, arising from $\langle (AB)_q Z_n(z) Z_1 \rangle \rightarrow 0$. For simplicity of discussion let's first consider the 1-loop amplitude. This pole corresponds to cutting the loop momentum running between n and 1, and is therefore given by a tree-amplitude with two additional particles sandwiched-between $n, 1$, with momenta $q, -q$, summing-over the multiplet of states running around the loop. These single-cuts associated with “forward-limits” of lower-loop integrands are precisely the objects that make an appearance in the context of the Feynman tree theorem [103]. The geometry of the forward limit is shown below for both in the dual x -space and momentum-twistor space:

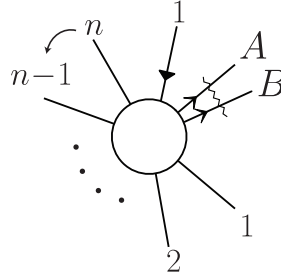


Here, between particles 5 and 1, we have particles 6, 7 with momenta $q^\mu, -q^\mu$, where $q^\mu = x_1^\mu - x_7^\mu$ is a null vector. In momentum-twistor space, the null condition means that the line (76) intersects (15), while in the forward limit both Z_6 and Z_7 approach the intersection point $(76) \cap (15)$.

In a generic gauge theory, the forward limits of tree amplitudes suffer from collinear divergences and are not obviously well-defined. However remarkably, as pointed out in [103], in supersymmetric theories the sum over the full multiplet makes these objects completely well-defined and equal to single-cuts!

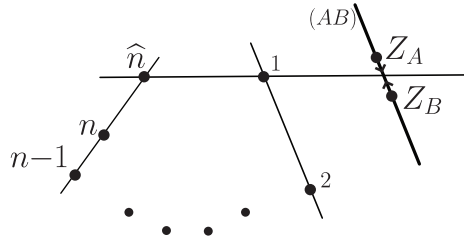
Indeed, we can go further and express this single-cut “forward limit” term in a manifestly Yangian-invariant way. It turns out to be a beautiful object, combining

the entangled removal of two particles with the “merge” operation:



Here a particle $(n + 1)$ is added adjacent to A, B as a k -increasing inverse soft factor, then A, B are removed by entangled integration. The GL_2 -contour is chosen to encircle points where both points A, B on the line (AB) are located at the intersection of the line (AB) with the plane $(n-1 \ n \ 1)$. Note that there is no actual integral to be done here; the GL_2 -integral is done on residues and is computed purely algebraically. Finally, the added particle $(n + 1)$ is merged with 1.

As in our discussion of the BCFW bridge, this form can be easily understood by looking at the deformations induced by the “1” inverse soft factors; the associated momentum-twistor geometry turns out to be

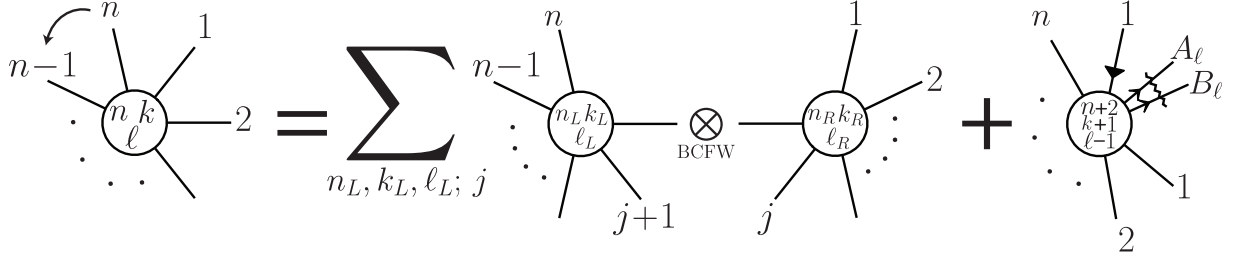


exactly as needed. The picture is the same for taking the single cut of any Yangian-invariant object.

Note that we were able to identify the BCFW terms in a straightforward way since the residues of the poles *of the integrand* have obvious “factorization” and “cut” interpretations. This is another significant advantage of working with the integrand, since as is well known, the full loop amplitudes (after integration) have more complicated factorization properties [111]. This is due to the IR-divergences which occur when the loop momenta becomes collinear to external particles, when the integration is performed.

II. BCFW For All Loop Amplitudes

Putting the pieces together, we can give the recursive definition for all loop integrands in planar $\mathcal{N} = 4$ SYM as



To be fully explicit, the recursion relation is

$$\begin{aligned}
 M_{n,k,\ell}(1, \dots, n) &= M_{n-1,k,\ell}(1, \dots, n-1) \\
 &+ \sum_{n_L, k_L, \ell_L; j} [j \ j+1 \ n-1 \ n \ 1] M_{n_R, k_R, \ell_R}^R(1, \dots, j, I_j) M_{n_L, k_L, \ell_L}^L(I_j, j+1, \dots, \hat{n}_j) \\
 &+ \int_{GL_2} [AB \ n-1 \ n \ 1] \times M_{n+2, k+1, \ell-1}(1, \dots, \hat{n}_{(AB)}, \hat{A}, B). \tag{2.4.29}
 \end{aligned}$$

where $n_L + n_R = n + 2$, $k_L + k_R = k - 1$, $\ell_L + \ell_R = \ell$ and the shifted momentum (super-)twistors that enter are

$$\begin{aligned}
 \hat{n}_j &= (n-1 \ n) \cap (j \ j+1 \ 1), & I_j &= (j \ j+1) \cap (n-1 \ n \ 1); \\
 \hat{n}_{(AB)} &= (n-1 \ n) \cap (AB \ 1), & \hat{A} &= (AB) \cap (n-1 \ n \ 1).
 \end{aligned} \tag{2.4.30}$$

Beyond 1-loop, it is understood that this expression is to be fully-symmetrized with equal weight in all the loop-integration variables $(AB)_\ell$; it is easy to see that this correctly captures the recursive combinatorics. Recall again that GL_2 -integral is done on simple residues and is thus computed purely algebraically; the contour is chosen so that the points A, B are sent to $(AB) \cap (n-1 \ n \ 1)$. Recursively using the BCFW form for the lower-loop amplitudes appearing in the forward limit allows us to carry out the GL_2 -integral completely explicitly, but the form we have given here will suffice for this chapter.

III. Simple Examples

In [?], we will describe the loop-level BCFW computations in detail; here we will just highlight some of the results for some simple cases, to illustrate some of the important

properties of the recursion and the amplitudes that result. We start by giving the BCFW formula for all one-loop MHV amplitudes.

In this case the second line in the above formula vanishes, and the recursion relation trivially reduces to a single sum. To compute the NMHV tree amplitudes which enters through the third line, it is convenient to use the tree BCFW deformation $\tilde{\mathcal{Z}}_B = \mathcal{Z}_B + z\hat{\mathcal{Z}}_A$ which leads to

$$M_{\text{MHV}}^{1\text{-loop}} = \int_{(AB)} \int_{GL_2} \sum_j [AB j j+1 1] \times \left(\sum_{i < j} [\hat{A} B 1 i i+1] + \dots \right), \quad (2.4.31)$$

where we have defined

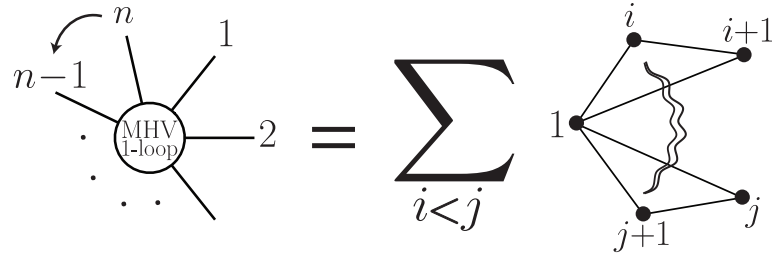
$$\int_{(AB)} \equiv \int \left[\frac{d^{4|4} \mathcal{Z}_A d^{4|4} \mathcal{Z}_B}{\text{vol}(GL_2)} \right], \quad (2.4.32)$$

and where the omitted terms are independent of \mathcal{Z}_B and vanish upon Fermionic-integration. The GL_2 - and Fermion-integrals are readily evaluated, as explained above, reducing this to

$$M_{\text{MHV}}^{1\text{-loop}} = \int_{(AB)} \sum_{i < j} \frac{\langle AB (1 i i+1) \cap (1 j j+1) \rangle^2}{\langle AB 1 i \rangle \langle AB i i+1 \rangle \langle AB i+1 1 \rangle \langle AB 1 j \rangle \langle AB j j+1 \rangle \langle AB j+1 1 \rangle}. \quad (2.4.33)$$

This is the full one-loop integrand for MHV amplitudes.

As expected on general grounds from Yangian-invariance, and also as familiar from BCFW recursion at tree-level, the individual terms in this formula contain both local and non-local poles. We will graphically denote a factor $\langle AB xy \rangle$ in the denominator by drawing a line (xy) ; the numerators of tensor integrals (required by dual conformal invariance) will be denoted by wavy- and dashed-lines—the precise meaning of which will be explained shortly. In this notation, this result is



Notice that all the terms have 6 factors in the denominator, and hence by dual conformal invariance we must have two factors containing (AB) in the numerators.

These are denoted by the wavy lines: the numerator is $\langle AB(1\ i\ i+1) \cap (1\ j\ j+1) \rangle^2 \equiv (\langle A\ 1\ i\ i+1 \rangle \langle B\ 1\ j\ j+1 \rangle - \langle B\ 1\ i\ i+1 \rangle \langle A\ 1\ j\ j+1 \rangle)^2$, where the power of 2 has been indicated by the line's multiplicity.

Notice that when $i + 1 = j$, the numerator cancels the two factors $\langle AB\ 1\ j \rangle^2$ in the denominator: by a simple use of the Schouten identity it is easy to see that

$$[\langle A\ 1\ j-1\ j \rangle \langle B\ 1\ j\ j+1 \rangle - \langle A\ 1\ j\ j+1 \rangle \langle B\ 1\ j-1\ j \rangle]^2 = [\langle AB\ 1\ j \rangle \langle 1\ j-1\ j\ j+1 \rangle]^2. \quad (2.4.34)$$

In general, all of these terms contain both physical as well as spurious poles. Physical poles are denominator factors of the form $\langle AB\ i\ i+1 \rangle$ and $\langle i\ i+1\ j\ j+1 \rangle$ while spurious poles are all other denominator factors. We often refer to physical poles as local poles and to spurious poles as non-local. A small explanation for the “non-local” terminology is in order. Consider the 5-particle amplitude as an example, where there are three terms in the integrand. These three terms are

$$\frac{\langle 1234 \rangle^2}{\langle AB\ 12 \rangle \langle AB\ 23 \rangle \langle AB\ 34 \rangle \langle AB\ 14 \rangle} + \frac{\langle AB(123) \cap (145) \rangle^2}{\langle AB\ 12 \rangle \langle AB\ 23 \rangle \langle AB\ 31 \rangle \langle AB\ 14 \rangle \langle AB\ 45 \rangle \langle AB\ 51 \rangle} \\ \frac{\langle 3451 \rangle^2}{\langle AB\ 34 \rangle \langle AB\ 45 \rangle \langle AB\ 51 \rangle \langle AB\ 31 \rangle}. \quad (2.4.35)$$

The spurious poles are $\langle AB\ 14 \rangle$ and $\langle AB\ 13 \rangle$. The line defined by Z_1 and Z_3 corresponds to a complex point, but what makes $\langle AB\ 13 \rangle$ non-local? The reason is that in field theory $1/\langle AB\ 13 \rangle$ could only come from a loop integration, *e.g.* it is generated by a local one-loop integral of the form

$$\int \left[\frac{d^4 Z_C d^4 Z_D}{\text{vol}(GL_2)} \right] \frac{\langle CD(512) \cap (234) \rangle}{\langle CD\ AB \rangle \langle CD\ 51 \rangle \langle CD\ 12 \rangle \langle CD\ 23 \rangle \langle CD\ 34 \rangle}. \quad (2.4.36)$$

(This is also the secret origin of the non-local poles in BCFW at tree-level.)

Back to the 5-particle example, $\langle AB\ 14 \rangle$ and $\langle AB\ 31 \rangle$ occur each in two of the three terms and they cancel in pairs. Indeed upon collecting denominators we find, after repeated uses of the Schouten identity, the result for the sum

$$\frac{\langle AB\ 12 \rangle \langle 2345 \rangle \langle 1345 \rangle + \langle AB\ 23 \rangle \langle 1345 \rangle \langle 1245 \rangle + \langle AB\ 13 \rangle \langle 1245 \rangle \langle 3245 \rangle + \langle AB\ 45 \rangle \langle 1234 \rangle \langle 1235 \rangle}{\langle AB\ 12 \rangle \langle AB\ 23 \rangle \langle AB\ 34 \rangle \langle AB\ 45 \rangle \langle AB\ 51 \rangle}. \quad (2.4.37)$$

This is furthermore cyclically-invariant, albeit in a nontrivial way involving Schouten identities.

Let us also briefly discuss the 6-particle NMHV amplitude at 1-loop. The full integrand has 16 terms which differs even more sharply from familiar local forms of writing the amplitude. As we will review in the next section, the usual box decomposition of 1-loop amplitudes does not match the full integrand (only the “parity-even” part of the integrand); even so, there is a natural generalization of the basis of integrals that can be used to match the full integrand in a manifestly dual conformal invariant form. Any such representation, however, will have the familiar form “leading singularity/Grassmannian residue \times loop integral”. However, this is *not* the form we encounter with loop-level BCFW. Instead, the supersymmetric η -variables are entangled with the loop integration variables in an interesting way. For instance, one of the terms from the forward limit contribution to the 6-particle NMHV amplitude integrand is the following,

$$\frac{\delta^{0|4} \left(\begin{array}{l} \eta_1 \langle AB 1(23) \cap (456) \rangle + \eta_2 \langle 4561 \rangle \langle AB 31 \rangle + \eta_3 \langle 4561 \rangle \langle AB 12 \rangle \\ + \eta_4 \langle AB (123) \cap (561) \rangle + \eta_5 \langle AB 1(46) \cap (123) \rangle + \eta_6 \langle AB 1(123) \cap (45) \rangle \end{array} \right)}{\langle 4561 \rangle \langle AB 45 \rangle \langle AB 61 \rangle \langle AB 12 \rangle \langle AB 23 \rangle \langle AB 13 \rangle \langle AB 41 \rangle \langle AB (123) \cap (456) \rangle \langle AB (123) \cap (561) \rangle}$$

Note the presence of the explicit (AB) -dependence in the argument of the Fermionic δ -function. Seemingly miraculously, when the residues of this integral are computed on its leading singularities, the η -dependence precisely reproduces the standard NMHV R -invariants. Of course this miracle is guaranteed by our general arguments about the Yangian-invariance of these objects.

IV. Unitarity as a Residue Theorem

The BCFW construction of tree-level amplitudes make Yangian-invariance manifest, but are not manifestly cyclic-invariant. The statement of cyclic-invariance is then a remarkable identity between rational functions. Of course one could say that the field theory derivation of the recursion relation gives a proof of these identities, but this is quite a circuitous argument. One of the initial striking features of the Grassmannian picture for tree amplitudes was that these identities were instead a direct consequence of the global residue theorem applied to the Grassmannian integral. This observation ultimately led to the “particle interpretation” picture for the tree contour, giving a completely autonomous and deeper understanding of tree amplitudes, removed from the crutch of their field theory origin.

In complete analogy with BCFW at tree-level, the BCFW construction of the loop integrand is not manifestly cyclically-invariant. Again cyclic-invariance is a remarkable identity between rational functions, and again this identity can be thought of as a consequence of the field theory derivation of the recursion relation. But of course we strongly suspect that there is an extension of the “particle interpretation” picture that gives a completely autonomous and deeper understanding of loop amplitudes, independent of any field theoretic derivation.

Just as at tree-level, a first step in this direction is to find a new understanding of the cyclic-invariance identities. To wit, we have understood how the cyclic-identity for the 1-loop MHV amplitude can be understood as a residue theorem. The idea is to identify the terms appearing in the MHV 1-loop formulas as the residues of a new Grassmannian integral. All the terms in the MHV 1-loop formula can actually be thought of as arising from $\int d^{3|4} \mathcal{Z}_A d^{3|4} \mathcal{Z}_B Y_{n+2,k=2}(\mathcal{Z}_A, \mathcal{Z}_B, \dots)$, where $Y_{n+2,k=2}$ is computed from the $G(2, n+2)$ Grassmannian integral. Note that $\mathcal{Z}_A, \mathcal{Z}_B$ appear in the δ -functions of the integral in the combination $C_{\beta A} \mathcal{Z}_A + C_{\beta B} \mathcal{Z}_B$, so the GL_2 -action on $(\mathcal{Z}_A, \mathcal{Z}_B)$ also acts on $(C_{\beta A}, C_{\beta B})$. Performing the $\eta_{A,B}$ and GL_2 -integrals leaves us with a new Grassmannian integral:

$$\int d^{2 \times (n+2)} C_{\beta a} \frac{\delta^4(C_{\beta i} Z_i + C_{\beta A} Z_A + C_{\beta B} Z_B)(AB)^2}{(12)(23) \cdots (n1)}. \quad (2.4.38)$$

By construction, this integral has a GL_2 -invariance acting on columns (A, B) and (Z_A, Z_B) , and hence all of its residues are only a function of the line $(Z_A Z_B)$. In particular all terms appearing in the MHV 1-loop formula, after GL_2 integration, are particular residues of this Grassmannian integral.

The equality of cyclically-related BCFW expressions of the 1-loop amplitude follows from a residue theorem applied to this integral. In fact, it can be shown that the *only* combination of these residues that is free of spurious poles is the physical 1-loop amplitude.

At tree level, the cyclic-identity applied to *e.g.* NMHV amplitudes ensures the absence of spurious poles. The same is true at 1-loop level. Since the BCFW formula manifestly guarantees that one of the single cuts is correctly reproduced, cyclicity guarantees that *all* the single cuts are correct. Having all correct single cuts, auto-

matically ensures that all higher cuts—and in particular unitarity cuts—are correctly reproduced. Unitarity then finds a deeper origin in this residue theorem.

2.5 Final remarks

I. Origin of Loops

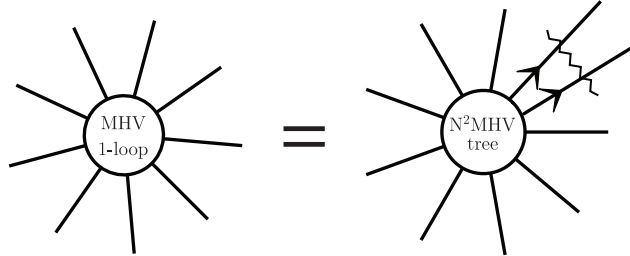
A few years ago, the tree-level BCFW recursion relations sat at an interesting crossroads between the usual formulation of field theory, where space-time locality is manifest, and a hoped for dual description, where space-time should be emergent. On the one hand, the recursion relations were directly derived from field theory—without the field-theoretic motivation, it was hard to imagine the motivation for gluing lower-point objects together in the prescribed way. On the other hand, the presentation of the amplitude was very different from anything normally seen in field theory. The amplitudes could be presented in many different forms, with remarkable identities guaranteeing their equivalence. The simplicity of the answers resulted directly from the presence of non-local poles. These properties, together with the dual superconformal invariance of all terms in the BCFW expansions, strongly motivated the search for a dual theory which would make these features obvious, and which would furthermore give an intrinsic definition of the tree amplitudes on its own turf.

The Grassmannian duality for leading singularities provides this dual understanding of tree amplitudes in a satisfying way. The Yangian symmetry is manifest (for all leading singularities and not just tree amplitudes). The amplitude can be presented in many forms since it is a contour integral, with many representatives for a given homology class. The remarkable identities guaranteeing cyclic-invariance (together with important physical properties at loop-level) indeed find a new interpretation as higher-dimensional residue theorems. And finally, giving the contour integral over the Grassmannian a “particle interpretation” poses a natural question, intrinsic to the Grassmannian picture, whose answer yields the tree amplitude, along the way exposing a (still quite mysterious) connection with twistor string theory. We strongly suspect that a generalization of this picture exists that extends the duality to only to

incorporate loop amplitudes but also explain why loops must be computed to begin with.

Our extension of BCFW to all loop orders puts loop amplitudes in the same position at the cross-roads between field theory and a sought-after dual description that tree amplitudes occupied a few years ago. This should set the stage for fully exposing the dual picture, and we have already made some inroads to uncovering its structure. For instance we saw that the remarkable identities guaranteeing cyclic-invariance of the MHV 1-loop amplitude indeed have an origin as a residue theorem in a new Grassmannian integral closely associated to the “master” integral computing leading singularities/Yangian-invariants. The nature of the “seed” for loops, arising from removing particles, is also clearly intimately related to the particle interpretation, which has already played a central role in the emergence of locality at tree-level.

Along these lines, here we give another presentation of the 1-loop MHV amplitudes, which differs from the form we obtained using the recursion relation. Consider the tree-level N^2 MHV amplitude $M_{n,k=2}(\mathcal{Z}_1, \dots, \mathcal{Z}_n, \mathcal{Z}_A, \mathcal{Z}_B)$. The 1-loop MHV amplitude arises directly from the entangled removal of A and B :



Here it is easy to see, using the BCFW form of the tree amplitude, that there is a unique GL_2 -contour of integration associated with each term. This formula differs term-by-term from the BCFW form of this amplitude. We can however recognize all the terms as residues of the same auxiliary Grassmannian integral in equation (2.4.38), and we have shown that the equivalence to the BCFW form follows from a residue theorem. While this formula does not directly generalize for other amplitudes, its form is certainly suggestive.

Progress on all these questions would likely be accelerated by finding an explicit solution to the recursion relation for all (n, k, ℓ) , generalizing the explicit solution already known for tree-amplitudes [100].

As a final comment, our analysis of loops in this chapter has been greatly aided by working in momentum-twistor space; these variables allow us to recognize loop integrals in their familiar momentum-space setting. However, given that all the elements in the recursion relation were described in manifestly Yangian-invariant ways, it must be possible to translate these results into ordinary twistor space. It is likely that the twistor-space formulation will be most fundamental, amongst other things it could offer a natural understanding of non-planar loop amplitudes as well.

The results of this chapter also give a renewed hope for extracting loop-information from twistor-string theory. As we have seen, loop amplitudes can easily hide in plain sight in subtle ways, masquerading as a formal way of representing “1” in terms of IR-divergent integrals in (3, 1)-signature! It is likely that a deeper understanding of the contours associated with the “Hodges diagrams” [73, 112], already for twistor-space tree-amplitudes in (3, 1)-signature, will be important to make progress here.

II. Simplicity of Integrals and IR-Anomalies

Putting aside these highbrow issues, we are confronted with a much more urgent question: does our understanding of the integrand help us to carry out the integrations to obtain the physical amplitudes? Are the symmetries of the integrand of any use?

In fact the manifestly Yangian-invariant way of presenting the integrand *does* strongly suggest that the integrals themselves will be “simple”. The “super” part of super-dual conformal invariance is already an extremely powerful constraint. Consider MHV amplitudes for simplicity. The statement of super-dual conformal invariance is

$$\sum_a \eta_a^K \frac{\partial}{\partial Z_a^J} M_{\text{MHV}} = 0 \rightarrow \frac{\partial}{\partial Z_a^J} M_{\text{MHV}} = 0 \text{ for all } a, \quad (2.5.39)$$

where we use the fact that the MHV amplitude has no η_a dependence. Thus, the only super-dual conformally invariant amplitude is forced to be a constant! This reflects the well-known fact that the only Yangian invariant with $k = 0$ is the MHV tree amplitude (=1 in momentum-twistor space). Now, we have expressed the integrand for the MHV amplitude in a manifestly super-dual conformal (indeed Yangian)-invariant way. Consider for instance the 1-loop amplitude, which has the form

$$M_{\text{MHV}} = \int d^{3|4} Z_A d^{3|4} Z_B F(Z_A, Z_B; Z_a), \quad (2.5.40)$$

with an entangled contour of integration for $\mathcal{Z}_{A,B}$; we suppress the explicit expression for F . The statement of super-dual conformal invariance is perfectly well-defined at the level of the integrand, which turns into a total derivative:

$$\sum_a \eta_a^K \frac{\partial}{\partial Z_a^J} M_{\text{MHV}} = \int d^{3|4} \mathcal{Z}_A d^{3|4} \mathcal{Z}_B \left(\eta_A^K \frac{\partial}{\partial Z_A^J} + \eta_B^K \frac{\partial}{\partial Z_B^J} \right) F. \quad (2.5.41)$$

After doing the $\eta_{A,B}$ and GL_2 -integrals, we have

$$\frac{\partial}{\partial Z_a^J} M_{\text{MHV}} = \int \frac{d^4 Z_A d^4 Z_B}{\text{vol}(GL_2)} \left(\frac{\partial}{\partial Z_A^J} G_A^a + \frac{\partial}{\partial Z_B^J} G_B^a \right), \quad (2.5.42)$$

where we suppress the explicit forms of $G_{A,B}^a$. We see that super-dual conformal-invariance continues to be manifest at the level of the Bosonic loop integrand in the dual co-ordinate space, also at all loop orders.

This symmetry therefore guarantees that no matter how complicated the integrand looks, on any contour of integration where the integral is completely well-defined, it can only integrate to a constant, “1”! The integral is not “1” *only* because we choose a contour of integration over lines (AB) corresponding to real $(3, 1)$ -signature points in dual spacetime, and this integral is IR-divergent. We see that IR-divergences are not an annoying side-feature of loop amplitudes, they are the sole reason these amplitudes are non-trivial; in this Yangian-invariant form, the loop amplitudes are telling us “I diverge, therefore I am”⁹. This is a powerful statement that should be turned into an engine to simplify the computation of the loop integrals. Due to the IR-divergences, the Yangian generators will not quite annihilate the loop amplitude, but they should localize the integral to the IR-divergent regions of loop momentum-space collinear to the external particles. In the dual co-ordinate space, this is the region localized to the edges of the null-polygonal Wilson loop. It seems likely that these IR-anomalies fully control the structure of the amplitude. Amongst other things, they must lie behind the astonishing simplicity recently uncovered in the structure of the remainder function for the 2-loop, 6-particle MHV amplitude [22]. In the same line of thought, it is conceivable that there is a very direct link between the Yangian structure we uncovered and the very beautiful connections made at strong coupling with integrable systems, Y-systems, TBA equations and the Yang-Yang functional [54, 113]. Already these developments have allowed a bridge to weak coupling by computing sub-leading corrections to collinear limits [55, 114, 115].

⁹We thank Peter Goddard for this remark.

Having said all of this, there is a very important issue that must be addressed to make progress in directly computing these Yangian-“invariant” but non-local integrals. The question is of course how to handle IR-regularization for these objects. Dimensional regularization has long been the preferred method for regulating IR-divergences in gauge theories, but it does particularly violent damage to the structure of the integrand, and is not useful for our purposes. Fortunately, there is a better regulator, both conceptually and computationally. Physically, the IR-divergences are removed by moving out on the Coulomb branch [67]. This gives a beautifully simple way to regulate the integrals in momentum-twistor space which is also useful for practical computations [116, 117]. With the loop integrand written in local form, one simply deforms the local propagators as $\langle AB \ j-1 \ j \rangle \mapsto \langle AB \ j-1 \ j \rangle + m^2 \langle AB \rangle \langle j-1 \ j \rangle$. The physics is always four dimensional. The ambiguities in this regulator occur at an irrelevant level $\mathcal{O}(m^2)(\log(m^2))^p$. In particular there are no issues with the notorious “ μ -terms” in dimensional regularization, and we don’t encounter the ubiquitous ϵ/ϵ effects either. This is clearly the physically correct regularization for our set-up.

How should we use this regularization to compute the non-local integrals of interest? One can glibly regulate all 4-brackets $\langle AB \ xy \rangle \mapsto \langle AB \ xy \rangle + m^2 \langle AB \rangle \langle xy \rangle$, but this is not physically correct: the regularization of the local propagators is reflecting the (local!) masses induced by Higgsing; and so it is not clear how the non-local propagators should be regularized. Indeed, we have checked that for the 1-loop MHV amplitudes, this very naïve regularization of the integrals does not produce the standard result. Of course, since the Yangian invariant form of the full amplitude can be expanded in terms of local integrals, we can in principle work backwards to see how the correct local regulator affects the non-local integrand; the question is whether there is a sensible way of computing these non-local integrals directly. We intend to return to these questions in near future.

We have emphasized that the Yangian-invariant presentation of the loop integrand strongly suggests that the integrals should be simple. But as we have seen in a number of examples, even the local forms of the integrand, when written in terms of the natural chiral basis of momentum-twistor space integrals with unit leading singularities, look surprisingly elegant. In fact, these integrals with unit leading singularities should also be “simple”. The reason is precisely that their leading singularities are

“1” or “0”; these are the only possible values of the integrals on any closed contour of integration, independent of the kinematic variables. This means that *e.g.* $\partial/\partial Z_a^I$ acting on these integrals should also be a total derivative with respect to the loop variables, and that they too should be localized to regions with collinear singularities. Since these are local integrals their regularization is well defined. Indeed, as we pointed out in our multi-loop examples, the naïvely “hardest” integrals are even IR-finite. The integrals for our form of the two-loop 6-point MHV amplitude have been computed analytically passing all non-trivial checks. The simplicity of these partial results strongly supports the idea that the full amplitude computed with these integrals are also simple.

III. Other Planar Theories

We end by stressing that many of the ideas in this chapter are likely to generalize beyond the very special case of $\mathcal{N} = 4$ SYM. Since the integrand is well-defined in any planar theory, one can try to determine it with recursion relations just as we have done for $\mathcal{N} = 4$ SYM. In [103], it was argued that the single-cuts of the 1-loop amplitude are well-defined for any theory with at least $\mathcal{N} = 1$ SUSY (or $\mathcal{N} = 2$ in the presence of massive particles), so the BCFW recursion determines amplitudes at least up to 1-loop in these theories too, with or without maximal SUSY and Yangian-invariance. In non-supersymmetric theories, further progress on these questions will require a better understanding of single-cuts. One difficulty is that the naïve forward limit of tree amplitudes is ill-defined. It is plausible that this is closely related to presence of rational terms in 1-loop amplitudes, which have a beautiful and fascinating structure which is strongly suggestive of a deeper origin.

Chapter 3 *Scattering Amplitudes and Positive Grassmannian*

3.1 Overview of the chapter

All the developments in the field of scattering amplitudes have made completely clear that there are powerful new mathematical structures underlying the extraordinary properties of scattering amplitudes in gauge theories. If history is any guide, formulating and understanding the physics in a way that makes the symmetries manifest should play a central role in the story. The Grassmannian picture does this, but up to this point there has been little understanding for why this formulation exists, exactly how it works, or where it comes from physically. Our primary goal in this chapter is to resolve this unsatisfactory state of affairs.

This new way of thinking about scattering amplitudes involves many novel physical and mathematical ideas. Our presentation will be systematic, and we have endeavored to make it self contained and completely accessible to physicists. While we will discuss a number of mathematical results—some of them new—we will usually be content with the physicist’s level of rigor. While the essential ideas here are all very simple, they are tightly interlocking, and range over a wide variety of areas—most of which are unfamiliar to most physicists. Thus, before jumping into the detailed exposition, as a guide to the reader we end this introductory section by giving a roadmap of the logical structure and content of the chapter.

In section 3.2, we introduce the central physical idea motivating our work, which is to focus on *on-shell diagrams*, obtained by gluing together fundamental 3-particle amplitudes and integrating over the on-shell phase space of internal particles. These objects are of central importance to the understanding scattering amplitudes. We will see that scattering amplitudes in planar $\mathcal{N}=4$ SYM—to all loop orders—can be represented *directly* in terms of on-shell processes. In this picture, “virtual particles”

make no appearance at all. We should emphasize that we are not merely using on-shell information to determine scattering amplitudes, but rather seeing that the amplitudes can be directly computed in terms of fully on-shell processes. The off-shell, virtual particles familiar from Feynman diagrams are replaced by internal, *on-shell* particles (with generally complex momenta).

In our study of on-shell diagrams, we will see that different diagrams related by certain elementary moves can be physically equivalent, leading to the natural question of how to invariantly characterize their physical content. Remarkably, the invariant content of on-shell diagrams turns out to be characterized by *permutations*. We discuss this in detail in section 3.3 where we show how a long-known and beautiful connection between permutations and scattering amplitudes in integrable (1+1)-dimensional theories generalizes to more realistic theories in (3+1) dimensions.

In section 3.4 we turn to actually calculating on-shell diagrams and find that the most natural way of carrying out the computations is to associate each diagram with a certain differential form on an auxiliary Grassmannian. In sections 3.5 and 3.6 we show how the invariant, combinatorial content of an on-shell diagram is reflected in the Grassmannian directly. This is described in terms of a surprisingly simple stratification of the configurations of k -dimensional vectors endowed with a cyclic ordering, classified by the linear dependencies among consecutive chains of vectors. For the real Grassmannian, this stratification can be equivalently described in an amazingly simple and beautiful way as nested ‘boundaries’ of the *positive part* of the Grassmannian, [43], which is motivated by the theory of totally positive matrices, [38, 118, 119]. Each on-shell diagram can then be associated with a particular configuration or “stratum” among the boundaries of the positive Grassmannian.

In section 3.7 we make contact with the Grassmannian contour integral of reference [16], which is now seen as a compact way of representing the natural, invariant top-form on the positive Grassmannian. This form of the measure allows us to easily identify the conformal and dual conformal symmetries of the theory which are related by a simple mapping of permutations described in section 3.8. In section 3.9, we show that the invariance of scattering amplitudes under the action of the level-one generators of the Yangian has a transparent interpretation: these generators correspond to the leading, non-trivial diffeomorphisms that preserve all the cells of the positive

Grassmannian.

In section 3.10 we begin a systematic classification of Yangian invariants and their relations by first describing a combinatorial test to determine whether an on-shell diagram has non-vanishing kinematical support (and if so, how many points of support exist). In section 3.11 a geometric basis is given for all the myriad, highly non-trivial identities satisfied among Yangian-invariants. This completes the classification of *all* Yangian Invariants together with *all* their relations.

In section 3.12 we show that the story for scattering amplitudes in integrable (1+1)-dimensional theories—in particular, the Yang-Baxter relation—can be understood as a special case of our general results regarding on-shell diagrams. We further show that scattering amplitudes for the ABJM theory in (2+1) dimensions, [120], can also be computed in terms of a natural specialization of on-shell diagrams: those associated with the null orthogonal Grassmannian. And we initiate the study of on-shell diagrams in theories with less (or no) supersymmetry in section 3.13.

In section 3.14 we move beyond the discussion of individual on-shell diagrams and describe the particular combinations which represent scattering amplitudes. We present a self-contained direct proof—using on-shell diagrams alone—that the BCFW construction of the all-loop integrand generates an object with precisely those singularities dictated by quantum field theory. We then show that the Grassmannian representation of loop-integrands are always given in a remarkable, “*dlog*” form, which we illustrate using examples of simple, one- and two-loop amplitudes. We discuss the implications of this representation for the transcendental functions that arise after the loop integrands are integrated.

We conclude our story in section 3.15 with a discussion of a number of the outstanding, open directions for further research.

3.2 On-Shell Diagrams

Theoretical explorations in field theory have been greatly advanced by focusing on interesting classes of observables—from local correlation functions and scattering amplitudes, to Wilson and 't Hooft loops, surface operators and line defects, to partition functions on various manifolds (see e.g. [121, 122]). The central physical idea of our work is to study *on-shell scattering processes* as a new set of objects of fundamental interest.

I. On-Shell Building Blocks: the Three-Particle Amplitudes

The fundamental building blocks for all on-shell scattering processes are the three-particle amplitudes, which are completely determined (up to an overall coupling constant) by Poincaré invariance. This is a consequence of the unique simplicity of three-particle kinematics. It is very easy to show that momentum conservation can only be satisfied if either: (A) all the λ 's are proportional to each other, or (B) all the $\tilde{\lambda}$'s are proportional:

$$\lambda_1 \tilde{\lambda}_1 + \lambda_2 \tilde{\lambda}_2 + \lambda_3 \tilde{\lambda}_3 = 0 \iff \left\{ \begin{array}{l} (A) : \lambda_1 \propto \lambda_2 \propto \lambda_3 \\ (B) : \tilde{\lambda}_1 \propto \tilde{\lambda}_2 \propto \tilde{\lambda}_3 \end{array} \right\}. \quad (3.2.1)$$

Because of this, in the kinematic configuration where all the λ 's are proportional, the amplitude can *only* depend non-trivially on the $\tilde{\lambda}$'s, and vice-versa. The dependence on $\lambda(\tilde{\lambda})$ is fully determined by the weights, together with the requirement that the amplitude is non-singular in the limit where the momenta are taken real (see equation (3.2.5)).

We will denote the three-particle amplitude associated with the configuration where all the λ 's ($\tilde{\lambda}$'s) are parallel with a white (black) three-point vertex. In a non-supersymmetric theories, i.e. with only gluons, these are associated with helicity configurations involving one (two) negative-helicity gluons:

$$\begin{array}{ccc} \begin{array}{c} 2^+ \\ \diagup \\ \text{---} \text{O} \text{---} \\ \diagdown \\ 3^+ \\ 1^- \end{array} & \text{and} & \begin{array}{c} 2^- \\ \diagup \\ \text{---} \text{O} \text{---} \\ \diagdown \\ 3^- \\ 1^+ \end{array} \end{array} \quad (3.2.2)$$

The corresponding helicity amplitudes are given by,

$$\begin{aligned} A_3^{(1)}(-, +, +) &= \frac{[23]^3}{[12][31]} \delta^{2 \times 2} (\lambda_1 \tilde{\lambda}_1 + \lambda_2 \tilde{\lambda}_2 + \lambda_3 \tilde{\lambda}_3); \\ A_3^{(2)}(+, -, -) &= \frac{\langle 23 \rangle^3}{\langle 12 \rangle \langle 31 \rangle} \delta^{2 \times 2} (\lambda_1 \tilde{\lambda}_1 + \lambda_2 \tilde{\lambda}_2 + \lambda_3 \tilde{\lambda}_3). \end{aligned} \quad (3.2.3)$$

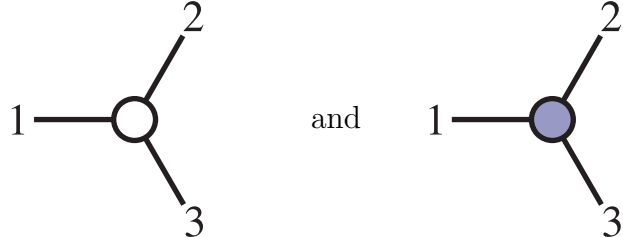
Here, we have made use of the Lorentz-invariants constructed out of the spinors,

$$\langle a b \rangle \equiv \det\{\lambda_a, \lambda_b\} \quad \text{and} \quad [a b] \equiv \det\{\tilde{\lambda}_a, \tilde{\lambda}_b\}. \quad (3.2.4)$$

These amplitudes are of course what we get from the two-derivative Yang-Mills Lagrangian. Amplitudes involving all-plus or all-minus helicities are also fixed by Poincaré invariance in the same way, but arise only in theories with higher-dimension operators like F^3 or R^3 . In general, Poincaré invariance fixes the kinematical dependence of the three-particle amplitude involving massless particles with arbitrary helicities to be, [123]:

$$A_3(h_1, h_2, h_3) \propto \begin{cases} [12]^{h_1+h_2-h_3} [23]^{h_2+h_3-h_1} [31]^{h_3+h_1-h_2} & \sum h_a > 0; \\ \langle 12 \rangle^{h_3-h_1-h_2} \langle 23 \rangle^{h_1-h_2-h_3} \langle 31 \rangle^{h_2-h_3-h_1} & \sum h_a < 0. \end{cases} \quad (3.2.5)$$

As mentioned above, in maximally supersymmetric theories all helicity states are unified in a single super-multiplet, and so there is no need to distinguish among the particular helicities of particles involved; and so, we may consider the simpler, cyclically-invariant amplitudes:



$$1 \text{ --- } \bigcirc \begin{matrix} / 2 \\ \backslash 3 \end{matrix} \quad \text{and} \quad 1 \text{ --- } \bigcirc \begin{matrix} / 2 \\ \backslash 3 \end{matrix} \quad (3.2.6)$$

The first includes among its components the $(-, +, +)$ amplitude of (3.2.2), while the latter includes the $(+, -, -)$ amplitude. These super-amplitudes are given by,

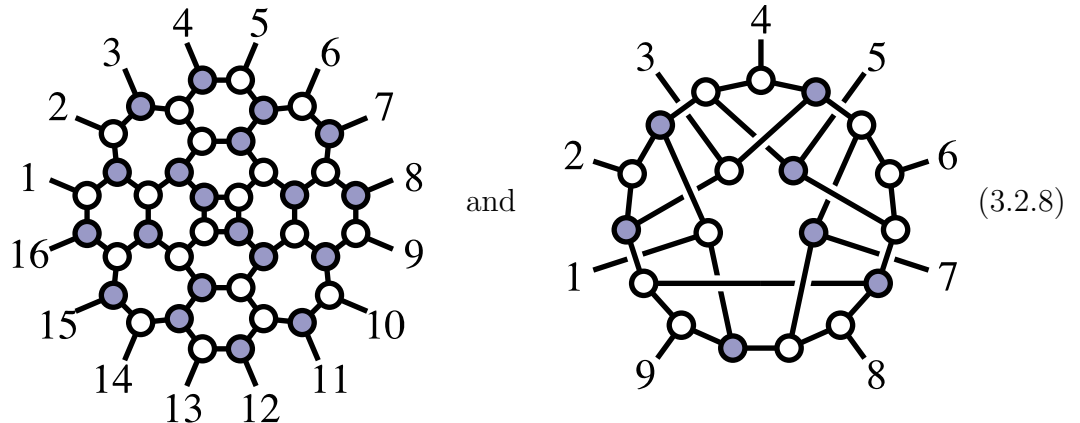
$$\begin{aligned} \mathcal{A}_3^{(1)} &= \frac{\delta^{1 \times 4} ([23] \tilde{\eta}_1 + [31] \tilde{\eta}_2 + [12] \tilde{\eta}_3)}{[12][23][31]} \delta^{2 \times 2} (\lambda_1 \tilde{\lambda}_1 + \lambda_2 \tilde{\lambda}_2 + \lambda_3 \tilde{\lambda}_3); \\ \mathcal{A}_3^{(2)} &= \frac{\delta^{2 \times 4} (\lambda_1 \tilde{\eta}_1 + \lambda_2 \tilde{\eta}_2 + \lambda_3 \tilde{\eta}_3)}{\langle 12 \rangle \langle 23 \rangle \langle 31 \rangle} \delta^{2 \times 2} (\lambda_1 \tilde{\lambda}_1 + \lambda_2 \tilde{\lambda}_2 + \lambda_3 \tilde{\lambda}_3). \end{aligned} \quad (3.2.7)$$

(Although not essential for our present considerations, it may be of some interest that these objects can be made fully *permutation* invariant by including also a prefactor f^{a_1, a_2, a_3} depending on the ‘colors’ a_i of the particles involved (where ‘color’ is

simply a label denoting the possible distinguishable states in the theory). General considerations of quantum mechanics and locality (see e.g. [123]) require that any such prefactor must be fully antisymmetric and satisfy a Jacobi identity—implying that color labels combine to form the adjoint representation of a Lie algebra. The most physically interesting case is when this is the algebra of $U(N)$; in this case, N can be viewed as a *parameter* of the theory, and scattering amplitudes can be expanded in powers of $1/N$ to all orders of perturbation theory, [124]. In this chapter, we will mostly concern ourselves with the leading-terms in $1/N$ —the *planar* sector of the theory.)

II. Gluing Three-Particle Amplitudes Into On-Shell Diagrams

It is remarkable that three-particle amplitudes are totally fixed by Poincaré symmetry; they carry all the essential information about the particle content and obvious symmetries of the physical theory. It is natural to “glue” these elementary building blocks together to generate more complicated objects we will call *on-shell diagrams*. Such objects will be our primary interest in this chapter; examples of these include:



We draw both planar and non-planar examples here to stress that on-shell diagrams have nothing to do with planarity. In this chapter, however, we will focus on the case of planar $\mathcal{N} = 4$; we leave a systematic exploration of non-planar on-shell diagrams to future work.

Note that on-shell diagrams such as those of (3.2.8) are *not* Feynman diagrams! There are no “virtual” or “off-shell” internal particles involved: *all the lines in these pictures are on-shell* (meaning that their momenta are null). Each internal line represents a sum over all possible particles which can be exchanged in the theory, with

(often complex) momenta constrained by momentum conservation at each vertex—integrating over the on-shell phase space of each. If I denotes an internal particle with momentum $p_I = \lambda_I \tilde{\lambda}_I$ and helicity h_I , then p_I flows into one vertex with helicity h_I , and $(-p_I)$ flows into the other with helicity $(-h_I)$. In pure (non-supersymmetric) Yang-Mills we would have, [51],

$$\sum_{h_I=\pm} \int \frac{d^2 \lambda_I d^2 \tilde{\lambda}_I}{\text{vol}(GL(1))}, \quad (3.2.9)$$

for each internal line; in a theory with maximal supersymmetry we would have,

$$\int \frac{d^2 \lambda_I d^2 \tilde{\lambda}_I}{\text{vol}(GL(1))} d^4 \tilde{\eta}. \quad (3.2.10)$$

Here, the on-shell phase-space integral is clearly over $\lambda, \tilde{\lambda}$, modulo the $GL(1)$ -redundancy of the little group—rescaling $\lambda_I \mapsto t_I \lambda_I$ and $\tilde{\lambda}_I \mapsto t_I^{-1} \tilde{\lambda}_I$.

In general, we have some number of integration variables corresponding to the (on-shell) internal momenta, and δ -functions enforcing momentum-conservation at each vertex. We may have just enough δ -functions to *fully localize* all the internal momenta; in this case the on-shell diagram becomes an ordinary *function* of the external data, which has historically been called a “leading singularity” in the literature [11, 68]. If there are more δ -functions than necessary to fix the internal momenta, the left-over constraints will impose conditions on the external momenta; such an object is said to be a *singularity* or to have “singular support”. If there are fewer δ -functions than necessary to fix the internal momenta, there will be some degrees of freedom left over; the on-shell diagram then leaves us with some *differential form* on these extra degrees of freedom which we are free to integrate over any contour we please. But there is no fundamental distinction between these cases; and so we will generally think of an on-shell diagram as providing us with an “on-shell form”—a differential form defined on the space of external *and* internal on-shell momenta. If we define the (super) phase space factor of the on-shell particle denoted a by,

$$\Omega_a = \frac{d^2 \lambda_a d^2 \tilde{\lambda}_a}{\text{vol}(GL(1))} d^4 \tilde{\eta}_a, \quad (3.2.11)$$

then we can think of the 3-particle amplitude involving particles a, b, c also as a *form*:

$$\mathcal{A}_3 \Omega_a \Omega_b \Omega_c. \quad (3.2.12)$$

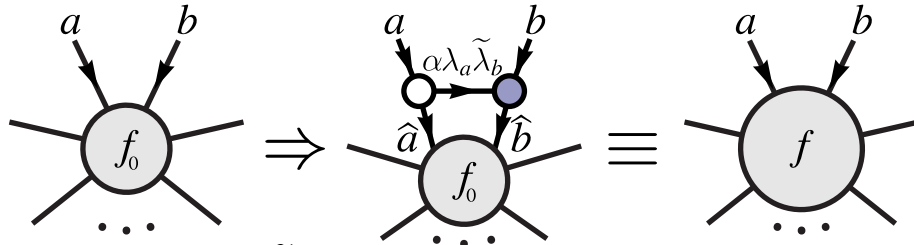
Putting all the 3-particle amplitudes in an on-shell diagram together gives rise to a (typically high-dimensional) differential form on the space of external and internal

momenta. The on-shell form associated with a diagram is then obtained by taking residues of this high-dimensional form on the support of all the δ -function constraints (thought of *holomorphically*—as representing poles which enforce their arguments to vanish); this produces a lower-dimensional form defined on the support of any remaining δ -functions.

Individual Feynman diagrams are *not* gauge invariant and thus don't have any physical meaning. By contrast, each on-shell diagram *is* physically meaningful and corresponds to some particular on-shell scattering process. Note that although on-shell diagrams almost always involve ‘loops’ of internal particles, these internal particles often have momenta *fixed* by the constraints (or are otherwise free). On-shell forms are simply the products of on-shell 3-particle amplitudes; as such, they are always well-defined, finite objects—free from either infrared or ultraviolet divergences. This makes them ideal for exposing symmetries of a theory which are often obscured by such divergences.

III. The BCFW “Bridge”

One particularly simple way of building-up more complicated on-shell diagrams from simpler ones will play an important role in our story. Starting from any on-shell diagram, we can pick two external lines, and attach a “BCFW-bridge” to make a new diagram as follows:



Note that the momentum $\lambda_I \tilde{\lambda}_I$ flowing through the *bridge*, as indicated by the arrow, is very special: the white vertex on the left forces $\lambda_I \propto \lambda_a$, and the black vertex on the right forces $\tilde{\lambda}_I \propto \tilde{\lambda}_b$; thus, $\lambda_I \tilde{\lambda}_I = \alpha \lambda_a \tilde{\lambda}_b$ for some α . The momenta entering the rest of the graph through legs $(a b)$ are deformed according to:

$$\left\{ \begin{array}{l} \lambda_a \mapsto \lambda_{\hat{a}} = \lambda_a \\ \tilde{\lambda}_a \mapsto \tilde{\lambda}_{\hat{a}} = \tilde{\lambda}_a - \alpha \tilde{\lambda}_b \end{array} \right\} \quad \text{and} \quad \left\{ \begin{array}{l} \lambda_b \mapsto \lambda_{\hat{b}} = \lambda_b + \alpha \lambda_a \\ \tilde{\lambda}_b \mapsto \tilde{\lambda}_{\hat{b}} = \tilde{\lambda}_b \end{array} \right\}. \quad (3.2.13)$$

For theories with supersymmetry, there is also a deformation of $\tilde{\eta}_a$ according to $\tilde{\eta}_a \mapsto \tilde{\eta}_a - \alpha \tilde{\eta}_b$. (It is useful to remember that $\tilde{\eta}$ *always* transforms as $\tilde{\lambda}$ does.)

Thus, attaching a BCFW-bridge adds one new variable, α , to an on-shell form f_0 , and gives rise to a new on-shell form f given by,

$$\begin{aligned} f(\dots; \lambda_a, \tilde{\lambda}_a, \tilde{\eta}_a; \lambda_b, \tilde{\lambda}_b, \tilde{\eta}_b; \dots) &= \frac{d\alpha}{\alpha} f_0(\dots; \lambda_{\tilde{a}}, \tilde{\lambda}_{\tilde{a}}, \tilde{\eta}_{\tilde{a}}; \lambda_{\tilde{b}}, \tilde{\lambda}_{\tilde{b}}, \tilde{\eta}_{\tilde{b}}; \dots); \\ &= \frac{d\alpha}{\alpha} f_0(\dots; \lambda_a, \tilde{\lambda}_a - \alpha \tilde{\lambda}_b, \tilde{\eta}_a - \alpha \tilde{\eta}_b; \lambda_b + \alpha \lambda_a, \tilde{\lambda}_b, \tilde{\eta}_b; \dots). \end{aligned} \quad (3.2.14)$$

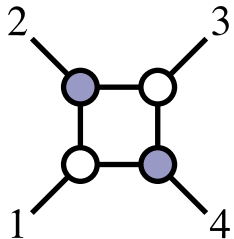
Notice that *very* complex on-shell diagrams (both planar and non-planar alike) can be generated by successively attaching BCFW-bridges to a small set of ‘simple’ diagrams. As we will soon understand, it turns out that *all* (physically-relevant) on-shell diagrams can be constructed in this way.

IV. On-Shell Recursion for All-Loop Amplitudes

While on-shell diagrams are interesting in their own right, for planar $\mathcal{N}=4$ SYM, we will see that they are of much more than purely formal interest. Scattering amplitudes at all-loop order can be directly represented and computed as on-shell scattering processes. This is quite remarkable, considering the ubiquity of “off-shell” data in the more familiar Feynman expansion.

Of course by now we have become accustomed to the idea that amplitudes can be ‘determined’ using on-shell data—as evidenced, for instance, by the BCFW recursion relations at tree-, [14, 82], and loop levels, [65] (see also [125–128]). But our statement goes beyond this: the claim is not just that an off-shell object such as “the loop integrand” can be *determined* using only on-shell information, but rather that they can be *directly represented* by fully on-shell objects.

Before discussing loops, let us look at some examples of “tree-level” amplitudes. Recall from [129] that the four-particle tree-amplitude $\mathcal{A}_4^{(2)}$ can be represented by a single on-shell diagram—its “BCFW representation”:



$$(3.2.15)$$

This is very far from what would be obtained using Feynman diagrams which would have represented (3.2.15) as the sum of three terms,

$$(3.2.16)$$

the first two of which involve *off-shell* gluon exchange. (The terms “tree-amplitude” and “loop-amplitude” are artifacts of such Feynman-diagrammatic expansions.) Another striking difference is that, despite the fact that we’re discussing a *tree*-amplitude, the on-shell diagram (3.2.15) looks like a loop! To emphasize this distinction, consider a (possibly more familiar) “tree-like” on-shell graph such as:

$$(3.2.17)$$

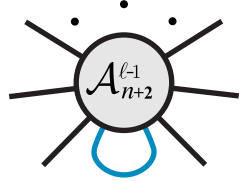
Since the internal line in this graph must be on-shell, the diagram imposes a δ -function constraint $\delta((p_1 + p_2)^2)$ on the external momenta; and so, (3.2.17) corresponds to a singularity—a *factorization channel*. The extra leg in (3.2.15) that makes the “loop” allows for a non-vanishing result for *generic* (on-shell, momentum-conserving) external momenta. It is interesting to note that we can interpret (3.2.15) as having been obtained by attaching a “BCFW-bridge” to *any* of the factorization channels of the four-particle amplitude—such as that of (3.2.17). This makes it possible for the single diagram (3.2.15) to *simultaneously* exhibit *all* the physical factorization channels.

This simple example illustrates the fundamental physical idea behind the BCFW description of an amplitude—not just at tree-level, but at all loop orders: any amplitude can be *fully* reconstructed from the knowledge of its singularities; and the singularities of an amplitude are determined by entirely by on-shell data. At tree-level, the singularities are simply the familiar factorization channels,

$$(3.2.18)$$

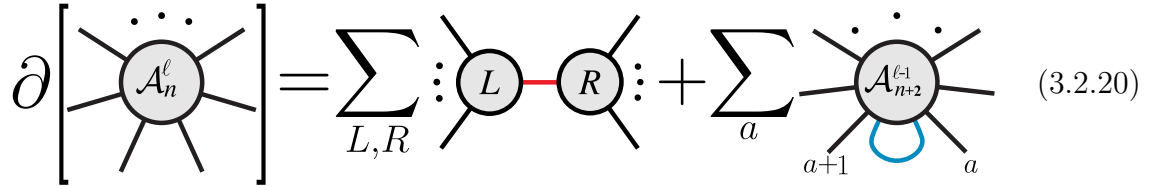
where the left- and right-hand sides are both fully on-shell scattering amplitudes. At loop-level, all the singularities of the integrand can be understood as factorizations

like that of (3.2.18), or those for which an *internal* particle is put on-shell; at least for $\mathcal{N} = 4$ SYM in the planar limit, these singularities are given by the “forward-limit” [103] of an on-shell amplitude with one fewer loop and two extra particles, where any two adjacent particles have equal and opposite momenta, denoted:



$$(3.2.19)$$

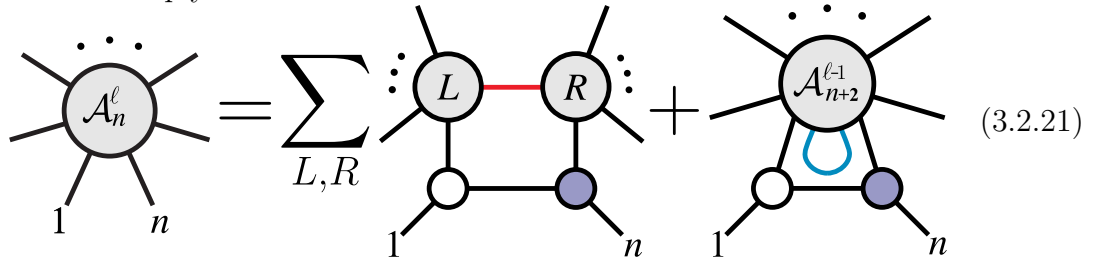
Combining these two terms, the singularities of the *full amplitude* are, [65]:



$$(3.2.20)$$

Here we have suggestively used the symbol “ ∂ ” to signify “singularity of”. Of course, the symbol ∂ is often used to denote “boundary” or “derivative”; we will soon see that all of these senses are appropriate.

Equation (3.2.20) can be understood as defining a “differential equation” for scattering amplitudes; and it turns out to be possible to ‘integrate’ it directly. This is precisely what is accomplished by the BCFW recursion relations. For planar $\mathcal{N} = 4$ SYM, the all-loop BCFW recursion relations, when represented in terms of on-shell diagrams are simply:



$$(3.2.21)$$

The structure of this solution will be discussed in much greater detail in section 3.14. For instance, notice that this presentation only makes *some* of the factorization channels and forward-limits manifest, and seems to break the cyclic symmetry of the amplitude by singling-out legs (1 n). In other words, working intrinsically with on-shell diagrams, it is not obvious that the sum (3.2.21) includes *all* the required singularities of an amplitude. Of course Feynman diagrams *do* make it manifest that such an

object exists; but it would be nice to understand this more directly, without recourse to the usual formalism of field theory. We will show how this works in subsection I., demonstrating that (3.2.21) has all the necessary singularities purely from within the framework of on-shell diagrams.

The seed of loop integrands in the recursion relation are the “forward-limit” terms as the three-point amplitudes are fixed by Poincaré invariance to all loop-orders. Each loop is accompanied by four integration variables: three of these are given by the phase space of the forward-limit momentum $\lambda_{AB}\tilde{\lambda}_{AB}$ (from merging legs ‘A’ and ‘B’), and the BCFW deformation parameter α is the fourth. Of course, all the objects appearing in these expressions are completely on-shell, and so do not seem to contain anything that looks like the conventional “ $\int d^4\ell$ ” with which we are accustomed (where ℓ is the momentum of a generally off-shell, *virtual* particle). However, it is easy to convert the parameters of the on-shell forward-limit to the more familiar one via the identification:

$$\ell \equiv \lambda_{AB}\tilde{\lambda}_{AB} + \alpha \lambda_1\tilde{\lambda}_n \quad \text{with} \quad d^4\ell = \frac{d^2\lambda_{AB}d^2\tilde{\lambda}_{AB}}{\text{vol}(GL(1))}d\alpha \langle 1 \lambda_{AB} \rangle [n \tilde{\lambda}_{AB}]. \quad (3.2.22)$$

At L loops, the all-loop recursion relation produces a $4L$ -form, and we can identify the $4L$ integration variables with loop momenta at each order via (3.2.22). Integrating these on-shell forms over a contour which restricts each loop-momentum to be *real* (i.e. in $\mathbb{R}^{3,1}$) generates the final, physical amplitude.

Thus, as advertised, on-shell diagrams are of much more than mere academic interest: they *fully* determine the amplitude in planar $\mathcal{N}=4$ SYM to *all loop-orders*.

V. Physical Equivalences Among On-Shell Diagrams

We have seen that on-shell diagrams are objects of fundamental importance to the physics of scattering amplitudes. It is therefore natural to try and compute the forms associated with on-shell diagrams more explicitly, and better understand their structure. At first sight, the class of on-shell diagrams may look as complicated as Feynman diagrams. For instance, even for a fixed number of external particles, there are obviously an infinite number of such diagrams (by continuously adding BCFW bridges, for example). As we will see however, at least for $\mathcal{N}=4$ SYM in the planar limit, this complexity is entirely illusory. The reason is that apparently very different

graphs actually give rise to exactly the same differential form—differing only by a change of variables.

The first instance of this phenomenon is extremely simple and trivial. Consider an analog of the “factorization channel” diagram (3.2.17), but connecting two black vertices. Because these vertices require that all the $\tilde{\lambda}$'s be parallel, it makes no physical difference how they are connected. And so, on-shell diagrams related by,

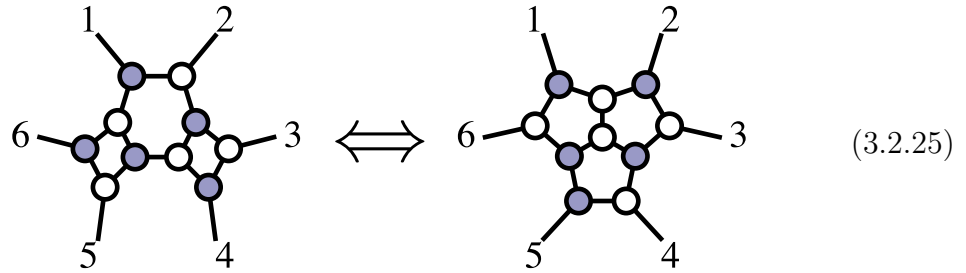
(3.2.23)

represent the same on-shell form. Thus, we can collapse and re-expand any chain of connected black vertices in anyway we like; the same is obviously true for white vertices. Because of this, for some purposes it may be useful to define composite black and white vertices with any number of legs. By grouping black and white vertices together in this way, on-shell diagrams can always be made *bipartite*—with (internal) edges only connecting white to black vertices. We will, however, preferentially draw trivalent diagrams because of the fundamental role played by the three-particle amplitudes.

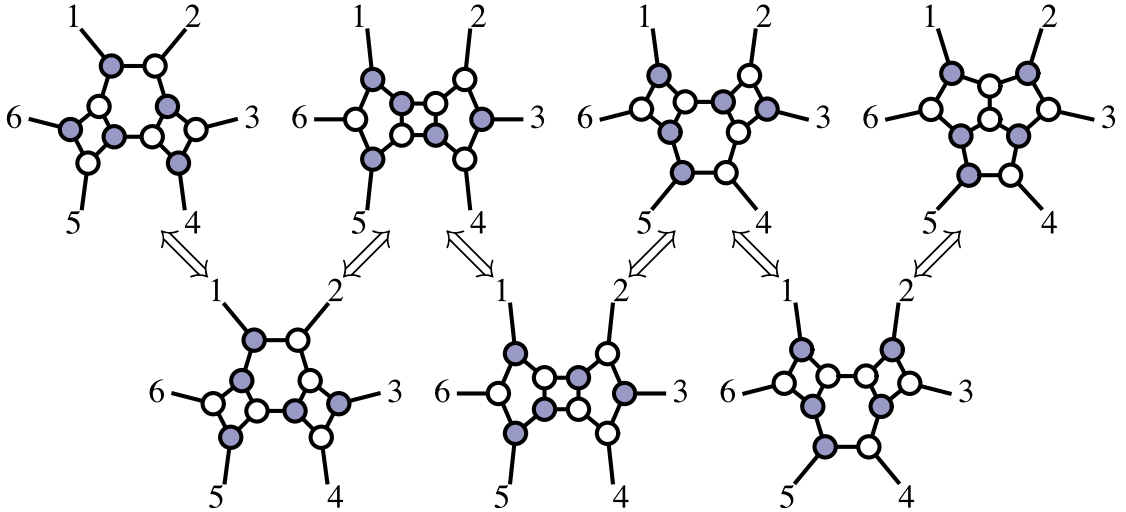
There is also a more interesting equivalence between on-shell diagrams that will play an important role in our story. We can see this already in the BCFW representation of the four-particle amplitude given above, (3.2.15). The *picture* is obviously not cyclically invariant—as a rotation would exchange its black and white vertices. But the four-particle *amplitude* of course *is* cyclically invariant; and so there is another generator of equivalences among on-shell diagrams, the “square move”, [112]:

(3.2.24)

The merger and square moves can be used to show the physical equivalence of many seemingly different on-shell diagrams. For instance, the following two diagrams generate physically equivalent on-shell forms:

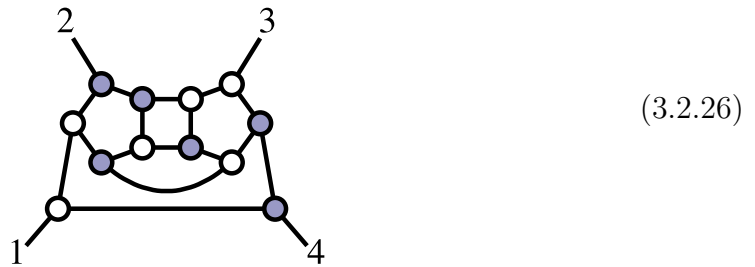


We can see this by explicitly constructing the chain of moves which brings one graph into the other:



Here, each step down involves one or more square-moves, and each step up involves one or more mergers.

To give another example, the on-shell diagram representing the one-loop four-particle amplitude—as obtained directly from BCFW recursion—is given by:



Using a series of mergers and square moves, it can be brought to the beautifully symmetric, bipartite form:

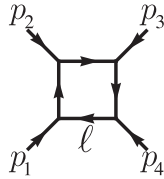


These forms are completely equivalent, but suggest very different physical interpretations. The first, (3.2.26), clearly exposes its origin as a forward-limit—arising through the gluing of two of the external particles of the six-particle tree-amplitude. The second form, (3.2.27), does not look like this at all; instead, it appears to represent four BCFW-bridges attached to an internal square—which is of course the four-particle tree-amplitude. Thus, in this picture, we can think of the one-loop amplitude as an integral over a four-parameter deformation of the tree-amplitude!

This is more than mere amusement. It immediately tells us that with an appropriate choice of variables representing the BCFW-shifts, the one-loop amplitude can be represented in a remarkably simple form:

$$\mathcal{A}_4^{\ell=1} \propto \mathcal{A}_4^{\ell=0} \times \int \frac{d\alpha_1}{\alpha_1} \frac{d\alpha_2}{\alpha_2} \frac{d\alpha_3}{\alpha_3} \frac{d\alpha_4}{\alpha_4}. \quad (3.2.28)$$

Of course, this does not look anything like the more familiar expression, [130],

$$\mathcal{A}_4^{\ell=1} \propto \mathcal{A}_4^{\ell=0} \times \int \frac{d^4\ell}{\ell^2(\ell+p_1)^2(\ell+p_1+p_2)^2(\ell-p_4)^2} \cdot \quad (3.2.29)$$


In this form, it is not at all obvious that there is any change of variables that reduces the integrand to the “ $d\log$ ”-form of (3.2.28). However, following the rule for identifying off-shell loop momenta in terms of on-shell data, (3.2.22), we may easily identify the map which takes us from the ℓ of (3.2.29) to the α_i of (3.2.28):

$$\begin{aligned} & \frac{d^4\ell}{\ell^2(\ell+p_1)^2(\ell+p_1+p_2)^2(\ell-p_4)^2} \\ &= d\log\left(\frac{\ell^2}{(\ell-\ell^*)^2}\right) d\log\left(\frac{(\ell+p_1)^2}{(\ell-\ell^*)^2}\right) d\log\left(\frac{(\ell+p_1+p_2)^2}{(\ell-\ell^*)^2}\right) d\log\left(\frac{(\ell-p_4)^2}{(\ell-\ell^*)^2}\right), \end{aligned} \quad (3.2.30)$$

where ℓ^* is either of the two points null separated from all four external momenta. This expression will be derived in detail in subsection III..

As we will see, the existence of this “ $d\log$ ” representation for loop integrands is a completely general feature of all amplitudes at all loop-orders. But the possibility of such a form even existing was never anticipated from the more traditional formulations of field theory. Indeed, even for the simple example of the four-particle one-loop amplitude, the existence of a change of variables converting $d^4\ell$ to four $d\log$ ’s went

unnoticed for decades. We will see that these “ $d\log$ ”-forms follow directly from the on-shell diagram description of scattering amplitudes generated by the BCFW recursion relations, (3.2.21). Beyond their elegance, these $d\log$ -forms suggest a completely new way of carrying out loop integrations, and more directly expose an underlying, “motivic” structure of the final results which will be a theme pursued in a later, more extensive work.

The equivalence of on-shell diagrams related by mergers and square-moves clearly represents a major simplification in the structure on-shell diagrams; but these alone cannot reduce the seemingly infinite complexities of graphs with arbitrary numbers of ‘loops’ (faces) as neither of these operations affect the number of faces of a graph. However, using mergers and square-moves, it may be possible to represent an on-shell diagram in a way that exposes a “bubble” on an internal line. As one might expect, there is a sense in which such diagrams can be *reduced* by eliminating bubbles:

(3.2.31)

Of course this can’t literally be true: there is one more integration variable in the diagram with the bubble than the one without. What “reduction” actually means is that there is a concrete *and simple* change of variables for which this extra degree of freedom, say α , factors-out of the on-shell form cleanly as $d\log \alpha$ —which, upon taking the residue on a contour around $\alpha = 0$, yields the reduced diagram and the associated on-shell form.

Before completing our discussion, it is worth mentioning that there are other—somewhat trivial—operations on diagrams which leave the corresponding on-shell form invariant; these include, adding or deleting a bivalent vertex (of either color) along a line, or exchanging the colors involved in a bubble such as that in (3.2.31).

It turns out that using mergers, square-moves *and* bubble-deletion, all planar on-shell diagrams involving n external particles can be reduced to a *finite* number of diagrams. This shows that the essential content of on-shell diagrams are encapsulated by the finite list of *reduced* objects. And as we will see, the extra, “irrelevant” variables

associated with bubble-deletion also have a purpose in life: they represent the loop integration variables.

Reduced diagrams are still not unique of course: they can still be transmuted into each other using mergers and square-moves. Given that the same on-shell form can be represented by many different on-shell diagrams, it is natural to ask for some *invariant* way to characterize them. For instance, if we are given two complicated on-shell diagrams such as those of (3.2.25), how can we decide whether they can be morphed into each other using the merge and square-moves? The answer to this question ends up being simple and striking: the invariant data associated with reduced on-shell diagram is encoded by a *permutation* of the particle labels! We will describe this connection in detail in the next section.

It is amazing that a connection between scattering amplitudes in (3+1) dimensions and combinatorics exists at all, let alone that it will play a central role in the story. This is the tip of an iceberg of remarkable connections between on-shell diagrams and rich mathematical structures only recently explored in the literature. We will spend much of the rest of this chapter outlining these connections in greater detail. But we will start by recalling that this is not the first time scattering theory has been related to permutations in an important way: a classic example of such a connection is for integrable theories in (1+1) dimensions. In addition to providing us with some historical context, revisiting this story will give us an interesting perspective on recent developments.

3.3 Permutations and Scattering Amplitudes

I. Combinatorial Descriptions of Scattering Processes

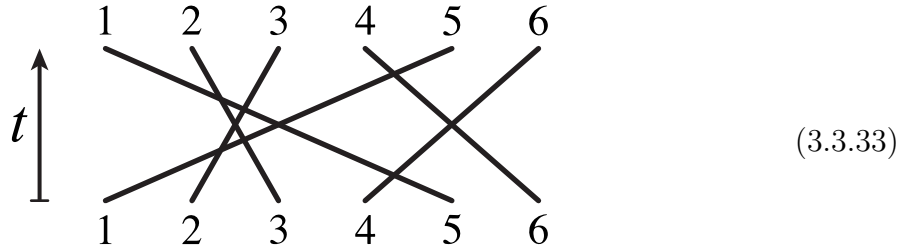
To a physicist, scattering is perhaps the most fundamental physical process; but scattering amplitudes are rather sophisticated functions of the helicities and momenta of the external particles. If we strip-away all of this data, all that would be left would be the arbitrary labels identifying the particles involved, which we will denote simply by $(1, \dots, n)$. The simplest kind of “interaction” that could be associated with just this data would be a *permutation*; because of the central role played by permutations in combinatorics, we might fancifully say that a permutation is the combinatorial analog of the physicists’ S -matrix.

At first sight, it certainly seems as if a “combinatorial S -matrix” would be far too simple an object to capture anything remotely resembling the richness of physical scattering amplitudes. However, we will see that this is not the case: in a specific sense, our study of on-shell diagrams will be fully determined by a novel way of thinking about permutations.

Indeed something very much like this happens for integrable theories in (1+1) dimensions, [131, 132]. Consider for instance the permutation given by

$$\begin{pmatrix} 1 & 2 & 3 & 4 & 5 & 6 \\ \downarrow & \downarrow & \downarrow & \downarrow & \downarrow & \downarrow \\ 5 & 3 & 2 & 6 & 1 & 4 \end{pmatrix}. \quad (3.3.32)$$

Its relationship to physics can be seen by representing it graphically as:



This can be thought of as a space-time picture for a scattering process in (1+1) dimensions, where time flows upwards. First, particles 4 and 5 scatter, then 1 and 2, then 2 and 3, and so on. The time-ordering of these scatterings corresponds to one way of representing the permutation as a product of adjacent transpositions. Of course, this decomposition is not unique: there are many ways of drawing the same

picture with different time-orderings for the various $2 \rightarrow 2$ processes. In a general theory with only 4-point interactions, the amplitude for different orderings would be different, and therefore the amplitude for the scattering process would not be completely determined by the permutation alone. For the amplitude to depend *only on the permutation and nothing else*, the $2 \rightarrow 2$ amplitudes must satisfy the famous Yang-Baxter relation, [131, 132]:

$$\begin{array}{ccc}
 1 & 2 & 3 \\
 \diagdown & | & / \\
 & \times & \\
 / & | & \diagdown \\
 1 & 2 & 3
 \end{array}
 \iff
 \begin{array}{ccc}
 1 & 2 & 3 \\
 / & | & \diagdown \\
 & \times & \\
 \diagdown & | & / \\
 1 & 2 & 3
 \end{array}
 \tag{3.3.34}$$

It is natural to ask whether such a picture can be generalized to more realistic theories in higher dimensions. This seems impossible at first sight, since the pictures drawn above only make physical sense in (1+1) dimensions (not only because they are drawn on a plane). The fact that particles can only move in one spatial dimension is what makes it possible to describe all interactions as a sequence of local $2 \rightarrow 2$ scattering processes. Also important is the absence of any particle creation or destruction, allowing us to label the final-states by the same labels as the initial-states. Neither of these features hold for the higher-dimensional theories in which we are primarily interested: for planar $\mathcal{N} = 4$ SYM, particle creation and destruction plays a fundamental role; and the most primitive processes are not $2 \rightarrow 2$ amplitudes, but rather the 3-particle amplitudes discussed above, (3.2.6).

An important starting-point for describing higher-dimensional scattering processes is to forgo the traditional meaning of the “ S -matrix”—an operator which maps initial states to final states. Rather, we find it much more convenient to treat all the external particles on equal footing, using crossing symmetry to formulate the S -matrix as a process for which *all* the external particles are taken to be *incoming*.

One lesson we can take from (1+1) dimensions is that any connection between scattering and permutations *must* involve *on-shell* processes. In (3+1) dimensions, this leads us to trivalent, on-shell diagrams with black and white vertices discussed in the previous section. And so we are led to try and associate a permutation with these diagrams. As it turns out, just such a connection exists between two-colored,

planar graphs and permutations, and has recently been studied in the mathematical literature, [43] (see also [46]).

Let’s jump-in and describe how it works. The way to read-off a permutation from an on-shell graph is as follows. For each external leg a (with clockwise ordering), follow the graph inward from a , turning left at each white vertex, and turning right at each black vertex; this “left-right path” will terminate at some external leg, denoted $\sigma(a)$. For example, the three-particle building blocks of $\mathcal{N}=4$, (3.2.6), are associated with permutations in the following way:

$$\begin{array}{c}
 \begin{array}{ccc}
 \text{Diagram 1} & \Leftrightarrow & \begin{pmatrix} 1 & 2 & 3 \\ \downarrow & \downarrow & \downarrow \\ 2 & 3 & 1 \end{pmatrix} \\
 \text{Diagram 2} & \Leftrightarrow & \begin{pmatrix} 1 & 2 & 3 \\ \downarrow & \downarrow & \downarrow \\ 3 & 1 & 2 \end{pmatrix}
 \end{array} \\
 \text{and}
 \end{array}
 \quad (3.3.35)$$

Of course, this works equally-well for more complex on-shell graphs; for example, the graph which gives the four-particle tree-amplitude, (3.2.15), is associated with the following permutation:

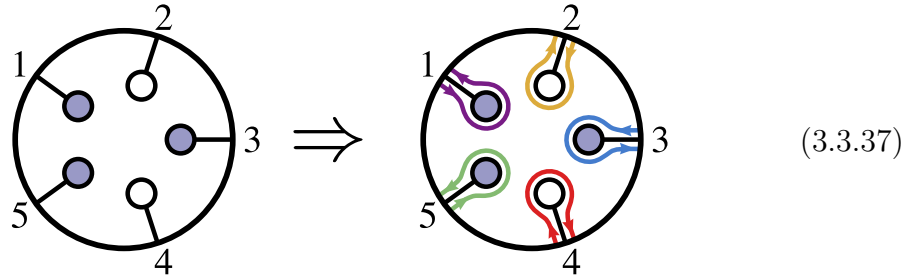
$$\begin{array}{ccc}
 \text{Diagram} & \Leftrightarrow & \begin{pmatrix} 1 & 2 & 3 & 4 \\ \downarrow & \downarrow & \downarrow & \downarrow \\ 3 & 4 & 1 & 2 \end{pmatrix} \\
 & & (3.3.36)
 \end{array}$$

It is very easy to see that such “left-right paths” allow us to define a permutation for any planar graph constructed with black and white vertices (not only those which are trivalent). Starting from any external leg of such a graph, this path will always lead back out to the boundary; and because any path can be trivially reversed (by exchanging the roles of black and white), it is clear that every external leg is the terminus of some such path. And so, the left-right paths do indeed define a *permutation* of the external legs.

Actually, left-right paths associate each graph with a slight generalization of an ordinary permutation known as a *decorated* permutation—a generalization which al-

lows for two types of fixed-points. By convention, we always consider a left-right path to permute each label ‘to its right’—in other words, we think of the paths as being associated with a map $\sigma: \{1, \dots, n\} \mapsto \{1, \dots, 2n\}$ such that $a \leq \sigma(a) \leq a+n$ and taking $\sigma(a) \bmod n$ would be an ordinary permutation. The two types of fixed points correspond to the cases of $\sigma(a) = a$ or $\sigma(a) = a+n$. For the sake of simplicity, for the rest of this chapter we will refer to these *decorated* permutations simply as ‘permutations’ and denote them by “ $\{\sigma(1), \dots, \sigma(n)\}$ ”.

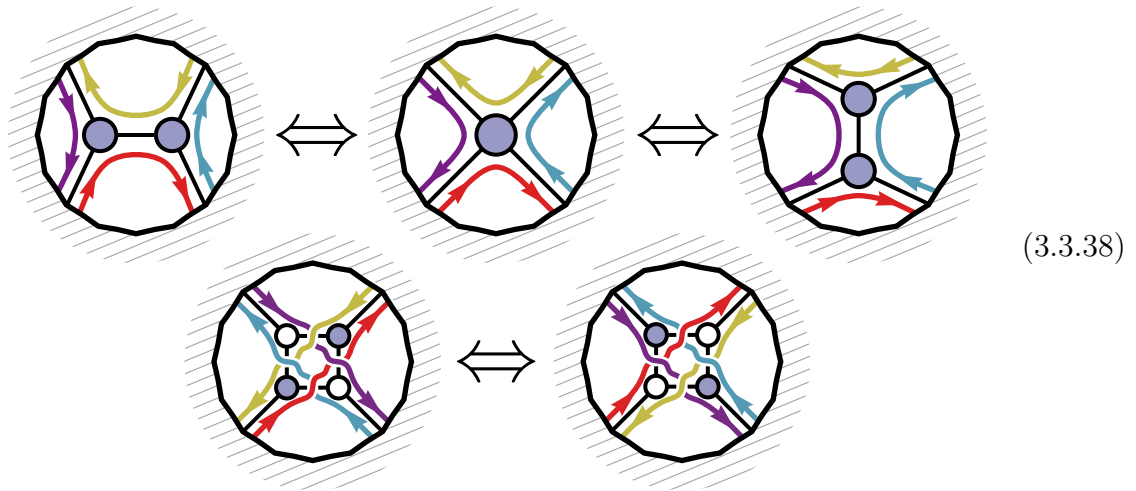
This allows us to differentiate between 2^n possible ‘decorations’ of the trivial permutation. Such ‘decorations’ arise for graphs such as,



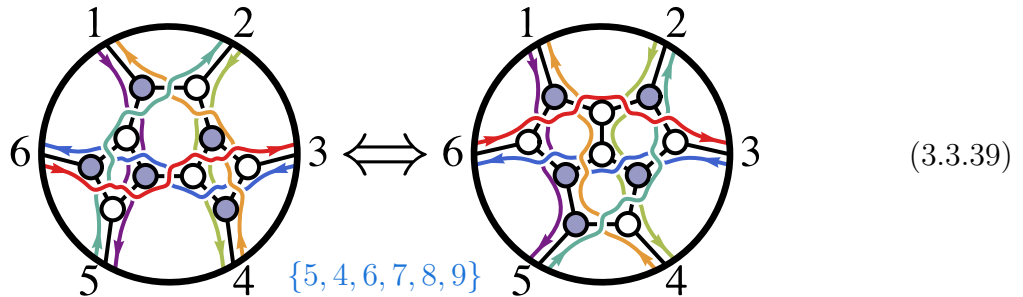
which would be labeled by a ‘permutation’ $\{1, 7, 3, 9, 5\}$. Although such empty graphs are themselves of little direct relevance to physics, they will play an important role in the general toolbox—as we will see in the following subsection.

Associated with any permutation is a number, k , which is the number of $a \in \{1, \dots, n\}$ which are mapped ‘beyond n ’ by σ —that is, for which $\sigma(a) > n$. This number is also given by the mean value of $\sigma(a) - a$: $k \equiv \frac{1}{n} \sum_a (\sigma(a) - a)$. To see this, notice that while the mean of any *ordinary* permutation always vanishes, our requirement that $a \leq \sigma(a) \leq a+n$ means that σ must be shifted by n relative to an ordinary permutation for some k elements. For example, both the 4-point graph, (3.3.36), and the 5-particle graph, (3.3.37), have $k = 2$.

The reason why the permutations associated with on-shell graphs are so important is that in many cases they *invariantly* encode the physical information about the graph and the on-shell form associated with it. Recall that graphs related by mergers, (3.4.105), or square-moves, (3.2.24), represent the same physical form. These operations also leave permutations invariant:



Bubble-deletion, however, *does* change the permutation associated with an on-shell diagram; it also changes the number of faces. But by deleting bubbles, any graph can be ‘reduced’—and any two *reduced* graphs labeled by the same permutation always represent the same physical form. More explicitly, all physical information in reduced graphs is captured by the corresponding permutation. To see a simple example of this, recall the pair of inequivalent graphs given in (3.2.25) which were related by a rather long sequence of mergers and square-moves; it is much easier to test the equivalence of the permutations which label them:



We should note in passing that there is something very special about $\mathcal{N}=4$ SYM and integrability which allows us to *fully* characterize on-shell diagrams in this way. Just as the Yang-Baxter relation (3.3.34) was the prerequisite for (1+1)-dimensional theories to be ‘combinatorial’ in nature, it is the square-move (3.2.24) which does this for $\mathcal{N}=4$: recall that in a non-supersymmetric theory, all 3-particle vertices would need to be dressed by the helicities of the particles involved—such as in (3.2.2); this dressing represents *extra* data which must be supplied in order to specify the physical process, and this data is *not* left invariant under square-moves. That being said,

however, the purely combinatorial story of $\mathcal{N} = 4$ will play a central role even for non-supersymmetric theories. This will be described more completely in section 3.13.

II. The BCFW-Bridge Construction of Representative Graphs

We have seen that every on-shell graph is associated with a permutation; quite beautifully, the converse is also true: *all* permutations can be represented by an on-shell graph. A constructive procedure for building a representative graph for any permutation was described in [43] (and in somewhat different terms by D. Thurston in [46]). Here, we will describe a different method—motivated by simple physical and combinatorial considerations and by analogy with physics in (1+1) dimensions—where graphs are constructed out of simple, adjacent transpositions. Of course, in (3+1) dimensions, there is no space-time evolution analogue of successive $2 \rightarrow 2$ scattering; and so we must find some way to ‘build-up’ on-shell objects directly from the “vacuum” (a trivial permutation).

The key is understanding what an adjacent transposition means in terms of on-shell graphs. The answer is extremely simple: an adjacent transposition is nothing but the addition of the BCFW-bridge:

Notice that any number of ‘hanging legs’—those which map to themselves under σ —can be inserted between a and “ $a+1$ ” without consequence; and so, we will consider any transposition (ac) to be “adjacent” so long as for all b between a and c , $\sigma(b) = b \pmod n$. (Although the bridge drawn in (3.3.40) will be sufficient for most applications, the oppositely-colored bridge—where black and white vertices are exchanged—could also be used; the principle difference being that such a bridge would transpose the *pre*-images of a and $a+1$ under σ instead of the images).

Because adjacent transpositions simply correspond to adding BCFW-bridges, any decomposition of a permutation σ into a sequence of such transpositions acting on a trivial permutation can be read as *instructions* for building-up a *representative* on-

shell graph for σ by successively adding BCFW-bridges to an empty graph like that of (3.3.37).

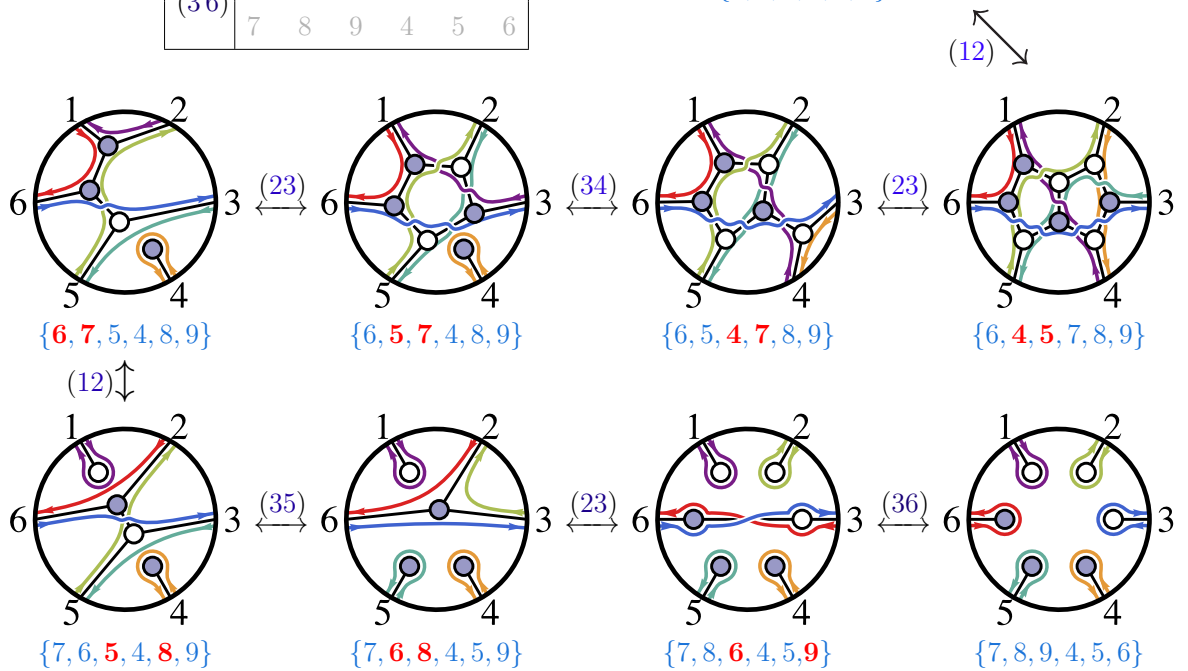
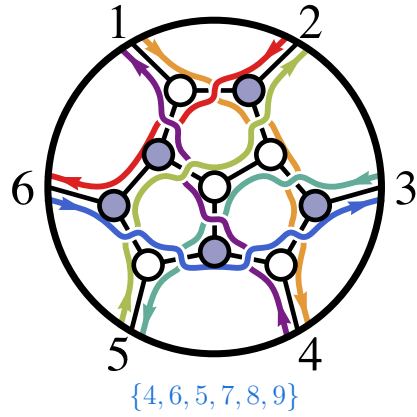
Of course, adding a BCFW bridge may potentially give us a reducible on-shell diagram. However, it turns out that when adding a bridge to a reduced graph, so long as $\sigma(a+1) < \sigma(a)$ —that is, the are paths arranged as drawn in (3.3.40)—then the resulting graph is guaranteed to be reduced. We will not prove this statement now, but its proof will become trivial after the discussions in section 3.5.

And so, when breaking-down a permutation into adjacent transpositions, we want to find pairs (ac) with $a < c$ (separated only by external legs b self-identified under σ) such that $\sigma(a) < \sigma(c)$; then when we decompose σ as $(ac) \circ \sigma'$ with $\{\sigma(a), \sigma(c)\} = \{\sigma'(c), \sigma'(a)\}$, adding a BCFW-bridge to a *reduced* on-shell diagram labeled by σ' will result in a *reduced* on-shell diagram labeled by σ . Of course, there are *many* ways of decomposing a permutation σ into such a chain of adjacent transpositions, and *any* such decomposition will result in a representative, reduced graph whose left-right permutation is σ . But for the sake of concreteness, let us describe one very specific, *canonical* procedure to decompose any permutation—one which will turn out to have rather special properties discussed in subsection IV..

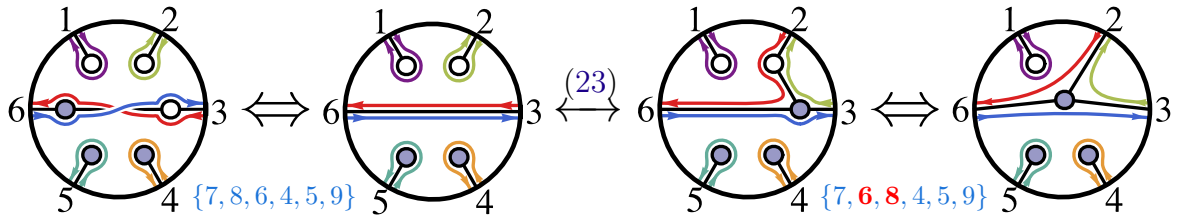
BCFW-Bridge Decomposition: Starting with any permutation σ , if σ is not a decoration of the identity, then decompose σ as $(ac) \circ \sigma'$ where $1 \leq a < c \leq n$ is the *lexicographically-first* pair separated only by legs b which are self-identified under σ and for which $\sigma(a) < \sigma(c)$; repeat until σ is the identity.

To illustrate this procedure, let's see how it generates a representative, reduced on-shell diagram which is labeled by the permutation $\{4, 6, 5, 7, 8, 9\}$:

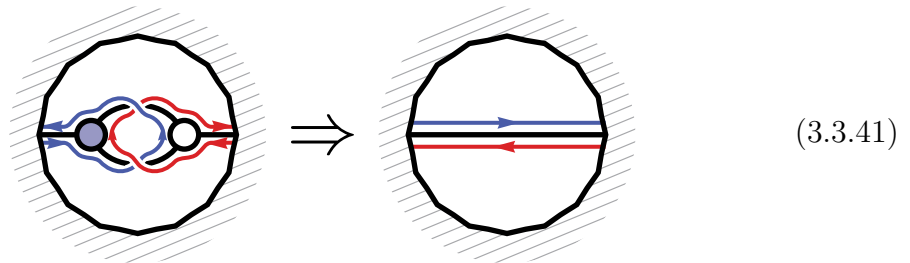
| | | | | | | |
|--------|--------------|--------------|--------------|--------------|--------------|--------------|
| | 1 | 2 | 3 | 4 | 5 | 6 |
| τ | \downarrow | \downarrow | \downarrow | \downarrow | \downarrow | \downarrow |
| | 4 | 6 | 5 | 7 | 8 | 9 |
| (12) | 6 | 4 | 5 | 7 | 8 | 9 |
| (23) | 6 | 5 | 4 | 7 | 8 | 9 |
| (34) | 6 | 5 | 7 | 4 | 8 | 9 |
| (23) | 6 | 7 | 5 | 4 | 8 | 9 |
| (12) | 7 | 6 | 5 | 4 | 8 | 9 |
| (35) | 7 | 6 | 8 | 4 | 5 | 9 |
| (23) | 7 | 8 | 6 | 4 | 5 | 9 |
| (36) | 7 | 8 | 9 | 4 | 5 | 6 |



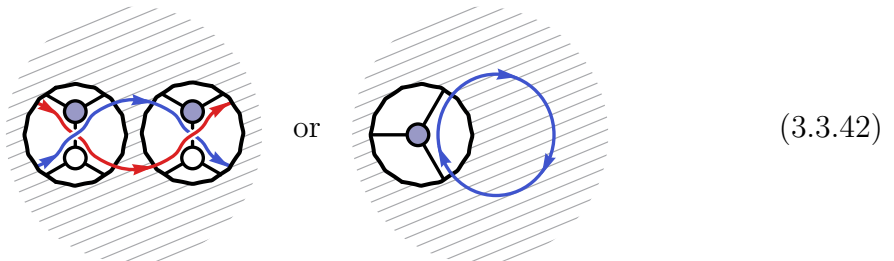
In the sequence of figures drawn above, we often made use of the fact that any bivalent or (non-boundary) monovalent vertex can be deleted without changing the permutation. So, for example, adding the BCFW bridge '(23)' to the second graph (from the bottom-right) results in the succeeding graph drawn via the sequence of (essentially trivial) moves:



This procedure provides us with a combinatorial test of a graph’s reducibility: because the BCFW-bridge construction always produces a *reduced* representative graph for any permutation, and each step in the construction adds one face to the graph as it is built, a graph is reduced if and only if the number of its faces minus one is equal to the number of steps in the BCFW-bridge decomposition of the permutation which labels it. If not, then the graph is reducible, and has some number of faces which can be deleted by bubble reduction:



A more intrinsic way to identify a reducible graph is if any pair of left-right paths $a \rightarrow \sigma(a)$ and $b \rightarrow \sigma(b)$ cross each other along more than one edge in the graph in the manner known as a “bad double crossing”, or if there is any purely-internal path.



A bad double-crossing is distinguished from those double-crossings of the form:



Double-crossings such as that above do not indicate that a graph is reducible.

We thus have a complete dictionary between (reduced) on-shell graphs and permutations. As we will discuss in section 3.12, this new picture actually contains the (1+1)-dimensional story as a special case. Another closely related special case is relevant for describing on-shell diagrams (and all-loop amplitudes) of the ABJM theory in (2+1) dimensions!

But let us now move beyond the purely combinatorial aspects of the story, and turn towards actually *computing* on-shell diagrams. This will lead us to uncover beautiful structures in algebraic geometry also described by decorated permutations, ultimately connecting on-shell graphs to the “positive” Grassmannian of our title.

3.4 From On-Shell Diagrams to the Grassmannian

In this section we will show that the computation of on-shell diagrams is most efficiently and transparently carried out by associating each diagram with an auxiliary structure: a matrix C representing an element of the Grassmannian $G(k, n)$. But let us begin by reviewing some elementary properties about Grassmannian manifolds in general, and describe the first appearance of these spaces in the story of scattering amplitudes, as they arise in the description of external kinematical data.

I. The Grassmannian of k -Planes in n Dimensions, $G(k, n)$

The Grassmannian $G(k, n)$ is the space of k -dimensional planes passing through the origin in an n -dimensional space (see e.g. [71]). We can specify a k -plane in n dimensions by giving k vectors $C_\alpha \in \mathbb{C}^n$, whose span defines the plane. We can assemble these vectors into a $(k \times n)$ -matrix C , whose components are $c_{\alpha a}$ for $\alpha = 1, \dots, k$ and $a = 1, \dots, n$.

Under $GL(k)$ -transformations, $C \mapsto \Lambda \cdot C$ —with $\Lambda \in GL(k)$ —the row vectors will change, but the plane spanned by them is obviously unchanged. Thus, the Grassmannian $G(k, n)$ can be thought of as the space of $(k \times n)$ -matrices modulo this $GL(k)$ “gauge” redundancy. From this, we see that the dimension of $G(k, n)$ is $k \times n - k^2 = k(n - k)$. In practice, we can “gauge-fix” the $GL(k)$ redundancy by choosing any k of the columns of the matrix to form the $(k \times k)$ identity matrix. For instance, we can represent a generic point in $G(2, 5)$ in the following gauge-fixed form:

$$C = \begin{pmatrix} 1 & 0 & c_{13} & c_{14} & c_{15} \\ 0 & 1 & c_{23} & c_{24} & c_{25} \end{pmatrix}. \quad (3.4.44)$$

This coordinate chart does not cover the *entire* Grassmannian—though of course the collection of all $\binom{n}{k}$ such charts would obviously suffice.

The $GL(k)$ -invariant information associated with C is easily specified. First, notice that the only $SL(k)$ -invariants of $C \in G(k, n)$ are the minors constructed out of the *columns* of C ,

$$(a_1 \cdots a_k) \equiv \det\{c_{a_1}, \dots, c_{a_k}\}. \quad (3.4.45)$$

$GL(k)$ -invariants are then simply ratios of these:

$$\frac{(a_1 \cdots a_k)}{(b_1 \cdots b_k)}. \quad (3.4.46)$$

While the (ratios of) minors are $GL(k)$ -invariant, the number of these, $\binom{n}{k}$, is much greater than the dimensionality of the Grassmannian, $\dim(G(k, n)) = k(n-k)$, and so the minors represent a highly-redundant set of data to describe C . The identities among minors arise from the simple fact that any k -vector can be expanded in a basis of any k linearly-independent k -vectors—a statement that is equivalent to the identity known as *Cramer's rule*:

$$c_{a_1}(a_2 \cdots a_{k+1}) - c_{a_2}(a_1 a_3 \cdots a_{k+1}) + \cdots + (-1)^{k-1} c_{a_{k+1}}(a_1 \cdots a_k) = 0, \quad (3.4.47)$$

for any $c_a \in \mathbb{C}^k$. Contracting each of the vectors in (3.4.47) with another set of vectors $c_{b_1}, \dots, c_{b_{k-1}}$ generates the identities known as the Plücker relations,

$$(b_1 \cdots b_{k-1} a_1)(a_2 \cdots a_{k+1}) + \cdots + (-1)^{k-1} (b_1 \cdots b_{k-1} a_{k+1})(a_1 \cdots a_k) = 0. \quad (3.4.48)$$

Associated with any k -plane C is a natural $(n-k)$ -plane denoted C^\perp , the “orthogonal complement” of C , which is defined by,

$$C^\perp \cdot C = 0. \quad (3.4.49)$$

Therefore, there is a natural isomorphism between $G(k, n)$ and $G(n-k, n)$, which is reflected in the invariance of $\dim(G(k, n)) = k(n-k)$ under the exchange $k \leftrightarrow (n-k)$. The minors of C^\perp are fully determined by the minors of C in the obvious way: for any complementary sets $\{a_1, \dots, a_k\}$ and $\{b_1, \dots, b_{n-k}\}$ (whose union is $\{1, \dots, n\}$), we have

$$(a_1 \cdots a_k)|_C = \pm (b_1 \cdots b_{n-k})|_{C^\perp}. \quad (3.4.50)$$

To be completely explicit, suppose we represent C in a gauge where columns c_A with $A \equiv \{a_1, \dots, a_k\}$ are taken as the identity; then the $n-k$ columns of C in the complementary set $B \equiv A^c$, c_b for $b \in B$ —whose components we write as c_{ba} —encode the $k(n-k)$ degrees of freedom of C ; then the matrix C^\perp has components,

$$c_{ab}^\perp = -c_{ba}. \quad (3.4.51)$$

For example, the plane $C^\perp \in G(3, 5)$ orthogonal to $C \in G(2, 5)$ given in (3.4.44) is:

$$C^\perp = \begin{pmatrix} -c_{13} & -c_{23} & 1 & 0 & 0 \\ -c_{14} & -c_{24} & 0 & 1 & 0 \\ -c_{15} & -c_{25} & 0 & 0 & 1 \end{pmatrix} \quad (3.4.52)$$

Finally, we will eventually be talking about a certain top-dimensional differential form on the Grassmannian, so it is useful to discuss what general forms on the

Grassmannian look like in the coordinates c_{ab} . Consider first the familiar example of a form on the projective space $G(1, 2)$. We can think of this as a (1×2) matrix $C = (c_1 \ c_2)$, modulo the $GL(1)$ -action of $C \rightarrow tC$. Any top-form can be written as

$$\Omega = \frac{d^2 C}{\text{vol}(GL(1))} \frac{1}{f(C)}, \quad (3.4.53)$$

where $f(C)$ must have homogeneity $(+2)$ under rescaling C ; that is, $f(tC) = t^2 f(C)$. In practice, modding-out by the $GL(1)$ -action is trivial: one can simply gauge-fix the $GL(1)$ so that, say, $C \mapsto C^* = (1 \ c_2)$; and then $\Omega = dc_2/f(C^*)$. We can also say this more invariantly, by writing,

$$\Omega = \langle CdC \rangle \frac{1}{f(C)}. \quad (3.4.54)$$

The generalization of this simple case to an arbitrary Grassmannian is straightforward. We can write,

$$\Omega = \frac{d^{k \times n} C}{\text{vol}(GL(k))} \frac{1}{f(C)}, \quad (3.4.55)$$

where $GL(k)$ -invariance implies, in particular, that $f(C)$ must be a function of the minors of C with homogeneity under rescaling

$$f(tC) = t^{k \times n} f(C). \quad (3.4.56)$$

In the coordinate chart where we gauge-fix k of the columns to the identity as above, then $\Omega = d^{k \times (n-k)} c_{a,b}/f(C)$. Said more invariantly, we have

$$\Omega = \langle C_1 \cdots C_k (dC_1)^{(n-k)} \rangle \cdots \langle C_1 \cdots C_k (dC_k)^{(n-k)} \rangle \frac{1}{f(C)}, \quad (3.4.57)$$

where C_α is a row-vector of C and, e.g.,

$$\langle C_1 \cdots C_k (dC_1)^{(n-k)} \rangle \equiv \epsilon^{a_1 a_2 \cdots a_n} c_{1, a_1} \cdots c_{k, a_k} dc_{1, a_{k+1}} \wedge \cdots \wedge dc_{1, a_n}. \quad (3.4.58)$$

II. Grassmannian Description of Kinematical Data: the 2-Planes λ and $\tilde{\lambda}$

In a moment, we will establish a very direct connection between on-shell diagrams and the Grassmannian; but let us first pause to point out an even more basic way in which the Grassmannian makes an appearance in scattering amplitudes: in the very way we encode external kinematical data. We normally think of this data as simply being specified by n 2-component spinors λ_a^α and $\tilde{\lambda}_a^{\dot{\alpha}}$; but of course we may also think of this data as given by a pair of $(2 \times n)$ -matrices—which we denote collectively by λ and $\tilde{\lambda}$. For example, the λ 's are naturally associated with the $(2 \times n)$ -matrix,

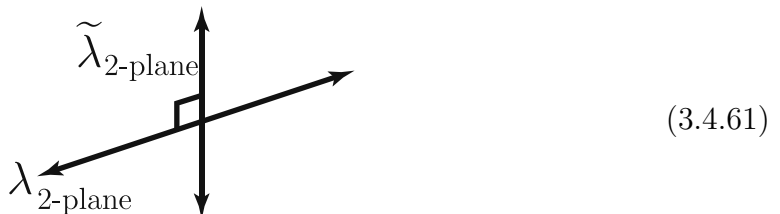
$$\lambda \equiv \begin{pmatrix} \lambda_1^1 & \lambda_2^1 & \cdots & \lambda_n^1 \\ \lambda_1^2 & \lambda_2^2 & \cdots & \lambda_n^2 \end{pmatrix} \Leftrightarrow (\lambda_1 \ \lambda_2 \ \cdots \ \lambda_n). \quad (3.4.59)$$

Instead of focusing on the *columns* of the matrix λ , let us think about it as two row-vectors. Each of these is a vector in an n -dimensional space. Under Lorentz transformations, these two vectors change, but since Lorentz transformations act on the λ 's by $SL(2)$ -transformations on their α indices, the two new vectors will simply be a linear combination of the original ones. Therefore, while the vectors themselves change, the *plane* that is spanned by them is invariant under Lorentz transformations. Quite beautifully then, the Lorentz-invariant information encoded by the λ 's is really just this 2-*plane* in n dimensions—an element of $G(2, n)$ as realized in [16]. The same is obviously true for the $\tilde{\lambda}$'s. Of course, the Lorentz group is only the $SL(2)$ part of $GL(2)$ and on-shell forms do transform under “global” little group transformations which correspond to the $GL(1)$ subgroup of $GL(2)$.

In terms of spinor helicity variables, momentum conservation is simply,

$$\sum_a \lambda_a^\alpha \tilde{\lambda}_a^{\dot{\alpha}} = 0, \quad (3.4.60)$$

which has the geometric interpretation that the plane λ is *orthogonal* to the plane $\tilde{\lambda}$, [16]:



This geometric understanding of momentum-conservation also nicely explains the unique nature of its application to the case of three-particles: two 2-planes in 3 dimensions *cannot* be orthogonal in general. The only solution, therefore, is for one of the planes to actually be a 1-plane in disguise. For example, suppose that we have three generic $\tilde{\lambda}$'s. Momentum conservation requires that $\lambda \subset \tilde{\lambda}^\perp$, but $\tilde{\lambda}^\perp$ is a 1-plane! A $GL(1)$ -representative of $\tilde{\lambda}^\perp$ is given by

$$\tilde{\lambda}^\perp \equiv \left([2\ 3] \quad [3\ 1] \quad [1\ 2] \right), \quad (3.4.62)$$

for which $\tilde{\lambda}^\perp \cdot \tilde{\lambda} = 0$ follows as a trivial instance of Cramer's rule, (3.4.47):

$$\tilde{\lambda}^\perp \cdot \tilde{\lambda} = [2\ 3]\tilde{\lambda}_1 + [3\ 1]\tilde{\lambda}_2 + [1\ 2]\tilde{\lambda}_3 = 0. \quad (3.4.63)$$

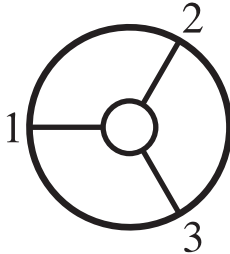
Because this is the *unique* plane orthogonal to $\tilde{\lambda}$, momentum conservation requires that the λ -plane be spanned by it. In particular, this means that all the λ 's must be proportional: in a Lorentz frame where $\lambda_1 = \begin{pmatrix} [2\ 3] \\ 0 \end{pmatrix}$, we have

$$\lambda \equiv (\lambda_1 \quad \lambda_2 \quad \lambda_3) = \begin{pmatrix} [2\ 3] & [3\ 1] & [1\ 2] \\ 0 & 0 & 0 \end{pmatrix}. \quad (3.4.64)$$

III. Grassmannian Representation of On-Shell Diagrams

Let us begin to more explicitly calculate the differential form associated with a given on-shell diagram. We use the momentum-conserving δ -functions at the vertices to localize as many of the internal momenta as we can. This looks highly non-trivial because momentum conservation is a quadratic constraint on the $\lambda, \tilde{\lambda}$ in general. But a moment's reflection suggests that the situation may be easier to understand. We know that for 3-particle amplitudes, momentum conservation implies a very simple geometric situation—where either the λ 's or the $\tilde{\lambda}$'s are forced to be parallel to each other. However, our representation of the three-particle amplitude, simple and elegant though it is, does not make this simple fact manifest. This motivates us to try to express the 3-particle amplitude in a slightly different form—one which makes the geometry of the λ 's and $\tilde{\lambda}$'s in each case as transparent as possible.

Let's start with the $\mathcal{A}_3^{(1)}$ vertex:



$$\Leftrightarrow \mathcal{A}_3^{(1)} = \frac{\delta^{1 \times 4} ([2\ 3] \tilde{\eta}_1 + [3\ 1] \tilde{\eta}_2 + [1\ 2] \tilde{\eta}_3)}{[1\ 2][2\ 3][3\ 1]} \delta^{2 \times 2} (\lambda \cdot \tilde{\lambda}). \quad (3.4.65)$$

Notice that the coefficients of the $\tilde{\eta}$'s are the same as the factors that appear in the denominator of $\mathcal{A}_3^{(1)}$, and coincide with the 1-plane $\tilde{\lambda}^\perp$ orthogonal to $\tilde{\lambda}$. We can make this geometry manifest by introducing an *auxiliary* 1-plane $W \in G(1, 3)$, and demand that it be orthogonal to $\tilde{\lambda}$ and that it contains the plane λ . This latter constraint is equivalent to the somewhat less concise condition that the orthogonal complement of W^\perp is orthogonal to λ . Thus, we can represent,

$$\mathcal{A}_3^{(1)} = \int \frac{d^{1 \times 3} W}{\text{vol}(GL(1))} \frac{\delta^{1 \times 4} (W \cdot \tilde{\eta})}{(1)(2)(3)} \delta^{1 \times 2} (W \cdot \tilde{\lambda}) \delta^{2 \times 2} (\lambda \cdot W^\perp), \quad (3.4.66)$$

where $W \in G(1, 3)$ is given by the (1×3) -matrix

$$W \equiv \begin{pmatrix} w_1 & w_2 & w_3 \end{pmatrix}, \quad (3.4.67)$$

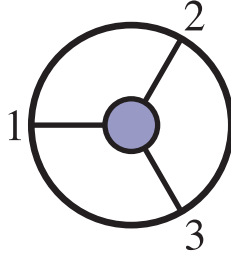
$(a) \equiv \det\{w_a\}$ is a (1×1) -‘minor’ of the matrix W and $\tilde{\eta} \equiv (\tilde{\eta}_1 \tilde{\eta}_2 \tilde{\eta}_3)$. The δ -function $\delta^{1 \times 2}(W \cdot \tilde{\lambda})$ fixes $W \mapsto W^* = \tilde{\lambda}^\perp$ (written above, in (3.4.62)). On the support of the point $W^* \in G(1, 3)$, the remaining δ -functions in (3.4.66),

$$\delta^{1 \times 4}(W^* \cdot \tilde{\eta}) \delta^{2 \times 2}(\lambda \cdot (W^*)^\perp), \quad (3.4.68)$$

simply become ordinary super-momentum conservation.

A comment is in order here. To make the invariance of the integrand under $GL(1)$ manifest one has to find a $GL(1)$ invariant way of writing $\delta^{2 \times 2}(\lambda \cdot W^\perp)$. As usual, this is achieved by introducing auxiliary variables as explained in detail (and more generality) in section II.

We can of course make the same generalization for the $\mathcal{A}_3^{(2)}$ vertex:



$$\Leftrightarrow \mathcal{A}_3^{(2)} = \frac{\delta^{2 \times 4}(\lambda_1 \tilde{\eta}_1 + \lambda_2 \tilde{\eta}_2 + \lambda_3 \tilde{\eta}_3)}{\langle 12 \rangle \langle 23 \rangle \langle 31 \rangle} \delta^{2 \times 2}(\lambda \cdot \tilde{\lambda}). \quad (3.4.69)$$

We can think of this as an integral over an auxiliary 2-plane $B \in G(2, 3)$ according to:

$$\mathcal{A}_3^{(2)} = \int \frac{d^{2 \times 3} B}{\text{vol}(GL(2))} \frac{\delta^{2 \times 4}(B \cdot \tilde{\eta})}{(12)(23)(31)} \delta^{2 \times 2}(B \cdot \tilde{\lambda}) \delta^{2 \times 1}(\lambda \cdot B^\perp). \quad (3.4.70)$$

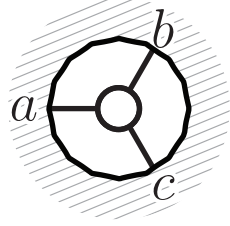
In this case, we can use the constraint $\delta^{2 \times 1}(\lambda \cdot B^\perp)$ to localize the integral over B , (somewhat trivially) fixing $B \mapsto B^* = \lambda$, and the minors in the measure trivially become $(12)(23)(31) \mapsto \langle 12 \rangle \langle 23 \rangle \langle 31 \rangle$. As before, the remaining δ -functions in (3.4.70),

$$\delta^{2 \times 4}(B^* \cdot \tilde{\eta}) \delta^{2 \times 2}(B^* \cdot \tilde{\lambda}), \quad (3.4.71)$$

encode super-momentum conservation.

The crucial feature of these Grassmannian representations of the three-particle amplitudes is that the constraints on the kinematical data λ and $\tilde{\lambda}$ are now decoupled, and occur *linearly* in the δ -function constraints. This makes it essentially trivial to perform the phase space integral over the internal lines, making any on-shell graph simply a collection of auxiliary 1-planes $W \in G(1, 3)$ and 2-planes $B \in G(2, 3)$ associated with the white and black vertices—each carrying with it all the constraints to impose momentum-conservation.

To summarize, for each white vertex involving the (possibly internal) legs (a, b, c) we introduce a 1-plane $W \in G(1, 3)$,

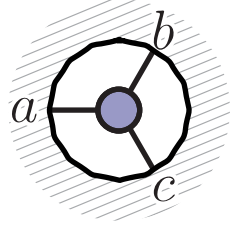


$$\Leftrightarrow W \equiv \begin{pmatrix} w_a & w_b & w_c \end{pmatrix}, \quad (3.4.72)$$

carrying with it an integration measure,

$$d\Omega_w \equiv \frac{d^{1 \times 3} W}{\text{vol}(GL(1))} \frac{1}{(a)(b)(c)}, \quad (3.4.73)$$

and corresponding constraints; similarly, for each black vertex involving legs (a, b, c) we have a plane $B \in G(2, 3)$,



$$\Leftrightarrow B \equiv \begin{pmatrix} b_a & b_b & b_c \end{pmatrix}, \quad (3.4.74)$$

together with its associated integration measure,

$$d\Omega_b \equiv \frac{d^{2 \times 3} B}{\text{vol}(GL(2))} \frac{1}{(a b)(b c)(c a)}, \quad (3.4.75)$$

and corresponding constraints. Each white vertex imposes *one* relation among $\tilde{\lambda}$'s:

$$W \cdot \tilde{\lambda} = w_a \tilde{\lambda}_a + w_b \tilde{\lambda}_b + w_c \tilde{\lambda}_c = 0; \quad (3.4.76)$$

and each black vertex imposes *two* relations (as the columns b_a of B are two-vectors):

$$B \cdot \tilde{\lambda} = b_a \tilde{\lambda}_a + b_b \tilde{\lambda}_b + b_c \tilde{\lambda}_c = 0. \quad (3.4.77)$$

Thus, for a graph with n_b black vertices, n_w white vertices, and n_I internal edges, we have a total of $2n_b + n_w$ constraints; from these, one constraint is needed to fix (and eliminate) each internal $\tilde{\lambda}_I$ —leaving us with a total of:

$$k \equiv 2n_b + n_w - n_I \quad (3.4.78)$$

linear constraints relating the external $\tilde{\lambda}$'s for any given graph. We may write this collection of constraints as $C \cdot \tilde{\lambda} = 0$ for some $(k \times n)$ -matrix C , where

$$n = 3n_V - 2n_I, \quad (3.4.79)$$

with $n_V = n_b + n_w$. Because these are *linear* constraints among the $\tilde{\lambda}$'s, the matrix C is of course only well-defined up to an arbitrary re-shuffling of its k equations (a

$GL(k)$ -transformation of C); and so, C actually represents a point in $G(k, n)$! Of course, integrating-out the internal $\tilde{\eta}$'s follows identically to the $\tilde{\lambda}$, giving us the same final constraints among the external $\tilde{\eta}$'s as for the $\tilde{\lambda}$'s.

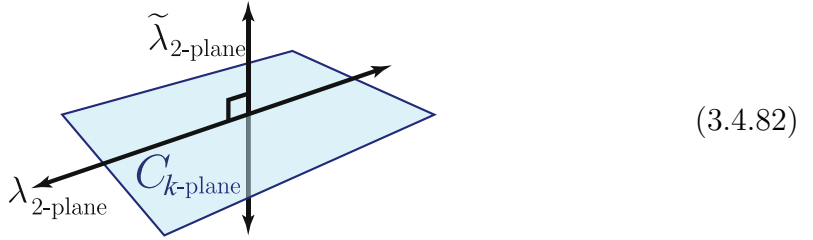
Thus, eliminating the internal $\tilde{\lambda}_I$ and $\tilde{\eta}_I$ combines all the “little Grassmannians” $W \in G(1, 3)$ and $B \in G(2, 3)$ associated with the vertices, and gives us finally a point in the Grassmannian $G(k, n)$ represented by some matrix C which encodes the relations satisfied among the $\tilde{\lambda}$'s and $\tilde{\eta}$'s via the δ -functions,

$$\delta^{k \times 4}(C \cdot \tilde{\eta}) \delta^{k \times 2}(C \cdot \tilde{\lambda}). \quad (3.4.80)$$

Following the same logic, but exchanging each plane B and W for their orthogonal complements, gives us the complementary set of relations involving the λ 's. Not surprisingly, these are simply given by the δ -functions,

$$\delta^{2 \times (n-k)}(\lambda \cdot C^\perp). \quad (3.4.81)$$

Geometrically, the ordinary δ -functions constrain the matrix C to be *orthogonal to* $\tilde{\lambda}$ and to *contain* λ :



Putting everything together, each on-shell diagram is associated with a differential-form obtained by integration over,

$$\prod_{\substack{\text{internal} \\ \text{edges } e}} \left(\frac{1}{\text{vol}(GL(1)_e)} \right) \prod_w d\Omega_w \prod_b d\Omega_b \delta^{k \times 4}(C \cdot \tilde{\eta}) \delta^{k \times 2}(C \cdot \tilde{\lambda}) \delta^{2 \times (n-k)}(\lambda \cdot C^\perp). \quad (3.4.83)$$

Notice that while freely using the δ -functions to fix each internal λ_I and $\tilde{\lambda}_I$, we have not modded-out by the $GL(1)$ -redundancies acting on these momenta (which explains the appearance of the $1/\text{vol}(GL(1))$ factors in (3.4.83)). It is natural to refer to the net number of auxiliary variables—after modding-out by all these $GL(1)$ -redundancies—as the *dimension* of the space of configurations $C \in G(k, n)$. As each vertex carries two auxiliary degrees of freedom, and each $GL(1)$ from the internal lines can be used to remove one of them, the ‘dimension’ associated with an on-shell graph is simply:

$$\dim(C) = 2n_V - n_I. \quad (3.4.84)$$

We should mention that this can be counted in a more direct way from the graph as follows. Because each on-shell graph is trivalent, we have $3n_V = 2n_I + n$ so that

$\dim(C) = 2n_V - n_I = n_I - n_V + n$; and restricting our attention to planar graphs, Euler's formula tells us that $(n_F - n) - n_I + n_V = 1$ (where n_F is the number of faces of the graph *including* the n faces of the boundary). Putting these two facts together shows that:

$$\dim(C) = n_F - 1. \quad (3.4.85)$$

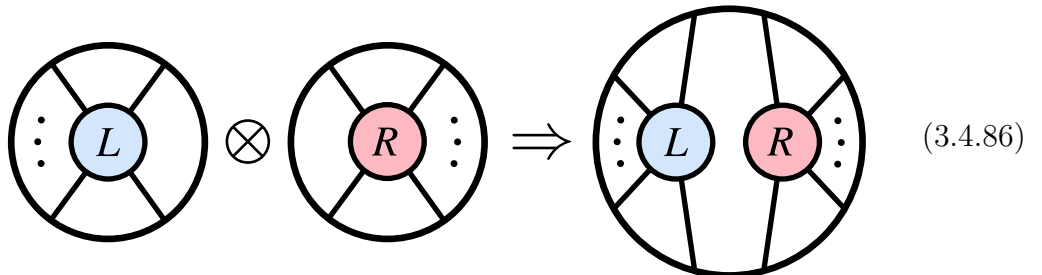
We will soon see that this is not an accident: there is a natural way in which the degrees of freedom associated with a graph are encoded by its *faces*.

So far, we've described in general terms how to compute the differential-form associated with a given on-shell graph. In the next subsection, we will describe how this can be done systematically using only two very simple, elementary operations; and in section V., we'll show how these two operations can be efficiently automated to construct an explicit representative of the plane C expressed in terms of variables associated with either a graph's *edges* or *faces*.

IV. Amalgamation of On-Shell Graphs

General on-shell graphs can be built-up in steps from more elementary ones using two simple operations: *direct-products* and *projections*. Collectively, we refer to this step-wise construction of more complicated graphs from simpler ones as *amalgamation* (see [42] for a mathematical construction and [17, 107] for some early steps in the physical setup). In this subsection, we describe both operations in turn, and show how they completely determine the k -plane C associated with any on-shell graph. Since all the $GL(k)$ -invariant information about C is given by the ratios of its minors, $(a_1 \cdots a_k)/(b_1 \cdots b_k)$, it suffices for us to simply describe how these two primitive operations act on the minors of C .

The first operation is rather trivial: starting with any two graphs, we can take their *direct-product*:



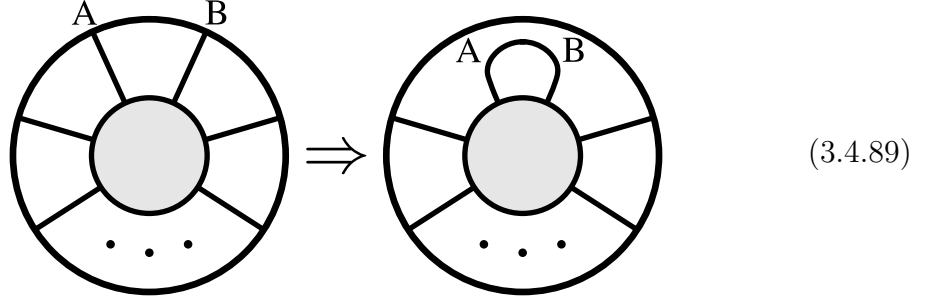
If the left-graph is associated with the plane $C_L \in G(k_L, n_L)$, and the right-graph is associated with the plane $C_R \in G(k_R, n_R)$, the direct-product produces a plane $C_L \otimes C_R \mapsto C \in G(k_L + k_R, n_L + n_R)$ according to:

$$\left(\begin{array}{|c|} \hline L \\ \hline \end{array} \right) \otimes \left(\begin{array}{|c|} \hline R \\ \hline \end{array} \right) \Rightarrow \left(\begin{array}{|cc|} \hline L & 0 \\ \hline 0 & R \\ \hline \end{array} \right) \quad (3.4.87)$$

The non-vanishing minors of C are easily expressed in terms of those of C_L and C_R :

$$(a_1 \cdots a_{k_L} b_1 \cdots b_{k_R})|_C = (a_1 \cdots a_{k_L})|_{C_L} \times (b_1 \cdots b_{k_R})|_{C_R}. \quad (3.4.88)$$

The second operation, *projection*, is more interesting. It corresponds to the identification of two (external) legs—say A and B —of a graph:

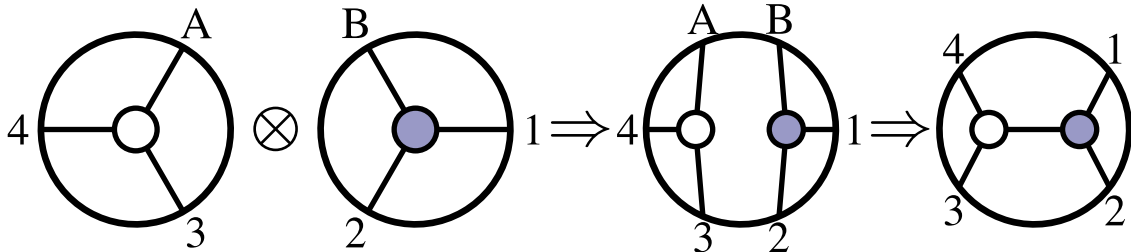


We call this operation “projection” because it takes a plane $C \in G(k+1, n+2)$, and produces a plane $\widehat{C} \in G(k, n)$, which is the *projection of C* onto the quotient of the column space of C modulo $(c_A - c_B)$. This follows directly from how the plane C associated with an on-shell graph is interpreted geometrically as constraints imposed on the external momenta.

For convenience, let us suppose that the $n+2$ particles of the configuration before projection are ordered $(A, B, 1, \dots, n)$. Then the minors of the projection’s image $\widehat{C} \in G(k, n)$ will be given in terms of the minors of $C \in G(k+1, n+2)$ according to:

$$(a_1 \cdots a_k)|_{\widehat{C}} = (A a_1 \cdots a_k)|_C + (B a_1 \cdots a_k)|_C. \quad (3.4.90)$$

Let us consider a simple case where these two operations are used to construct an on-shell graph. For example, consider the sequence,

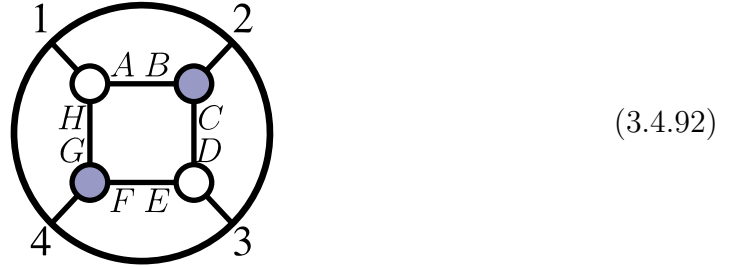


which builds-up the 4-particle factorization graph by first taking the direct-product of $W \in G(1, 3)$ and $B \in G(2, 3)$ to produce a graph associated with a plane $\widehat{C} \in G(3, 6)$, then merge legs A and B to produce the final graph associated with a plane $C \in G(2, 4)$. As we have described, minors of the final plane $C \in G(2, 4)$ are fully specified by those of its constituents; e.g.,

$$(13)|_C = (A13)|_{\widehat{C}} + (B13)|_{\widehat{C}} = 0 + (B1)|_{B \times (3)}|_W; \quad (3.4.91)$$

and $(24)|_C = (A24)|_{\widehat{C}} + (B24)|_{\widehat{C}} = 0 + (B2)|_{B \times (4)}|_W.$

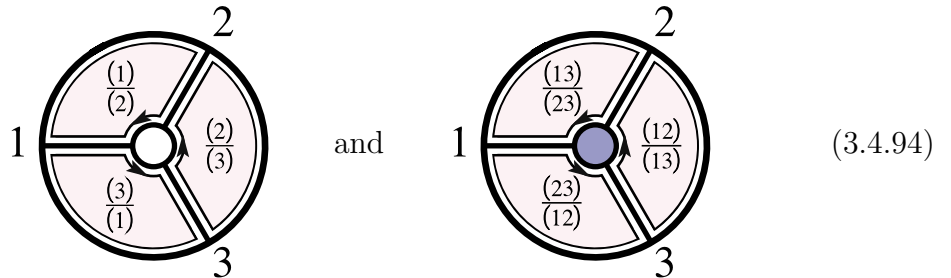
Let us look at one more interesting example: the amalgamation of graphs generating the 4-particle tree-amplitude:



Following the amalgamation rules described above, we find, for example that

$$\frac{(24)}{(13)} = \left(\frac{(F4)(H)}{(GF)(1)} \right) \left(\frac{(B2)(D)}{(CB)(3)} \right) + \left(\frac{(C2)(A)}{(BC)(1)} \right) \left(\frac{(G4)(E)}{(GF)(3)} \right). \quad (3.4.93)$$

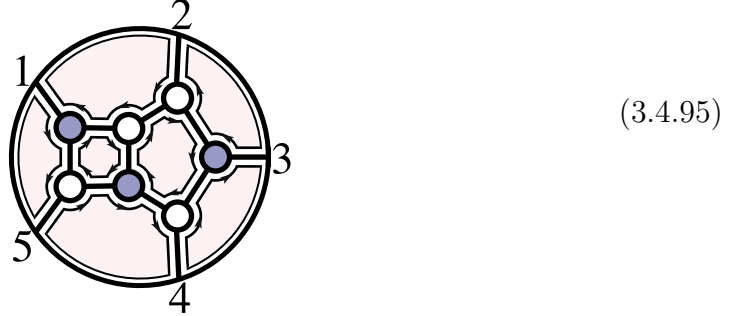
Notice that the amalgamation picture makes it clear that C will only depend on special combinations of the minors of the matrices associated with its constituent vertices. This ultimately stems from the fact that the only $GL(k)$ -invariant data associated with the vertices themselves are the ratios of minors. These appear, for example, as the face variables of the three-particle graphs:



Here, we have used arrows to show how the ratios transform under the little group.

Now, a very simple but important observation is that the final point in $G(k, n)$ obtained from amalgamation must obviously be completely invariant under the little group rescaling of any internal line. This means that only combinations of minors that are invariant under these scaling are ultimately relevant to our description of C .

Graphically, it is clear that these are given by products of such ratios, as following along the boundary of a face we form a closed path. A face variable, then, can be built as the product of these variables along its boundary. To illustrate the point, consider the following graph—associated with a generic plane in $G(2, 5)$:



Thus, while the variables describing the matrix C can be constructed from the variables of the planes B and W attached to each vertex, we may alternatively view C as being described by variables f_i associated with its *faces*. Note that the product of the face variables for each $G(1, 3)$ $G(2, 3)$ vertex is manifestly equal to 1 (see (3.4.94)); and so, it is easy to see that there are only *two* independent degrees of freedom per vertex—matching our calculation that $\dim(C) = n_F - 1$. This clearly persists to larger graphs, ensuring that $\prod_i f_i = 1$, which always accounts for the “minus 1” in the formula for the dimension of C . And so, the degrees of freedom are all but one of the face variables, say f_* . Rescaling $f_i \mapsto \hat{f}_i \equiv f_i/f_*$, the integration measure (3.4.83) for the auxiliary parameters in C becomes simply,

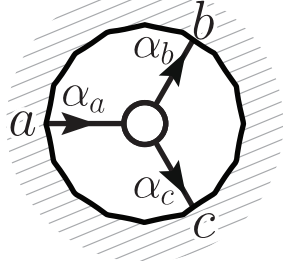
$$\prod_{\text{internal edges } e} \left(\frac{1}{\text{vol}(GL(1)_e)} \right) \prod_w d\Omega_w \prod_b d\Omega_b = \prod_{\text{rescaled faces } \hat{f}_i} \frac{d\hat{f}_i}{\hat{f}_i}. \quad (3.4.96)$$

V. “Boundary Measurements” and Canonical Coordinates

Let us now turn to the problem of explicitly determining a matrix representative C associated with a given on-shell graph. We will first do this in a very efficient—but somewhat overly redundant—way by attaching variables α_e to all the *edges* of a graph; and then, we will see how this procedure can be translated (with less redundancy) in terms of variables attached to a graph’s *faces*.

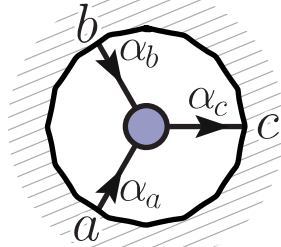
One strategy for explicitly constructing the k -plane C encoding the system of constraints (3.4.82) associated with an on-shell graph is to put the degrees of freedom associated with each vertex in a way which allows us to eliminate all internal momenta

as efficiently as possible. Of course, each vertex carries with it only two degrees of freedom. But it turns out to be useful to introduce an additional $GL(1)$ -redundancy at each vertex, so that every *leg* attached to a given vertex carries its own degree of freedom (making it easier to pair-up the degrees of freedom attached to internal lines between vertices). To further simplify the elimination of internal momenta from the ultimate system of equations relating the $\tilde{\lambda}$, it will be helpful also to provide an orientation to each edge, so that each white (black) has one (two) edges directed inward. With these decorations, each white vertex corresponds to:



$$\Leftrightarrow W \equiv \begin{pmatrix} a & b & c \\ \alpha_a^{-1} & -\alpha_b & -\alpha_c \end{pmatrix} \Rightarrow \tilde{\lambda}_a = \alpha_a(\alpha_b \tilde{\lambda}_b + \alpha_c \tilde{\lambda}_c); \quad (3.4.97)$$

and each black-vertex corresponds to:



$$\Leftrightarrow B \equiv \begin{pmatrix} a & b & c \\ \alpha_a^{-1} & 0 & -\alpha_c \\ 0 & \alpha_b^{-1} & -\alpha_c \end{pmatrix} \Rightarrow \left\{ \begin{array}{l} \tilde{\lambda}_a = \alpha_a \alpha_c \tilde{\lambda}_c \\ \tilde{\lambda}_b = \alpha_b \alpha_c \tilde{\lambda}_c \end{array} \right\}. \quad (3.4.98)$$

Decorating a graph in this way is called giving it a *perfect orientation*; and it is a general fact that all two-colored, trivalent graphs *relevant to physics* can be given a perfect orientation.

(The only graphs which cannot be given a perfect orientation are those which contain a sub-graph with $k \leq 0$ or $k \geq \nu$ (where ν denotes the number of legs of the *sub-graph*). This obstruction is closely tied to an inability to eliminate some internal line's λ_I or $\tilde{\lambda}_I$ from the complete system of equations. But this subtlety plays no role in our story, as the differential-form associated with such a graph *always* vanishes due to the $\tilde{\eta}_I$ integration. And so, these 'pathological' graphs never contribute to physically-relevant processes.)

Once we have given a perfect orientation, the system of equations $C \cdot \tilde{\lambda}$ becomes trivial to construct: each vertex can be viewed as giving an equation which expands the $\tilde{\lambda}$'s of the vertex's *sources* in terms of those of its *sinks*. Combining all such equations then gives us an expansion of the external sources' $\tilde{\lambda}$'s in terms of those of the

external sinks. Notice that when identifying two legs, (I_{in}, I_{out}) during amalgamation the degree of freedom lost in the process is accounted for via the replacement of the pair $(\alpha_{I_{in}}, \alpha_{I_{out}})$ with the single variable $\alpha_I \equiv \alpha_{I_{in}} \alpha_{I_{out}}$.

If we denote the external sources of a graph by $\{a_1, \dots, a_k\} \equiv A$, then the final linear relations imposed on the $\tilde{\lambda}$'s can easily be seen to be given by,

$$\tilde{\lambda}_A + c_{Aa} \tilde{\lambda}_a = 0, \quad (3.4.99)$$

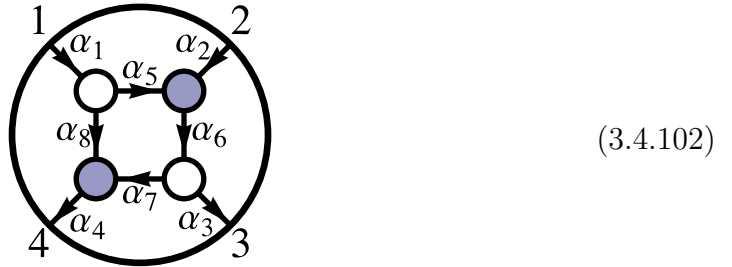
with

$$c_{Aa} = - \sum_{\Gamma \in \{A \rightsquigarrow a\}} \prod_{e \in \Gamma} \alpha_e, \quad (3.4.100)$$

and where $\Gamma \in \{A \rightsquigarrow a\}$ is any (directed) path from A to a in the graph. (If there is a closed, directed loop, then the geometric series should be summed—we will see an example of this in (3.4.107).) The entries of the matrix c_{Aa} are called the “boundary measurements” of the on-shell graph. The on-shell form on $C(\alpha) \in G(k, n)$ can then be written in terms of the variables c_{Aa} according to:

$$\left(\prod_{\text{vertices } v} \frac{1}{\text{vol}(GL(1)_v)} \right) \left(\prod_{\text{edges } e} \frac{d\alpha_e}{\alpha_e} \right) \delta^{k \times 4}(C \cdot \tilde{\eta}) \delta^{k \times 2}(C \cdot \tilde{\lambda}) \delta^{2 \times (n-k)}(\lambda \cdot C^\perp). \quad (3.4.101)$$

Let us consider a simple example to see how this works. Consider the following perfectly oriented graph:

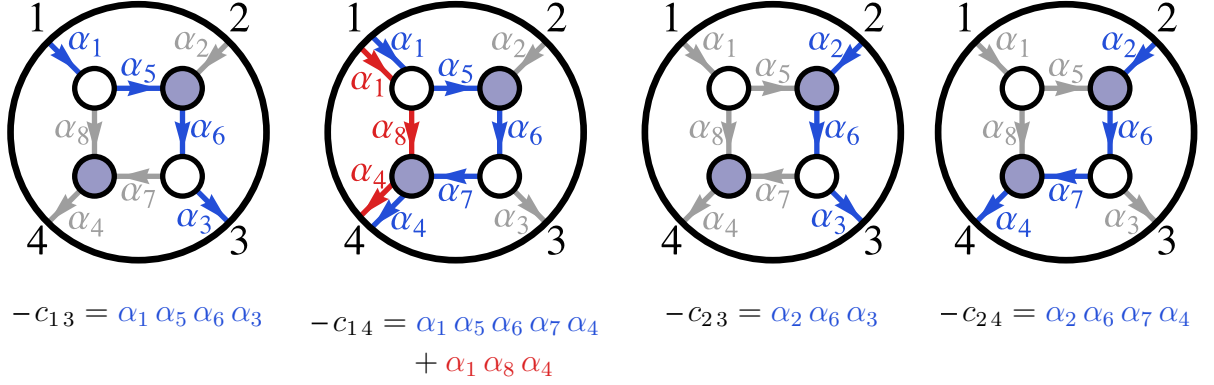


$$(3.4.102)$$

Using the equations for each directed 3-particle vertex, we can easily expand the $\tilde{\lambda}$ of each source—legs 1 and 2—in terms of those of the sinks—legs 3 and 4; e.g.,

$$\tilde{\lambda}_2 = \alpha_2 \alpha_6 (\alpha_3 \tilde{\lambda}_3 + \alpha_7 (\alpha_4 \tilde{\lambda}_4)). \quad (3.4.103)$$

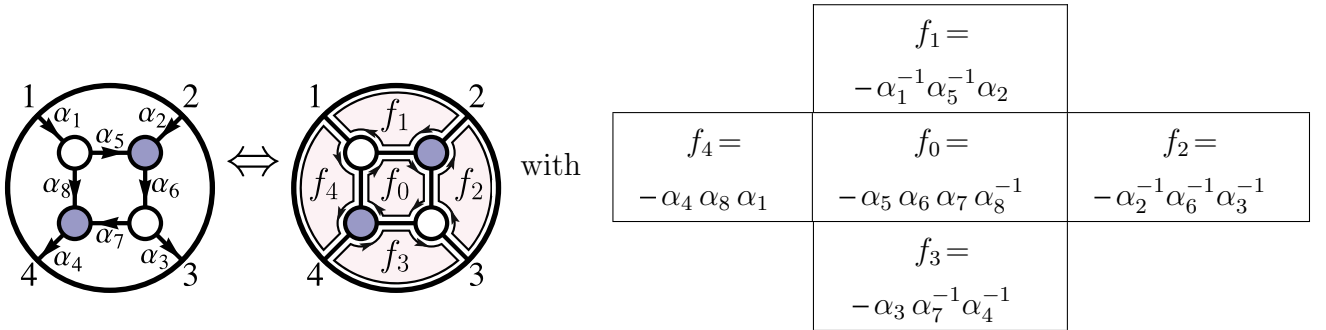
Such expansions obviously result in (3.4.100): the coefficient c_{Aa} of $\tilde{\lambda}_a$ in the expansion of $\tilde{\lambda}_A$ is simply (minus) the product of all edge-variables α_e along any path $\Gamma \in \{A \rightsquigarrow a\}$. Doing this for all the c_{Aa} of our example above, we find,



Thus, the final relations involving the $\tilde{\lambda}$'s is encoded by the matrix $C \equiv \begin{pmatrix} 1 & 0 & c_{13} & c_{14} \\ 0 & 1 & c_{23} & c_{24} \end{pmatrix}$.

Notice that only certain combinations of edge-weights appear in the equations. This happens for a very simple—and by now familiar—reason. Think of the $GL(1)$ -redundancy of each vertex as a gauge-group, with the variable of a directed edge charged as a “bi-fundamental” of the $GL(1) \times GL(1)$ of the vertices it connects. Since the configuration C must be invariant under these “gauge groups”, only gauge-invariant combinations of the edge variables can appear. And just as we saw in the previous subsection, these combinations are those familiar from lattice gauge theory and can be viewed as encoding the flux through each closed loop in the graph—that is, each of its faces. Fixing the orientation of each face to be clockwise, the flux through it is given by the product of α_e (α_e^{-1}) for each aligned (anti-aligned) edge along its boundary. For future convenience, we define the face *variables* f_i to be *minus* this product.

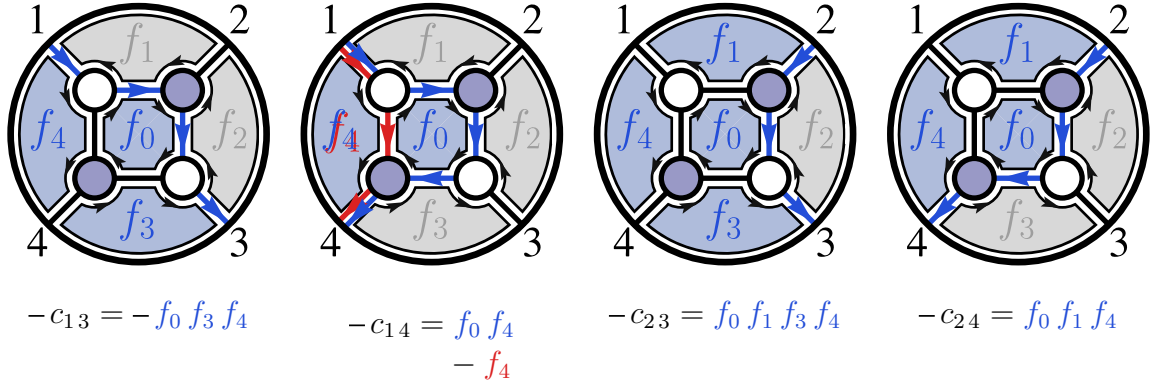
Applying this to the example above, we find:



The boundary-measurements c_{Aa} can then be expressed in terms of the faces by

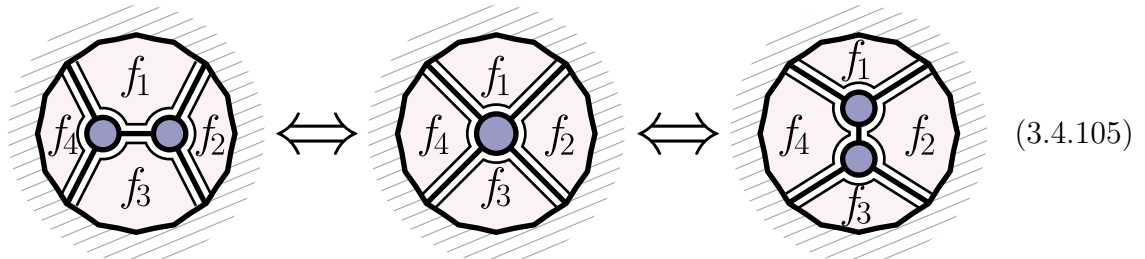
$$c_{Aa} = - \sum_{\Gamma \in \{A \rightsquigarrow a\}} \prod_{f \in \hat{\Gamma}} (-f), \quad (3.4.104)$$

where $\widehat{\Gamma}$ is the ‘clockwise’ closure of Γ . (If there are any closed, directed loops, the geometric series of faces enclosed should be summed.) The faces of course over-count the degrees of freedom by one, and this is reflected by the fact that $\prod_i (-f_i) = 1$.

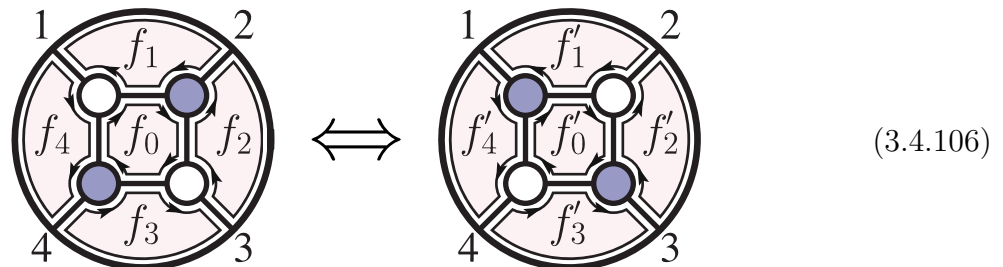


VI. Coordinate Transformations Induced by Moves and Reduction

Let us now examine how the identification of graphs via merge-operations, square-moves, and bubble-deletion is reflected in the coordinates—the edge- or face-variables—used to parameterize cells $C \in G(k, n)$. As usual, the simplest of these is the merge/un-merge operation which trivially leaves any set of coordinates unchanged. For example, in terms of the face variables, it is easy to see that



The square-move is more interesting. It is obvious that squares with opposite coloring both give us a generic configuration in $G(2, 4)$, but (as we will soon see), the square-move acts rather non-trivially on coordinates used to parameterize a cell,



Let us start by determining the precise way the face-variables f_i and f'_i of square-move related graphs are related to one another. To do this, we will provide perfect orientations (decorated with edge variables) for both graphs, allowing us to compare the resulting boundary-measurement matrices in each case. Because these two boundary measurement matrices must represent the same point in $G(2, 4)$, we will be able to explicitly determine how all the various coordinate charts are related—including the relationship between the variables f_i and f'_i . Our work will be considerably simplified if we remove the $GL(1)$ -redundancies from each vertex, leaving us with a non-redundant set of edge-variables. Of course, *any* choice of perfect orientations for the graphs, and any fixing of the $GL(1)$ -redundancies would suffice for our purposes; but for the sake of concreteness, let us consider the following:

$$\begin{pmatrix} 1 & -\alpha_1 & 0 & -\alpha_4 \\ 0 & -\alpha_2 & 1 & -\alpha_3 \end{pmatrix} \iff \begin{pmatrix} 1 & -\beta_2\beta_3\beta_4\Delta & 0 & -\beta_4\Delta \\ 0 & -\beta_2\Delta & 1 & -\beta_1\beta_2\beta_4\Delta \end{pmatrix} \quad (3.4.107)$$

Here, we have written the matrices $C(\alpha)$ and $C(\beta)$ obtained as boundary-measurements as discussed in section V.. The factor Δ in $C(\beta)$ is given by,

$$\Delta \equiv \frac{1}{1 - \beta_1\beta_2\beta_3\beta_4}, \quad (3.4.108)$$

and arises from summing the infinite geometric series of paths which circle-around the internal loop of the perfectly-oriented graph. The edge-variables in (3.4.107) used as coordinates in $G(2, 4)$ are closely-related to the face-variables in (3.4.106).

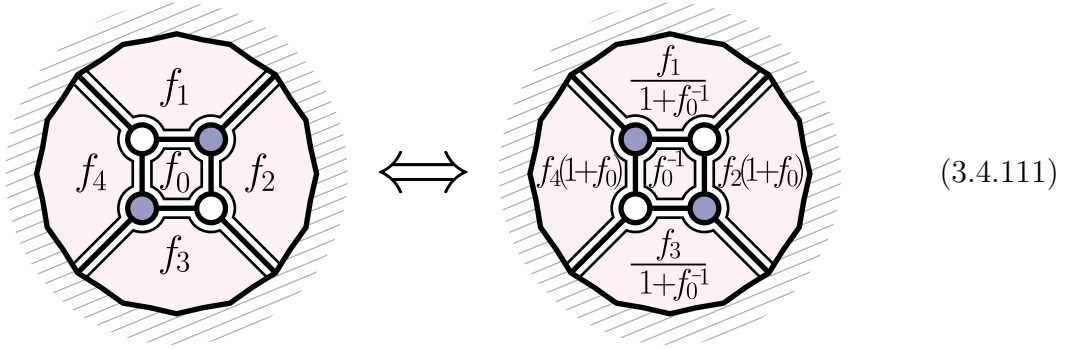
It is not hard to express the face variables in terms of the edge variables for the two orientations in (3.4.106). It is easy to see that,

$$\begin{aligned}
 f_0 &= -\alpha_1 \alpha_2^{-1} \alpha_3 \alpha_4^{-1}, & f_1 &= -\alpha_1^{-1}, & f_2 &= -\alpha_2, & f_3 &= -\alpha_3^{-1}, & f_4 &= -\alpha_4^{-1}; \\
 f'_0 &= -(\beta_1\beta_2\beta_3\beta_4)^{-1}, & f'_1 &= -\beta_1, & f'_2 &= -\beta_2, & f'_3 &= -\beta_3, & f'_4 &= -\beta_4.
 \end{aligned} \quad (3.4.109)$$

Because the boundary-measurements must represent the same point in the Grassmannian regardless of whether we use α or β coordinates, we see that:

$$\left\{ \begin{array}{l} \alpha_1 = \beta_2\beta_3\beta_4\Delta \\ \alpha_2 = \beta_2\Delta \\ \alpha_3 = \beta_1\beta_2\beta_4\Delta \\ \alpha_4 = \beta_4\Delta \end{array} \right\} \Rightarrow \left\{ \begin{array}{l} -\beta_1 = f'_1 = -\alpha_2^{-1}\alpha_3\alpha_4^{-1}\Delta = f_1f_0\Delta \\ -\beta_2 = f'_2 = -\alpha_2\Delta^{-1} = f_2\Delta^{-1} \\ -\beta_3 = f'_3 = -\alpha_1\alpha_2^{-1}\alpha_4^{-1}\Delta = f_3f_0\Delta \\ -\beta_4 = f'_4 = -\alpha_4\Delta^{-1} = f_4\Delta^{-1} \\ \therefore f'_0 = -\alpha_1^{-1}\alpha_2\alpha_3^{-1}\alpha_4 = f_0^{-1} \end{array} \right\}. \quad (3.4.110)$$

Observing that $\Delta = (1 + f_0^{-1})^{-1} = (1 + f_0)^{-1}$, we therefore conclude that a square-move alters face-variables according to:

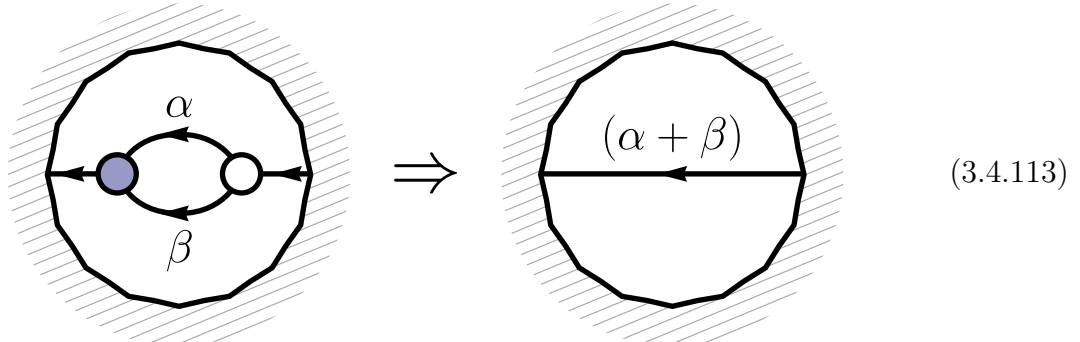


This transformation of the face variables is an example of a more general operation related to *cluster transformations*. Note that, crucially, our form is invariant under this transformation:

$$\prod_f \frac{df}{f} = - \prod_{f'} \frac{df'}{f'} \quad (3.4.112)$$

The invariance of the measure (modulo an overall sign) guarantees that the on-shell forms associated with diagrams related by square moves are the same—differing only by a change of coordinates used.

Let us now turn to bubble-deletion. It is easy to see that the following oriented subgraphs always lead to exactly the same boundary-measurements:



Following the same logic used to analyze the square-move, we find that the face-variables of these two graphs are related by:

$$(3.4.114)$$

Note again the crucial fact that the measure is invariant under this transformation:

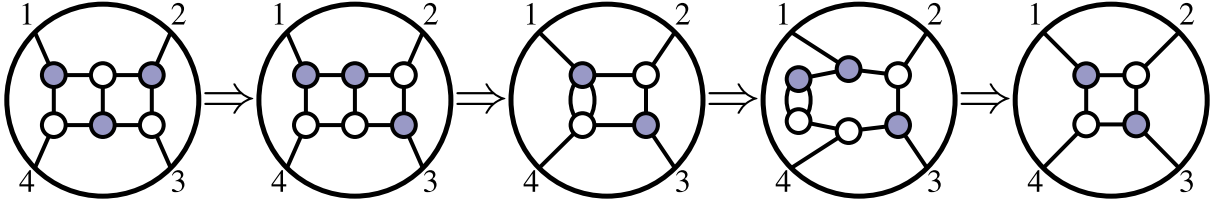
$$\frac{df_0}{f_0} \wedge \frac{df_1}{f_1} \wedge \frac{df_2}{f_2} = -\frac{df'_0}{f'_0} \wedge \frac{df'_1}{f'_1} \wedge \frac{df'_2}{f'_2}, \quad (3.4.115)$$

where $f'_0 = f_0^{-1}$. The change of variables from $f \rightarrow f'$ eliminates all dependence on f_0 associated with the bubble from the final point in the Grassmannian. Of course, the variable f_0 *remains in the measure*, but it cleanly factors out as an overall prefactor of $d\log(f_0)$. As we will see later on, MHV amplitude integrands—to all loop-orders—are always the tree-amplitude, dressed with many additional $d\log$ -factors arising from bubble-deletion. These “irrelevant” factors in the measure encode the internal degrees of freedom of the loop-momenta.

If instead of the *integrand* for scattering amplitudes, we were interested in the *residues* of the on-shell differential form—to compute, *e.g.* “leading singularities”—then these “irrelevant” $d\log$ -factors *really are irrelevant*: any residue involving them will give either one or zero.

Due to reduction, then, the number of interesting *residues* of general (non-reduced) on-shell diagrams turns is in fact finite despite the seemingly-infinite number of possible diagrams. Notice that in our way of thinking about ‘leading singularities’ and on-shell diagrams, we’ve made no distinction whatsoever between what have historically been called “ordinary” versus “composite” objects, [72, 133]. Historically, *reducible* on-shell diagrams were those with “irrelevant” additional degrees of freedom which could be systematically trivialized-away.

One example of such an on-shell form is the ‘double-box’ involving four-particles; this on-shell diagram has been known to include *one* unfixed degree-of-freedom which factorizes-out of diagram trivially upon bubble-deletion:



As discussed in generality above, the variable “lost” during bubble-deletion is in reality just a bare $d\log(\alpha)$ in the measure.

VII. Relation to Composite Leading Singularities

When all the auxiliary degrees of freedom of an on-shell form can be localized by kinematical constraints, we can think of it as having been obtained by starting with the $(n_F - n)$ -loop integrand for the scattering amplitude, and successively putting (off-shell) Feynman propagators on-shell (‘cutting them’) until the on-shell diagram is obtained. Such on-shell diagrams are referred to as “leading singularities”. Thought of in this way, they are secondary—derived—quantities obtained from the ‘primary’ object, the loop integrand. An important physical point of our present work (discussed more thoroughly in section 3.14) is that it is much more fruitful to take the opposite viewpoint: that ‘loop-integrands’ are in fact ‘derived’ from on-shell diagrams. However, since the concept of a “leading singularity” will likely be more familiar to most readers, in this subsection we will briefly review how leading singularities have been used to inform us about scattering amplitudes, and discuss in particular the subtle issue of *composite* leading singularities—which is closely related to reducibility. (This discussion is meant only to make contact with this point in previous literature, and isn’t especially germane to the rest of our chapter.)

The reduction procedure is related to what was called the “computation of composite leading singularities” in the physics literature, [70, 72, 133, 134] (see [135–137] for recent developments). In order to make the connection between the modern and the old procedures transparent let us explain what a composite leading singularity means for the four-point example already examined above. Starting with the diagram with two faces one realizes that any of the two squares actually represents a full four-particle amplitude. Choose the left one for example and draw the equivalent figure,

$$(3.4.116)$$

At this point the attentive reader can recognize this as a BCFW bridge on a physical scattering amplitude and it is given by the differential form

$$(3.4.117)$$

where the α -dependence of $\mathcal{A}_4^{(2)}$ results from that of the shifted momenta $\hat{2}$ and $\hat{3}$. This on-shell form has only two poles in α : a trivial pole at $\alpha = 0$, and another where the $\mathcal{A}_4^{(2)}$ factorizes. Of course, as there are *only two* poles in the α -plane, their residues sum to zero, and hence differ only by a sign; as the $\alpha = 0$ residue is manifestly the *undeformed* tree-amplitude $\mathcal{A}_4^{(2)}(\alpha = 0)$, so is the other (up to a sign).

The composite leading singularity technique was based on the observation that the pole at $(p_1 + p_2)^2 = 0$ is guaranteed to be there simply as a pole of the physical $\mathcal{A}_4^{(2)}(\alpha)$ tree amplitude. Therefore the pole at $(p_1 + p_2)^2 = 0$, in combination with the other three on-shell conditions on the loop momenta already in the figure, can be used to determine a residue. This gives rise to,

$$(3.4.118)$$

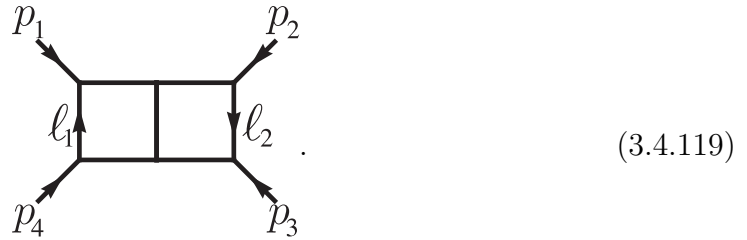
which is nothing but the on-shell diagram for a four-point amplitude $\mathcal{A}_4^{(2)}$.

We note in passing that this gives yet another ideal use of bubbles. Suppose that one is given an on-shell diagram corresponding to a leading singularity, i.e., an on-shell diagram which evaluates to an algebraic function of external momenta (conditions for this to happen are discussed in section 3.11). Next, apply a BCFW

bridge to the diagram and ask what its possible poles and corresponding residues are as a function of the BCFW variable α . Let again return to discussing to the same four-particle example. We can ask how could we have known that there was a pole in the ‘ $s_{12}(\alpha) \rightarrow 0$ channel’ and not in any other channel, by only manipulating the graph. The answer is already in figure at the end of the previous subsection: find a bubble and the channel of the bubble becomes the pole required by unitarity!

Composite leading singularities were first developed in order to compute two-loop amplitudes following a technique that was very successful at one loop [69]. While Feynman diagrams are even hard to write down explicitly for loop amplitudes, it is known that loop integrals can be reduced to a linear combination of basic standard integrals [64]. The idea is then to start with the most general linear combination of such basic integrals and find ways of computing the coefficients. This is known as the “unitarity-based method”, [12, 80, 138–140] (for recent applications of these techniques, see e.g. [137, 141]). In more modern language, the key idea is to use contour integrals to compute the coefficients. At one loop, $\mathcal{N} = 4$ super Yang-Mills only requires integrals with four propagators. Thus, the four dimensional contour for computing a given coefficient is then obviously defined by the four propagators of the given integral.

At two loops and four particles the basis of integrals must include one such as,



Now there are eight integration variables but only seven propagators. Naively it seems that this integral does not have any non-vanishing residues. The key observation is that the propagators are non-linear functions of the integration variables and therefore computing the ℓ_1 integral using the T^4 contour defined by the left box gives rise to $1/s_{12}(\ell_2)s_{41}$, which is ℓ_2 -dependent. This can then be used together with the three-propagators already present on the right to define a second T^4 contour and hence a non-vanishing residue. The ℓ_2 depend pole, $1/s_{12}(\ell_2)$, generated in this form is precisely what is needed for the new computation to be that of a single scalar box on-shell diagram.

In this way of thinking about things, the existence of composite residues is unexpected, and are made possible from “hidden” poles that are produced by Jacobian factors which appear as residues are taken. In our new picture, *all* the singularities are manifestly exposed in our “ $d\log$ ” measure for edge or face variables. There is no distinction between “composite” and “ordinary” singularities, and they are all treated together in a systematic and unified way.

3.5 Configurations of Vectors and the Positive Grassmannian

We have seen that every on-shell graph is associated with a $(k \times n)$ -matrix C , where a reduced graph with n_F faces gives us an $(n_F - 1)$ -dimensional sub-manifold of the Grassmannian $G(k, n)$. We have also seen that the invariant content of an on-shell diagram is given by the permutation which labels it. We will now link these two observations by showing that the sub-manifold in the Grassmannian associated with an on-shell graph is also characterized—for geometric reasons—by the *same* permutation which labels the graph.

Our discussion will be most transparent if we think of the Grassmannian in a complementary way to our presentation so far: instead of viewing the $k \times n$ matrix C *horizontally*, as a k -plane spanned by its rows, we want to now view C *vertically*—as a collection of n , k -dimensional columns. The $GL(k)$ -invariant data to describe any configuration are ratios of minors:

$$\frac{(a_1 \cdots a_k)}{(b_1 \cdots b_k)}, \tag{3.5.120}$$

Intuitively, a *generic* plane C would be one for which none of its minors vanish. Such a configuration would have $k(n - k)$ degrees of freedom. The vanishing of any minor of C implies some linear-dependence among its columns. Allowing for all possible linear-dependencies among the columns of C leads to the “matroid stratification” [142] of configurations, which is known to be arbitrarily complicated. Indeed, it was proven in [143] that *all* algebraic varieties are part of this matroid stratification, so understanding this amounts to *completely* taming the entire category of algebraic varieties! However, if we impose one small restriction on the set of admissible linear-dependencies, we will find a that rich, simple, and very beautiful structure emerges.

I. The Geometry and Combinatorics of the Positroid Stratification

Notice that any configuration C associated with an on-shell, planar graph is endowed with a cyclic-ordering for the columns $\{c_1, \dots, c_n\}$. It is therefore natural to consider a stratification of $G(k, n)$ that involves only linear-dependencies among (cyclically)

consecutive chains of columns. This is known as the *positroid stratification*, [43, 44] (see also [38, 144]), and will turn out to be precisely what is relevant to the physics of on-shell diagrams. In order to understand the connection most clearly, we will first discuss the stratification in some detail on its own, and show how these configurations are characterized by permutations. We will then see how the geometrically-defined permutation which characterizes C is precisely the one which would label the graph.

Before describing the stratification generally, it may help to consider some simple examples. Since the kinematical data describing the external particles enjoys a rescaling symmetry, we often find it useful to transfer this symmetry to the columns of C , identifying $c_a \sim t_a c_a$, so that (non-vanishing) columns c_a can be thought of as elements in $\mathbb{P}^{(k-1)}$ (vanishing columns simply being absent from the space). This makes it a little easier to visualize configurations—at least for small k . Consider a generic configuration $C \in G(3, 6)$, whose 6 columns—viewed as points in \mathbb{P}^2 —are arranged according to:

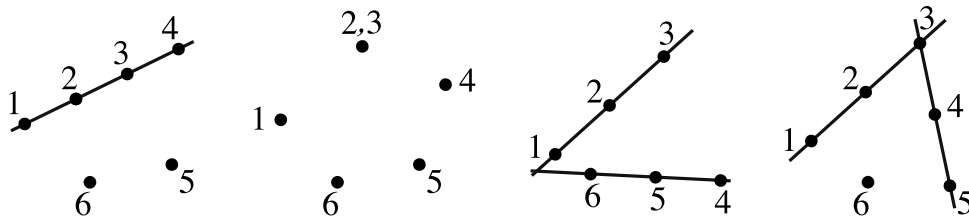
$$(3.5.121)$$

As no three of the columns are linearly-dependent, this indeed represents a generic configuration in $G(3, 6)$, and has $3(6-3) = 9$ degrees of freedom.

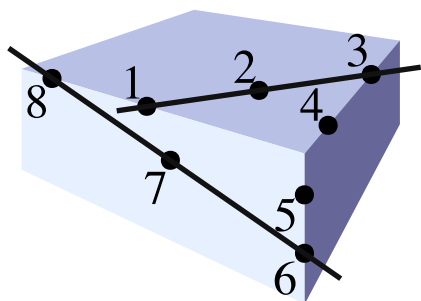
The simplest *consecutive* constraint we could impose on (3.5.121) would be to force any 3 consecutive columns to become linearly-dependent—projectively, collinear. For example, we could require that the minor (123) vanish:

$$(3.5.122)$$

From this configuration, seven possible further restrictions are possible, including:



For $k \leq 3$, it is easy to describe such configurations geometrically—being easily visualizable. But such geometric descriptions rapidly become cumbersome as k increases: even for $k = 4$ —which is still possible to visualize in three-dimensional space—configurations obtainable using only consecutive constraints can become impressively complex. Consider for example the following configuration in $G(4, 8)$:



| consec. chains of columns | span |
|---------------------------------|----------------|
| (1) (2) (3) (4) (5) (6) (7) (8) | \mathbb{P}^0 |
| (123) (34) (45) (56) (678) (81) | \mathbb{P}^1 |
| (56781) (81234) (3456) | \mathbb{P}^2 |

(3.5.123)

A more systematic way to describe any configuration in this stratification would be to list the *ranks* of spaces spanned by all consecutive chains of columns. Labeling columns mod n , let us define,

$$r[a; b] \equiv \text{rank}\{c_a, c_{a+1}, \dots, c_b\}; \quad (3.5.124)$$

then knowing $r[a; b]$ for all n^2 pairs of columns $a \leq b$ would suffice to reconstruct any particular configuration. This data is obviously highly redundant: for example, $r[a; a+n-1] = k$ for all a . We can discover how this data can be encoded more efficiently if by first organizing it in a clever way (we thank Pierre Deligne for suggesting this to us):

| | | | | | | |
|--------------|----------------|---------|------------------|-------------------|----------|----------|
| | | | | $r[n ; 2n-1]$ | \dots | $2n-1$ |
| | | | | $r[n-1 ; 2n-2]$ | \vdots | $2n-2$ |
| | | \dots | \vdots | \vdots | \dots | \vdots |
| | $r[2 ; n+1]$ | \dots | $r[n-1 ; n+1]$ | $r[n ; n+1]$ | \dots | $n+1$ |
| $r[1 ; n]$ | \vdots | \dots | $r[n-1 ; n]$ | $r[n ; n]$ | | n |
| \vdots | \vdots | \dots | $r[n-1 ; n-1]$ | | | $n-1$ |
| $r[1 ; 3]$ | $r[2 ; 3]$ | \dots | | | | \vdots |
| $r[1 ; 2]$ | $r[2 ; 2]$ | | | | | 2 |
| $r[1 ; 1]$ | | | | | | 1 |
| 1 | 2 | \dots | $n-1$ | n | \dots | |

The advantages of arranging the ranks in this way will become clear momentarily. Notice that for each pair of adjacent columns $(a, a+1)$ there is some b sufficiently large such that $r[a; b] = r[a+1; b]$, as $r[a; b]$ is bounded above by k and strictly increases with b (moving vertically in (3.5.125)). Moreover, it is easy to see that if $r[a; b] = r[a+1; b]$ for some b , then $r[a; c] = r[a+1; c]$ for all $c \geq b$, as we would have $c_a \in \text{span}\{c_{a+1}, \dots, c_b\}$, and so $\text{span}\{c_a, \dots, c_b\} \subset \text{span}\{c_a, \dots, c_c\}$ for all $c \geq b$. The same argument shows that, moving from right to left along each pair of consecutive rows in (3.5.125), for any c there exists a b such that $r[b; c] = r[b; c+1]$, and that for all $a < b$, $r[a; c] = r[a; c+1]$.

Because $r[a; b] \geq r[a+1; b]$ in general, for each a there must be a *nearest* column, which we will denote (suggestively) as ' $\sigma(a)$ ' $\geq a$ such that $r[a; \sigma(a)] = r[a+1; \sigma(a)]$. Notice that this implies that $r[a; \sigma(a)] = r[a; \sigma(a)-1] > r[a+1; \sigma(a)-1]$, as otherwise $\sigma(a)$ would not be the nearest. Similarly, we see that a must be the *maximal* column $a \leq \sigma(a)$ such that $r[a; \sigma(a)] = r[a; \sigma(a)-1]$. Thus, there is a *unique* point vertically along each pair of consecutive columns and a *unique* point horizontally along each pair of consecutive rows where the table locally looks like:

| | |
|------------------------|-------------------------|
| $r[a ; \sigma(a)]$ | $r[a+1; \sigma(a)]$ |
| $r[a ; \sigma(a)-1]$ | $r[a+1; \sigma(a)-1]$ |

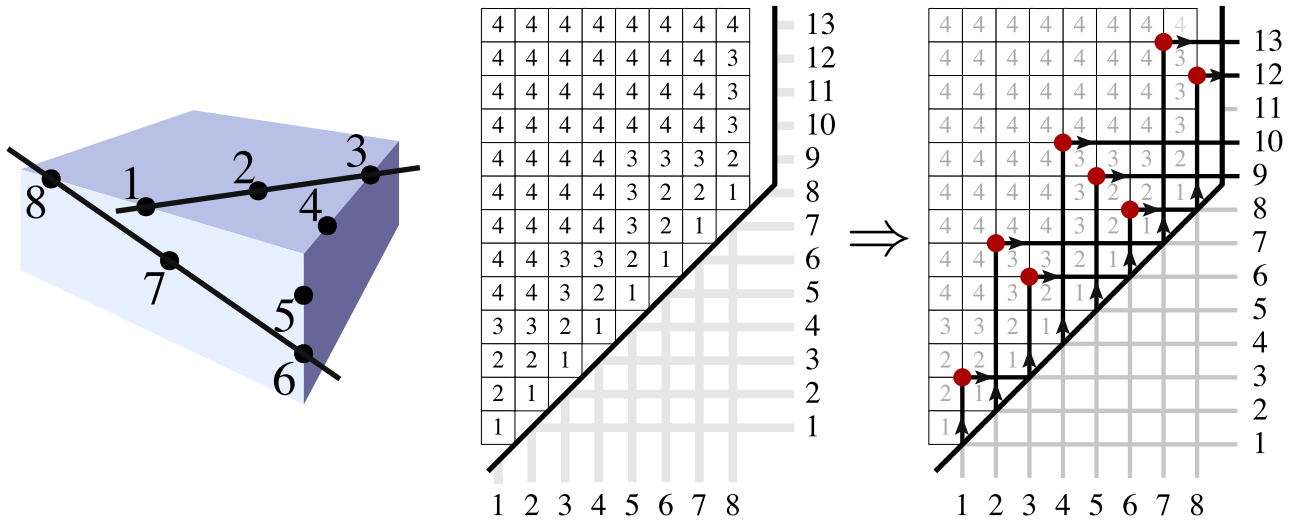
 \Leftrightarrow

| | |
|--------|--------|
| ℓ | ℓ |
| ℓ | |

(3.5.126)

These “hooks” show that σ is in fact a *permutation* among the labels $\{1, \dots, n\}$ of the column-vectors. Actually, because this definition of σ differentiates between $\sigma(a) = a$ (which occurs whenever $r[a; a] = 0$) and $\sigma(a) = a + n$, σ is automatically a *decorated* permutation as defined in section I..

We can see how the permutation encoded by these hooks can be read-off from the table of ranks, (3.5.125), by considering the example configuration given above, (3.5.123):



(This picture of the permutation σ is similar to the “juggling patterns” illustrated in [44].) And so this configuration is associated with the permutation,

$$\sigma \equiv \begin{pmatrix} 1 & 2 & 3 & 4 & 5 & 6 & 7 & 8 \\ \downarrow & \downarrow \\ 3 & 7 & 6 & 10 & 9 & 8 & 13 & 12 \end{pmatrix}. \quad (3.5.127)$$

The definition of σ can be restated in an equivalent, but more transparently geometric form:

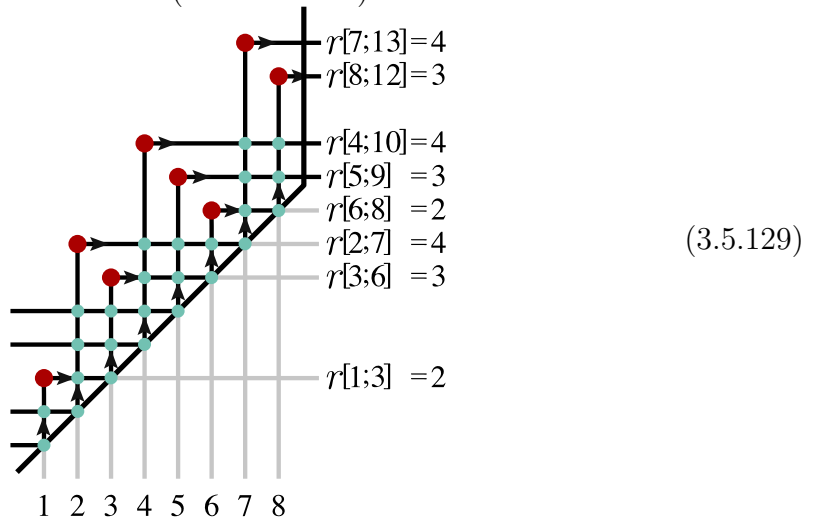
Definition: For each $a \in \{1, \dots, n\}$, the permutation $\sigma(a) \geq a$ labels the *first* column $c_{\sigma(a)}$ such that $c_a \in \text{span} \{c_{a+1}, \dots, c_{\sigma(a)}\}$.

(Notice that if $c_a = \vec{0}$, then $\sigma(a) = a$, as $\vec{0}$ is spanned by the *empty* chain $\{c_{a+1}, \dots, c_a\}$.)

This definition is useful in practice. For example, it makes it easy to understand how the dimensionality of a configuration is encoded by its permutation. Notice that because $c_a \in \text{span}\{c_{a+1}, \dots, c_{\sigma(a)}\}$, we may expand c_a into the $r[a; \sigma(a)]$ -dimensional space spanned by $\{c_{a+1}, \dots, c_{\sigma(a)}\}$; therefore, specifying c_a requires $r[a; \sigma(a)]$ degrees of freedom. And so, remembering to subtract the k^2 degrees of freedom absorbed by the overall $GL(k)$ -redundancy, we find that:

$$\dim(C_\sigma) = \sum_{a=1}^n r[a; \sigma(a)] - k^2. \quad (3.5.128)$$

Notice that $r[a; \sigma(a)]$ is nothing but the number of other hooks which intersect the vertical (or horizontal) part of any particular hook $a \mapsto \sigma(a)$. Thus, for our example in $G(4, 8)$ given above, the ranks $r[a; \sigma(a)]$ can be read-off as the number of intersections (marked in green) along each vertical (or horizontal) line:

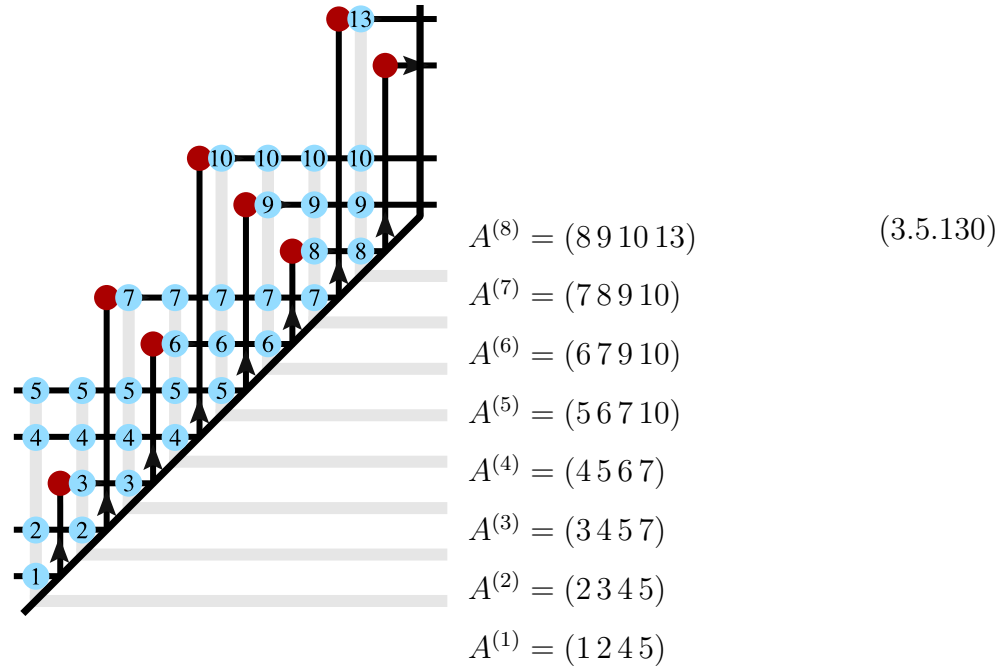


which shows that this configuration has $25 - 4^2 = 9$ degrees of freedom.

It is not hard to see how the permutation encodes *all* the ranks $r[a; b]$, thereby demonstrating that σ *fully* characterizes any configuration in the positroid stratification. If we let $q[a; b]$ denote the number of $c \in \{b-n, \dots, a\}$ such that $\sigma(c) \in \{b, \dots, a+n\}$, then $r[a; b] = k - q[a; b]$. Graphically, $q[a; b]$ is the number of hooks whose corners are above and to the left of $r[a; b]$ in the table (3.5.125).

The permutation is the most compact, most invariant way of describing the consecutive linear dependencies of a configuration of vectors. A more redundant, but sometimes useful alternative characterization of a configuration is known as the *Grassmannian necklace*, [43]: a list of n , k -tuples $A^{(a)} \equiv (A_1^{(a)}, \dots, A_k^{(a)})$ denoting the

lexicographically-minimal non-vanishing minors starting from each of the n columns. Geometrically, $A^{(a)}$ encodes the labels of the *first* k column-vectors beyond (or possibly including) c_a , for which $\text{rank}\{c_{A_1^{(a)}}, \dots, c_{A_k^{(a)}}\} = k$. In terms of the hooks described above, $A^{(a)}$ simply lists the k horizontal lines which pass above the a^{th} column (which often do not cross the hook going from $a \mapsto \sigma(a)$). In the $G(4, 8)$ example above, (3.5.123), the Grassmannian necklace can be read-off as follows:



II. Canonical Coordinates and the Equivalence of Permutation Labels

In section 3.4, we saw that every on-shell graph is associated with both a permutation (via left-right paths) and also a k -plane in n dimensions $C \in G(k, n)$ encoding the linear-relations involving the external data. And we have just seen that any such plane C , viewed as a configuration of column-vectors, can *also* be labeled by a permutation. We will now demonstrate that these permutation labels match—that the configuration $C \in G(k, n)$ associated with an on-shell graph labeled by the left-right-path permutation σ , is labeled *geometrically* by the *same* permutation σ .

The proof of the equivalence of these permutation labels is both simple and constructive. Recall from subsection II. that a representative, reduced on-shell graph can be constructed for any permutation σ by decomposing it into a sequence of ‘adjacent’ transpositions acting on a trivial permutation, where each successive transposition in the decomposition adds a BCFW-bridge to the graph according to:

$$(3.5.131)$$

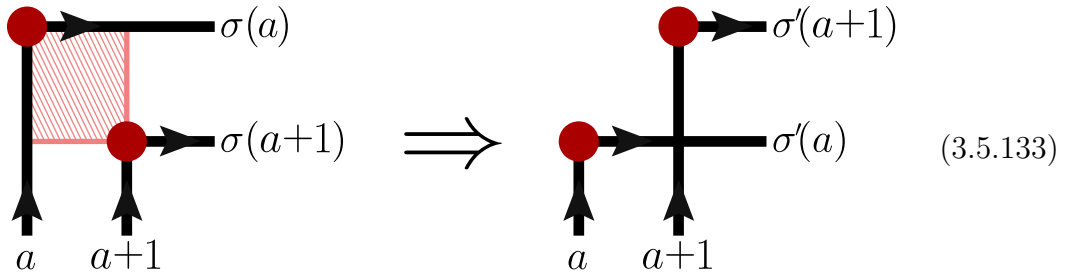
(As before, recall that two columns are to be considered ‘adjacent’ if separated only by columns which are self-identified under σ .) Now, just as we can build-up a representative on-shell graph in this way for any permutation, we can also build-up a representative matrix $C_\sigma \in G(k, n)$, which we will find to be labeled *geometrically* by the same permutation. As a bonus, this construction will provide us with explicit coordinates for any cell of the positroid, and these coordinates will have many nice properties.

What action on the columns of C corresponds to adding a BCFW bridge, (3.5.131)? In terms of the matrices associated with on-shell graphs, adding a bridge shifts,

$$c_{a+1} \mapsto c_{\widehat{a+1}} \equiv c_{a+1} + \alpha c_a; \quad (3.5.132)$$

recall also this shift changes the measure on the Grassmannian by adding a factor of $d\log(\alpha)$.

Notice that if we take a residue about $\alpha = 0$, we restore the original configuration; thus, $\alpha \mapsto 0$ can be viewed as deleting the new edge from the graph in (3.5.131). Of course, in terms of the left-right path permutations, the BCFW bridge transposes the images of a and $a+1$ under σ . What we need to show, therefore, is that the shift (3.5.132) has this same effect on the geometric permutation defined by the columns of C :

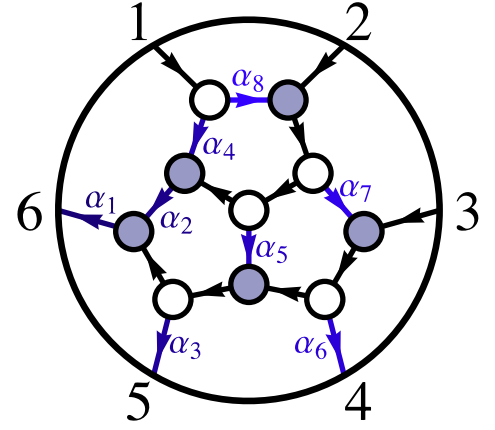


Let us now show that this is indeed the change induced by (3.5.132). Clearly, the transformation (3.5.132) can at most affect the ranks of chains which *include* c_{a+1} and *not* c_a . After the shift, $c_{\widehat{a+1}}$ is no longer spanned by $\{c_{a+2}, \dots, c_{\sigma(a+1)}\}$, because c_a is not; but $c_{\widehat{a+1}}$ is spanned by $\{c_{a+2}, \dots, c_{\sigma(a)}\}$; and so, $\sigma(a+1) \mapsto \sigma'(a+1) = \sigma(a)$. Similarly, after the shift c_a is trivially in the span of $\{c_{\widehat{a+1}}, \dots, c_{\sigma(a+1)}\}$ as $\text{span}\{c_{\widehat{a+1}}, \dots, c_{\sigma(a+1)}\} = \text{span}\{c_a, c_{a+1}, \dots, c_{\sigma(a+1)}\}$; and so, $\sigma(a) \mapsto \sigma'(a) = \sigma(a+1)$. And we are done.

Therefore, just as successive BCFW-bridges, (3.5.131), can be used to construct a representative, reduced on-shell graph for any permutation, they also provide us with a representative matrix for the configuration—and the BCFW-shift parameters, denoted α_i , provide us with coordinates.

We can see how this works explicitly by revisiting the example given in section II. where we used successive BCFW-bridges to construct a representative on-shell graph for the permutation $\{4, 6, 5, 7, 8, 9\}$. Repeating the same construction as before, but now decorating each BCFW-bridge with its corresponding shift-parameter α_i gives rise to the following:

| τ | 1 | 2 | 3 | 4 | 5 | 6 | BCFW shift |
|--------|---|---|---|---|---|---|----------------------------------|
| | ↓ | ↓ | ↓ | ↓ | ↓ | ↓ | |
| (12) | 4 | 6 | 5 | 7 | 8 | 9 | $c_2 \mapsto c_2 + \alpha_8 c_1$ |
| (23) | 6 | 4 | 5 | 7 | 8 | 9 | $c_3 \mapsto c_3 + \alpha_7 c_2$ |
| (34) | 6 | 5 | 4 | 7 | 8 | 9 | $c_4 \mapsto c_4 + \alpha_6 c_3$ |
| (23) | 6 | 7 | 5 | 4 | 8 | 9 | $c_3 \mapsto c_3 + \alpha_5 c_2$ |
| (12) | 7 | 6 | 5 | 4 | 8 | 9 | $c_2 \mapsto c_2 + \alpha_4 c_1$ |
| (35) | 7 | 6 | 8 | 4 | 5 | 9 | $c_5 \mapsto c_5 + \alpha_3 c_3$ |
| (23) | 7 | 8 | 6 | 4 | 5 | 9 | $c_3 \mapsto c_3 + \alpha_2 c_2$ |
| (36) | 7 | 8 | 9 | 4 | 5 | 6 | $c_6 \mapsto c_6 + \alpha_1 c_3$ |

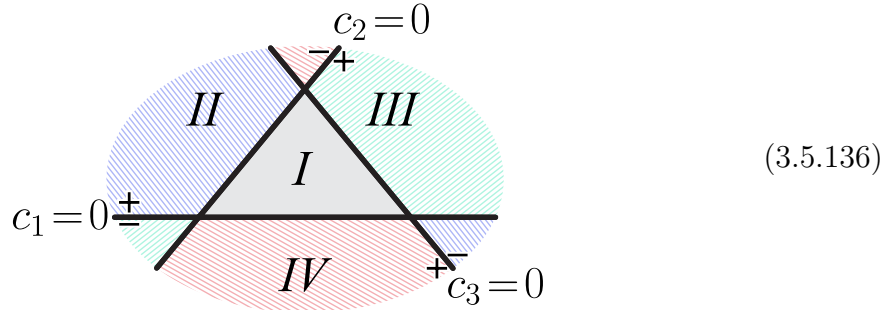


Starting with the zero-dimensional configuration labeled by $\{7, 8, 9, 4, 5, 6\}$ and performing each successive BCFW-shift generates the following representation of C :

$$C(\vec{\alpha}) \equiv \begin{pmatrix} 1 & (\alpha_4 + \alpha_8) & \alpha_4(\alpha_5 + \alpha_7) & \alpha_4\alpha_5\alpha_6 & 0 & 0 \\ 0 & 1 & (\alpha_2 + \alpha_5 + \alpha_7) & (\alpha_2 + \alpha_5)\alpha_6 & \alpha_2\alpha_3 & 0 \\ 0 & 0 & 1 & \alpha_6 & \alpha_3 & \alpha_1 \end{pmatrix}. \quad (3.5.134)$$

describe this object intrinsically, and then return to on-shell diagrams and show how the amalgamation picture described in section IV. makes it obvious that on-shell diagrams—whether reduced or not—are always associated with points in $G_+(k, n)$, and demonstrate how this works explicitly for the reduced graphs obtained via the BCFW-bridge decomposition described in the previous section.

Perhaps the best way to motivate the positive Grassmannian is by starting with the simplest case, $G_{\mathbb{R}}(1, n) \simeq \mathbb{RP}^{n-1}$. Here, the column ‘vectors’ c_a of a 1-plane $C \equiv (c_1, \dots, c_n)$ are simply homogeneous coordinates on \mathbb{RP}^{n-1} , and the ‘positive part’ of \mathbb{RP}^{n-1} is simply the part of projective space where all the homogeneous coordinates are positive, which is nothing but a simplex. Consider for example \mathbb{RP}^2 corresponding to the 1-plane $C = (c_1, c_2, c_3)$:



The ‘positive part’ of \mathbb{RP}^2 is defined by the region where all the homogeneous coordinates c_a are positive—corresponding to the (open) region labeled “I” above. Of course, because we often allow ourselves to rescale each $c_a \sim t_a c_a$, *any* relative signs among the homogeneous coordinates will describe an open-region of \mathbb{RP}^2 essentially equivalent to region I, dividing \mathbb{RP}^2 into four “positive parts” as indicated in (3.5.136). Continuing this logic to higher n , it is clear that the “positive part” of \mathbb{RP}^{n-1} should be defined as the (open) simplex for which all homogeneous coordinates are positive.

For higher k , the “positive part” of $G(k, n)$ is a natural generalization of the notion of a simplex in $G(1, n)$. Thinking of the homogeneous coordinates c_a as (1×1) -‘minors’ of $C \in G(1, n)$, it is natural to define the positive part of $G(k, n)$ to be the region for which all *ordered* minors $(a_1 \cdots a_k)$, with $a_1 < \cdots < a_k$, are positive. (Notice that without a fixed ordering of the columns, it would be meaningless to discuss the positivity of minors as they are antisymmetric with respect to ordering.)

Although this definition of the positive part of $G(k, n)$ requires an ordering of the columns, no reference was made to any *cyclic* structure. But cyclicity emerges

automatically. Naïvely, it would seem that there could be a distinct positive part for each of the $n!$ orderings of the columns, but some of these are actually the same. Suppose that $C \in G_+(k, n)$ for columns ordered according to $\{c_1, \dots, c_n\}$. Then the change

$$c_1 \rightarrow c_2, c_2 \rightarrow c_3, \dots, c_n \rightarrow (-1)^{k+1} c_1, \quad (3.5.137)$$

gives a positive configuration in the rotated ordering. This is referred to as a “twisted” cyclic symmetry.

Notice that the definition of $G_+(k, n)$ has so far made no reference to *consecutivity* of the constraints involved in its boundary configurations (where some minors are allowed to vanish). The reason why consecutivity plays a role is that not all minors are independent—recall from section I. that they satisfy Plücker relations following from Cramer’s rule, (3.4.47). The relevance of this will become clear in a simple example. Consider the case of $G(2, 4)$, where we have

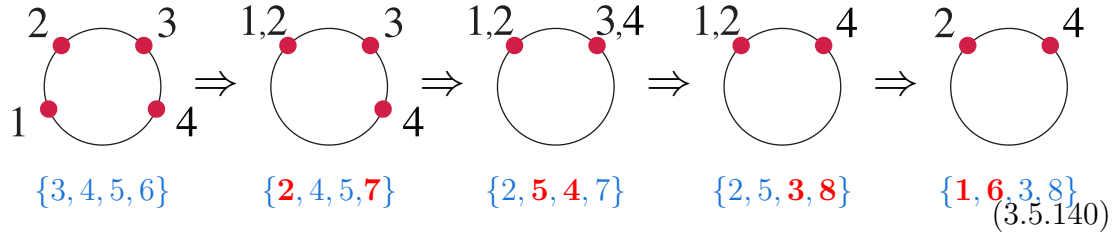
$$(13)(24) = (12)(34) + (14)(23). \quad (3.5.138)$$

Notice the presence of the *plus* sign on the right-hand side. It implies that if we start with a configuration in $G_+(2, 4)$, the minor (13) can only vanish if at least two other ordered minors also vanish.

We can see how consecutivity matters more generally for $G(2, n)$ by thinking of the column-vectors projectively as points in \mathbb{RP}^1 . If we rescale the columns to be of the form $c_a \sim \begin{pmatrix} \beta_a \\ 1 \end{pmatrix}$, then $(ab) = (\beta_a - \beta_b)$, and so a positive configuration is simply one for which $\beta_a > \beta_b$ for all $a < b$. That is, the positive part of $G(2, n)$ is nothing but configurations of *ordered* points on a circle:

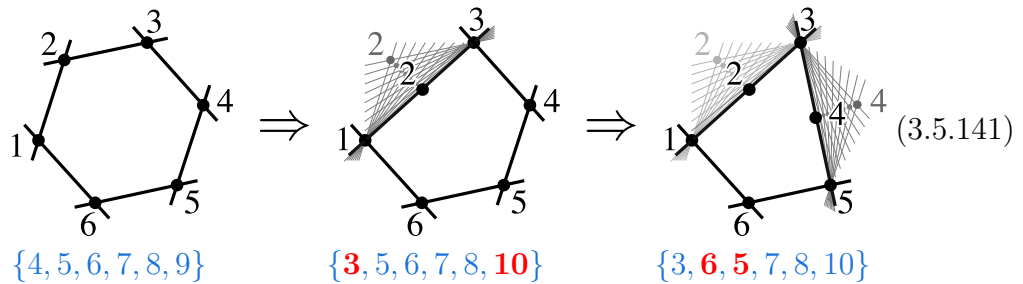


As such, it is clear that co-dimension one boundaries should correspond to the vanishing of only *consecutive* minors—the collision of adjacent points in \mathbb{RP}^1 . In $G(2, 4)$, for example, the following sequence of boundaries connect a generic configuration to one without any degrees of freedom:



In order to see that this phenomenon is not peculiar to $G(2, n)$, and to get a better picture for what is going on, let us look again at $G(3, n)$. We may use the rescaling symmetry to write each column as $c_a \sim \begin{pmatrix} \hat{c}_a \\ 1 \end{pmatrix}$, where each \hat{c}_a is in \mathbb{R}^2 . It is then easy to check that the requirement of positivity for all ordered minors translates into the geometric statement that the points \hat{c}_a form the vertices of a *convex* polygon in the plane.

Because of convexity, it is easy to see that going to boundaries can only involve linear relations between *consecutive* chains of columns. For instance, below we draw a projective representation of a generic configuration $G(3, 6)$, and some of the boundaries obtainable while preserving convexity:



From the generic configuration, it is possible to make any consecutive minor vanish such as (123) shown above. Projectively, a minor will vanish whenever three points become collinear. However, note that for instance the non-consecutive minor (135) cannot be made to vanish without either: 1. destroying convexity, or 2. forcing *additional* minors to vanish along the way. And so, we find the same stratification of successive boundaries as those obtained by consecutive constraints.

These examples suffice to motivate a remarkable connection, which we will shortly understand in a simple and general way. In the first part of this section, we discussed a stratification of the *complex* Grassmannian, in terms of specified linear dependencies between consecutive column vectors. We now see that this structure is beautifully characterized by the structure of the *real* Grassmannian: the cell decomposition of

the positive Grassmannian is precisely specified by giving linear dependencies between consecutive vectors.

But first, let us step back and understand the simple and direct connection between on-shell diagrams and the positive Grassmannian. Recall that we can construct the configuration $C \in G(k, n)$ for any on-shell diagram by simply “amalgamating” the 1- and 2-planes associated with the white, and black vertices, respectively. We saw in section IV. that only two operations were needed to construct the plane $C \in G(k, n)$ for any on-shell graph: combining graphs via *direct-products*, and gluing legs together by *projecting-out* on-shell pairs of particles. Let us briefly recall how these two operations act on the minors of the planes involved, and verify the wonderful fact that *amalgamation preserves positivity*.

The proof is simple. First, observe that we can always use rescaling symmetry to make any configuration in $G(1, 3)$ or $G(2, 3)$ positive (see, e.g. (3.5.136)). Therefore, an on-shell graph can always be constructed by attaching these positive cells to each vertex, and then proceeding with amalgamation as described in section IV.. Recall that the simplest of the two operations, taking direct-products, acts trivially on minors: suppose that the columns of $C_L \in G(k_L, n_L)$ are ordered $\{c_1, \dots, c_{n_L}\}$, and that those of $C_R \in G(k_R, n_R)$ are ordered $\{c_{n_L+1}, \dots, c_{n_L+n_R}\}$, then all the non-vanishing minors $C_L \otimes C_R \mapsto C \in G(k_L+k_R, n_L+n_R)$ will be given by,

$$(a_1 \cdots a_{k_L} b_1 \cdots b_{k_R})|_C = (a_1 \cdots a_{k_L})|_{C_L} \times (b_1 \cdots b_{k_R})|_{C_R} ; \quad (3.5.142)$$

and so, if C_L and C_R are both *positive*, then C will be as well.

The second fundamental operation, *projection*, takes a configuration $C \in G(k+1, n+2)$ and produces a configuration $\widehat{C} \in G(k, n)$, obtained by projecting C into the orthogonal-complement of $(c_A - c_B)$, for two *adjacent* legs (AB) . In terms of minors, this operation acts according to:

$$(a_1 \cdots a_k)|_{\widehat{C}} = (A a_1 \cdots a_k)|_C + (B a_1 \cdots a_k)|_C . \quad (3.5.143)$$

If (AB) are the *first two* labels for the columns of $C \in G_+(k+1, n+2)$, then both terms on the right hand side are trivially positive; if (AB) are not the first two columns, then they can always be brought to this position at the trivial cost of rescaling some columns by (-1) as described during our discussion of the twisted cyclic structure of $G_+(k, n)$ in section III..

IV. Canonically Positive Coordinates for Positroids

We have seen many ways to describe the configuration $C \in G(k, n)$ associated with an on-shell diagram, including procedures which explicitly generate a matrix representative of C parameterized by variables attached to the *faces* or the *edges* of a graph (see section V.). And in section II., we saw that “canonical” coordinates for any cell $C \in G(k, n)$ in the positroid stratification can be systematically generated (along with a representative, reduced graph) by applying successive BCFW-shifts. In this subsection, we demonstrate that a slight-modification of these BCFW-bridge coordinates (see equation (3.5.149)) have the remarkable property that when the coordinates α_i are themselves positive, then $C(\alpha_i) \in G_+(k, n)$! We will refer to any such coordinates which have this property as “positive”.

Before we describe how the BCFW-bridge coordinates make positivity manifest in this way, let us first describe a more intuitive way to parameterize generic configurations in $G(k, n)$ with coordinates which share this property. It will turn out that this geometrically-motivated parameterization of $G(k, n)$ will be essentially identical to that which is generated by the BCFW-bridge construction, and so this slight detour will prove itself quite useful later (see section 3.7).

Observe that any homogeneous coordinates for $G(1, n) \simeq \mathbb{P}^{n-1}$ are trivially positive:

$$C^{(1,n)} \equiv \left(\beta_{1,1} \quad \beta_{1,2} \quad \cdots \quad \beta_{1,n-1} \quad \beta_{1,n} \right), \quad (3.5.144)$$

because $C^{(k,n)}(\beta) \in G_+(1, n)$ whenever all the variables $\beta_{1,a} > 0$.

The first non-trivial case is for $G(2, n)$. Recall from our discussion above that if we rescale all the column vectors of $C \in G(2, n)$ to be of the form $c_a \sim \begin{pmatrix} \hat{c}_a \\ 1 \end{pmatrix}$, then $(ab) = \hat{c}_a - \hat{c}_b$; and so any set of ordered numbers $\hat{c}_1 > \cdots > \hat{c}_n$ will parameterize a point in $G_+(2, n)$. One natural way to create such an ordered list of positive numbers would be to have $\hat{c}_a = \hat{c}_{a+1} + \beta_{1,a+1}$ for arbitrary, positive $\beta_{1,a+1}$ —where we have intentionally named these ‘arbitrary’ positive parameters according to our parameterization of $G_+(1, n)$ in (3.5.144). Restoring the degrees of freedom which rescale each column vector, we obtain the following:

$$C^{(2,n)} \equiv \begin{pmatrix} \beta_{2,1}(\beta_{1,2} + \cdots + \beta_{1,n}) & \beta_{2,2}(\beta_{1,3} + \cdots + \beta_{1,n}) & \cdots & \beta_{2,n-1}(\beta_{1,n}) & 0 \\ & \beta_{2,1} & & \beta_{2,n-1} & \beta_{2,n} \end{pmatrix}. \quad (3.5.145)$$

It is easy to verify that if $\beta_{\alpha,a} > 0$, then $C^{(2,n)}(\beta) \in G_+(2, n)$.

This construction naturally continues recursively, generating positive coordinates for any (generic) configuration in $G(k, n)$ as follows:

$$C^{(k,n)} \equiv \begin{pmatrix} \beta_{k,1} \widehat{c}_1^{(k,n)} & \cdots & \beta_{k,n-1} \widehat{c}_{n-1}^{(k,n)} & 0 \\ \beta_{k,1} & \cdots & \beta_{k,n-1} & \beta_{k,n} \end{pmatrix} \quad \text{with} \quad \widehat{c}_a^{(k,n)} \equiv \sum_{j=(a+1)}^n c_j^{(k-1,n)}. \quad (3.5.146)$$

Surprisingly, after using $GL(k)$ -redundancy to remove the excess degrees of freedom in the parameterization of $C^{(k,n)}(\beta)$, it turns out that these are (essentially) identical to the coordinates produced by the BCFW-bridge construction described in section II.. Indeed, the only distinction is a relabeling of bridge-variables α_i according to:

| | | | | | | | | | | | | | | | | |
|-----------------|-----------------|----------|-----------------|---------------|-------------------|-----------------------|----------------|----------|---------------------|----------|-------------------|---------------|----------|----------|-----------------------|------------|
| $\beta_{1,k+1}$ | $\beta_{1,k+2}$ | \cdots | $\beta_{1,n-1}$ | $\beta_{1,n}$ | \Leftrightarrow | α_d | α_{d-2} | \cdots | \cdots | \cdots | \cdots | α_ℓ | \cdots | \cdots | $\alpha_{k(k-1)/2+1}$ | |
| $\beta_{2,k+1}$ | $\beta_{2,k+2}$ | \cdots | $\beta_{2,n-1}$ | $\beta_{2,n}$ | | α_{d-1} | \cdots | \cdots | \cdots | \cdots | $\alpha_{\ell+1}$ | \cdots | \cdots | \cdots | \cdots | α_2 |
| \vdots | \vdots | \ddots | \vdots | \vdots | | \vdots | \cdots | \cdots | \cdots | \cdots | \cdots | \cdots | \cdots | \cdots | \cdots | α_3 |
| $\beta_{k,k+1}$ | $\beta_{k,k+2}$ | \cdots | $\beta_{k,n-1}$ | $\beta_{k,n}$ | | $\alpha_{d-k(k-1)/2}$ | \cdots | \cdots | $\alpha_{\ell+k-1}$ | \cdots | \cdots | \cdots | \cdots | \cdots | \cdots | α_1 |
| $\beta_{k,k+1}$ | $\beta_{k,k+2}$ | \cdots | $\beta_{k,n-1}$ | $\beta_{k,n}$ | | $\alpha_{d-k(k-1)/2}$ | \cdots | \cdots | $\alpha_{\ell+k-1}$ | \cdots | \cdots | \cdots | \cdots | \cdots | \cdots | α_1 |

Let us now show that positivity is a *manifest* property of the BCFW-bridge coordinates for *all* positroid cells. This will also complete the connection between on-shell graphs, the stratification of configurations of vectors given by prescribing linear dependencies between consecutive vectors, and the cell decomposition of the *positive* Grassmannian.

We begin by observing that the minors of C transform nicely under BCFW-shifts:

$$(\cdots a+1 \cdots) \mapsto (\cdots \widehat{a+1} \cdots) = (\cdots a+1 \cdots) + \alpha (\cdots a \cdots). \quad (3.5.147)$$

And so, if we start with a configuration C in the positive Grassmannian, and if a and $a+1$ are *strictly* adjacent—with no columns between them self-identified under σ —then the BCFW-shift preserves positivity, because whenever $(\cdots a+1 \cdots)$ is ordered, so is $(\cdots a \cdots)$.

However, we must remember that the decomposition of a permutation into ‘adjacent’ transpositions allows for a and “ $a+1$ ” to be separated by any number of columns which map to themselves (mod n) under σ . Because $\sigma(b) = b$ (as opposed to $\sigma(b) = b+n$) implies that $c_b = 0$, all minors involving b vanish; and so, skipping-over these columns will not affect any non-vanishing minors. However, $\sigma(b) = b+n$ if and only if $c_b \notin \text{span}\{c_{b+1}, \dots, c_{b+n-1}\}$, implying that c_b is not spanned by the rest of the columns of C ; as such, $\sigma(b) = b+n$ implies that b *must* be involved in any

non-vanishing $(k \times k)$ -minor of C . And so, when this happens, the shift in (3.5.147) may not preserve ordering for both of the terms.

To illustrate this minor subtlety, consider the very simplest case in which it arises: the one-dimensional configuration $C \in G(2, 3)$ labeled by the permutation $\sigma \equiv \{3, 5, 4\}$. The decomposition of σ into ‘adjacent’ transpositions involves only one step: (13)—an ‘adjacent’ transposition which skips-over column c_2 because $\sigma(2) = 2+3$. Explicitly, the BCFW-coordinates of C_σ would be generated as follows:

| | | | | |
|--------|---|---|---|----------------------------------|
| τ | 1 | 2 | 3 | BCFW shift |
| | ↓ | ↓ | ↓ | |
| (13) | 3 | 5 | 4 | $c_3 \mapsto c_3 + \alpha_1 c_1$ |
| | 4 | 5 | 3 | |

$$\begin{pmatrix} 1 & 0 & 0 \\ 0 & 1 & 0 \end{pmatrix} \xrightarrow[\alpha_1]{(13)} \begin{pmatrix} 1 & 0 & \alpha_1 \\ 0 & 1 & 0 \end{pmatrix}$$

$\{4, 5, 3\}$
 $\{3, 5, 4\}$

(3.5.148)

Notice that the minor (23), which vanishes before the shift, becomes $(23) \mapsto (\widehat{23}) = (23) + \alpha_1(21) = -\alpha_1(12)$ after the shift. And so, if we wish to make the final configuration C *positive*, we must take α_1 to be negative; alternatively, we could redefine the rule for BCFW-shifts so that the transposition (13) actually corresponds to a shift $c_3 \mapsto c_3 - \alpha_1 c_1$. Of the two alternatives, we prefer the latter as then positivity of the BCFW-shift coordinates would directly imply that a configuration were positive.

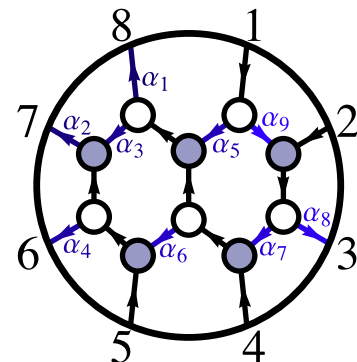
It is easy to see how this simple example generalizes: in order to preserve the positivity of minors *and* the coordinates, we should redefine the BCFW-shift so that the transposition of a and “ $a+1$ ” changes the columns of C according to

$$c_{a+1} \mapsto c_{a+1} + (-1)^q \alpha c_a, \tag{3.5.149}$$

where q is the number of columns b between a and “ $a+1$ ” such that $\sigma(b) = b+n$. In this modified form, the BCFW-shift is *guaranteed* to preserve positivity. And so, restricting all the coordinates α_i to be positive will always result in a configuration $C(\vec{\alpha})$ in the *positive* Grassmannian $G_+(k, n)$.

To see how these *signed* BCFW-shifts make positivity manifest—and as one further example of the BCFW-bridge construction described in section II.—consider the following coordinates constructed for the configuration in $G(4, 8)$ given in (3.5.123):

| | | 1 | 2 | 3 | 4 | 5 | 6 | 7 | 8 | BCFW shift | |
|--------|-----|---|----|---|----|----|---|----|----|----------------------------------|--|
| τ | q | ↓ | ↓ | ↓ | ↓ | ↓ | ↓ | ↓ | ↓ | | |
| (12) | 0 | 3 | 7 | 6 | 10 | 9 | 8 | 13 | 12 | $c_2 \mapsto c_2 + \alpha_9 c_1$ | |
| (23) | 0 | 7 | 3 | 6 | 10 | 9 | 8 | 13 | 12 | $c_3 \mapsto c_3 + \alpha_8 c_2$ | |
| (24) | 0 | 7 | 6 | 3 | 10 | 9 | 8 | 13 | 12 | $c_4 \mapsto c_4 + \alpha_7 c_2$ | |
| (45) | 0 | 7 | 10 | 3 | 6 | 9 | 8 | 13 | 12 | $c_5 \mapsto c_5 + \alpha_6 c_4$ | |
| (14) | 1 | 7 | 10 | 3 | 9 | 6 | 8 | 13 | 12 | $c_4 \mapsto c_4 - \alpha_5 c_1$ | |
| (56) | 0 | 9 | 10 | 3 | 7 | 6 | 8 | 13 | 12 | $c_6 \mapsto c_6 + \alpha_4 c_5$ | |
| (45) | 0 | 9 | 10 | 3 | 7 | 8 | 6 | 13 | 12 | $c_5 \mapsto c_5 + \alpha_3 c_4$ | |
| (57) | 0 | 9 | 10 | 3 | 8 | 7 | 6 | 13 | 12 | $c_7 \mapsto c_7 + \alpha_2 c_5$ | |
| (48) | 1 | 9 | 10 | 3 | 8 | 13 | 6 | 7 | 12 | $c_8 \mapsto c_8 - \alpha_1 c_4$ | |
| | | 9 | 10 | 3 | 12 | 13 | 6 | 7 | 8 | | |



$$\begin{pmatrix}
 1 & \alpha_9 & 0 & -\alpha_5 & -\alpha_5 \alpha_6 & 0 & 0 & 0 \\
 0 & 1 & \alpha_8 & \alpha_7 & 0 & 0 & 0 & 0 \\
 0 & 0 & 0 & 1 & \alpha_3 + \alpha_6 & \alpha_3 \alpha_4 & 0 & -\alpha_1 \\
 0 & 0 & 0 & 0 & 1 & \alpha_4 & \alpha_2 & 0
 \end{pmatrix}$$

It is easy to verify that all the non-vanishing minors of $C(\alpha) \in G(4, 8)$ are positive when $\alpha_i \in \mathbb{R}_+$. For example, consider the minor,

$$(2457) = \alpha_2 \alpha_3 \alpha_5 + \alpha_2 \alpha_3 \alpha_7 \alpha_9 + \alpha_2 \alpha_6 \alpha_7 \alpha_9, \quad (3.5.150)$$

the positivity of which requires, for example, the *signed* BCFW-shift $c_4 \mapsto c_4 - \alpha_5 c_1$.

3.6 Boundary Configurations, Graphs, and Permutations

I. Physical Singularities and Positroid Boundaries

Recall that an on-shell diagram labeled by the permutation σ corresponds to a differential form f_σ obtained via integration over the configuration $C_\sigma(\alpha) \in G(k, n)$ subject to the constraints that C_σ be orthogonal to $\tilde{\lambda}$ and contain λ :

$$f_\sigma = \int_{C_\sigma} \frac{d\alpha_1}{\alpha_1} \wedge \dots \wedge \frac{d\alpha_d}{\alpha_d} \delta^{k \times 4}(C_\sigma \cdot \tilde{\eta}) \delta^{k \times 2}(C_\sigma \cdot \tilde{\lambda}) \delta^{2 \times (n-k)}(\lambda \cdot C_\sigma^\perp), \quad (3.6.151)$$

where α_i are *canonical* (e.g. BCFW-bridge) coordinates for the configuration C_σ . Because the δ -functions encode $(2n-4)$ constraints in general (together with the 4 constraints of momentum-conservation), cells with $(2n-4)$ degrees of freedom can be fully-localized, while those of lower dimension leave-behind further δ -functions which impose constraints on the external kinematical data.

On-shell differential forms which impose constraints on the external data (beyond momentum conservation) represent physical *singularities*: places in the space of kine-

mathematical data where higher-degree forms develop poles. As we saw in section IV., such singularities are of primary physical interest: for example, knowing the singularity-structure of scattering amplitudes suffices to fix them completely to all loop-orders via the BCFW recursion relations, (3.2.21).

The physical singularities of on-shell differential forms, therefore, correspond to the *boundaries* of the corresponding configurations in the Grassmannian. Suppose we consider a *reduced* graph with n_F faces; then, because such a graph is associated with an $(n_F - 1)$ -dimensional configuration C , it is easy to see that its boundaries are those graphs obtained by deleting edges (reducing the number of faces by one). However, sometimes a graph obtained in this way is no longer reduced, and actually corresponds to a configuration in the Grassmannian whose dimension has been lowered by more than one. This raises the question: which edges in a graph can be removed while keeping a graph reduced? Such edges will be called *removable*. It turns out that this question is easiest to answer not in terms of on-shell graphs directly, but in terms of the geometry of their corresponding configurations in the Grassmannian and the combinatorics of their permutations.

II. Boundary Configuration Combinatorics in the Positroid Stratification

The boundaries of a configuration C , denoted $\partial(C)$, in the positroid stratification are those configurations obtained by imposing any one additional constraint involving consecutive chains of columns. Before describing the combinatorial rule for finding boundary configurations, let us first build some intuition through simple examples. Recall from section I. the configuration in $G_+(3, 6)$ whose boundaries included:

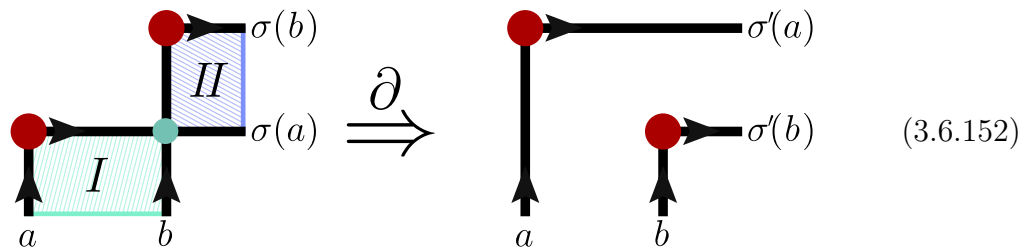
$$\partial \left(\begin{array}{c} \bullet 1 \quad \bullet 2 \quad \bullet 3 \\ \bullet 4 \\ \bullet 5 \\ \bullet 6 \end{array} \right) = \left\{ \begin{array}{c} \bullet 1 \quad \bullet 2 \quad \bullet 3 \quad \bullet 4 \\ \bullet 6 \\ \bullet 5 \end{array} \right\}, \left\{ \begin{array}{c} \bullet 2,3 \\ \bullet 4 \\ \bullet 5 \\ \bullet 6 \end{array} \right\}, \left\{ \begin{array}{c} \bullet 1 \quad \bullet 2 \quad \bullet 3 \\ \bullet 6 \quad \bullet 5 \quad \bullet 4 \end{array} \right\}, \left\{ \begin{array}{c} \bullet 1 \quad \bullet 2 \quad \bullet 3 \\ \bullet 6 \\ \bullet 4 \\ \bullet 5 \end{array} \right\}, \dots$$

{3, 5, 6, 7, 8, 10}
 {3, 4, 6, 7, 8, 11}
 {5, 3, 6, 7, 8, 10}
 {3, 6, 5, 7, 8, 10}
 {3, 5, 7, 6, 8, 10}

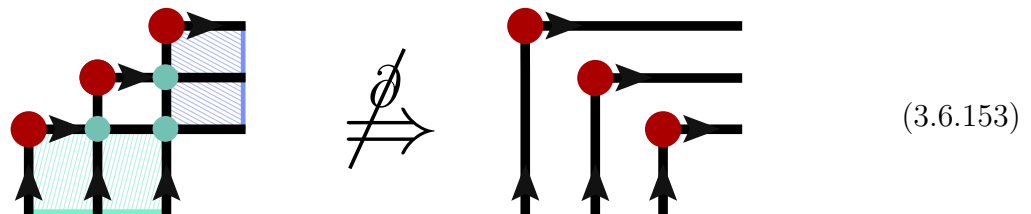
where we have highlighted how the permutation changes for each boundary-

element.

And so—if it weren't sufficiently obvious already—this example makes it clear that boundary elements of a configuration labeled by σ are those labeled by σ' which are related to σ by a transposition of its images. However, not all transpositions lower the dimension of the configuration, and some transpositions lower the dimensionality by more than one. The way to identify the transpositions which lower the dimension by precisely one is easily understood from the way dimensionality is encoded by a configuration's permutation: if we view the permutation as given by the 'hooks' described in section I., then the dimension of a configuration is counted by the number of intersections of its hooks (minus k^2). Therefore, boundaries are those transpositions which eliminate any *one* such intersection:



Here, it is important that $a < b \leq \sigma(a) < \sigma(b) \leq (a+n)$, and that there are no hooks from $c \in I$ to $\sigma(c) \in II$ as otherwise the dimensionality would be lowered by more than one:



Restated in terms of on-shell graphs decorated by left-right paths, this rule identifies *removable* edges as those along which two paths cross, $a \rightarrow \sigma(a)$ and $b \rightarrow \sigma(b)$ with $a < b \leq \sigma(b) < \sigma(a) \leq (a+n)$, provided that there is no path $c \rightarrow \sigma(c)$ with $c \in I$ and $\sigma(c) \in II$:

These two definitions of the boundary elements of a configuration are of course equivalent; but without the combinatorial rule for counting dimensions, it would have been considerably more difficult to see that these—and only these—edges are removable.

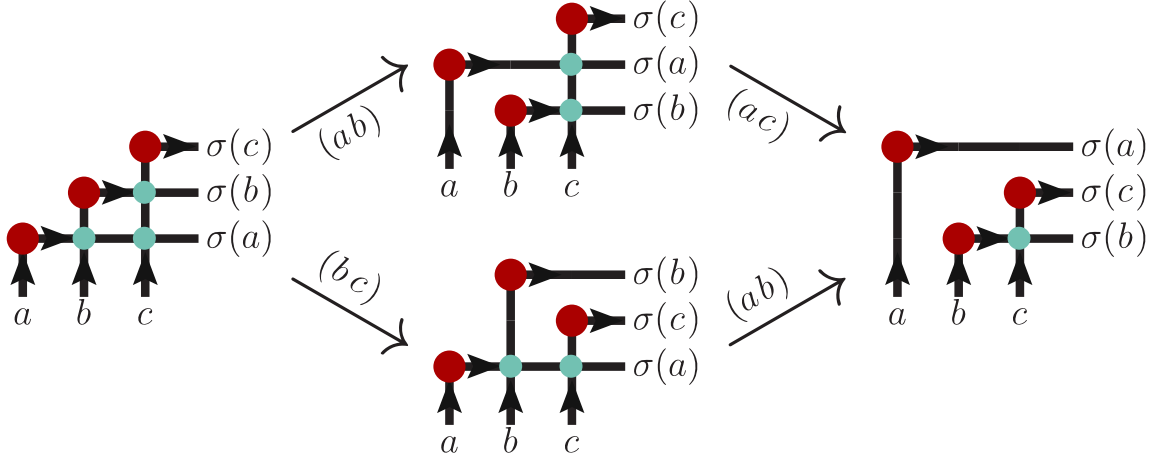
III. (Combinatorial) Polytopes in the Grassmannian

The boundary operator ∂ given above *defines* the positroid stratification of $G(k, n)$; and this stratification is a very special one, with many nice features. For one thing, it allows us to view every positroid configuration in $G_+(k, n)$ is *something like* a ‘polytope’ in $G(k, n)$. By this we mean that the inclusions induced by ∂ (viewed as a strong Bruhat covering relation) define an *Eulerian poset*—the key combinatorial property of the poset of faces of an ordinary polytope.

We will not prove that ∂ defines an Eulerian poset (this was proven in [145]), but let us at least demonstrate that $\partial^2 = 0 \pmod{2}$ —which is of course a prerequisite for ∂ to actually have the meaning of a homological ‘boundary’ operator. It turns out that every configuration in $\partial^2(C)$ is found as the boundary of precisely *two* configurations in $\partial(C)$ (a fact which follows trivially from the more complete statement that ∂ defines an Eulerian poset). This is not hard to prove, and it trivially implies that $\partial^2 = 0 \pmod{2}$. To see this, notice that each configuration in $\partial[C_\sigma]$ is labeled by σ' related to σ by a transposition. It is easy to see that the pair of transpositions must involve at least three distinct labels. If the pair involved four labels, say (ab) and (cd) , then obviously the two transpositions can be taken in either order. When the pair involves three labels, say $\{abc\}$, then there are only four possible scenarios to check:

$$\begin{aligned}
 (ab) \circ (ac) &\simeq (bc) \circ (ab) & (ab) \circ (bc) &\simeq (bc) \circ (ac) \\
 (ab) \circ (bc) &\simeq (ac) \circ (ab) & (ac) \circ (bc) &\simeq (bc) \circ (ab)
 \end{aligned}
 \quad ; \quad (3.6.155)$$

the first of these, for example, can be understood graphically in terms of hooks as,

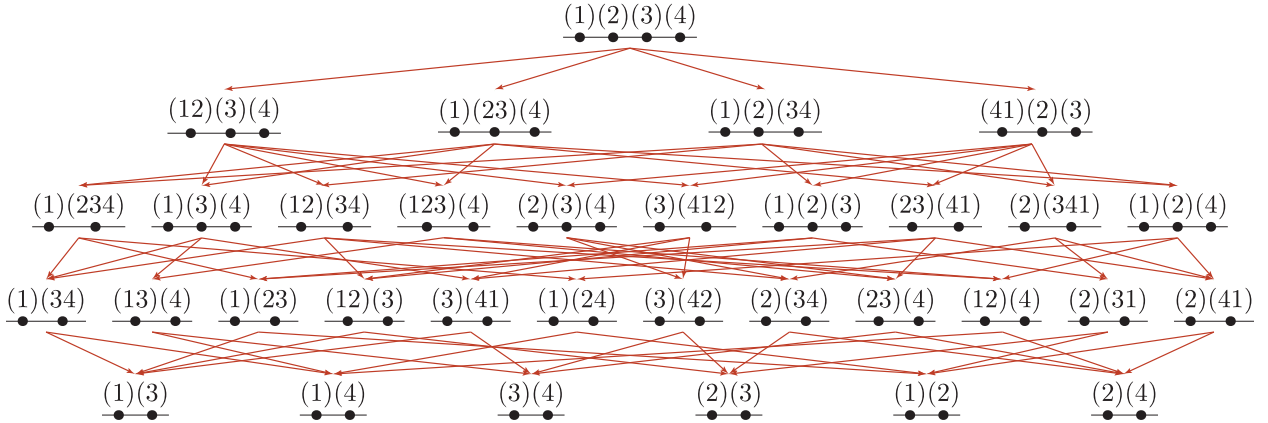


A more immediate, but somewhat indirect proof of this fact follows from the association of each permutation σ with a reduced, on-shell graph. Recall that the graphs in the boundary of an on-shell graph labeled by σ are those for which *one* edge has been removed. Because each pair of left-right paths $a \rightarrow \sigma(a)$ and $b \rightarrow \sigma(b)$ cross on *at most one* edge of any *reduced* graph (if the edge is removable), it is clear that graphs in ∂^2 are those obtained by removing a pair of edges. As such, the pair of edges can be removed in any order, proving that there are two paths from any graph to each graph in ∂^2 .

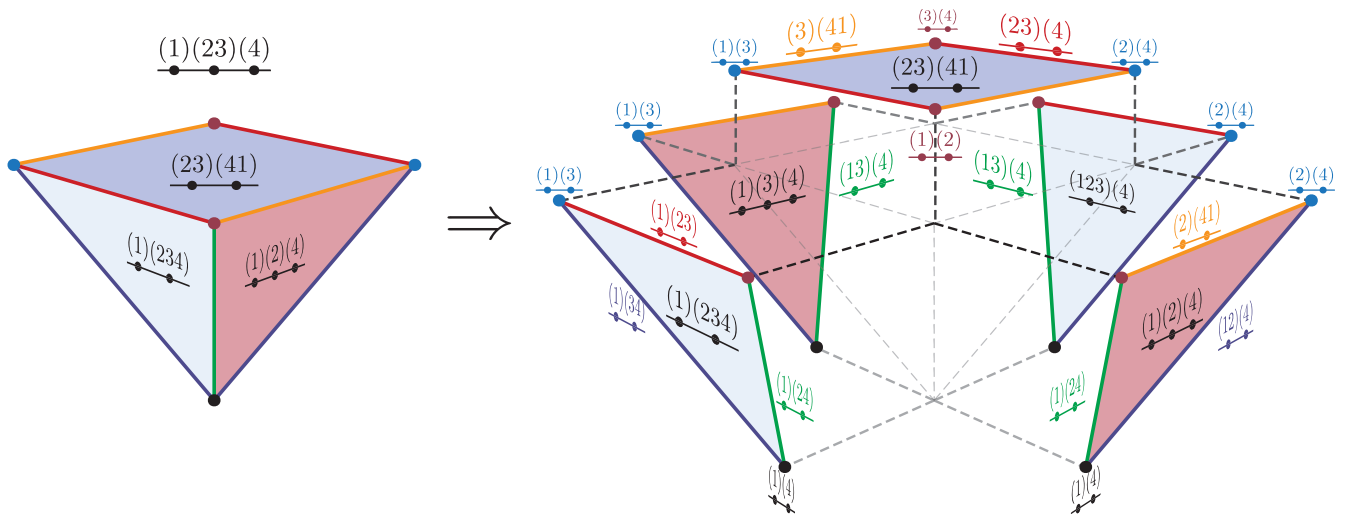
(We should mention briefly that it remains an open and important problem to refine the definition of ∂ so that elements in $\partial(C)$ are decorated with signs ± 1 such that $\partial^2 = 0$ directly—not merely modulo 2.)

As mentioned above, an amazing feature of the positroid stratification is that the combinatorial structure of the inclusions induced by ∂ have the property that every positroid configuration defines an Eulerian poset—a combinatorial polytope. Because of this, we can loosely view each positroid configuration as a region of $G(k, n)$ with essentially the topology of an open ball—even though such a picture is only strictly known to be valid for relatively simple cases such as $G(2, n)$.

In the case of the positroid $G_+(2, 4)$, the polytope is relatively easy to visualize. The four-dimensional top-cell has four, three-dimensional boundary configurations; and the boundaries of these cells collectively involve ten two-dimensional configurations, etc. Starting with the generic configuration in $G_+(2, 4)$, we find the boundaries defined by ∂ given as follows [146]:



Although it is hard to draw the complete four-dimensional polytope, its four three-dimensional faces each define square-pyramidal regions of $G(2, 4)$. For example, the polytope corresponding to the configuration $(1)(23)(4)$ of $G(2, 4)$ labeled by the permutation $\{4, 3, 5, 6\}$ is arranged as follows:



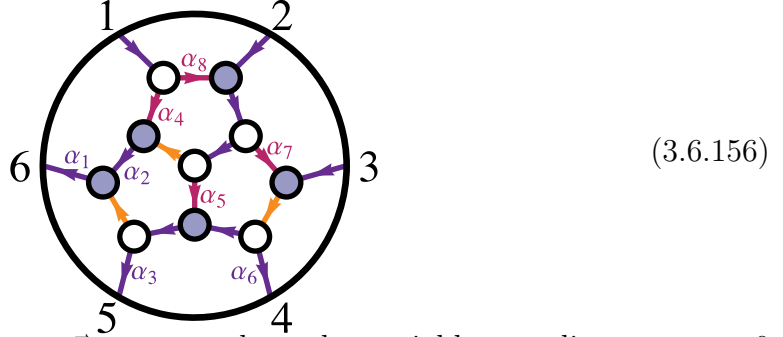
IV. Approaching Boundaries in Canonical Coordinates

Recall that the singularities of an on-shell differential form associated with an on-shell diagram are simply the residues of its poles. When written in terms of canonical coordinates on the Grassmannian as described above (see equation (3.6.151)), it is tempting to identify the manifestly-logarithmic singularities in the measure with configurations in the ‘boundary’. But there are two important points which make such a correspondence a bit more delicate than it may appear at first-glance:

1. the coordinate chart $\vec{\alpha}$ used to cover C_σ may degenerate when some $\alpha_i \rightarrow 0$ —such a degeneration would be signaled by the appearance of additional singularities in the Jacobian arising from the δ -functions in (3.6.151);

2. no *single* coordinate chart $\vec{\alpha}$ covers *all* of the boundaries of C_σ .

We can illustrate both points by considering a simple example. Recall from equation (3.5.134) the BCFW-bridge coordinates generated for the graph labeled by $\{4, 6, 5, 7, 8, 9\}$:



Because the BCFW coordinates $\vec{\alpha}$ correspond to edge-variables, sending any $\alpha_i \rightarrow 0$ will have the effect of deleting the corresponding edge from the graph. The first subtlety mentioned above is reflected in the fact that some edge-variables—here, $\{\alpha_1, \alpha_2, \alpha_3, \alpha_6\}$ —are attached to *irremovable* edges; the second subtlety is reflected in the fact that three of the seven removable edges—colored orange in the figure—are *not* dressed with edge-variables. Of course, if we introduce additional $GL(1)$ -redundancies at each vertex as we did in section V., every removable edge could be dressed by a variable whose vanishing would give the corresponding boundary; this would make all the boundaries accessible, but at the cost of introducing vast redundancy.

A surprising fact—not very difficult to prove—is that *all* the boundaries of any cell $C \in G_+(k, n)$ can be found at the zero-locus of single-coordinates in at least one chart from an atlas composed only of those charts generated by the BCFW-bridge construction (see section II.) in all its n cyclic manifestations (taking each of the n labels as the cyclic ‘starting-point’ for the decomposition). To be clear, this claim only applies for the *specific scheme* described in section II. used to decompose a permutation into adjacent transpositions—no other scheme is known to have this remarkable property.

3.7 The Invariant Top-Form and the Positroid Stratification

We have seen that, associated with any d -dimensional cell of the positive Grassmannian, there is a natural associated form. In any of our natural coordinate charts, this d -form is just the “ $d\log$ ” measure,

$$\frac{d\alpha_1}{\alpha_1} \wedge \cdots \wedge \frac{d\alpha_d}{\alpha_d}, \quad (3.7.157)$$

which is a special case of a more general cluster volume. This form makes it obvious that boundary configurations are associated with residues for some $\alpha_i = 0$. It is also clear that we can view all cells $C \in G_+(k, n)$ as iterated residues of the *top-form* Ω^{top} on a *generic* configuration $C \in G_+(k, n)$.

A natural question is whether this top-form Ω^{top} can be written directly in terms of the ‘matrix-coordinates’ $c_{\alpha a}$ of C . In terms of matrix-coordinates $C \equiv c_{\alpha a}$, the desired measure $G(k, n)$ would have the form,

$$\Omega = \frac{d^{k \times n} C}{\text{vol}(GL(k))} \frac{1}{f(C)}, \quad (3.7.158)$$

where $f(C)$ must be a function of the *minors* of C , and must scale uniformly as $f(tC) = t^{k \times n} f(C)$. Moreover, because the top-cell $G_+(k, n)$ *always* has precisely n co-dimension one boundaries—corresponding to any k consecutive columns becoming linearly-dependent—it is clear that $f(C)$ must have *at least* the n cyclic-minors as factors:

$$f(C) = (1 \cdots k) \cdots (n \cdots k-1) f'(C). \quad (3.7.159)$$

Because the product of the cyclic minors scale as $f(C)$ must, $f'(C)$ must be scale-invariant: $f'(tC) = f'(C)$. And so, $f'(C)$ can at most involve ratios of minors. However, any non-consecutive minors appearing as factors in $f'(C)$ would generate new, unwanted singularities for the top-cell—poles corresponding to co-dimension one boundaries not in the positroid stratification—and any consecutive minors in $f'(C)$ would make a double-pole, spoiling the logarithmic singularities corresponding to one of the *necessary* boundary configurations. Therefore, we are forced to conclude that the only choice is to take $f'(C) \rightarrow 1$. This means that the *only* viable ansatz for a measure on $G(k, n)$ with the desired properties is:

$$\Omega = \frac{d^{k \times n} C}{\text{vol}(GL(k))} \frac{1}{(1 \cdots k) \cdots (n \cdots k-1)}. \quad (3.7.160)$$

This strikingly-simple form was first encountered in connection with “leading singularities” in reference [16].

It is not hard to see the plausibility of a guess that $\Omega = \Omega^{\text{top}}$. We have just established that the poles of Ω and Ω^{top} are the same, and furthermore Ω does not have any zeroes on the Grassmannian. Thus $\Omega^{\text{top}}/\Omega$ is a function of the Grassmannian with no poles, and any such function must be a constant. So, we have

$$\frac{d^{k \times n} C}{\text{vol}(GL(k))} \frac{1}{(1 \cdots k) \cdots (n \cdots k-1)} = \frac{d\alpha_1}{\alpha_1} \wedge \cdots \wedge \frac{d\alpha_{k(n-k)}}{\alpha_{k(n-k)}}. \quad (3.7.161)$$

This representation of the top form will be crucial for most transparently seeing the dual conformal symmetry and Yangian invariance of the theory.

We will momentarily prove that $\Omega = \Omega^{\text{top}}$ by direct computation as well, but let us first step-back and observe some remarkable properties of Ω . It is rather surprising that a form as simple as (3.7.160)—which has only n poles!—should be able to capture all of the intricate and beautiful structure of the positive Grassmannian in its iterated singularities. The reason why this isn’t obviously impossible is that each of these n factors are generally k^{th} -degree polynomials in the variables $c_{\alpha a}$, and whenever one such minor vanishes, other minors typically factorize, exposing further singularities and more structure below.

Let us consider an example which illustrates how the iterated factorizations of the consecutive minors exposes all the cells in the positroid stratification. Consider the top-cell of $G(3, 6)$,

$$\begin{array}{c}
 \bullet 2 \quad \bullet 3 \\
 \bullet 1 \quad \bullet 4 \\
 \bullet 6 \quad \bullet 5
 \end{array}
 \iff
 \frac{d^{3 \times 6} C}{\text{vol}(GL(3))} \frac{1}{(123)(234)(345)(456)(561)(612)}. \quad (3.7.162)$$

Upon restricting this form to the residue where $(234) \rightarrow 0$, the configuration becomes:

$$\begin{array}{c}
 \bullet 2 \quad \bullet 3 \quad \bullet 4 \\
 \bullet 1 \\
 \bullet 6 \quad \bullet 5
 \end{array}
 \quad (3.7.163)$$

Now, as described in section 3.5, this configuration contains 7 boundary configurations. How are we to see *seven* logarithmic singularities arising from the *five* remain-

ing cyclic minors of (3.7.162)? The answer is simple: let us parameterize the pole $(234) \rightarrow 0$ by sending $c_3 \rightarrow \beta_{32}c_2 + \beta_{34}c_4$, under which the minors (123) and (345) each factorize:

$$\frac{1}{(123)(234)(345)(456)(561)(612)} \xrightarrow[c_3 = \beta_{32}c_2 + \beta_{34}c_4]{(234) \rightarrow 0 \text{ via}} \frac{1}{\underbrace{\beta_{34}(124)}_{(123)} \underbrace{\beta_{32}(245)}_{(345)} (456)(561)(612)},$$

exposing all seven of the boundary configurations! To further illustrate this point, let us now take a residue of this measure about the configuration setting $(561) \rightarrow 0$, by setting $c_6 \mapsto \beta_{65}c_5 + \beta_{61}c_1$; as before, this leads to the factorization of minors (456) and (612), leaving us with,

$$\frac{1}{\beta_{34}(124)\beta_{32}(245)(456)(561)(612)} \xrightarrow[c_6 = \beta_{65}c_5 + \beta_{61}c_1]{(561) \rightarrow 0 \text{ via}} \frac{1}{\beta_{34}(124)\beta_{32}(245) \underbrace{\beta_{61}(461)}_{(456)} \underbrace{\beta_{65}(512)}_{(612)}},$$

which shows that this configuration has *eight* further boundary configurations. Proceeding in this way we can reconstruct all the cells of $G_+(3, 6)$.

I. Proving Equivalence with the Canonical Positroid Measure

In section IV. we showed that we can construct canonical coordinates for the top-cell of $G_+(k, n)$ recursively by first introducing coordinates

$$C^{(1,n)} \equiv \left(\beta_{1,1} \ \beta_{1,2} \ \cdots \ \beta_{1,n-1} \ \beta_{1,n} \right), \quad (3.7.164)$$

for $G(1, n)$, and then building-up coordinates for any $G(k, n)$ recursively via:

$$C^{(k,n)} \equiv \begin{pmatrix} \beta_{k,1} \widehat{c}_1^{(k,n)} & \cdots & \beta_{k,n-1} \widehat{c}_{n-1}^{(k,n)} & 0 \\ \beta_{k,1} & \cdots & \beta_{k,n-1} & \beta_{k,n} \end{pmatrix} \quad \text{with} \quad \widehat{c}_a^{(k,n)} \equiv \sum_{j=(a+1)}^n c_j^{(k-1,n)}. \quad (3.7.165)$$

Recall that these coordinates match those obtained by the BCFW bridge construction upon the trivial relabeling:

| | | | | | | | | | |
|-----------------------|----------------|----------|---------------------|----------|-------------------|---------------|----------|------------|-----------------------|
| α_d | α_{d-2} | \cdots | \cdots | \cdots | \cdots | α_ℓ | \cdots | \cdots | $\alpha_{k(k-1)/2+1}$ |
| α_{d-1} | \cdots | \cdots | \cdots | \cdots | $\alpha_{\ell+1}$ | \cdots | \cdots | \cdots | \vdots |
| \vdots | \cdots | \cdots | \cdots | \cdots | \cdots | \cdots | \cdots | \cdots | α_2 |
| $\alpha_{d-k(k-1)/2}$ | \cdots | \cdots | $\alpha_{\ell+k-1}$ | \cdots | \cdots | \cdots | \cdots | α_3 | α_1 |

 \Leftrightarrow

| | | | | |
|-----------------|-----------------|----------|-----------------|---------------|
| $\beta_{1,k+1}$ | $\beta_{1,k+2}$ | \cdots | $\beta_{1,n-1}$ | $\beta_{1,n}$ |
| $\beta_{2,k+1}$ | $\beta_{2,k+2}$ | \cdots | $\beta_{2,n-1}$ | $\beta_{2,n}$ |
| \vdots | \vdots | \ddots | \vdots | \vdots |
| $\beta_{k,k+1}$ | $\beta_{k,k+2}$ | \cdots | $\beta_{k,n-1}$ | $\beta_{k,n}$ |

and the gauge-choice of setting the first k column-vectors to the identity matrix. The motivation for relabeling the coordinates in this way is that the BCFW-coordinates give rise a gauge-fixed parameterization of $C(\beta_{\alpha,a})$ of the form,

$$\begin{array}{c}
1 \quad 2 \cdots k \qquad \qquad \qquad k+1 \qquad \qquad \qquad \cdots \qquad \qquad \qquad \cdots \qquad \qquad \qquad n \\
\hline
1 \left(\begin{array}{c|ccc}
1 & 0 \cdots 0 & & \\
0 & 1 \ddots & & \\
\vdots & \vdots \ddots & & \\
0 & \cdots 0 & 1 &
\end{array} \right. \begin{array}{l}
(\beta_{1,k+1} \cdots \beta_{k,k+1}) + \cdots \quad (\beta_{1,k+2} \cdots \beta_{k,k+2}) + \cdots \quad \cdots \quad (\beta_{1,n} \cdots \beta_{k,n}) + \cdots \\
(\beta_{2,k+1} \cdots \beta_{k,k+1}) + \cdots \quad (\beta_{2,k+2} \cdots \beta_{k,k+2}) + \cdots \quad \cdots \quad (\beta_{2,n} \cdots \beta_{k,n}) + \cdots \\
\vdots \qquad \qquad \qquad \vdots \qquad \qquad \qquad \vdots \qquad \qquad \qquad \vdots \\
\beta_{k,k+1} \qquad \qquad \qquad \beta_{k,k+2} \qquad \qquad \qquad \cdots \qquad \qquad \qquad \beta_{k,n}
\end{array} \right)
\end{array} \tag{3.7.166}$$

Here, we have used color to highlight the fact that $c_{\alpha,a} \propto \beta_{\alpha,a}(\beta_{\alpha+1,a} \cdots \beta_{k,a}) + \cdots$, and that only this factor contributes to the Jacobian in going from coordinates $c_{\alpha,a}$ to coordinates $\beta_{\alpha,a}$. In particular, it is easy to see that the entire Jacobian from this change of variables is simply,

$$J \equiv \left| \frac{dc_{\alpha,a}}{d\beta_{\alpha,a}} \right| = \prod_{\alpha,a} (\beta_{\alpha,a})^{\alpha-1}. \tag{3.7.167}$$

Somewhat less obviously, the cyclic minors are all simply expressed in these coordinates: each is the product of all the *highlighted* $\beta_{\alpha,a}$ in the lower-right triangle of the corresponding sub-matrix of (3.7.166):

$$(\ell \cdots \ell+k-1) = \prod_{\alpha=1}^k \left(\prod_{a=1}^{\alpha} \beta_{\alpha,(k+\ell-a)} \right) \Leftrightarrow \begin{array}{c} \left| \begin{array}{cccc}
\beta_{1,\ell} & \cdots & \cdots & \beta_{1,\ell+k-1} \\
\vdots & \cdots & \beta_{2,\ell+k-2} & \beta_{2,\ell+k-1} \\
\vdots & \cdots & \vdots & \vdots \\
\beta_{k,\ell} & \cdots & \beta_{k,\ell+k-2} & \beta_{k,\ell+k-1}
\end{array} \right|, \end{array} \tag{3.7.168}$$

where the product of β 's only ranges over relevant columns: $k+1 \leq (k+\ell-a) \leq n$. And so, the product of all the consecutive minors is simply,

$$(1 \cdots k)(2 \cdots k+1) \cdots (n \cdots k-1) = \prod_{\alpha,a} (\beta_{\alpha,a})^{\alpha}. \tag{3.7.169}$$

Therefore, combining the product of all the cyclic minors with the necessary Jacobian given in (3.7.167) we have:

$$\frac{d^{k \times n} c_{\alpha,a}}{\text{vol}(GL(k)) (1 \cdots k) \cdots (n \cdots k-1)} = \left(\prod_{\alpha,a} d\beta_{\alpha,a} \right) \frac{J}{\prod_{\alpha,a} (\beta_{\alpha,a})^{\alpha}} = \prod_{\alpha,a} \frac{d\beta_{\alpha,a}}{\beta_{\alpha,a}} \tag{3.7.170}$$

as desired.

Let us briefly consider one concrete example of this equivalence. Consider the top-cell of $G(3, 6)$, where the BCFW-bridge construction gives the matrix-representative,

$$C(\alpha) = \begin{pmatrix}
1 & 0 & 0 & \alpha_9 \alpha_8 \alpha_6 & \alpha_7 \alpha_5 \alpha_3 + \alpha_3 \alpha_9 (\alpha_5 + \alpha_8) & \alpha_4 \alpha_2 \alpha_1 + \alpha_1 (\alpha_7 (\alpha_2 + \alpha_5) + \alpha_9 (\alpha_2 + \alpha_5 + \alpha_8)) \\
0 & 1 & 0 & -\alpha_8 \alpha_6 & -\alpha_5 \alpha_3 - \alpha_3 \alpha_8 & -\alpha_2 \alpha_1 - \alpha_1 (\alpha_5 + \alpha_8) \\
0 & 0 & 1 & \alpha_6 & \alpha_3 & \alpha_1
\end{pmatrix},$$

which, upon relabeling the variables according to,

$$\begin{array}{|c|c|c|} \hline \alpha_9 & \alpha_7 & \alpha_4 \\ \hline \alpha_8 & \alpha_5 & \alpha_2 \\ \hline \alpha_6 & \alpha_3 & \alpha_1 \\ \hline \end{array} \Rightarrow \begin{array}{|c|c|c|} \hline \beta_{1,4} & \beta_{1,5} & \beta_{1,6} \\ \hline \beta_{2,4} & \beta_{2,5} & \beta_{2,6} \\ \hline \beta_{3,4} & \beta_{3,5} & \beta_{3,6} \\ \hline \end{array}, \quad (3.7.171)$$

becomes,

$$C(\beta) = \begin{pmatrix} 1 & 0 & 0 & \beta_{1,4}\beta_{2,4}\beta_{3,4} & \beta_{1,5}\beta_{2,5}\beta_{3,5} + \dots & \beta_{1,6}\beta_{2,6}\beta_{3,6} + \dots \\ 0 & 1 & 0 & -\beta_{2,4}\beta_{3,4} & -\beta_{2,5}\beta_{3,5} - \dots & -\beta_{2,6}\beta_{3,6} - \dots \\ 0 & 0 & 1 & \beta_{3,4} & \beta_{3,5} & \beta_{3,6} \end{pmatrix}. \quad (3.7.172)$$

It is easy to see that the cyclic minors are given by,

$$\begin{aligned} (123) &= 1 & (456) &= \beta_{1,6} \beta_{2,5} \beta_{2,6} \beta_{3,4} \beta_{3,5} \beta_{3,6} \\ (234) &= \beta_{1,4} \beta_{2,4} \beta_{3,4} & (561) &= \beta_{2,6} \beta_{3,5} \beta_{3,6} \\ (345) &= \beta_{1,5} \beta_{2,4} \beta_{2,5} \beta_{3,4} \beta_{3,5} & (612) &= \beta_{3,6} \end{aligned} \quad (3.7.173)$$

so that their product gives,

$$(123) \cdots (612) = (\beta_{1,4} \beta_{1,5} \beta_{1,6})^1 (\beta_{2,4} \beta_{2,5} \beta_{2,6})^2 (\beta_{3,4} \beta_{3,5} \beta_{3,6})^3; \quad (3.7.174)$$

and the Jacobian of going from $c_{\alpha,a}$ to $\beta_{\alpha,a}$ is easily seen to be,

$$J \equiv \left| \frac{dc_{\alpha,a}}{d\beta_{\alpha,a}} \right| = (\beta_{1,4} \beta_{1,5} \beta_{1,6})^0 (\beta_{2,4} \beta_{2,5} \beta_{2,6})^1 (\beta_{3,4} \beta_{3,5} \beta_{3,6})^2, \quad (3.7.175)$$

so that

$$\frac{d^{3 \times 6} C}{\text{vol}(GL(3)) (123)(234)(345)(456)(561)(612)} = \prod_{\alpha,a} \frac{d\beta_{\alpha,a}}{\beta_{\alpha,a}}. \quad (3.7.176)$$

3.8 (Super) Conformal and Dual Conformal Invariance

In this section, we will describe how the Grassmannian formulation of on-shell diagrams makes all the symmetries of the theory—both the super-conformal *and dual* super-conformal symmetries—completely manifest. Along the way, we will find it useful to recast the on-shell differential form's dependence on external kinematical data in a way which more transparently reflects the geometry of momentum-conservation; doing so, we will discover a correspondence between (some) cells $C \in G(k, n)$ with cells $\widehat{C} \in G(k-2, n)$.

I. The Grassmannian Geometry of Momentum Conservation

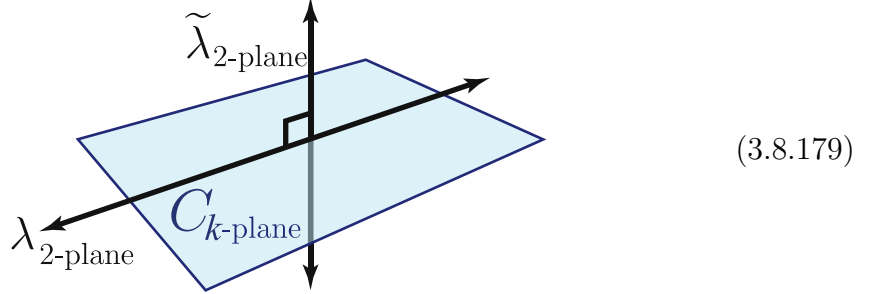
Consider an arbitrary on-shell graph associated with the cell $\Gamma_\sigma \in G(k, n)$ labeled by the permutation σ associated with an on-shell differential form $f_\sigma^{(k)}(1, \dots, n)$. Using any of the canonical coordinates for the cell $C(\alpha_1, \dots, \alpha_d) \subset \Gamma_\sigma \in G(k, n)$, this form is given by:

$$f_\sigma^{(k)} = \int \frac{d\alpha_1}{\alpha_1} \wedge \dots \wedge \frac{d\alpha_d}{\alpha_d} \delta^{k \times 4}(C \cdot \tilde{\eta}) \delta^{k \times 2}(C \cdot \tilde{\lambda}) \delta^{2 \times (n-k)}(\lambda \cdot C^\perp). \quad (3.8.177)$$

As we saw in section 3.7, this can also be written as a residue of the top-form,

$$f_\sigma^{(k)} = \oint_{C \subset \Gamma_\sigma} \frac{d^{k \times n} C}{\text{vol}(GL(k))} \frac{\delta^{k \times 4}(C \cdot \tilde{\eta})}{(1 \dots k) \dots (n \dots k-1)} \delta^{k \times 2}(C \cdot \tilde{\lambda}) \delta^{2 \times (n-k)}(\lambda \cdot C^\perp). \quad (3.8.178)$$

Recall from section 3.4, the (ordinary) δ -functions in (3.8.178) have the geometric interpretation of constraining the k -plane C to be *orthogonal to* the 2-plane $\tilde{\lambda}$ and to *contain* the 2-plane λ , [16]:



Because $\tilde{\lambda} \subset \lambda^\perp$, 4 of the $2n (= 2(n-k) + 2k)$ constraints always represent momentum-conservation, leaving $(2n-4)$ constraints imposed on C in general. Therefore, cells of $G(k, n)$ with precisely $(2n-4)$ degrees of freedom can be *fully-localized* by these constraints, and become *ordinary* super-functions of the external momenta; cells of lower dimension become functions with δ -function support, and cells of higher dimension represent *integration measures* on auxiliary, *internal* degrees of freedom (which may represent, for example, the degrees of freedom of internal loop-momenta).

The simplest example illustrating this localization is for $k = 2$. Here the 2-plane C is just identified with the λ -plane, and equation (3.8.178) directly becomes the familiar Parke-Taylor formula for tree-level MHV super-amplitudes, [51, 147]:

$$\begin{aligned} \mathcal{A}_n^{(2)} &= \int \frac{d^{2 \times n} C}{\text{vol}(GL(2))} \frac{\delta^{2 \times 4}(C \cdot \tilde{\eta})}{(12)(23) \dots (n1)} \delta^{2 \times 2}(C \cdot \tilde{\lambda}) \delta^{2 \times (n-2)}(\lambda \cdot C^\perp), \\ &= \frac{\delta^{2 \times 4}(\lambda \cdot \tilde{\eta})}{\langle 12 \rangle \langle 23 \rangle \dots \langle n1 \rangle} \delta^{2 \times 2}(\lambda \cdot \tilde{\lambda}). \end{aligned} \quad (3.8.180)$$

Let us look at a less trivial example of how this localization works for $k > 2$. One of the on-shell diagrams contributing to the 6-particle $k = 3$ tree-amplitude is (see section 3.14),

$$(3.8.181)$$

which is labeled by the permutation $\{3, 5, 6, 7, 8, 10\}$. It is easy to see that (a $GL(3)$ -representative of) the point C^* in this positroid cell which satisfies the kinematical constraints is:

$$C^* = \begin{pmatrix} \lambda_1^1 & \lambda_2^1 & \lambda_3^1 & \lambda_4^1 & \lambda_5^1 & \lambda_6^1 \\ \lambda_1^2 & \lambda_2^2 & \lambda_3^2 & \lambda_4^2 & \lambda_5^2 & \lambda_6^2 \\ 0 & 0 & 0 & [5\ 6] & [6\ 4] & [4\ 5] \end{pmatrix}, \quad (3.8.182)$$

where $[ab] \equiv \det\{\tilde{\lambda}_a, \tilde{\lambda}_b\}$ is a minor of the matrix $\tilde{\lambda}$. (Notice that $C^* \cdot \tilde{\lambda} = 0$ because $\lambda \cdot \tilde{\lambda} = 0$, and the third-row dotted-into $\tilde{\lambda}$ gives an instance of (3.4.47).) Supported at this point, (3.8.178) generates the on-shell super-function,

$$f_{\{3,5,6,7,8,10\}}^{(3)} = \frac{\delta^{3 \times 4}(C^* \cdot \tilde{\eta}) \delta^{2 \times 2}(\lambda \cdot \tilde{\lambda})}{\underbrace{\langle 2\ 3 \rangle [5\ 6]}_{(234)|_{C^*}} \underbrace{(\langle 3\ 4 \rangle [6\ 4] + \langle 5\ 3 \rangle [5\ 6])}_{(345)|_{C^*}} \underbrace{s_{456}}_{(456)|_{C^*}} \underbrace{(\langle 6\ 1 \rangle [6\ 4] + \langle 1\ 5 \rangle [4\ 5])}_{(561)|_{C^*}} \underbrace{\langle 1\ 2 \rangle [4\ 5]}_{(612)|_{C^*}}, \quad (3.8.183)$$

where

$$s_{456} \equiv (p_4 + p_5 + p_6)^2 = \langle 4\ 5 \rangle [4\ 5] + \langle 4\ 6 \rangle [4\ 6] + \langle 5\ 6 \rangle [5\ 6].$$

The particular $GL(3)$ -representative of C^* given in (3.8.182) was chosen so that the Jacobian from all the δ -functions is 1, making the residue of (3.8.178) about the pole $(123) = 0$ easy to read-off from C^* . Let us briefly mention that (3.8.183) makes *super* momentum-conservation manifest: in addition to the obvious $\delta^{2 \times 2}(\lambda \cdot \tilde{\lambda})$ in (3.8.183), the (fermionic) δ -functions $\delta^{3 \times 4}(C^* \cdot \tilde{\eta})$ includes the factor $\delta^{2 \times 4}(\lambda \cdot \tilde{\eta})$ —the supersymmetric-extension of ordinary momentum conservation.

II. Twistor Space and the Super-Conformal Invariance of On-Shell Forms

In order to see the conformal symmetry of any theory, it is often wise to use *twistor* variables, [61, 148–151]. Not surprisingly then, it is *twistor* space—not momentum-

space—which gives us the simplest basis in which to describe scattering amplitudes conformally. Formally, we go to twistor space by assuming that $\lambda, \tilde{\lambda}$ are independent, real variables, and then Fourier-transform with respect to either the λ or $\tilde{\lambda}$ variables, [13]. It is not hard to see how this Fourier transform makes the action of conformal transformations particularly transparent. Working with spinor-helicity variables, the generators of translations, $P_{\alpha\dot{\beta}}$, Lorentz transformations, $J_{\alpha\beta}$ and $\bar{J}_{\dot{\alpha}\dot{\beta}}$, dilatations D , and special conformal transformations, $K_{\alpha\dot{\beta}}$, all look very different:

$$P_{\alpha\dot{\beta}} = \lambda_\alpha \tilde{\lambda}_{\dot{\beta}}, \quad J_{\alpha\beta} = \frac{i}{2} \left(\lambda_\alpha \frac{\partial}{\partial \lambda^\beta} + \lambda_\beta \frac{\partial}{\partial \lambda^\alpha} \right), \quad \text{and} \quad K_{\alpha\dot{\beta}} = \frac{\partial^2}{\partial \lambda^\alpha \partial \tilde{\lambda}^{\dot{\beta}}}. \quad (3.8.184)$$

(\bar{J} is defined analogously to J .) However, if we Fourier-transforms with respect to each of the λ 's, say, using $\int d^{2 \times n} \lambda e^{i\lambda \cdot \tilde{\mu}}$, denoting the $(2 \times n)$ -matrix of conjugate variables by $\tilde{\mu}$, the generators (3.8.184) become, (see [13] for a detailed discussion):

$$P_{\dot{\alpha}\dot{\beta}} = i \tilde{\lambda}_{\dot{\alpha}} \frac{\partial}{\partial \tilde{\mu}^{\dot{\beta}}}, \quad J_{\dot{\alpha}\dot{\beta}} = \frac{i}{2} \left(\tilde{\mu}_{\dot{\alpha}} \frac{\partial}{\partial \tilde{\mu}^{\dot{\beta}}} + \tilde{\mu}_{\dot{\beta}} \frac{\partial}{\partial \tilde{\mu}^{\dot{\alpha}}} \right), \quad \text{and} \quad K_{\dot{\alpha}\dot{\beta}} = i \tilde{\mu}_{\dot{\alpha}} \frac{\partial}{\partial \tilde{\lambda}^{\dot{\beta}}}. \quad (3.8.185)$$

These are easy to recognize as the generators of $SL(4)$ -transformations on *twistor* variables, denoted w_a , which combine $\tilde{\lambda}$ and $\tilde{\mu}$ according to:

$$w_a \equiv \begin{pmatrix} \tilde{\mu}_a \\ \tilde{\lambda}_a \end{pmatrix}. \quad (3.8.186)$$

Very nicely, under the action of the little group, the $\tilde{\mu}$'s transform oppositely to the λ 's so that the twistors transform uniformly like the $\tilde{\lambda}$'s: $w_a \sim t_a^{-1} w_a$. Thus, we should view each w_a projectively as a point in \mathbb{P}^3 . Furthermore, we can combine these ordinary variables w_a with the anti-commuting $\tilde{\eta}$'s to form *super-twistors* \mathcal{W}_a , [152],

$$\mathcal{W}_a \equiv \begin{pmatrix} w_a \\ \tilde{\eta}_a \end{pmatrix}, \quad (3.8.187)$$

for which the generators of the super-conformal group are simply those of $SL(4|4)$ —acting in the obvious way as super-linear transformations on the \mathcal{W} 's.

Now, given any of our on-shell forms, the Fourier-transform with respect to the λ variables is straightforward as the only dependence on λ is in the term $\delta^{2 \times (n-k)}(\lambda \cdot C^\perp)$. It will be useful to re-write this to more directly reflect its geometric origin: the requirement that the plane C *contains* λ . This means that there should exist a linear combination of the k row-vectors of C which *exactly* match λ . In other words, if we parameterize such a linear combination by a $(2 \times k)$ -matrix ρ , we should be able to

find a ρ for which $\rho \cdot C = \lambda$. Re-written in terms of this auxiliary matrix ρ , the constraint that C contains λ becomes,

$$\delta^{2 \times (n-k)}(\lambda \cdot C^\perp) = \int d^{2 \times k} \rho \delta^{2 \times n}(\rho \cdot C - \lambda), \quad (3.8.188)$$

which makes it trivial to Fourier-transform to twistor space:

$$\int d^{2 \times n} \lambda e^{i\lambda \cdot \tilde{\mu}} \int d^{2 \times k} \rho \delta^{2 \times n}(\rho \cdot C - \lambda) = \int d^{2 \times k} \rho e^{i(\rho \cdot C) \cdot \tilde{\mu}} = \delta^{k \times 2}(C \cdot \tilde{\mu}). \quad (3.8.189)$$

Therefore, in twistor space the constraints $\delta^{k \times 2}(C \cdot \tilde{\lambda})$ and $\delta^{2 \times (n-k)}(\lambda \cdot C^\perp)$ together with the fermionic $\delta^{k \times 4}(C \cdot \tilde{\eta})$ combine into the extremely elegant,

$$\delta^{k \times 4}(C \cdot \tilde{\eta}) \delta^{k \times 2}(C \cdot \tilde{\lambda}) \delta^{k \times 2}(C \cdot \tilde{\mu}) \Rightarrow \delta^{4k|4k}(C \cdot \mathcal{W}), \quad (3.8.190)$$

which makes the $SL(4|4)$ -invariance of on-shell forms completely manifest. And so, in twistor space, the general on-shell form, (3.8.178), is simply,

$$f_\sigma^{(k)} = \oint_{C \in \Gamma_\sigma} \frac{d^{k \times n} C}{\text{vol}(GL(k))} \frac{\delta^{4k|4k}(C \cdot \mathcal{W})}{(1 \cdots k) \cdots (n \cdots k-1)}. \quad (3.8.191)$$

Note that our brief passage to twistor space was done mostly for formal reasons: in order to make the super-conformal symmetry of on-shell forms manifest. One disadvantage of this formalism, however, is that—at first glance—it appears that the integral over $C \in \Gamma_\sigma$ could be localized by all $4k$ (ordinary) δ -function constraints, while we know that on-shell forms associated with non-vanishing functions for generic (momentum-conserving) kinematical data correspond to $(2n-4)$ -dimensional cells $\Gamma_\sigma \in G(k, n)$. The mismatch is due to the fact that Fourier-transforming to twistor space does not produce functions which are non-vanishing for a *generic* set of twistors. Instead, we get distributions on twistor space, imposing constraints on the twistor variables. Indeed, only $(2n-4)$ of the $4k$ δ -functions in (3.8.191) can be used to localize the Grassmannian integral while the remaining impose constraints on the configuration of external twistors.

III. Momentum-Twistors and Dual Super-Conformal Invariance

In this subsection, we will review the arguments presented in [18] in order to discover that on-shell forms are quite surprisingly *also* invariant under an additional

super-conformal symmetry. This new symmetry, called *dual* super-conformal invariance, combines with ordinary super-conformal symmetry to generate an infinite-dimensional symmetry algebra of on-shell forms known as *the Yangian*, [74,93,96,97]. (Dual super-conformal invariance was first noticed in multi-loop perturbative calculations, [59], and then at strong coupling, [84]; this led to a remarkable connection between null-polygonal Wilson loops and scattering amplitudes—see e.g. [84–92].)

Let us start by reconsidering the condition that the plane C contains the plane λ . Because this constraint is ubiquitous for on-shell forms, it is natural to sharpen our focus to the $(k-2) \equiv \widehat{k}$ -plane—denoted \widehat{C} —which is the *projection of C* onto the orthogonal-complement of λ . To be a bit more precise, suppose we have an operator $Q: \mathbb{C}^n \rightarrow \mathbb{C}^n$ with $\ker(Q) = \lambda$ so that,

$$Q \cdot \lambda = 0. \quad (3.8.192)$$

With such an operator, we may define $\widehat{C} \equiv C \cdot Q$ so that $\widehat{C} \cdot \lambda = 0$ trivially.

Now, super momentum-conservation is of course the statement that the planes $\widetilde{\lambda}$ and $\widetilde{\eta}$ are both in λ^\perp —which is the image of Q . And so we may use Q to express $\widetilde{\lambda}$ and $\widetilde{\eta}$ in terms of some new, *generic* variables μ and η according to:

$$\widetilde{\lambda} \equiv \mu \cdot Q \quad \text{and} \quad \widetilde{\eta} \equiv \eta \cdot Q. \quad (3.8.193)$$

Defined in this way, any *unconstrained* planes μ and η will *automatically* define super momentum-conserving planes $\widetilde{\lambda}$ and $\widetilde{\eta}$.

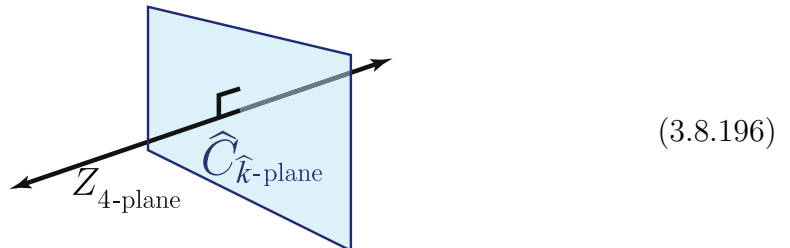
Let us now consider the constraint that C be orthogonal to the plane $\widetilde{\lambda}$. If Q were symmetric, then $C \cdot \widetilde{\lambda} = \widehat{C} \cdot \mu$; and similarly, $C \cdot \widetilde{\eta} = \widehat{C} \cdot \eta$. Putting all this together, the constraints imposed on the image \widehat{k} -plane \widehat{C} would become simply,

$$\delta^{k \times 2}(\widehat{C} \cdot \lambda) \delta^{k \times 2}(\widehat{C} \cdot \mu) \delta^{k \times 4}(\widehat{C} \cdot \eta) \Rightarrow \delta^{4k|4k}(\widehat{C} \cdot \mathcal{Z}), \quad (3.8.194)$$

where we have introduced the super *momentum-twistors* \mathcal{Z} , [60], according to:

$$\mathcal{Z}_a \equiv \begin{pmatrix} z_a \\ \eta_a \end{pmatrix} \quad \text{with} \quad z_a \equiv \begin{pmatrix} \lambda_a \\ \mu_a \end{pmatrix}. \quad (3.8.195)$$

Geometrically, the δ -functions $\delta^{k \times 4}(\widehat{C} \cdot \mathcal{Z})$ enforce that the plane \widehat{C} be orthogonal to the 4-plane Z :



Notice that these δ -functions are invariant under a *new* $SL(4|4)$ symmetry, and thus it appears that we have uncovered a new super-conformal symmetry—one acting on the super-twistor variables \mathcal{Z}_a . However there is one small catch: the measure of integration over the k -plane C does not necessarily descend to anything simple over the \widehat{k} -plane \widehat{C} . Indeed, depending on the choice of the projection operator Q , this resulting measure may have a complicated λ -dependence arising from the Jacobian of the change of variables from $(\widetilde{\lambda}, \widetilde{\eta})$ to (μ, η) , and this dependence on λ may break the $SL(4)$ conformal symmetry.

But it turns out that for what is perhaps the most natural choice of a projection operator Q , everything works like magic. To better understand the scope of choices we could make in specifying Q , observe that such a projector can always be constructed via the Cramer’s rule identities—the unique (up to rescaling) $(k+1)$ -term identity satisfied by generic k -vectors. For a 2-plane λ , Cramer’s rule encodes the identities:

$$\lambda_a \langle bc \rangle + \lambda_b \langle ca \rangle + \lambda_c \langle ab \rangle = 0, \quad (3.8.197)$$

or equivalently, (if we prefer the identity to transform under the little group like $\widetilde{\lambda}_b$),

$$\lambda_a \frac{1}{\langle ab \rangle} + \lambda_b \frac{\langle ca \rangle}{\langle ab \rangle \langle bc \rangle} + \lambda_c \frac{1}{\langle bc \rangle} = 0. \quad (3.8.198)$$

If we combine any such n cyclically-related identities, we will obtain a rank- $(n-2)$ -matrix Q which projects onto λ^\perp . In order for Q to be *symmetric* as a matrix (which was necessary for $C \cdot \widetilde{\lambda}$ to be identified with $\widehat{C} \cdot \mu$), we must have λ_a and λ_c equally-spaced about λ_b in (3.8.198). Of course, the most obvious and natural choice (and the only one which generates the magic we seek) would be to use the *consecutive* 3-term identities:

$$Q_{ab} \equiv \frac{\delta_{a-1b} \langle a a+1 \rangle + \delta_{ab} \langle a+1 a-1 \rangle + \delta_{a+1b} \langle a-1 a \rangle}{\langle a-1 a \rangle \langle a a+1 \rangle}. \quad (3.8.199)$$

For this choice of Q , it turns out that for any plane C containing λ , the plane $\widehat{C} \equiv C \cdot Q$ will have the property that for *any* consecutive chain of columns $\{c_a, \dots, c_b\}$, $\text{span}\{\widehat{c}_a, \dots, \widehat{c}_b\} \subset (\text{span}\{c_{a-1}, \dots, c_{b+1}\})$. That is, Q maps consecutive chains of columns onto consecutive chains of columns! An immediate consequence of this fact is that consecutive minors of C and \widehat{C} are proportional to one another:

$$(12 \cdots k-1 k)|_C = \langle 12 \rangle \langle 23 \rangle \cdots \langle k-1 k \rangle (23 \cdots k-2 k-1)|_{\widehat{C}}. \quad (3.8.200)$$

Thus, for this choice of Q —up to an overall λ -dependent factor (which combines with the Jacobian arising from changing variables $(\widetilde{\lambda}, \widetilde{\eta})$ to (μ, η))—the top-form measure

on $C \in G(k, n)$ given as the product of its consecutive minors, is mapped to the top-form on $\widehat{C} \in G(\widehat{k}, n)$ of precisely the same form. And so, Q maps positroid cells in $G(k, n)$ (which contain a generic 2-plane λ) to positroid cells in $G(\widehat{k}, n)$!

Conveniently, it turns out that the image of any cell $C \in G(k, n)$ in $G(\widehat{k}, n)$ is very easy to identify by its permutation label. Because $\text{span}\{\widehat{c}_a, \dots, \widehat{c}_b\} \subset (\text{span}\{c_{a-1}, \dots, c_{b+1}\})$, we have that $\widehat{r}[a; b] = r[a-1; b+1]-2$; and so, the entire table of ranks, (3.5.125), is preserved in going from C to \widehat{C} —merely shifted downward and to the right:

$$\begin{array}{|c|c|} \hline r[a ; \sigma(a)] & r[a+1; \sigma(a)] \\ \hline r[a ; \sigma(a)-1] & r[a+1; \sigma(a)-1] \\ \hline \end{array} \xrightarrow{\sigma(a)} \begin{array}{|c|c|} \hline \widehat{r}[a+1; \sigma(a)-1]-2 & \widehat{r}[a+2; \sigma(a)-1]-2 \\ \hline \widehat{r}[a+1; \sigma(a)-2]-2 & \widehat{r}[a+2; \sigma(a)-2]-2 \\ \hline \end{array} \xrightarrow{\sigma(a)-1}$$

And so, a configuration $C_\sigma \in G(k, n)$ labeled by the permutation σ will be mapped to a configuration $\widehat{C}_{\widehat{\sigma}} \in G(\widehat{k}, n)$ labeled by the permutation,

$$\widehat{\sigma}(a) \equiv \sigma(a-1) - 1. \quad (3.8.201)$$

One last remarkable aspect of this change of variables is that the combination of all the λ -dependent factors arising from (3.8.200) when mapping the cyclic minors of $G(k, n)$ to cyclic minors of $G(\widehat{k}, n)$ with the Jacobian of the change of variables from $(\widetilde{\lambda}, \widetilde{\eta})$ to (μ, η) turns out to be nothing but the Parke-Taylor (MHV) tree-amplitude, (3.8.180)! And so,

$$f_\sigma^{(k)}(\lambda, \widetilde{\lambda}, \widetilde{\eta}) = \frac{\delta^{2 \times 4}(\lambda \cdot \widetilde{\eta}) \delta^{2 \times 2}(\lambda \cdot \widetilde{\lambda})}{\langle 12 \rangle \langle 23 \rangle \dots \langle n1 \rangle} \times f_{\widehat{\sigma}}^{(\widehat{k})}(\mathcal{Z}), \quad (3.8.202)$$

where,

$$f_{\widehat{\sigma}}^{(\widehat{k})}(\mathcal{Z}) = \oint_{\widehat{C} \in \Gamma_{\widehat{\sigma}}} \frac{d^{\widehat{k} \times n} \widehat{C}}{\text{vol}(GL(\widehat{k}))} \frac{\delta^{4\widehat{k}|4\widehat{k}}(\widehat{C} \cdot \mathcal{Z})}{(1 \dots \widehat{k}) \dots (n \dots \widehat{k}-1)}. \quad (3.8.203)$$

This should not be too surprising, as the Parke-Taylor amplitude can be thought of as the most concise differential form consistent with super momentum conservation—and we know that any generic set of super-momentum-twistors \mathcal{Z} give rise to data $(\widetilde{\lambda}, \widetilde{\eta})$ which *manifestly* conserve super-momentum (This Grassmannian formula in terms of momentum twistor was introduced in [17]).

Let us briefly see how the dimensionality of cells $C_\sigma \in G(k, n)$ and their images $\widehat{C}_{\widehat{\sigma}} \in G(\widehat{k}, n)$ are related. Because the rank of each chain $\widehat{r}[a+1; \widehat{\sigma}(a+1)]$ is lowered by 2 relative to $r[a; \sigma(a)]$, recalling the way dimensionality is encoded by the permutation,

(3.5.128) we see that:

$$\begin{aligned}
\dim(\widehat{C}_{\widehat{\sigma}}) &= \dim(C_{\sigma}) - 2n + k^2 - (k-2)^2, \\
&= \dim(C_{\sigma}) - (2n-4) + 4\widehat{k}; \\
\therefore \dim(\widehat{C}_{\widehat{\sigma}}) - 4\widehat{k} &= \dim(C_{\sigma}) - (2n-4).
\end{aligned} \tag{3.8.204}$$

This is precisely as it should be: *generic* super momentum-twistors \mathcal{Z} give rise to *generic* super-momentum conserving spinor-helicity data $\lambda, \widetilde{\lambda}, \widetilde{\eta}$. Thus, the degree of the form $f_{\widehat{\sigma}}$ should be $\dim(\widehat{C}_{\widehat{\sigma}})$ minus the $4\widehat{k}$ ordinary δ -functions which enforce that \widehat{C} be orthogonal to the generic 4-plane Z .

We should make one small point regarding the (existence of the) map between $G(k, n) \rightarrow G(\widehat{k}, n)$: it is only well-defined for cells C_{σ} which contain a generic 2-plane λ (a point which is completely obvious from the geometry involved in the map's construction). In terms of the permutation σ which labels $C \in G(k, n)$, the criterion that C can contain a generic 2-plane λ translates into the statement that $\sigma(a) - a \geq 2$ for all a . This guarantees that the permutation $\widehat{\sigma}$ is well-defined as an *affine* permutation, that is, that $\widehat{\sigma}(a) \geq a$. Suppose that instead we had $\sigma(a) = a+1$, then $c_a \in \text{span}\{c_{a+1}\}$, and so $\lambda \subset C$ would require that $\langle a a+1 \rangle = 0$. This all makes perfect sense, of course, because $\langle a a+1 \rangle \rightarrow 0$ precisely corresponds to a singularity of the Parke-Taylor amplitude; and the Parke-Taylor amplitude being the *Jacobian* of the transformation to momentum-twistor space, any such singularity indicates that the change of variables is singular.

Let us conclude our discussion by illustrating the map to the ‘momentum-twistor Grassmannian’ for the example discussed above, (3.8.183), of the on-shell form associated with the cell in $G(3, 6)$ labeled by the permutation $\{3, 5, 6, 7, 8, 10\}$, (3.8.181). The image of this cell in the momentum-twistor Grassmannian $G(1, 6)$ is labeled by $\widehat{\sigma} = \{3, 2, 4, 5, 6, 7\}$. Since $\widehat{\sigma}(2) = 2$, we have that $\widehat{c}_2 = 0$. A $GL(1)$ -representative of the point \widehat{C}^* which is orthogonal to the Z -plane in this cell is,

$$\widehat{C}^* \equiv \left(\langle 3456 \rangle \quad 0 \quad \langle 4561 \rangle \quad \langle 5613 \rangle \quad \langle 6134 \rangle \quad \langle 1345 \rangle \right), \tag{3.8.205}$$

where $\langle a b c d \rangle \equiv \det\{z_a, z_b, z_c, z_d\}$ is a minor of the matrix Z , and $\widehat{C}^* \cdot Z = 0$ because of the 4-vector manifestation of Cramer's rule, (3.4.47). Supported on this point, (3.8.203) generates the momentum-twistor super-function,

$$f_{\{3,2,4,5,6,7\}}^{(1)} = \frac{\delta^{1 \times 4}(\widehat{C}^* \cdot \eta)}{\underbrace{\langle 3 \ 4 \ 5 \ 6 \rangle}_{(1)|_{\widehat{C}^*}} \underbrace{\langle 4 \ 5 \ 6 \ 1 \rangle}_{(3)|_{\widehat{C}^*}} \underbrace{\langle 5 \ 6 \ 1 \ 3 \rangle}_{(4)|_{\widehat{C}^*}} \underbrace{\langle 6 \ 1 \ 3 \ 4 \rangle}_{(5)|_{\widehat{C}^*}} \underbrace{\langle 1 \ 3 \ 4 \ 5 \rangle}_{(6)|_{\widehat{C}^*}}}. \quad (3.8.206)$$

And so, including the Parke-Taylor Jacobian, (3.8.202), we have:

$$f_{\{3,5,6,7,8,10\}}^{(3)} = \frac{\delta^{2 \times 4}(\lambda \cdot \tilde{\eta}) \delta^{2 \times 2}(\lambda \cdot \tilde{\lambda})}{\langle 1 \ 2 \rangle \langle 2 \ 3 \rangle \langle 3 \ 4 \rangle \langle 4 \ 5 \rangle \langle 5 \ 6 \rangle \langle 6 \ 1 \rangle} \frac{\delta^{1 \times 4}(\widehat{C}^* \cdot \eta)}{\langle 3 \ 4 \ 5 \ 6 \rangle \langle 4 \ 5 \ 6 \ 1 \rangle \langle 5 \ 6 \ 1 \ 3 \rangle \langle 6 \ 1 \ 3 \ 4 \rangle \langle 1 \ 3 \ 4 \ 5 \rangle}. \quad (3.8.207)$$

3.9 Positive Diffeomorphisms and Yangian Invariance

We have seen that the map from twistor space to momentum-twistor space has a natural origin, providing an obvious geometric basis for dual conformal invariance. Let us now consider another obvious symmetry of the positive Grassmannian—namely, diffeomorphisms of Grassmannian coordinates which preserve the structure of the positroid stratification (equivalently, diffeomorphisms which leave measure on $G_+(k, n)$ invariant). Preserving the positive structure of the Grassmannian, we call this subset of diffeomorphisms *positive diffeomorphisms*. In this section, we illustrate the remarkable fact that the leading generators of infinitesimal positive diffeomorphisms directly match the level-one generators of the Yangian as described in [74] (see also [93, 96, 97, 99]).

Let us begin by broadly characterizing the infinitesimal diffeomorphisms in which we are interested. Consider any infinitesimal variation δC of $C \in G_+(k, n)$ which we may expand as a power-series,

$$\delta C \sim C + CC + CCC + \dots \quad (3.9.208)$$

We view a general infinitesimal diffeomorphism of C in terms of the variations $\delta c_{\alpha a}$ for each matrix component of C . Because *positive* diffeomorphisms must preserve *all* positroid configurations, $\delta c_{\alpha a}$ must vanish whenever c_a does; this restricts the class of diffeomorphisms to those of the form,

$$\delta c_{\alpha a} = (\Omega_a[C])_{\alpha}^{\beta} c_{\beta a} \quad (\text{no summation on } a), \quad (3.9.209)$$

where each $\Omega_a[C]$ is itself expanded as a power-series in the components of C . Considering $\Omega_a[C]$ as a $(k \times k)$ -matrix, we may simplify our notation by writing:

$$\delta c_a = (\Omega_a[C]) \cdot c_a. \quad (3.9.210)$$

Note that any variation where Ω is proportional to the identity matrix is just an un-interesting (C -dependent) little group transformation. Note also that this variation takes the form of a different $GL(k)$ transformation on each column. We can always use the global $GL(k)$ -symmetry to bring the variation of any *one* column, say c_1 , to zero:

$$\delta c_1 = 0. \tag{3.9.211}$$

(And without loss of generality, we can always take c_1 to be a non-vanishing column.)

Let us now determine what conditions must be imposed on $\Omega_a[C]$ in order to ensure that the variations δc_a preserve *all* positroid configurations. We will now demonstrate that there are no *non-trivial* variations to leading order in C , and that the first non-trivial positive diffeomorphisms—those quadratic in C —precisely correspond to the level-one generators of the Yangian as described in reference [74].

To leading order, each Ω_a is a C -independent $(k \times k)$ -matrix. Consider any configuration for which $c_1 \propto c_2$, and let us use the $GL(k)$ -symmetry to fix the variation of c_1 to zero. It is not hard to see that the only variation of c_2 which preserves the configuration in question would be the rescaling $\delta c_2 = t c_2$. This variation can be fully compensated by a little group rescaling, allowing us to conclude that *no* non-trivial variation of c_2 is positive. Repeating this argument by starting with c_2 instead of c_1 , and so on, we therefore see that the only *positive* leading-order diffeomorphisms are overall $GL(k)$ -transformations and little group rescalings.

Non-trivial positive diffeomorphisms first arise at quadratic-order—when $\Omega_a[C]$ is linear in the components of C . Let us again consider any configuration for which $c_1 \propto c_2$, and use the $GL(k)$ -symmetry to fix the variation of c_1 to zero. Because positive diffeomorphisms must preserve $r[a; b] \equiv \text{rank}\{c_a, \dots, c_b\}$ generally—and $r[1; 2]$ in particular—it is clear that the only allowed variations would be of the form,

$$\delta c_2 = (c_1 \omega_1^\beta) c_{\beta 2} \equiv c_1 (\omega_1 \cdot c_2). \tag{3.9.212}$$

We ignore any variation quadratic in c_2 as it represents a little group rescaling. Here, ω_1^β is an arbitrary k -vector parameterizing the variation. Notice that (3.9.212) is just a simple $GL(k)$ -transformation of column c_2 by the matrix $M_\alpha^\beta \equiv (c_{\alpha 1} \omega_1^\beta)$. Applying the inverse of this transformation to *all* columns would of course trivialize $\delta c_2 \rightarrow 0$, allowing us to repeat the same logic to fix the most general form of δc_3 , and so on. Continuing in this manner and then undoing each step's $GL(k)$ -transformation so that we restore $\delta c_1 = 0$, the most general quadratic, positive diffeomorphism consistent with positivity would be of the form:

$$\begin{aligned}
\delta c_1 &= 0; \\
\delta c_2 &= c_1(\omega_1 \cdot c_2); \\
\delta c_3 &= c_1(\omega_1 \cdot c_3) + c_2(\omega_2 \cdot c_3); \\
&\vdots \\
\delta c_n &= c_1(\omega_1 \cdot c_n) + \cdots + c_{n-1}(\omega_{n-1} \cdot c_n);
\end{aligned} \tag{3.9.213}$$

which we may summarize:

$$\delta c_a = \sum_{b < a} c_b(\omega_b^\beta c_{\beta a}). \tag{3.9.214}$$

We fixed the form of this transformation by demanding that the cells where $c_1 \propto c_2$ are left invariant, but quite nicely, we can see that this transformation leaves *all* cells invariant! Note that $r[1; a] \equiv \text{rank}\{c_1, \dots, c_a\}$ is unchanged for all a , as the variations in (3.9.213) transform each c_a by factors proportional to columns which are always (trivially) spanned by the un-deformed chains. And so, (3.9.214) preserves all $r[1; b]$ —the entire first column of the table (3.5.125).

In order for the diffeomorphisms (3.9.214) to be *positive*, however, they must preserve the ranks $r[a; b]$ for *all* chains of columns; and so, we must find the subset which are independent of our choice to single-out δc_1 . These can be found by continuing the sequence of successive variations in (3.9.213) back to δc_1 , and requiring that this be consistent with our choice to fix $\delta c_1 = 0$:

$$\delta c_1 = c_1(\omega_1 \cdot c_1) + \cdots + c_n(\omega_n \cdot c_1) = \left(\sum_{b=1}^n c_b \omega_b^\beta \right) c_{\beta 1} = 0. \tag{3.9.215}$$

Because this must be satisfied for *all* configurations in $G_+(k, n)$, this must be independent of $c_{\beta 1}$. And so, the condition that ensures that (3.9.214) is positive is that,

$$\sum_{b=1}^n c_b \omega_b^\beta = 0. \tag{3.9.216}$$

This is simply the geometric statement that $\omega_a^\beta \subset C^\perp$ (for each index β separately). We have therefore constructed the most general set of infinitesimal, quadratic diffeomorphisms which preserve all cells in the positroid stratification of $G(k, n)$.

Recall that kinematical data—specified, say, in terms of super-twistor variables \mathcal{W} —is communicated to the Grassmannian via the constraint $\delta^{4k|4k}(C \cdot \mathcal{W})$. This means that any symmetry-transformation acting on the \mathcal{W} 's can be recast as a transformation on the configuration C . In reference [74], it was shown that the level-one

generators of the Yangian can be translated in this way to become symmetry generators acting on the matrix C by the operator:

$$\mathcal{Q} \equiv \sum_{a=1}^n \mathcal{Q}_a \quad \text{with} \quad \mathcal{Q}_a \equiv \left(\sum_{b<a} c_{\alpha b} \mathcal{W}_b^I(\xi_I^\beta c_{\beta a}) \right) \frac{\partial}{\partial c_{\alpha a}}, \quad (3.9.217)$$

which is easily seen to generate diffeomorphisms of the form,

$$\delta c_a = \sum_{b<a} c_b w_b^I(\xi_I^\beta c_{\beta a}), \quad (3.9.218)$$

which we immediately recognize as nothing but the leading positive diffeomorphisms (3.9.214), where w_b^β has been re-written as

$$w_b^\beta \equiv w_b^I \xi_I^\beta, \quad (3.9.219)$$

for some (arbitrary) $(4 \times k)$ -matrix ξ_I^β . Moreover, the condition on admissible variations, (3.9.216), is immediately seen to be *precisely* what is enforced by the constraint $\delta^{4k|4k}(C \cdot \mathcal{W})$ —which is imposed for all on-shell differential forms.

3.10 Combinatorics of Kinematical Support for On-Shell Forms

On-shell graphs with the right number of degrees of freedom to be completely localized for *generic*, (super-)momentum conserving kinematical data are obviously of particular interest. In momentum space, this requires that a configuration C associated with an on-shell graph admits solutions to both the constraint that it contains a generic 2-plane $\lambda \in G(2, n)$, and is contained within the geometric-dual of another 2-plane $\tilde{\lambda} \in G(2, n)$ satisfying $\lambda \cdot \tilde{\lambda} = 0$. In terms of the permutation σ associated with an on-shell graph, these constraints minimally require that for any a , $(a+2) \leq \sigma(a) \leq (a+n-2)$. (Recall that the condition that $\sigma(a) \geq (a+2)$ is *necessary* for a configuration in $G(k+2, n)$ to even have a momentum-twistor dual in $G(k, n)$.) However, not all configurations which meet these conditions admit solutions to the combined constraints.

In this section, we will describe a purely-combinatorial solution to the question of whether or not an on-shell graph vanishes for generic kinematical data; and if so, how many solutions to the kinematical constraints exist. This turns out to be much simpler to do for the momentum-twistor Grassmannian rather than for configurations directly associated with on-shell graphs. This is partly because the kinematical constraints are much simpler for momentum-twistors than for the λ 's and $\tilde{\lambda}$'s.

Recall that when kinematical data is specified by momentum-twistors, $Z \in G(4, n)$, the configuration $\overline{C}_\sigma \in G(k+2, n)$ *directly* associated with an N^k MHV *on-shell graph* is mapped to its momentum-twistor image $\overline{C}_\sigma \mapsto C_\sigma \in G(k, n)$, and the kinematical constraints become the simpler condition that $C \cdot Z = 0$. This imposes $4k$ constraints in general, and so we are most interested in $4k$ -dimensional cells of $G(k, n)$, as these can be completely isolated by generic kinematical data. In terms of the orthogonal complement Z^\perp of the twistors Z , the number of solutions to $C \cdot Z = 0$ is counted by the number of isolated points in $C \cap Z^\perp$.

As with any intersection-number problem in algebraic geometry, the solution can be found by decomposing both C and Z^\perp into a homological basis for which the intersection numbers are known, such as Schubert cycles whose intersection numbers

are given by the Littlewood-Richardson rule (see [71]). The decomposition of (the closure of) an arbitrary positroid cell into Schubert cycles was recently presented in ref. [44], and this provides us with a purely-combinatorial answer to the ‘number of intersections’ question in which we are interested. And it turns out that for the special case of *generic* kinematical data, the machinery of [44] simplifies considerably. (We are thankful to Thomas Lam and David Speyer for helpful discussions regarding this specialization of the general case.)

A complete discussion of this story would require more space than warranted here; but let us briefly describe the ultimate, combinatorial solution to the question of kinematical support. The first step is to generalize our discussion slightly, and consider kinematical data specified for any number of dimensions:

Definition: For any $(m \times k)$ -dimensional cell $C \in G_+(k, n)$, let $\Gamma^m(C)$ denote the number of isolated points in $C \cap Z^\perp$ for a *generic* m -plane $Z \in G(m, n)$.

The basic strategy is to define a *distinguished subset* $[\partial^k](C)$ of k^{th} -degree boundary elements of C which contain non-overlapping subsets of the intersection points as projected to these boundaries, such that each element $C' \in [\partial^k](C)$ contains precisely $\Gamma^{m-1}(C')$ points. If this can be done, then $\Gamma^m(C)$ will be determined recursively by,

$$\Gamma^m(C) = \sum_{C' \in [\partial^k](C)} \Gamma^{m-1}(C') \quad \text{with} \quad \Gamma^0(C) \equiv 1. \quad (3.10.220)$$

The magic, then, is entirely in the definition of the distinguished boundary elements $[\partial^k](C)$. Before we describe these in general, however, it may be helpful to build some intuition with two (very) simple cases for which (3.10.220) is easy to understand.

I. Kinematical Support of NMHV Yangian-Invariants

Although perhaps a bit trivial, it is worth noting that $\Gamma^m(C) = 1$ for *all* m -dimensional configurations in $G(1, n)$ —those relevant to NMHV amplitudes: given any generic m -plane Z , there is a unique configuration $C^* \in C \cap Z^\perp$ supplied by Cramer’s rule, (3.4.47)—the unique $(m+1)$ -term identity satisfied by generic m -vectors. This is of course obvious; but let us see what it suggests about how we may define the *distinguished* boundary elements $[\partial^1](C)$ which we seek to understand.

Just as $\Gamma^m(C) = 1$ for any m -dimensional configuration in $G(1, n)$, $\Gamma^{m-1}(C) = 1$ for any $(m-1)$ -dimensional configuration. Therefore, in order for the recursive formula (3.10.220) to give us the right answer, we need only define $[\partial^1](C)$ to systematically choose any *one* element of the boundary of C . One natural choice would be the configuration in ∂C which deletes the *first* non-vanishing column of C —that is, the boundary for which the maximum image of the configuration’s permutation is ‘raised.’

II. Kinematical Support for One-Dimensional Kinematics

Let us now consider the slightly less trivial case of one-dimensional kinematics, where $Z \in G(1, n)$ and we are interested in finding $\Gamma^1(C)$ for k -dimensional configurations in $G(k, n)$. Unlike the situation for $k = 1$, it is no longer the case that every k -dimensional configuration admits solutions to $C \cdot Z = 0$. The simplest example of a configuration for which $\Gamma^1(C) = 0$ occurs for the 2-dimensional configuration in $G(2, 4)$ labeled by the permutation $\{2, 3, 5, 8\}$:

$$C(\alpha) = \begin{pmatrix} 1 & \alpha_1 & \alpha_2 & 0 \\ 0 & 0 & 0 & 1 \end{pmatrix}. \quad (3.10.221)$$

Notice that $C \cdot Z = 0$ implies that $z_4 = 0$, which is obviously not satisfied by a generic set of (1-dimensional) momentum-twistors. In contrast, consider the configuration labeled by the permutation $\{2, 5, 4, 7\}$ represented by,

$$C(\alpha) = \begin{pmatrix} 1 & \alpha_1 & 0 & 0 \\ 0 & 0 & 1 & \alpha_2 \end{pmatrix}, \quad \text{for which} \quad C^* \equiv \begin{pmatrix} z_2 & -z_1 & 0 & 0 \\ 0 & 0 & z_4 & -z_3 \end{pmatrix} \quad (3.10.222)$$

is the unique solution to $C \cdot Z = 0$.

We can understand that a solution exists in the second case because each row of the matrix-representative of C has one degree of freedom—reducing each row to the simple case of $k = 1$ described above. In the first example, however, no solution exists because its second row has no degrees of freedom—which can itself be viewed as a zero-dimensional configuration in $G(1, n)$. Heuristically, then, in order for any solutions to $C \cdot Z = 0$ to exist, there must exist at least one degree of freedom in every row of any matrix-representative of C .

In terms of the permutation, the existence of a row without any degrees of freedom is indicated by any column a such that $\sigma(a) = a + n$. And so, a k -dimensional cell

$C \in G(k, n)$ admits solutions to $C \cdot Z = 0$ for a generic 1-plane Z if and only if $\sigma(a) \neq a + n$ for all a .

III. General Combinatorial Test of Kinematical Support

Combining the lessons learned from the two simple cases above, it is clear that solutions to $C \cdot Z = 0$ exist only if there are in some sense m degrees of freedom in each row of any matrix-representative of C . A systematic way to test this combinatorially would be to find boundary elements of C which successively remove one degree of freedom from each row of C . Let us now describe how such boundary configurations can be found.

Recall that the lexicographically-first non-vanishing minor $A(\sigma) \equiv (a_1, \dots, a_k)$ of any configuration C_σ is given simply by the images of σ which extend beyond n (see section I.). Because of this, we can always give a matrix-representative of C in the following, gauge-fixed form:

$$\begin{array}{c}
 \dots \dots a_1 \dots \dots a_2 \dots \dots a_k \dots \dots \\
 \hline
 1 \left(\begin{array}{cccccccccccc}
 0 & \dots & 0 & 1 & * & \dots & * & \dots & \dots & \dots & \dots & \dots & * \\
 0 & \dots & \dots & \dots & \dots & 0 & 1 & * & \dots & \dots & \dots & \dots & * \\
 \vdots & & \ddots & \ddots & \ddots & \ddots & \ddots & & \ddots & \ddots & \ddots & & \vdots \\
 k & 0 & \dots & \dots & \dots & \dots & \dots & \dots & 0 & 1 & * & \dots & *
 \end{array} \right). \quad (3.10.223)
 \end{array}$$

A boundary-element which removes one degree of freedom from the k^{th} -row of C , for example, would be any which ‘raises’ a_k —that is, if $\sigma(c_k) = a_k$, then a boundary for which $\sigma'(c_k) = a'_k > a_k$. After this, a degree of freedom can be removed from the $(k-1)^{\text{th}}$ row, and so on. Notice, however, that at each stage, $A(\sigma)$ must be *raised*: if $A(\sigma)$ remained unchanged, then it would not indicate that a degree of freedom from any particular row had been removed, as we desire.

With this picture serving as motivation, we define the distinguished, k^{th} -degree boundary-elements of C , $[\partial^k](C)$, as follows. Let σ be the permutation labeling the configuration C , and let us define $A(\sigma) \equiv (a_1, \dots, a_k)$ —with $a_1 < a_2 < \dots < a_k$ —to be the images of σ which extend beyond n (the necklace $A^{(1)}(\sigma)$). Then $[\partial^k](C)$ is the set of all k^{th} -degree boundaries of C obtained by a sequence of boundaries labeled by permutations $\sigma \xrightarrow{\partial} \sigma^{(1)} \xrightarrow{\partial} \sigma^{(2)} \xrightarrow{\partial} \dots \xrightarrow{\partial} \sigma^{(k)}$ such that, *lexicographically*,

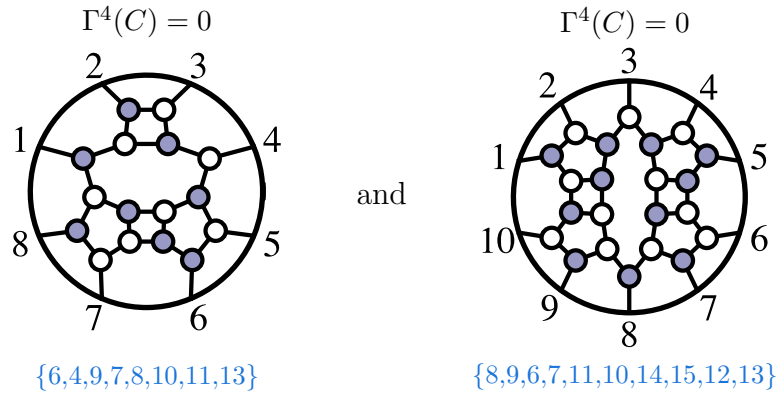
$$A(\sigma) < A(\sigma^{(1)}) < A(\sigma^{(2)}) < \dots < A(\sigma^{(k)}). \quad (3.10.224)$$

That is, if the configuration labeled by $\sigma^{(\ell-1)}$ with $A(\sigma^{(\ell-1)}) = (a_1, \dots, a_{k-\ell}, \dots, a_k)$ is found at the ℓ^{th} successive boundary, we take all $\sigma^{(\ell)}$ in its boundary for which $A(\sigma^{(\ell)}) = (a_1, \dots, a'_{k-\ell}, \dots, a_k)$ with $a_{k-\ell} < a'_{k-\ell}$.

In general, there can be many such elements of $[\partial^k](C)$, and each can contribute to $\Gamma^m(C)$. Putting all these contributions together, we find the recursive formula given above:

$$\Gamma^m(C) = \sum_{C' \in [\partial^k](C)} \Gamma^{m-1}(C') \quad \text{with} \quad \Gamma^0(C) \equiv 1. \quad (3.10.225)$$

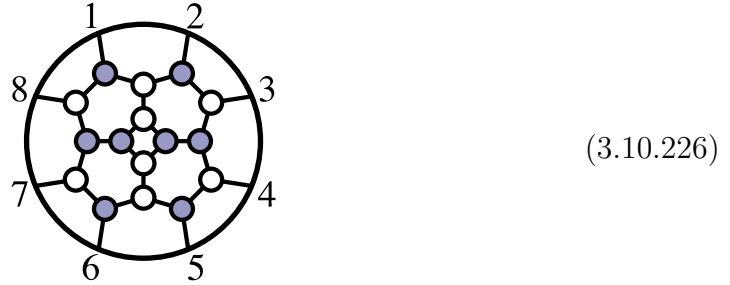
The utility of this combinatorial test is hard to overstate, as the number of $4k$ -dimensional cells in $G(k, n)$ with *non-vanishing* support become increasingly rare with large k and n . Cells with $\Gamma^4(C) = 0$ —for which $C \cap Z^\perp = \{\}$ —represent generally-vanishing functions which do not contribute to identities, for example. Many of these fail the simple test of $(a+2) \leq \sigma(a) \leq (n+a+2)$, but with increasing frequency, configurations fail to have kinematical support for much more subtle reasons—demonstrating the value of having a more robust yet simple combinatorial test available. For example, neither of the following on-shell graphs—in $G(4, 8)$ and $G(5, 10)$, respectively—have kinematical support:



Configurations for which $\Gamma^4(C) = 1$ correspond to manifestly *rational* functions of the kinematical data. More generally, however, when $\Gamma^4(C) > 1$ the isolation of internal degrees of freedom via $\delta^{k \times 4}(C \cdot Z)$ results in a (generally) *algebraic* function of the external twistors for each isolated solution $C^* \in C \cap Z^\perp$ —each point giving us a Yangian-invariant which is individually of some physical interest. However, a highly non-trivial but general result is that the function obtained by summing-over all isolated solutions to $C \cdot Z = 0$ is *always rational*. Throughout the rest of this chapter, whenever we speak of ‘the’ function associated with a graph for which $\Gamma^4 > 1$ —for

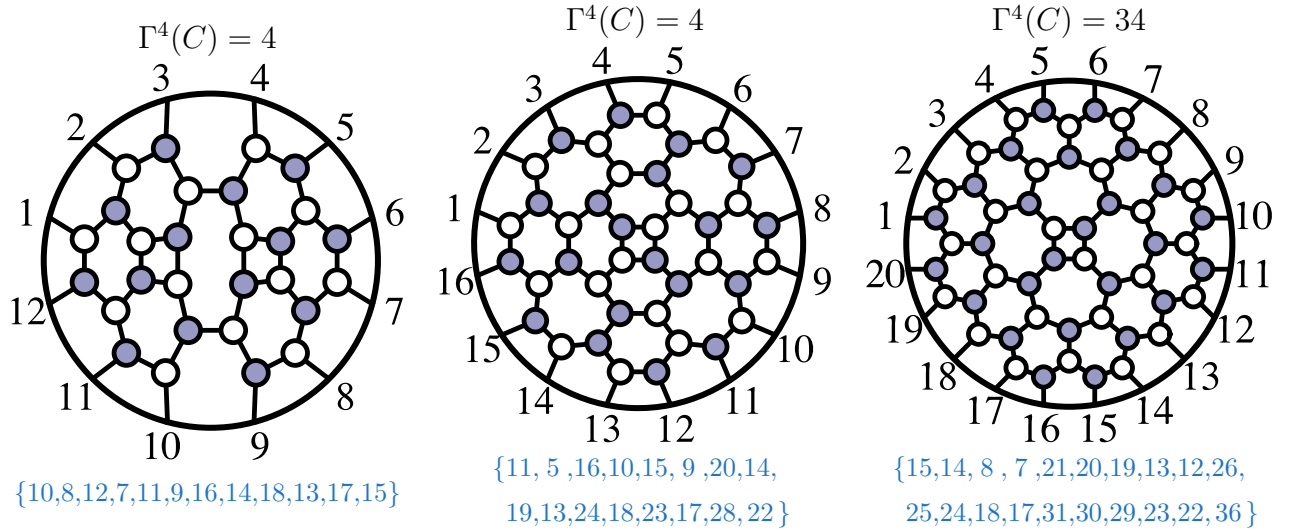
example, when appearing in an identity (see section 3.11)—we always implicitly mean the rational function obtained by summing-over all particular solutions to $C \cdot Z = 0$.

On-shell graphs which admit multiple solutions to the kinematical constraints are comparatively rare. The first on-shell graph for which more than one solution exists occurs for $G(4, 8)$ and is well-known to physicists as the ‘four-mass-box’:



The image of this configuration in the momentum-twistor Grassmannian is labeled by $\{2, 5, 4, 7, 6, 9, 8, 11\}$, for which we can calculate $\Gamma^4(C) = 2$.

Configurations admitting more than two solutions to $C \cdot Z = 0$ are even rarer—and their rarity increases dramatically with increasing Γ^4 . Indeed, almost no examples of Yangian-invariant functions for which $\Gamma^4(C) > 2$ were even known before the advent of the tools described in this section. But having the combinatorial test available allows us to systematically find and classify them. Three striking examples of on-shell graphs which admit many solutions to the kinematical constraints—for $G(6, 12)$, $G(8, 16)$, and $G(10, 20)$, respectively—are:



3.11 The Geometric Origin of Identities Among Yangian-Invariants

In this section, we will focus primarily on on-shell differential forms for which the integral over auxiliary Grassmannian degrees of freedom is fully localized by the δ -function constraints, without imposing any conditions on the external kinematical data other than momentum conservation. These are on-shell diagrams with $(2n-4)$ degrees of freedom or their momentum-twistor images with $4k$ degrees of freedom, and for which $\Gamma^4(C) > 0$; we will refer to such on-shell forms as *Yangian-invariants*, and frequently refer to them (improperly) as ‘functions’ of the kinematical variables.

One of the most remarkable and important properties about Yangian-invariants is that they satisfy many, intricate functional identities. Examples of such identities have long been known, and are crucial for our understanding of many important physical properties of scattering amplitudes. Perhaps the simplest and most familiar examples of such identities come from equating the various implementations of the BCFW recursion relations, (3.2.21); for example, for the 6-particle NMHV tree-level scattering amplitude, the BCFW recursion can alternatively lead to two distinct formulae depending on which pair of adjacent legs are singled-out by the recursion:

The diagrammatic identity is presented in two rows. Each row shows an equality between a single diagram on the left and a sum of three diagrams on the right. The diagrams are circular with six external legs labeled 1 through 6. The top row shows a diagram with a shaded central region (legs 1-6) equal to the sum of three diagrams with unshaded centers and different internal structures. The bottom row shows a diagram with an unshaded central region (legs 1-6) equal to the sum of three diagrams with unshaded centers and different internal structures. Blue text below each diagram in the right-hand side of both rows lists a set of legs: {4, 5, 6, 8, 7, 9}, {3, 5, 6, 7, 8, 10}, {4, 6, 5, 7, 8, 9} for the top row, and {4, 5, 7, 6, 8, 9}, {4, 5, 6, 7, 9, 8}, {5, 4, 6, 7, 8, 9} for the bottom row.

This identity is not easy to prove directly if each term is viewed as a multivariate, rational ‘function’ of the kinematical data. However, its veracity is crucial to our understanding of many important properties of the complete amplitude. For example,

although the BCFW-recursion breaks cyclicity by the choice of legs to deform, the entire amplitude—being cyclically-invariant—must be independent of this choice.

A wide variety of such identities can be generated simply by equating all the myriad BCFW ‘formulae’ obtained by recursing the left- and right-amplitudes appearing across the BCFW-bridge in all possible ways (at each stage of the recursion). For example, for the 8-particle N^2 MHV tree amplitude, there are many hundreds of ways to follow the recursion all the way down to a sum of 20 trivalent, on-shell diagrams; this multitude of BCFW ‘formulae’ involves a total of 176 distinct Yangian-invariants in $G(4, 8)$, and equating every pair leads to 74 linearly-independent, 40-term identities satisfied among them.

Other than the equality of different BCFW formulae, however, few identities among Yangian-invariants were known until the Grassmannian formulation—the contour integral “ $\mathcal{L}_{n,k}$ ” was discovered, [16]. But a complete understanding of the range of possible Yangian-invariants, and a systematic understanding of the relations they satisfy remained to be understood. In the remainder of this section, we will describe how *all* such identities arise *homologically* in the Grassmannian, and can be understood in purely geometric (even combinatorial) terms.

I. Homological Identities in the Grassmannian

The six-term identity described above which equates the two possible representations of the 6-particle $N^{(k=1)}$ MHV tree-amplitude turns out to generate *all* the identities among NMHV Yangian-invariants. In order to see how this can be, let us first descend to the somewhat simpler situation which arises in the momentum-twistor Grassmannian, where NMHV Yangian-invariants correspond to 4-dimensional cells of $G(1, n)$.

All NMHV Yangian-invariants are essentially equivalent, as any 4-dimensional configuration in $C \in G(1, n)$ involves precisely 5 non-vanishing ‘columns’; and so, such configurations differ only in which of the 5 columns are involved. In terms of canonical coordinates, such a configuration would be represented by,

$$C(\alpha) \equiv \left(\begin{array}{cccccccccccccccc} & & a & & & b & & & c & & & d & & & e & & & \\ \hline \cdots & 0 & 1 & 0 & \cdots & 0 & \alpha_1 & 0 & \cdots & 0 & \alpha_2 & 0 & \cdots & 0 & \alpha_3 & 0 & \cdots & 0 & \alpha_4 & 0 & \cdots \end{array} \right),$$

and would be labeled by a permutation,

$$\sigma \equiv \begin{pmatrix} a & b & c & d & e \\ \downarrow & \downarrow & \downarrow & \downarrow & \downarrow \\ b & c & d & e & a \end{pmatrix}, \quad (3.11.227)$$

with $\sigma(j) = j$ for all other columns. Instead of labeling the configuration by its permutation, it is tempting to label it instead by its 5 non-vanishing columns—as a *5-bracket*, $[abcde]$. Given any generic momentum-twistors $Z \in G(4, n)$, there is a unique point $C^* \in C \cap Z^\perp$, which can be represented by the matrix,

$$C^* \equiv \left(\begin{array}{ccccccccc} & a & & b & & c & & d & & e \\ 0 & \langle bcde \rangle & 0 & \langle cdea \rangle & 0 & \langle deab \rangle & 0 & \langle eabc \rangle & 0 & \langle abcd \rangle & 0 \end{array} \right),$$

for which it is easy to see that $C^* \cdot Z = 0$ as an instance of Cramer's rule, (3.4.47).

This leads to the general form of the essentially-unique NMHV Yangian-invariant,

$$\begin{array}{l} [abcde] \\ \{b,c,d,e,a\} \end{array} \Leftrightarrow \frac{\delta^{1 \times 4} (\eta_a \langle bcde \rangle + \eta_b \langle cdea \rangle + \eta_c \langle deab \rangle + \eta_d \langle eabc \rangle + \eta_e \langle abcd \rangle)}{\langle bcde \rangle \langle cdea \rangle \langle deab \rangle \langle eabc \rangle \langle abcd \rangle}. \quad (3.11.228)$$

(Notice that the 5-bracket $[abcde]$ as we have defined it is antisymmetric with respect to its arguments. This reflects the fact that the measure $d\log(\alpha_1) \wedge \cdots \wedge d\log(\alpha_4)$ is *oriented*. This 5-bracket is the simplest dual super-conformal invariant and was first found in the literature in [57] in momentum space).

If we considered instead a 5-dimensional configuration in $G(1, n)$, then the constraint $\delta^{1 \times 4}(C \cdot Z)$ would fix only four of the internal degrees of freedom, leaving us with a 1-dimensional integral over $G(1, n)$. In this case, Cauchy's theorem informs us that the sum of all the residues of this one-form will vanish. As each of these residues is itself a 4-dimensional configuration of the form above (3.11.228), this gives rise to an identity among 5-brackets. Motivated by the notation used above, let us denote a generic 5-dimensional configuration in $G(1, n)$ by the *6-bracket* $[abcdef]$; then we find,

$$\begin{array}{l} \partial[abcdef] \\ \{b,c,d,e,f,a\} \end{array} = \begin{array}{l} [abcde] \\ \{b,c,d,e,f,a\} \end{array} - \begin{array}{l} [abcdf] \\ \{b,c,d,e,f,a\} \end{array} + \begin{array}{l} [abcef] \\ \{b,c,d,e,f,a\} \end{array} - \begin{array}{l} [abdef] \\ \{b,c,d,e,f,a\} \end{array} + \begin{array}{l} [acdef] \\ \{b,c,d,e,f,a\} \end{array} - \begin{array}{l} [bcdef] \\ \{b,c,d,e,f,a\} \end{array} = 0.$$

(Here, the signs are important: they reflect the fact that our formula for the 5-bracket (3.11.228) corresponds to a *particular orientation* of the 4-dimensional cells; and so, when taking the boundary of $[abcdef]$ we must re-order the coordinates for each boundary cell accordingly—at the cost of introducing signs. Notice that the alternating signs here *precisely* capture the equality between two three-term, all-plus formulae as generated by equating BCFW formulae as described above.)

Notice that this 6-term identity precisely reproduces the identity among 6-particle NMHV Yangian invariants generated by equating BCFW recursion schemes. More importantly, however, because we understand that all NMHV Yangian-invariants are of the same basic form, the identity given above captures *all* the identities satisfied among NMHV Yangian-invariants.

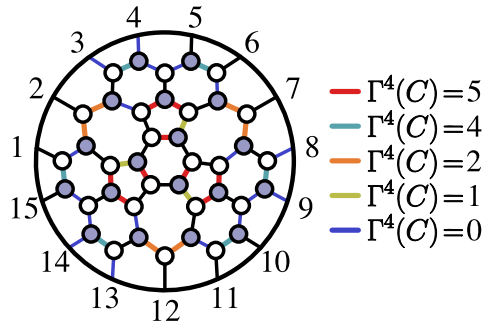
The essential point in the example above is that if we consider a configuration $C \in G(k, n)$ whose boundary includes those associated with Yangian-invariant ‘functions’, then the δ -function constraints will localize the Grassmannian integral to a 1-dimensional integral, allowing us to use Cauchy’s theorem to conclude that the sum of all the residues in the boundary will vanish; equivalently, that the combination of Yangian-invariants along any boundary $\partial(C)$ add to zero. This turns out to generate *all* the functional identities satisfied by Yangian-invariants, including many of impressive complexity.

Recall that the boundary of an on-shell diagram is the collection of diagrams obtained by deleting its *removable* edges. And so we can find identities among N^k MHV on-shell differential forms by taking the boundary of any $(2n-3)$ -dimensional cell in $G(k+2, n)$ for ordinary kinematical data, or any $(4k+1)$ -dimensional cell of $G(k, n)$ for momentum-twistor kinematical data. One example of an identity found in this way generates an identity among 8-particle N^2 MHV Yangian-invariants which is independent of all those identities found by equating various BCFW formulae, and can be understood as a way to represent the ‘four-mass box’ (which generally involves quadratic roots, as $\Gamma^4(C) = 2$) as a sum of purely-rational Yangian-invariants:

It is worth noting that we have only included the *non-vanishing* contributions to this identity—those graphs for which $\Gamma^4 > 0$; in addition to the nine graphs above, the boundary of $\{4,7,6,9,8,10,11,13\}$ also includes the graphs,

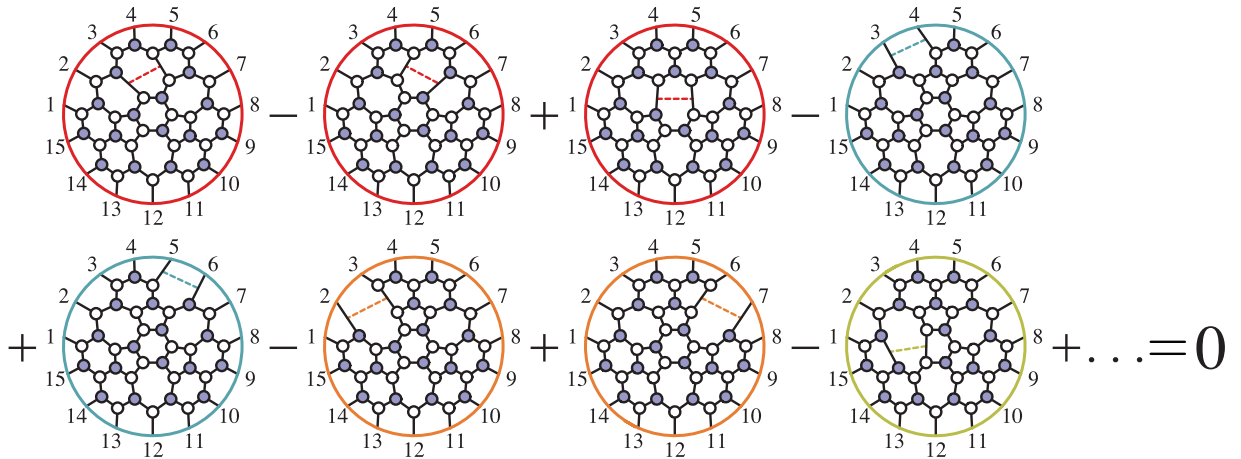
which all have $\Gamma^4 = 0$, and so lead to generally-vanishing functions of the external, kinematical data and therefore do not contribute to the identity.

Another particularly impressive example of an identity generated in this way is a 24-term identity among 15-particle N^4 MHV Yangian-invariants, generated by the boundary of the 27-dimensional cell,



{9,7,6,15,8,14,12,11,20,13,19,17,16,25,18}

which includes 8 cyclic classes of Yangian-invariants—three of which are quintic ($\Gamma^4(C) = 5$), two quartic, two quadratic, and one of which is rational:



where ‘ \dots ’ indicates a sum over cyclic classes.

3.12 The Yang-Baxter Relation and ABJM Theories

We began our discussion linking permutations and scattering amplitudes in section 3.3 by recalling the story of scattering in (1+1)-dimensional integrable theories (for a review see [153]). In this section, we will see that this familiar story is actually contained as a special case of our new picture linking permutations to on-shell diagrams. And there is another special case which will turn out to give a theory of on-shell graphs for the ABJM theory [120] (see also [154–157]) defined in (2+1) dimensions! Although both these stories are physically very rich on their own, we will content ourselves here by briefly sketching-out the main points involved, leaving more detailed exposition and exploration to future work.

I. The On-Shell Avatar of the Yang-Baxter Relation

Recall the basic structure of the (1+1)-dimensional amplitudes from our discussion in section 3.3, for which the fundamental interactions involved are 4-particle vertices. In order to relate these to our story, we must find a way to recast each 4-particle interaction (each carrying only one degree of freedom) in terms of an on-shell diagram with only trivalent vertices. The simplest way of doing this is to ‘blow-up’ each 4-point vertex according to:

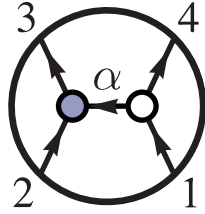
$$(3.12.229)$$

where only edges from blown-up vertices have weight different from unity.

Notice that the left-right path permutation moving from the bottom to the top of the graph agrees with the ‘(1+1)-permutation’, while the left-right path permutations from top to bottom are trivial:

$$(3.12.230)$$

Consider for example the 4-point vertex by itself,

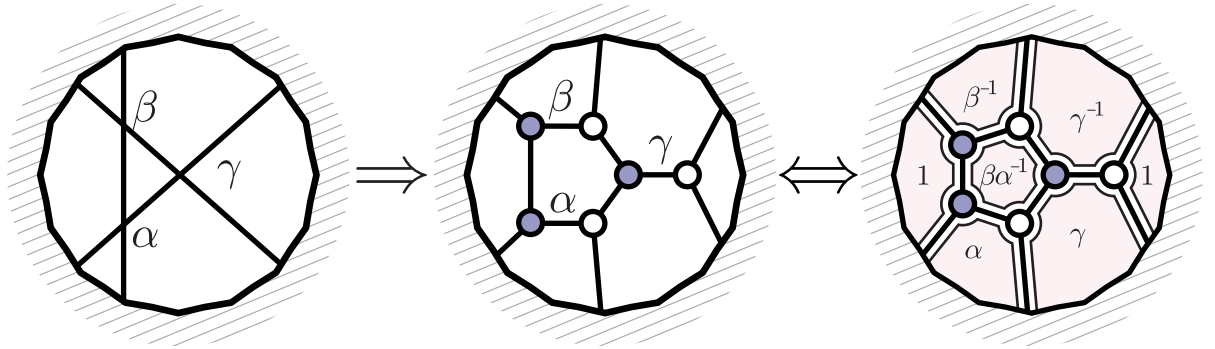


$$\Leftrightarrow C = \left(\begin{array}{cc|cc} 1 & 0 & -\alpha & -1 \\ 0 & 1 & -1 & 0 \end{array} \right) \equiv (1_{2 \times 2} | R_{12}), \quad (3.12.231)$$

where we have given the point in the Grassmannian C obtained using edge variables and the perfect-orientation indicated in the figure (see section V.), from which we can read-off the $2 \rightarrow 2$ “scattering-matrix” which we have denoted R_{12} . In general, blowing-up each 4-particle vertex allows us to translate any $(1+1)$ -scattering diagram into a trivalent, on-shell diagram from which we can identify an $(n \times n)$ scattering-matrix in the same way—identifying the point C in the Grassmannian in the gauge-fixed form,

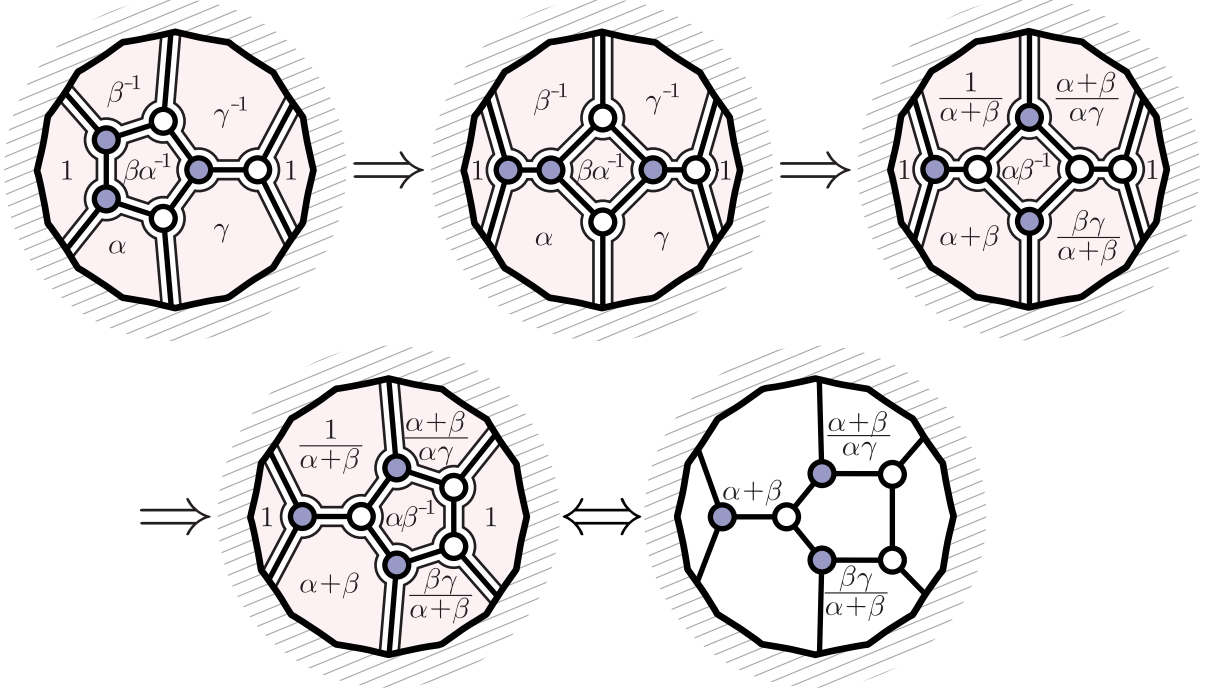
$$C_{n \times 2n} = (1_{n \times n} | R_{n \times n}) \quad (3.12.232)$$

As an example, let us look at the familiar configuration,

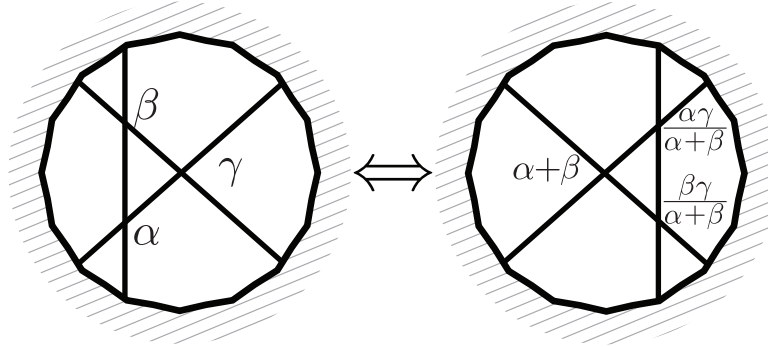


where on the right, we have recast the edge-variables into corresponding face-variables. Notice that because we are only putting non-trivial edge-weights on the “bridges” in the diagram, there are relations between the face variables.

Now, quite beautifully, we can see that the Yang-Baxter relation follows as a consequence of the more elementary actions of the merge- and square-moves! We can see this explicitly through the following sequence of moves, observing the effects induced on the face variables (see section VI.):



From this, we may conclude that,



This equivalence can be interpreted as a generalized Yang-Baxter relation for the R -matrices:

$$R_{12}(\beta)R_{13}(\gamma)R_{23}(\alpha) = R_{23}\left(\frac{\alpha\gamma}{\alpha+\beta}\right)R_{13}(\alpha+\beta)R_{12}\left(\frac{\beta\gamma}{\alpha+\beta}\right). \quad (3.12.233)$$

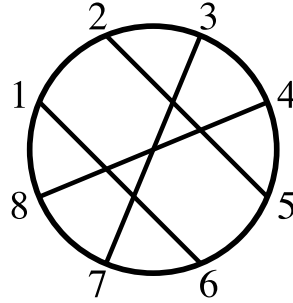
In particular, if we set $\alpha + \beta = \gamma$, we recover the familiar Yang-Baxter equation:

$$R_{12}(\beta)R_{13}(\alpha+\beta)R_{23}(\alpha) = R_{23}(\alpha)R_{13}(\alpha+\beta)R_{12}(\beta). \quad (3.12.234)$$

II. ABJM Theories

There is yet another natural way to associate a permutation with a scattering process. Suppose we have an even number, $2k$, of particle labels. We can divide them into two sets, A and B , of k elements each and draw arrows between them. Such a

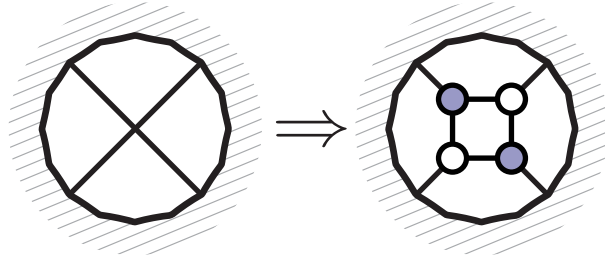
permutation takes some $a \rightarrow b$ and back via $b \rightarrow a$. We can then represent such a permutation graphically, with all labels on the boundary, as in the following:



| A | B |
|---|-------------------------|
| 1 | \longleftrightarrow 6 |
| 2 | \longleftrightarrow 5 |
| 3 | \longleftrightarrow 7 |
| 4 | \longleftrightarrow 8 |

(3.12.235)

We can then interpret this as an on-shell scattering process in a theory where each interaction is fundamentally a 4-particle vertex; and we can “blow-up” each four-particle vertex into an element of $G(2, 4)$, preserving the symmetrical nature of the permutation according to:


(3.12.236)

This structure was also recently considered in [45]. As in the (1+1)-dimensional example, it is natural to try and associated each vertex with a single degree of freedom. Unlike the (1+1)-dimensional example, however, this restriction should keep us within the top cell of $G(2, 4)$. A very simple way of doing this would be to impose the restriction that the 2-plane is *null*; that is,

$$C \cdot C = 0. \tag{3.12.237}$$

Notice that because the constraint $C \cdot C = 0$ is *symmetric*, it represents $k(k+1)/2$ constraints in general; for $C \in G(2, 4)$, this imposes only *three* constraints, leaving us with a single degree of freedom. In a canonical-gauge, we can write:

$$C = \left(\begin{array}{cc|cc} 1 & 0 & is & -ic \\ 0 & 1 & ic & is \end{array} \right), \tag{3.12.238}$$

where $c \equiv \cos(\theta)$ and $s \equiv \sin(\theta)$ for some angle θ .

Exactly this Grassmannian structure has been found to represent scattering amplitudes for the (2+1)-dimensional ABJM theory, [158–161]. As in (3+1) dimensions, we can motivate the appearance of the Grassmannian by first looking at the geometry

of external data. In (2+1) dimensions, the momenta are grouped into a *symmetric* (2×2) -matrix according to,

$$p^{\alpha\beta} = \begin{pmatrix} p^0 + p^2 & p^1 \\ p^1 & p^0 - p^2 \end{pmatrix}, \quad (3.12.239)$$

so that null momenta are given by,

$$p_a^{\alpha\beta} = \lambda_a^\alpha \lambda_a^\beta, \quad (3.12.240)$$

without any need for conjugate $\tilde{\lambda}$'s. The Lorentz group acts as a single copy of $SL(2)$, so the λ_a are still represented by a 2-plane in n dimensions. However, momentum-conservation,

$$\sum \lambda_a^\alpha \lambda_a^\beta = 0, \quad (3.12.241)$$

is now the statement that the λ plane is orthogonal to itself. Thus, the external data is given not by a general point in $G(2, n)$, but by a point in the *null* Grassmannian of 2-planes in n dimensions. It is therefore not surprising to find the null Grassmannian playing a role in ABJM theory.

ABJM theories have $\mathcal{N} = 6$ supersymmetries; if we diagonalize half of the supercharges, then the corresponding Grassmann coherent states are labeled by η^I for $I = 1, \dots, 3$. Thus, the on-shell data can be collected into,

$$\Lambda_a = \begin{pmatrix} \lambda_a \\ \eta_a \end{pmatrix}. \quad (3.12.242)$$

The ABJM amplitudes are not cyclically-invariant, but *are* invariant under a cyclic shift by *two*. Notice that since we only have λ 's, there is not the same little group rescaling symmetry as we had in three dimensions; rather, we have only the symmetry of sending $\lambda_a \rightarrow -\lambda_a$, under which on-shell differential forms transform according to $f(-\Lambda_a) = (-1)^a f(\Lambda_a)$.

Let us now return to the basic 4-point vertex, and determine the natural measure on the space of null 2-planes in 4 dimensions. This space is easily seen to be equivalent to $G(1, 2) \simeq \mathbb{P}^1$: the two rows of a (2×4) -matrix can be viewed as four-vectors p_1, p_2 which are null and mutually orthogonal; we can therefore write,

$$p_1 = \lambda \tilde{\lambda}_1, \quad p_2 = \lambda \tilde{\lambda}_2, \quad (3.12.243)$$

and use the $GL(2)$ -freedom to write $\tilde{\lambda}_1 \equiv (1, 0)$, $\tilde{\lambda}_2 \equiv (0, 1)$, and $\lambda \equiv (1, z)$. This demonstrates the equivalence of the null Grassmannian $C \subset G(2, 4)$ with \mathbb{P}^1 , and also

provides us with a natural measure: $d\log(z)$. Using this identification, we can write the null-plane $C \subset G(2, 4)$ in terms of z according to:

$$\begin{pmatrix} -i & -iz & z & 1 \\ -z & 1 & -i & iz \end{pmatrix}. \quad (3.12.244)$$

Performing a $GL(2)$ -transformation to recast this matrix-representative of C in a canonical-gauge brings it to the form given above in (3.12.238), with the identification:

$$s = \frac{2z}{z^2 + 1}, \quad \text{and} \quad c = \frac{z^2 - 1}{z^2 + 1}. \quad (3.12.245)$$

In terms of the natural measure $d\log(z)$ on the null subspace, the fundamental 4-point interaction in the ABJM theory can then be represented by,

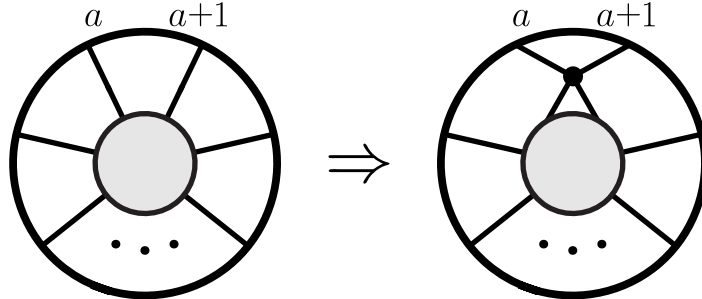
$$\mathcal{A}_4 = \int \frac{dz}{z} \delta^{4|6}(C(z) \cdot \Lambda); \quad (3.12.246)$$

equivalently, we may view this as having been obtained from a measure defined on all of $G(2, 4)$, but restricted to the null subspace by the constraint $\delta^3(C \cdot C)$:

$$\mathcal{A}_4 = \int \frac{d^{2 \times 4} C}{\text{vol}(GL(2))} \frac{1}{(12)(23)} \delta^3(C \cdot C) \delta^{4|6}(C \cdot \Lambda). \quad (3.12.247)$$

With this, we can define on-shell diagrams for the ABJM theory just as for $\mathcal{N} = 4$ by gluing together these basic 4-point vertices. Note that unlike for $\mathcal{N} = 4$, n and k are not independent for ABJM: we always have $n = 2k$.

It is easy to see that the on-shell representation of a BCFW shift is simply,

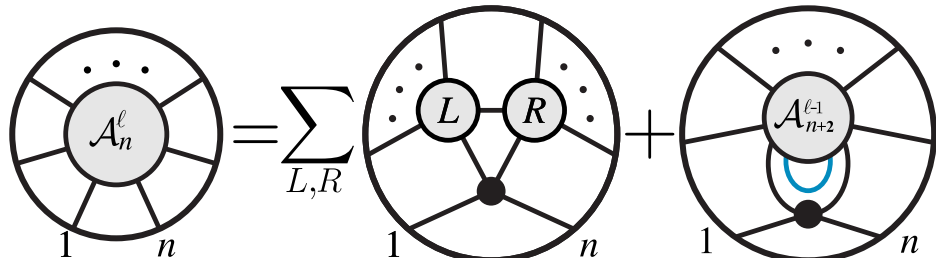


$$(3.12.248)$$

The action on the column-vectors is simply a rotation between c_a and c_{a+1} :

$$c_a \mapsto c c_a - s c_{a+1}, \quad c_{a+1} \mapsto s c_a + c c_{a+1}. \quad (3.12.249)$$

And the all-loop integrand can be given in terms of on-shell diagrams just as before:



$$(3.12.250)$$

(For recent computations at one and two loops see [162–165])

The rules for amalgamation are essentially identical to the $\mathcal{N} = 4$ case—the only difference being some factors of i that must be included. In (2+1) dimensions, because we write momenta as $p_a = \lambda_a \lambda_a$, switching $p_a \mapsto -p_a$ corresponds to taking $\lambda_a \mapsto i\lambda$. And so, when identifying two legs for the “projection” operation, instead of projecting relative to $(c_A - c_B)$, we must project relative to $(c_A - ic_B)$. The result is that minors of $C \in G(k, n)$ are related to those of the pre-image $\widehat{C} \in G(k+1, n+2)$ via:

$$(a_1 \cdots a_k)|_C = (Aa_1 \cdots a_k)|_{\widehat{C}} + i(Ba_1 \cdots a_k)|_{\widehat{C}}. \quad (3.12.251)$$

It is very easy to see that, starting with elementary 4-point vertices in the null Grassmannian, amalgamation preserves this property; translated in terms of minors, this is the statement that for all a ,

$$(c_1 \cdots c_{k-1}a)(d_1 \cdots d_{k-1}a) = 0. \quad (3.12.252)$$

This is trivial for the direct product. For projection, we easily verify that

$$\begin{aligned} (c_1 \cdots c_{k-1}a)(d_1 \cdots d_{k-1}a) &= [(Ac_1 \cdots c_{k-1}a) + i(Bc_1 \cdots c_{k-1}a)][(Ad_1 \cdots d_{k-1}a) + i(Bd_1 \cdots d_{k-1}a)] \\ &= (Ac_1 \cdots c_{k-1}B)(Ad_1 \cdots d_{k-1}B) - (Bc_1 \cdots c_{k-1}A)(Ad_1 \cdots d_{k-1}B) \\ &= 0. \end{aligned}$$

Thus, amalgamation of many little null $G(2, 4)$'s produces a point in the null Grassmannian $G(k, 2k)$, together with the measure,

$$\prod_{\text{vertices } v} d\log(z_v). \quad (3.12.253)$$

Notice that an important difference between this and the case of $\mathcal{N} = 4$ is that the fundamental variables are associated with the *vertices* of an on-shell graph, rather than its faces.

The measure on the top-cell can be given in terms of the C matrix via [159]

$$\frac{d^{k \times 2k} C}{\text{vol}(GL(k))} \frac{\delta^{k(k+1)/2}(C \cdot C)}{(1 \ 2 \cdots k) \cdots (k \ k+1 \cdots 2k-1)}. \quad (3.12.254)$$

It is also straightforward to find the analog of boundary measurements by summing over all the paths joining sources to sinks in a perfectly oriented graphs. We can orient each vertex with two incoming and two outgoing lines. Traversing any internal line contributes a factor of i , and at each vertex we get a is , ic or $-ic$ according to:

$$(3.12.255)$$

As an example, consider the following on-shell diagram involving 6 particles,

$$(3.12.256)$$

We find that this diagram is associated with a configuration C in the Grassmannian represented by,

$$C = -i \left(\begin{array}{ccc|ccc} i & 0 & 0 & s_\alpha s_\beta & s_\alpha c_\beta c_\gamma + c_\alpha s_\gamma & c_\alpha c_\gamma - s_\alpha c_\beta s_\gamma \\ 0 & i & 0 & -c_\alpha s_\beta & s_\alpha s_\gamma - c_\alpha c_\beta c_\gamma & s_\alpha c_\gamma + c_\alpha c_\beta s_\gamma \\ 0 & 0 & i & c_\beta & -s_\beta c_\gamma & s_\beta s_\gamma \end{array} \right). \quad (3.12.257)$$

In general, we can write the $(k \times 2k)$ -matrix representative $C \in G(k, 2k)$ associated with any such graph in the form,

$$C = -i (i1_{k \times k} | R_{k \times k}), \quad (3.12.258)$$

where R is an $SO(k)$ -rotation matrix. This gives us a pretty interpretation for amalgamation. The basic 4-point vertex is just a rotation in two dimensions. Amalgamation provides a way of building general rotations in higher dimensions by a composing many rotations in two-dimensional subspaces. The example above for 6 particles corresponds to a canonical way of representing three-dimensional rotations using Euler angles. The analog of the square move in ABJM looks much like the Yang-Baxter move, and represents the equality of two different Euler-angle representations of the same three-dimensional rotation.

Just as with $\mathcal{N}=4$ SYM, the invariant content of any reduced on-shell diagram is read-off from its associated permutation. We also have an analog of reduction, looking at the 4-point bubble diagram connecting two 4-particle vertices with parameters α and β :

$$(3.12.259)$$

Finally, we can take a boundary, lowering the dimension by one, by deleting a vertex, and re-connecting the lines according to:

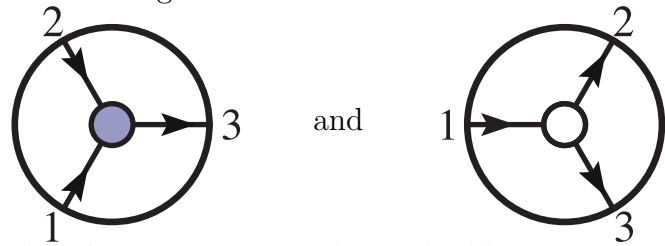
Diagrammatic equation (3.12.260) showing the decomposition of a sphere with a cross into two spheres with different internal structures. The left side shows a sphere with a cross (two intersecting diagonal lines) inside, surrounded by a hatched circular region. An arrow with a double underline and a script 'd' above it points to the right. The right side shows the sum of two spheres, each surrounded by a hatched circular region. The first sphere on the right has two curved lines inside, and the second sphere has two curved lines that meet at a central point.

$$\text{Sphere with cross} \xrightarrow{\mathcal{D}} \text{Sphere with two curves} + \text{Sphere with two curves meeting at center} \quad (3.12.260)$$

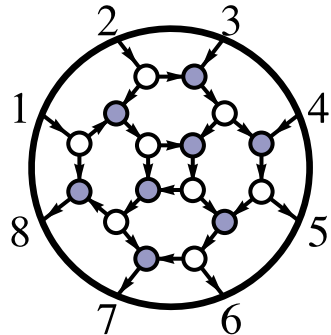
3.13 On-Shell Diagrams with $\mathcal{N} < 4$ Supersymmetries

On-shell diagrams can be defined for any theory with fundamental trivalent vertices, and in particular for gauge theories with any number, \mathcal{N} , of supersymmetries. There is obviously a rich structure to be unearthed here; in this short section we will content ourselves with setting-up some of the basic formalism and highlighting the central new mathematical object that makes an appearance—reflecting the physics of ultraviolet singularities which are present in theories with less supersymmetry.

Let us begin our discussion by focusing on non-supersymmetric theories, those of “ $\mathcal{N}=0$ ”. It is useful to represent the helicities involved in each basic 3-particle vertex by giving each of the edges an orientation:


(3.13.261)

We can then glue these vertices together to build-up more complex on-shell diagrams as before—leading to, for example:


(3.13.262)

In such decorated on-shell diagrams, the arrows are useful because they automatically encode the helicities of the internal particles involved. In general, we consider the particles as Grassmann coherent states labeled by $\tilde{\eta}^I$ for $I = 1, \dots, \mathcal{N}$. In theories with $\mathcal{N} < 4$ supersymmetry, we have “+” and “−” multiplets, which include gluons of helicity ± 1 as their top components, respectively; thus, on-shell diagrams must be labeled in exactly the same way for any $\mathcal{N} < 4$.

The Grassmannian formalism is just as powerful in integrating over the phase space of the internal particles regardless of the amount of supersymmetry. However,

when $\mathcal{N} < 4$, the diagrams really are fundamentally oriented, whereas for $\mathcal{N} = 4$ such an orientation merely encodes a convenient translation of the on-shell diagram into a particular gauge-fixed matrix-representative $C \in G(k, n)$. If the k incoming “source” indices are from a set A and the $(n - k)$ outgoing “sink” indices are from a , we find exactly the same linear relation between the external kinematical data:

$$\prod_A \delta^2(\tilde{\lambda}_A - c_{Aa} \tilde{\lambda}_a) \prod_A \delta^{\mathcal{N}}(\tilde{\eta}_A - c_{Aa} \tilde{\eta}_a) \prod_a \delta^2(\lambda_a + c_{Aa} \lambda_A), \quad (3.13.263)$$

where the c_{Aa} are exactly as in equation (3.4.100), which we reproduce below:

$$c_{Aa} = - \sum_{\Gamma \in \{A \rightsquigarrow a\}} \prod_{e \in \Gamma} \alpha_e. \quad (3.13.264)$$

The only difference between general \mathcal{N} and $\mathcal{N} = 4$ is the measure on the Grassmannian which ultimately encodes the on-shell differential form in terms of the auxiliary, Grassmannian degrees of freedom. For $\mathcal{N} = 4$, we didn’t have to include any Jacobian resulting from the elimination of internal variables, because the fermionic δ -functions always canceled the contributions between the internal bosons and internal fermions. However, when $\mathcal{N} < 4$, these two factors do not cancel, and leave a net Jacobian contribution to the measure which we may write as:

$$\left(\prod_{\text{vertices } v} \frac{1}{\text{vol}(GL(1)_v)} \right) \left(\prod_{\text{edges } e} \frac{d\alpha_e}{\alpha_e} \right) \times \mathcal{J}^{\mathcal{N}-4}. \quad (3.13.265)$$

If the vertices of the graph are labeled i, j , then we define the *adjacency matrix* A_{ij} of the graph by,

$$A_{ij} = \text{the weight of the directed edge } i \rightarrow j \text{ (if any);} \quad (3.13.266)$$

then the Jacobian \mathcal{J} is given by

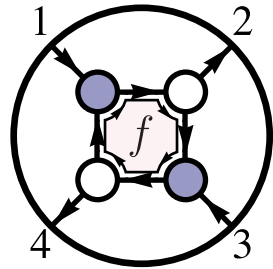
$$\mathcal{J} = \det(1 - A). \quad (3.13.267)$$

We know that the edge variables can only occur in the $GL(1)$ gauge-invariant “flux” combinations associated with faces, and we can give a simple formula for \mathcal{J} in terms of these face variables. In general, if we have a collection of closed, *orientated* loops bounding faces f_i , with *disjoint* pairs (f_i, f_j) , *disjoint* triples (f_i, f_j, f_k) , and so on, then \mathcal{J} is given by:

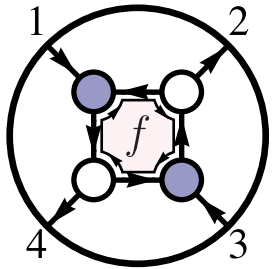
$$\mathcal{J} = 1 + \sum_{\text{faces}} f_i + \sum_{\substack{\text{disjoint} \\ \text{pairs } i,j}} f_i f_j + \sum_{\substack{\text{disjoint} \\ \text{triples } i,j,k}} f_i f_j f_k + \dots \quad (3.13.268)$$

For any oriented graph without any closed, oriented loops, the spectrum is trivial, and $\mathcal{J} = 1$; for any such oriented on-shell diagram, the maximally-supersymmetric and non-supersymmetric on-shell forms are identical. This is easy to understand because when an on-shell diagram is free of such oriented loops, only gluons propagate internally. In contrast, when there are oriented loops, the rest of the super-multiplet *can* propagate internally, differentiating theories with different amounts of supersymmetry.

When an oriented on-shell diagram has closed, oriented loops, the Jacobian is nontrivial. The simplest example occurs for four particles, where we can have,



A



B

(3.13.269)

for which the corresponding Jacobian is,

$$\mathcal{J}_A = 1 + f \quad \text{and} \quad \mathcal{J}_B = 1 + f^{-1}. \quad (3.13.270)$$

In order to compute the full on-shell process for fixed external sources and sinks, we have to sum-over all the possible orientations of the internal graph. And so, in this case we would be obliged to sum-over both diagrams, giving us a final contribution to the measure of:

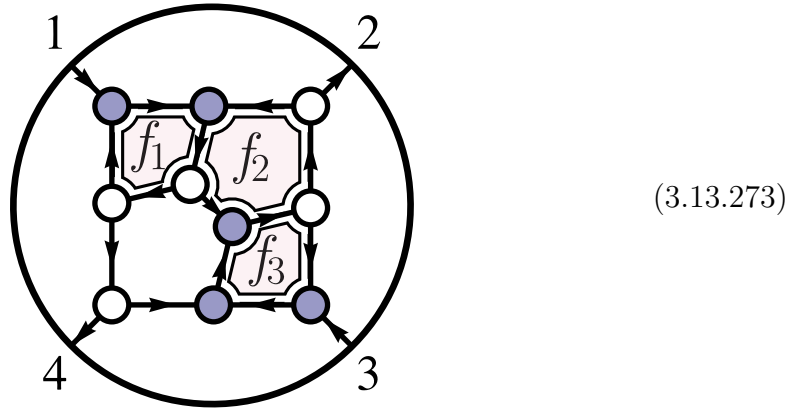
$$\mathcal{J}_A^{\mathcal{N}-4} + \mathcal{J}_B^{\mathcal{N}-4} = (1 + f)^{\mathcal{N}-4} + (1 + f^{-1})^{\mathcal{N}-4}. \quad (3.13.271)$$

Notice that when $\mathcal{N} = 3$, the complete contribution is simply:

$$\mathcal{J}_A^{-1} + \mathcal{J}_B^{-1} = (1 + f)^{-1} + (1 + f^{-1})^{-1} = 1. \quad (3.13.272)$$

This is good, because the “+” and “−” super-multiplets of $\mathcal{N} = 3$ combine to give us a complete $\mathcal{N} = 4$ super-multiplet. Of course, when $\mathcal{N} < 3$, the sum is not unity, and the result differs from what we would have found for $\mathcal{N} = 4$.

Let us consider a somewhat more interesting example:



$$(3.13.273)$$

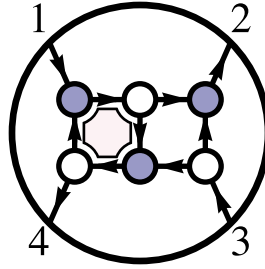
Here we have three faces bounding closed orientated paths, f_1, f_2, f_3 , but two of the faces f_1, f_3 are disjoint; and the complete Jacobian is:

$$\mathcal{J} = 1 + (f_1 + f_2 + f_3) + f_1 f_3. \quad (3.13.274)$$

We stress again that the point in the Grassmannian obtained from amalgamation is the same as it is for the maximally supersymmetric theory; the *only* difference between the theories is the presence of the Jacobian factor \mathcal{J} in the measure. The merge/un-merge moves still leaves the point in the Grassmannian and the rest of the form invariant; but now, the square-move and bubble-reduction—while leaving the point in the Grassmannian fixed—*can* change the measure.

If we consider a reduced graph with the dimension required to completely localize all the auxiliary variables associated with the matrix $C \in G(k, n)$, then the net effect is not particularly interesting—as theories with $\mathcal{N} < 4$ differ from those with maximal supersymmetry only by the prefactor of \mathcal{J} in the measure, evaluated at this particular point in $G(k, n)$. However, the situation is considerably more interesting when we consider on-shell graphs for which some auxiliary variables are not fixed by the δ -function constraints, leaving us with an integration measure over these internal degrees of freedom. Such graphs occur, for instance, in the forward-limits that generate loop integrands in the all-loop, on-shell BCFW recursion (3.2.21). In such cases, the factor of \mathcal{J} can lead to a qualitatively-new set of singularities where poles are generated by \mathcal{J} .

As a simple example of such a situation, consider a “wrong” BCFW-bridge acting on the four-particle tree amplitude’s on-shell graph:



(3.13.275)

The shift is “wrong” in the familiar sense of BCFW deforming the “wrong” helicities, for which the deformed amplitudes don’t vanish at infinity. This is reflected in the on-shell graph by the presence of a closed oriented loop (making the resulting on-shell differential form differ for theories with different amounts of supersymmetry). Because this graph’s measure includes the a non-trivial Jacobian \mathcal{J} , the corresponding function does not vanish in the deep ultraviolet—taking the shift-parameter $\alpha \rightarrow \infty$. This “pole at infinity” is characterized by the residue about $\mathcal{J} \mapsto 0$. Notice that this allows us to fully characterize the non-trivial, ultraviolet singularities present in theories with less than maximal supersymmetry. The presence of such poles indicate “lower-transcendentality” contributions to scattering amplitudes. For instance, the object above, (3.13.275) can be interpreted as the triple-cut of the one-loop four-particle amplitude, and the residue about $\mathcal{J} = 0$ computes the coefficient of the “triangle integral” for the amplitude. The coefficients of “bubbles” can be exposed in similar ways.

One of the most fundamental consequences of space-time locality is that the ultraviolet and infrared singularities are completely independent. It is fascinating to see that this physical fact is sharply captured by the Grassmannian formalism, where IR and UV singularities are associated with disparate contributions to the integration measure of the auxiliary Grassmannian: the positroid’s “ $d\log$ ” measure captures all the long-distance singularities—where internal particles go on-shell—and the prefactor \mathcal{J} captures ultraviolet singularities. This ultraviolet/infrared decoupling has an even more striking incarnation in the planar sector of the theory: it can be shown that \mathcal{J} is completely regular everywhere in the positive-part of $G(k, n)$ —literally *separating* the ultraviolet singularities of \mathcal{J} from infrared singularities of the positroid, their boundaries being completely disjoint!

3.14 On-Shell Representations of Scattering Amplitudes

Although we have focused on understanding individual on-shell diagrams for most of the chapter, let us return to a study of how these can combine to entire scattering amplitudes. As discussed in section 3.2, the defining property of the full amplitude is that it satisfies the “differential equation”,

$$\partial \left[\text{Diagram of } \mathcal{A}_n^\ell \right] = \sum_{L,R} \text{Diagram of } L \text{ and } R \text{ connected by a red line} + \sum_a \text{Diagram of } \mathcal{A}_{n+2}^{\ell-1} \text{ with a blue loop} \quad (3.14.276)$$

which specifies the two kinds of singularities it can have—corresponding to “factorization channels” (red) and “forward limits” (blue), respectively. All known representations of scattering amplitudes can be thought of as particular ways of building objects with these—and *only* these—(co-dimension one) singularities.

The usual Feynman-diagrammatic expansion for scattering amplitudes makes these singularities (together with conformal invariance) manifest, but at the cost of introducing unphysical, off-shell variables and gauge-redundancies which obscure the underlying Yangian-invariance of the theory. (The same can be said for the equivalent Wilson-loop representation—except that it is the *dual* conformal symmetry which is made manifest.) By contrast, the BCFW recursion relations,

$$\text{Diagram of } \mathcal{A}_n^{(k),\ell} = \sum_{\substack{\ell_L + \ell_R = \ell \\ k_L + k_R = k+1 \\ n_L + n_R = n+2}} \text{Diagram of } \mathcal{A}_{n_L}^{(k_L),\ell_L} \text{ and } \mathcal{A}_{n_R}^{(k_R),\ell_R} \text{ connected by a red line} + \text{Diagram of } \mathcal{A}_{n+2}^{(k+1),\ell-1} \text{ with a blue loop} \quad (3.14.277)$$

can be understood of as a *direct* integration of the defining equation (3.14.276), and provides us with a representation of scattering amplitudes for which *every term* enjoys the full Yangian-invariance of the theory. However, the recursion requires that two legs be singled-out to play a special role—in (3.14.277), these are the legs $(n\ 1)$. Although this choice is arbitrary, it breaks the cyclic-symmetry of the complete amplitude, and makes manifest only a rather small subset of the singularities required by (3.14.276).

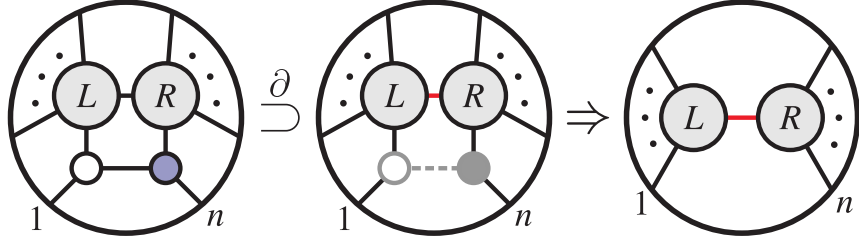
Of course, the BCFW recursion relations can be derived from field theory, starting either with the “scattering amplitude” [65] or “Wilson loop” [79, 166, 167] pictures (for the relation to light-like correlation functions, see [114, 115, 168–170]). We will however begin by showing how they can also be proven directly by induction. That is, we will show that the boundary of (3.14.277) includes *precisely* the singularities required by (3.14.276); this proof will be entirely *diagrammatic*. In section II. we will review some important features encountered in the tree-level ($\ell = 0$) version of the recursion relations, and in section III. we will see how the structure of tree amplitudes is reflected at loop-level, giving rise to a canonical—purely ‘dlog’—form for all loop-integrands.

I. (Diagrammatic) Proof of the BCFW Recursion Relations

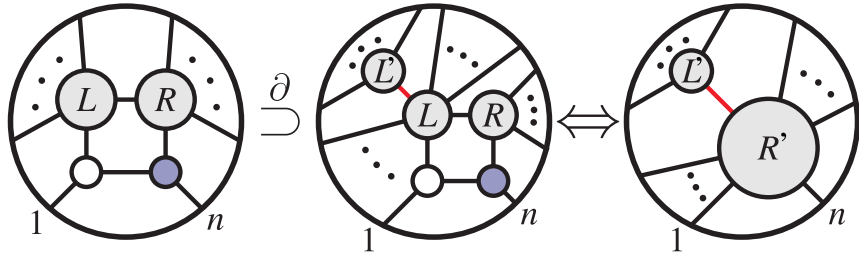
Let us take the BCFW recursion relations, (3.14.277) as an ansatz, and demonstrate inductively that its boundary includes *all* the correct factorization channels and forward limits, and no other singularities (for earlier work along these lines see [171, 172]). Recall that the four-point, tree-amplitude, $\mathcal{A}_4^{(2), \ell=0}$, manifestly has all the correct factorization channels in its boundary,

We may therefore suppose that the ansatz is correct for all amplitudes $\mathcal{A}_n^{(\hat{k}), \hat{\ell}}$ with $\hat{n} < n$, $\hat{k} \leq k$, and $\hat{\ell} \leq \ell$; we must show that this suffices to prove that it also holds for $\mathcal{A}_n^{(k), \ell}$. We may divide the argument into two parts: first, demonstrating that the boundary includes all the correct factorization channels; and then showing that it includes all the correct forward-limits.

Among the factorization channels, those for which particles 1 and n are on opposite sides are trivially present:

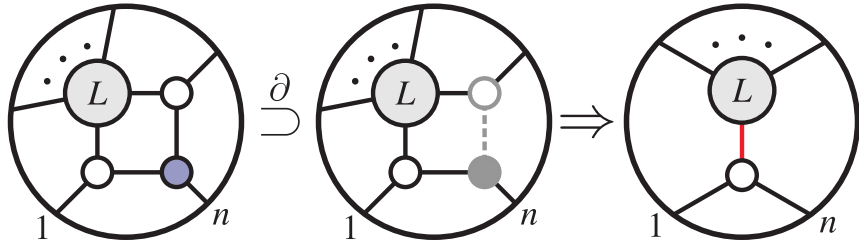


What we first need to check is that the BCFW recursion formula also generates all those factorizations for which 1 and n are on the same side. Factorization channels for which legs 1 and n are not alone on one side arise from the factorizations of the bridged amplitudes. For example, the boundaries of the left-amplitudes include:

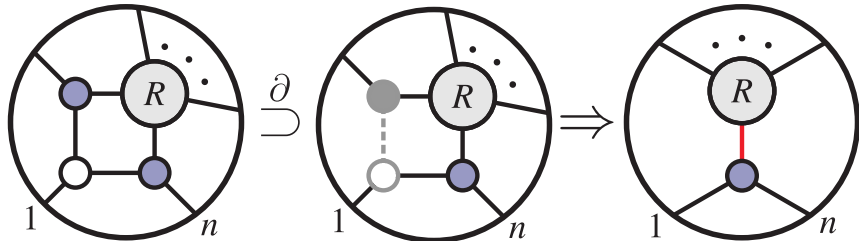


where we have used our induction hypothesis to identify the terms appearing on the right-side of the factorization as a lower-point amplitude denoted R' . We also have the analogous diagrams arising from the right-amplitudes.

The case of a two-particle factorization involving *just* 1 and n together, however, arises somewhat differently. The factorization for which particles 1 and n are connected via a $\mathcal{A}_3^{(1)}$ -vertex arises from the boundary,

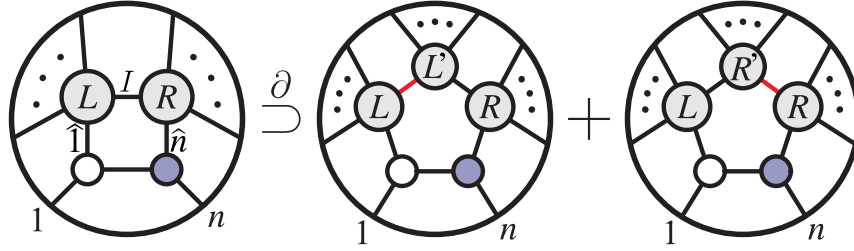


Similarly, the case where particles 1 and n are connected via a $\mathcal{A}_3^{(2)}$ -vertex arises from,



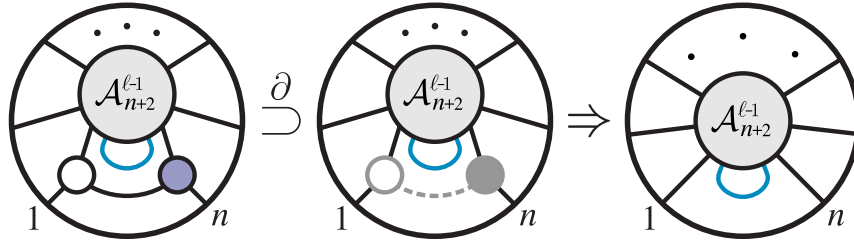
We have therefore shown that all factorization channels are present in the boundary of the BCFW ansatz. However, we must also show that these are the *only* such

boundaries. Our induction hypothesis would suggest that such ‘spurious’ poles could arise from factorizations of separating $(\hat{1}I)$ on the left, or $(I\hat{n})$ on the right:

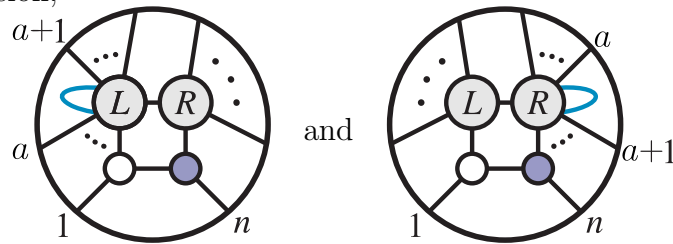


Conveniently, such boundaries are *always* generated symmetrically from the left- and right-amplitudes, and cancel in the sum.

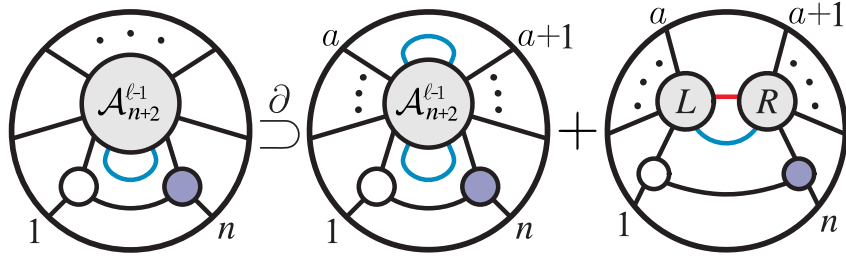
Let us now demonstrate that the BCFW recursion ansatz generates all the correct forward-limits as co-dimension one boundaries—and *only* these. As with the factorization channels, the BCFW recursion ansatz always makes one of the forward-limits manifest—those where the forward limit is taken between 1 and n :



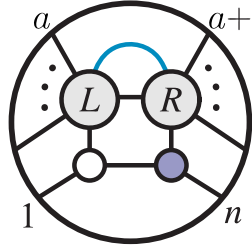
When the identified legs are not between $(n1)$, but say $(aa+1)$, something more interesting happens. Some of these arise trivially from the boundary of ‘bridged’ terms in the recursion,



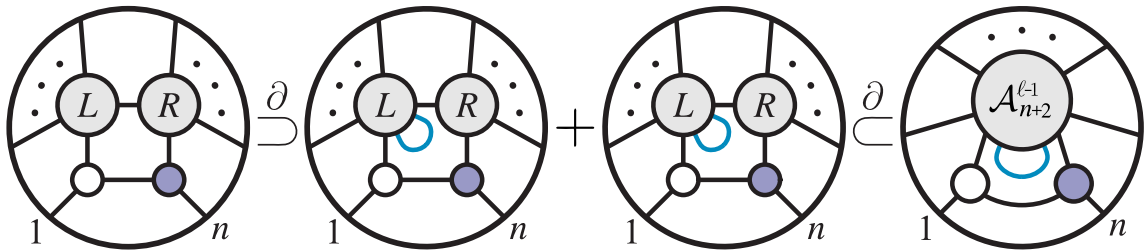
but these terms alone do not represent the complete BCFW-representation of the lower-loop, higher-point amplitude including the identified legs: the problem is that we are missing both the terms where the identified legs (before the forward-limit) are separated across the BCFW-bridge, and also the terms for which they are identified in the ‘forward-limit’ term. By our induction hypothesis, both of these terms arise from the boundary of the forward-limit term: as factorization and forward-limit boundaries of the forward-limit term, respectively:



The first of these is needed by ‘forward-limit’ term in the BCFW recursion ansatz, and the second term is needed to complete the ‘bridge’ term of the recursion ansatz; to see this more clearly, notice that the second term can be redrawn more suggestively:



And so, we have shown that the induction hypothesis ensures that all the necessary forward-limit terms are generated in the boundary of the BCFW recursion formula. But as with the factorization-channels studied earlier, we must show that no ‘spurious’ forward-limit terms are generated. Such spurious forward-limit terms can be generated by the ‘bridge’ term in the recursion—when the identified legs appear either between $(\hat{1} I)$ on the left, or between $(I \hat{n})$ on the right—or from the factorization-channels of the ‘forward-limit’ term; these are always generated in pairs, and cancel accordingly; for example,



II. The Structure of (Tree-)Amplitudes in the Grassmannian

The BCFW recursion relations provide us with a powerful description of scattering amplitudes to all-loop orders. Although the tree-level recursion relations have been largely understood for nearly a decade (see e.g. [10, 14, 82, 100, 171]), its extension to all-loop integrands remains relatively novel—and until now, has only been understood in terms of momentum-twistor variables (as described in [65]). Because of this novelty, it is worthwhile to explore some of the features of the recursion and the structures that emerge. In this subsection, we will mostly review aspects of tree-amplitudes that are well known to most practitioners; this will provide us with the background necessary to discuss some of the novelties that arise loop-level in section III.

When restricted to tree-level, the recursion relations (3.14.277) become,

$$\begin{aligned}
 & \text{Circle with } n \text{ legs } 1, \dots, n \text{ and central shaded region } \mathcal{A}_n^{(k)} \\
 &= \text{Circle with bridge between legs } 1 \text{ and } n, \text{ shaded region } \mathcal{A}_{n-1}^{(k-1)} \text{ on left} \\
 &+ \sum_{\substack{n_L, n_R \geq 4 \\ k_L + k_R = k+1 \\ n_L + n_R = n+2}} \text{Circle with bridge between legs } 1 \text{ and } n, \text{ shaded regions } \mathcal{A}_{n_L}^{(k_L)} \text{ and } \mathcal{A}_{n_R}^{(k_R)} \\
 &+ \text{Circle with bridge between legs } 1 \text{ and } n, \text{ shaded region } \mathcal{A}_{n-1}^{(k)} \text{ on left}
 \end{aligned}$$

Here, we have separated the terms in the recursion which involve a 3-particle amplitude on either side of the bridge; this is because one of the 3-particle amplitudes when bridged on either side will lead to an on-shell form with vanishing-support for generic kinematical data—for example, bridging $\mathcal{A}_3^{(1)}$ on the left would give,

$$\text{Circle with bridge between legs } 1 \text{ and } n, \text{ shaded region on left} \iff \text{Circle with bridge between legs } 1 \text{ and } n, \text{ shaded region on right}$$

which is only non-vanishing if $\lambda_1 \propto \lambda_2$. (Moreover, it turns out that these graphs are always reducible, and so have less than the necessary $(2n-4)$ independent degrees of freedom required to solve the kinematical constraints.)

Let us begin to build intuition about the structure that arises from the recursion by considering the simplest examples. Recall that the 4-particle amplitude is entirely given by the single on-shell graph, (3.2.15)—the familiar ‘box’,

$$\mathcal{A}_4^{(2)} = \mathcal{A}_3^{(2)} \otimes \mathcal{A}_3^{(1)} = \text{Diagram}$$

This of course follows trivially from the recursion relations. But it is not the only amplitude which is so simple: for example, the two 5-particle amplitudes are simply,

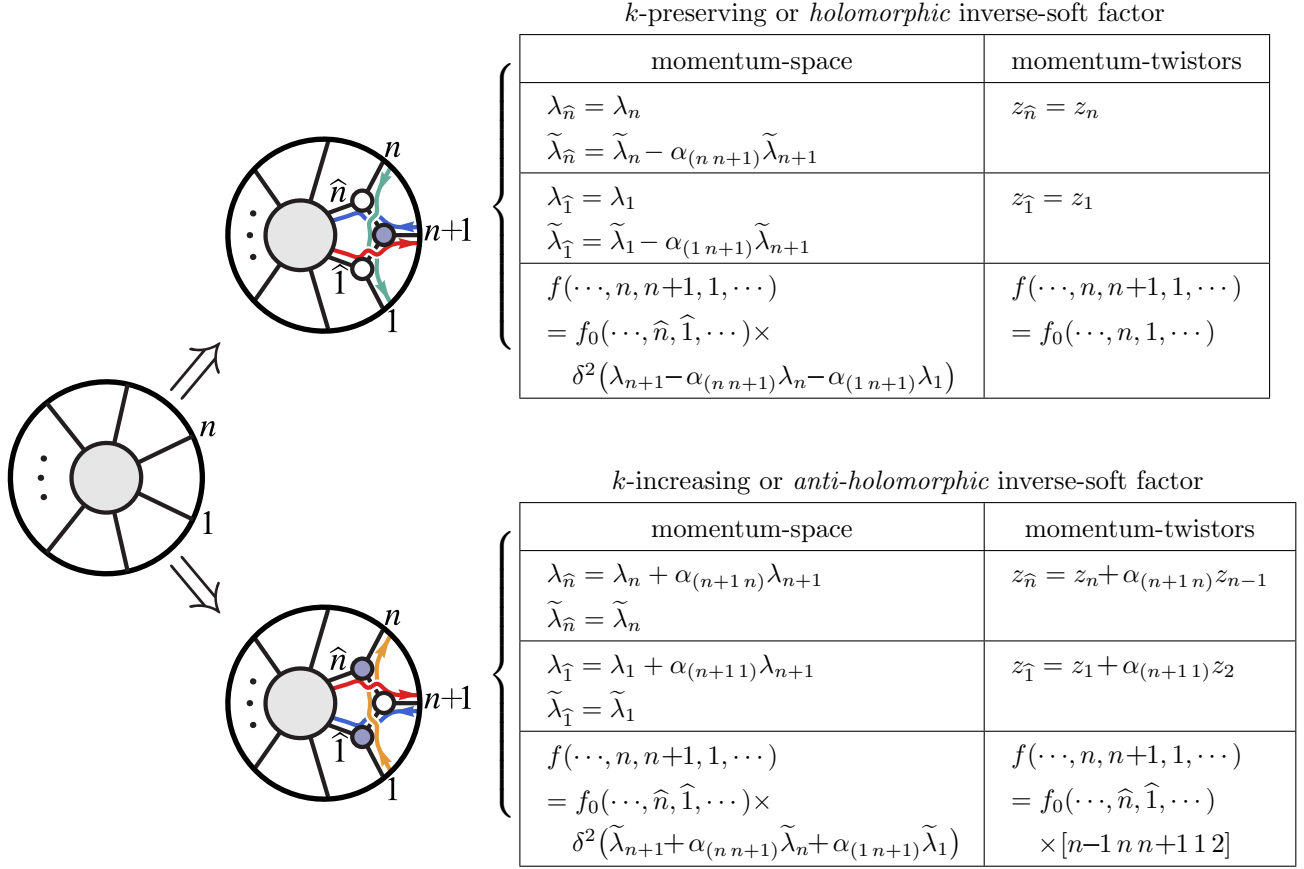
$$\mathcal{A}_5^{(2)} = \mathcal{A}_4^{(2)} \otimes \mathcal{A}_3^{(1)} = \text{Diagram} \quad \text{and} \quad \mathcal{A}_5^{(3)} = \mathcal{A}_3^{(2)} \otimes \mathcal{A}_4^{(2)} = \text{Diagram}$$

This trend continues for all MHV and $\overline{\text{MHV}}$ amplitudes, $\mathcal{A}_n^{(2)}$ and $\mathcal{A}_n^{(n-2)}$, respectively. For 6-particles, these amplitudes are:

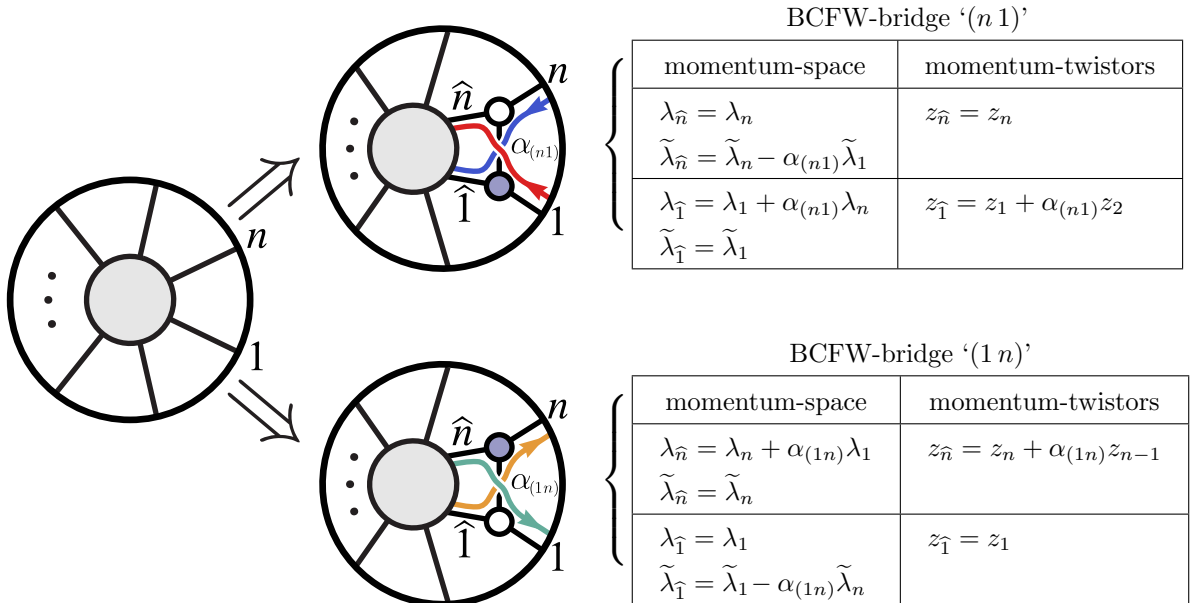
$$\mathcal{A}_6^{(2)} = \mathcal{A}_5^{(2)} \otimes \mathcal{A}_3^{(1)} = \text{Diagram} \quad \text{and} \quad \mathcal{A}_6^{(4)} = \mathcal{A}_3^{(2)} \otimes \mathcal{A}_5^{(3)} = \text{Diagram}$$

Thus, the BCFW-recursion *directly* represents all MHV (and $\overline{\text{MHV}}$) amplitudes as single terms—directly giving the famous formula guessed by Parke and Taylor, (3.8.180).

Although fairly trivial, notice that in obtaining these formulae, it is natural to view the act of attaching a 3-particle amplitude across the BCFW bridge as an operation which ‘adds a particle’. This operation is of course well-defined not just for the amplitude, but for any on-shell graph; thus, we have a way to add a particle in a way which ‘preserves k ’, $(\bullet \otimes \mathcal{A}_3^{(1)}) : G(k, n) \mapsto G(k, n+1)$, and in way which ‘increases k ’, $(\mathcal{A}_3^{(2)} \otimes \bullet) : G(k, n) \mapsto G(k+1, n+1)$. These are called ‘inverse-soft factors’. As a reference, these operations correspond to:



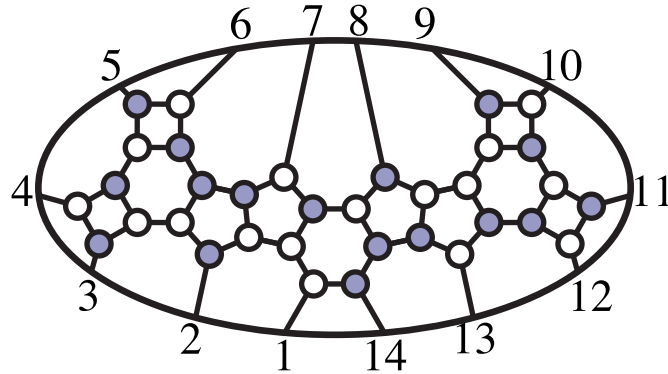
(Here, the $\tilde{\eta}$'s transform identically to the $\tilde{\lambda}$'s.) Each of these can be seen to follow from the action of two successive BCFW-bridges:



Notice that whenever an on-shell graph has a leg a such that $\sigma(a-1) = a+1$ or $\sigma(a+1) = a-1$ we can view it as having been obtained by adding particle a to a lower-point graph

using a k -preserving or k -increasing inverse soft-factor, respectively. In such cases, a is said to be an ‘inverse-soft factor’; and any on-shell graph which can be constructed by successively adding particles to a 3-particle amplitude using inverse-soft factors is said to be ‘inverse-soft *constructible*’.

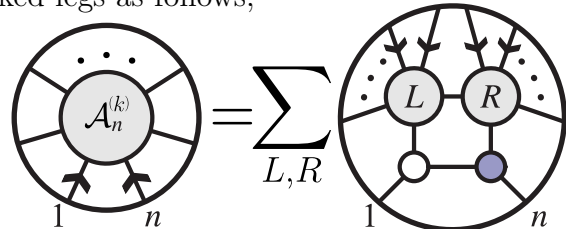
The notion of ‘inverse-soft constructibility’ proves useful because the auxiliary variables associated with any inverse-soft factor can be completely fixed by the associated δ -function constraint, making it very easy to recursively eliminate all the auxiliary, Grassmannian degrees of freedom. It turns out that for 13 or fewer legs, *all* on-shell forms generated by the tree-level recursion relations—*regardless* of how lower-point amplitudes are themselves recursed—are inverse-soft constructible. However, for 14 or more particles, some objects can be generated by the recursion relations which are *not* inverse-soft constructible, such as the following possible contribution to the 14-particle N^5 MHV tree-amplitude:



$$(3.14.278)$$

$$((\mathcal{A}_3^{(2)} \otimes (\mathcal{A}_4^{(2)} \otimes \mathcal{A}_4^{(2)})) \otimes \mathcal{A}_3^{(1)}) \otimes (\mathcal{A}_3^{(2)} \otimes ((\mathcal{A}_4^{(2)} \otimes \mathcal{A}_4^{(2)}) \otimes \mathcal{A}_3^{(1)}))$$

Notice that this graph was generated by always using *internal edges* to recurse the objects appearing across the BCFW-bridge— $(\hat{1} I)$ on the left and $(I \hat{n})$ on the right. (We should mention in passing that if one *always* recurses the lower-point amplitudes according to the marked legs as follows,



$$(3.14.279)$$

then *all* tree-amplitudes will be given in terms of only inverse-soft constructible graphs. This corresponds to the recursion ‘scheme’ $\{-2, 2, 0\}$ of reference [173].)

As described in section 3.11, the first amplitude which is given as the combination of several on-shell graphs is $\mathcal{A}_6^{(3)}$, the 6-particle NMHV tree-amplitude. This is given

by three terms, $\mathcal{A}_5^{(3)} \otimes \mathcal{A}_3^{(1)}$, $\mathcal{A}_4^{(2)} \otimes \mathcal{A}_4^{(2)}$, and $\mathcal{A}_3^{(2)} \otimes \mathcal{A}_5^{(2)}$:

$$\mathcal{A}_6^{(3)} = \begin{array}{c} \text{Diagram 1} \\ \{4, 5, 6, 8, 7, 9\} \end{array} + \begin{array}{c} \text{Diagram 2} \\ \{3, 5, 6, 7, 8, 10\} \end{array} + \begin{array}{c} \text{Diagram 3} \\ \{4, 6, 5, 7, 8, 9\} \end{array} \quad (3.14.280)$$

Although the on-shell graphs of each contribution appear quite different, it is easy to see from the permutations that they are all cyclically-related to one another:

$$\begin{array}{c} \text{Diagram 4} \\ \{3, 5, 6, 7, 8, 10\} \end{array} = \begin{array}{c} \text{Diagram 5} \\ \{3, 5, 6, 7, 8, 10\} \end{array} = \begin{array}{c} \text{Diagram 6} \\ \{3, 5, 6, 7, 8, 10\} \end{array} \quad (3.14.281)$$

The on-shell differential form drawn above—labeled by the permutation $\{3, 5, 6, 7, 8, 10\}$ —was given directly in terms of the kinematical variables $\lambda, \tilde{\lambda}$ in equation (3.8.183).

Because each term is cyclically-related, if we use ‘ r ’ to denote the operation that ‘rotates’ all particle labels forward by 1, we can write the entire tree-amplitude as:

$$\mathcal{A}_6^{(3)} = (1 + r^2 + r^4) \frac{\delta^{3 \times 4}(C^* \cdot \tilde{\eta}) \delta^{2 \times 2}(\lambda \cdot \tilde{\lambda})}{\langle 23 \rangle [56] (\langle 34 \rangle [64] + \langle 53 \rangle [56]) s_{456} (\langle 61 \rangle [64] + \langle 15 \rangle [45]) \langle 12 \rangle [45]} \quad (3.14.282)$$

where the matrix C^* was given in (3.8.182).

Although the precise set of on-shell graphs obtained using the BCFW recursion relations can vary considerably depending on which legs of the lower-point amplitudes are used for *their* recursion, the number of terms is of course scheme-independent. It is a relatively simple exercise to show that,

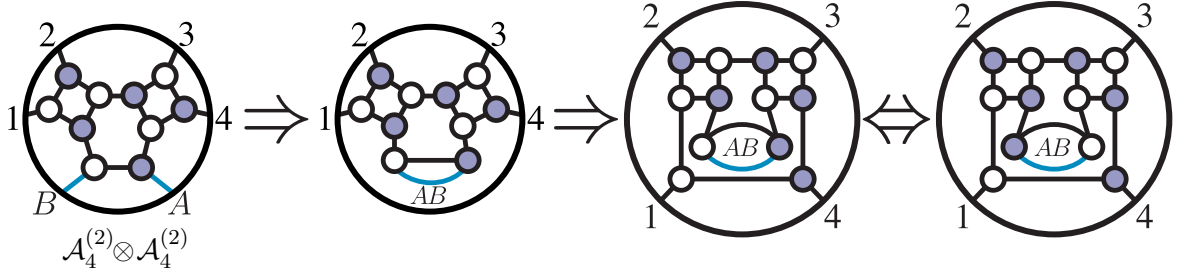
$$\# \text{ BCFW terms in the tree-amplitude } \mathcal{A}_n^{(k)}: \frac{1}{n-3} \binom{n-3}{k-1} \binom{n-3}{k-2}. \quad (3.14.283)$$

III. Canonical Coordinates for Loop Integrands

The all-loop generalization of the BCFW recursion relations was first described in [65] where it was formulated in terms of explicit operations acting directly on the ‘functions’ of momentum-twistor variables obtained after eliminating the auxiliary Grassmannian degrees of freedom. This led to formulae for the ‘loop integrands’ in the form of a ‘standard’ loop-integration measure $d^4\ell$ weighted by some rational function of the loop-momentum ℓ , or equivalently a function on the space of lines AB in momentum-twistor space with measure $d^4z_A d^4z_B/GL(2)$. When viewed as rational functions in this way, much of the underlying structure is hidden. However, by viewing each loop-momentum’s degrees of freedom as arising from canonical coordinates in the auxiliary Grassmannian, the integration measure is automatically generated in a much more illuminating, ‘canonical’ form: as a wedge-product of “ $d\log$ ” factors. The fact that loop amplitude integrands can be written in such a form—a fact which is essentially obvious using canonical coordinates on the Grassmannian—is far from obvious from any other method to compute scattering amplitudes.

We will postpone a systematic discussion of the loop amplitude integrands generated by the recursion relations (3.14.277) until a future work. Here, we merely want to demonstrate its most important physical implications through the context of simple examples. We first describe how one-loop integrands are generated by the recursion, using the case of MHV for illustration. At the end of this subsection, we will briefly describe the features observed for higher-loop amplitudes.

Let us begin with the simplest of all one-loop amplitudes, the 4-particle MHV amplitude. As there are no 3-particle one-loop integrands to appear in the ‘bridge’ term of the recursion, the 4-particle one-loop integrand is entirely generated as the forward-limit of the 6-particle NMHV tree-amplitude, $\mathcal{A}_6^{(3)}$. Let us denote the two particles identified in the forward-limit by (AB) , and use these two legs as the pair singled-out in the recursion of the 6-particle tree. Of the 3 terms appearing in the tree-amplitude $\mathcal{A}_6^{(3)}$, (3.14.280), only one is non-vanishing in the forward-limit (a fact that we will demonstrate momentarily); the forward-limit of the $\mathcal{A}_4^{(2)} \otimes \mathcal{A}_4^{(2)}$ -term is,

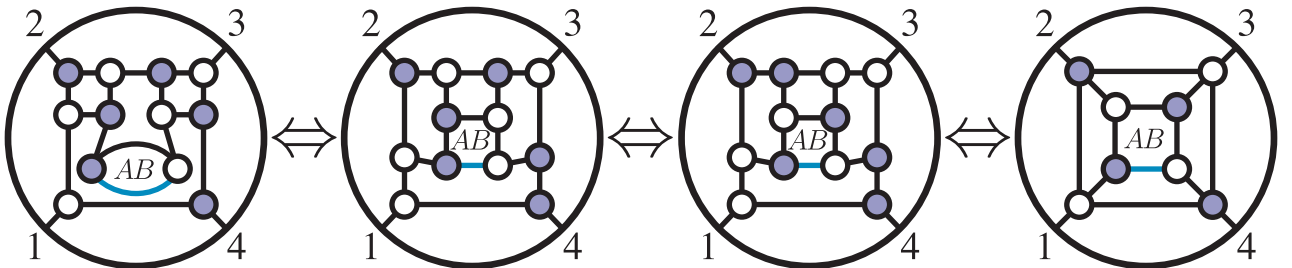


(The last move in this sequence was made only to make subsequent transformations more transparent.) It is easy to see that this diagram has four faces beyond that of the simple box, and thus four extra integration variables. Using reduction, we can of course reduce this diagram to the box, giving us the integrand. We can relate this new form of the integrand to a more familiar form, by identifying the usual loop momentum “ ℓ ” as,

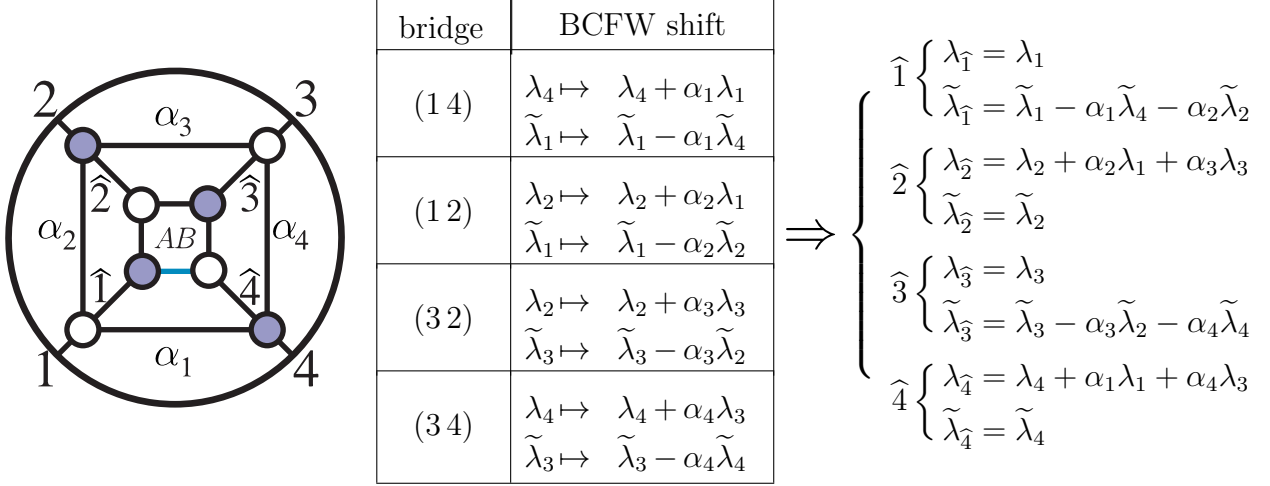
$$\ell = \alpha\lambda_1\tilde{\lambda}_4 + \lambda_{AB}\tilde{\lambda}_{AB}, \quad (3.14.284)$$

where $\lambda_{AB}\tilde{\lambda}_{AB}$ is the momentum of the highlighted line in figure above. We can of course determine $\lambda_{AB}, \tilde{\lambda}_{AB}$ in terms of the variables associated with the graph, and in this way trade the four ‘extra’ variables for those which parameterize ℓ .

While this is a straightforward exercise, it is more illuminating to carry out the reduction in a different way. We can use moves to give the on-shell diagram a different representation—as a sequence of BCFW bridges on a core 4-particle amplitude:



(In the last transformation, several mergers were made.) This allows us to think of the object as the usual box, but with ‘BCFW-shifted kinematical data’, given by,



Thus, the integrand is nothing but $d\log(\alpha_1) \wedge \cdots \wedge d\log(\alpha_4)$ times the shifted four-particle amplitude,

$$\frac{d\alpha_1}{\alpha_1} \frac{d\alpha_2}{\alpha_2} \frac{d\alpha_3}{\alpha_3} \frac{d\alpha_4}{\alpha_4} \frac{\delta^{2 \times 4}(\lambda \cdot \tilde{\eta})}{\langle \hat{1} \hat{2} \rangle \langle \hat{2} \hat{3} \rangle \langle \hat{3} \hat{4} \rangle \langle \hat{4} \hat{1} \rangle}. \quad (3.14.285)$$

If we strip-off the (unshifted) Parke-Taylor prefactor, the integrand for the one-loop ratio function—the loop amplitude divided by the tree-amplitude—is simply [73],

$$\begin{aligned} \frac{\mathcal{A}_4^{(2),1}}{\mathcal{A}_4^{(2),0}} &= \frac{d\alpha_1}{\alpha_1} \frac{d\alpha_2}{\alpha_2} \frac{d\alpha_3}{\alpha_3} \frac{d\alpha_4}{\alpha_4} \frac{\langle 12 \rangle \langle 23 \rangle \langle 34 \rangle \langle 41 \rangle}{\langle \hat{1} \hat{2} \rangle \langle \hat{2} \hat{3} \rangle \langle \hat{3} \hat{4} \rangle \langle \hat{4} \hat{1} \rangle}, \\ &= \frac{d\alpha_1}{\alpha_1} \frac{d\alpha_2}{\alpha_2} \frac{d\alpha_3}{\alpha_3} \frac{d\alpha_4}{\alpha_4} \frac{\langle 12 \rangle}{\langle 12 \rangle + \alpha_3 \langle 13 \rangle} \frac{\langle 23 \rangle}{\langle 23 \rangle + \alpha_2 \langle 13 \rangle} \frac{\langle 34 \rangle}{\langle 34 \rangle + \alpha_1 \langle 31 \rangle} \frac{\langle 41 \rangle}{\langle 41 \rangle + \alpha_4 \langle 31 \rangle}, \\ &= d\log\left(\frac{\alpha_1 \langle 34 \rangle}{\langle 34 \rangle + \alpha_1 \langle 31 \rangle}\right) d\log\left(\frac{\alpha_2 \langle 23 \rangle}{\langle 23 \rangle + \alpha_2 \langle 13 \rangle}\right) d\log\left(\frac{\alpha_3 \langle 12 \rangle}{\langle 12 \rangle + \alpha_3 \langle 13 \rangle}\right) d\log\left(\frac{\alpha_4 \langle 41 \rangle}{\langle 41 \rangle + \alpha_4 \langle 31 \rangle}\right) \end{aligned}$$

which is manifestly in a ‘dlog’-form.

Now, we can determine λ_{AB} and $\tilde{\lambda}_{AB}$ very simply in terms of the bridge variables. For a general box, the internal momentum on the bridge can be given in terms of the external data according to:



which allows us to identify,

$$\lambda_{AB} \tilde{\lambda}_{AB} = \frac{\langle \hat{1} \hat{2} \rangle}{\langle \hat{4} \hat{2} \rangle} \lambda_{\hat{4}} \tilde{\lambda}_{\hat{1}}. \quad (3.14.287)$$

And so in summary, the relation between the BCFW-bridge variables α_i and the usual loop momentum variables is given by,

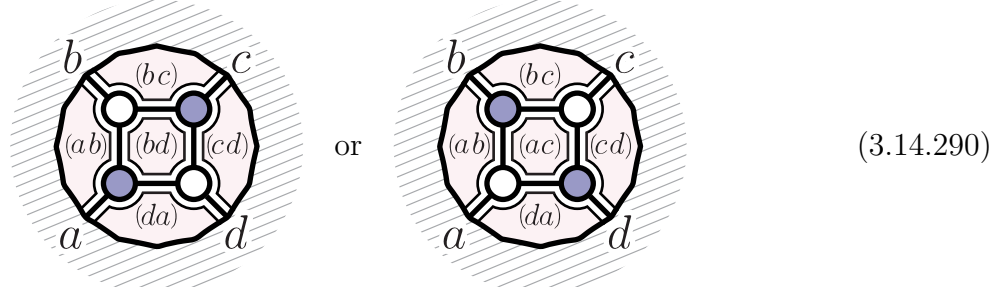
$$\ell = \frac{\langle 12 \rangle}{\langle 42 \rangle} \lambda_4 \tilde{\lambda}_1 + \alpha_1 \lambda_1 \tilde{\lambda}_4. \quad (3.14.288)$$

Using this change of variables, it is straightforward to re-cast the integrand (3.14.286) in the form which we gave earlier in section 3.2:

$$d\log\left(\frac{\ell^2}{(\ell - \ell^*)^2}\right) d\log\left(\frac{(\ell + p_1)^2}{(\ell - \ell^*)^2}\right) d\log\left(\frac{(\ell + p_1 + p_2)^2}{(\ell - \ell^*)^2}\right) d\log\left(\frac{(\ell - p_4)^2}{(\ell - \ell^*)^2}\right), \quad (3.14.289)$$

where $\ell^* = \frac{\langle 12 \rangle}{\langle 42 \rangle} \lambda_4 \tilde{\lambda}_1$.

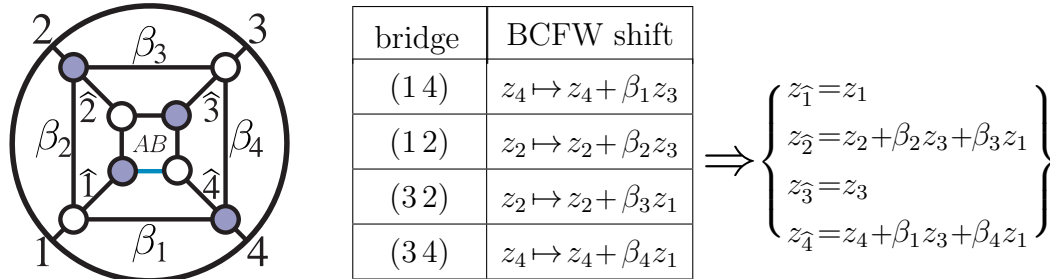
We can also interpret exactly the same pictures in momentum-twistor space. Recall that a BCFW bridge ‘(a-1 a)’—a white-to-black vertex from $a-1$ to a —has the effect of shifting the momentum twistor $z_a \mapsto z_a + \alpha z_{a+1}$ where α is the bridge variable. Generally speaking, lines in momentum-twistor space are associated with the faces of the momentum-space on-shell graph; we will not review these ideas here, but let us briefly summarize that the regions of a four-point box are associated with the lines in momentum-twistor space as indicated below:



Now, this means that if we identify the four unfixed degrees of freedom with the line (AB) in momentum-twistor space, we see that it corresponds to the line $(\hat{2}\hat{4})$ in



Performing the same sequence of shifts as before, but now using momentum-twistor variables, we find:



This uniquely fixes the auxiliary, Grassmannian parameters β_i in terms of the momentum-twistor line (AB) according to:

$$\beta_1 = \frac{\langle AB 41 \rangle}{\langle AB 13 \rangle}, \quad \beta_2 = \frac{\langle AB 12 \rangle}{\langle AB 31 \rangle}, \quad \beta_3 = \frac{\langle AB 23 \rangle}{\langle AB 31 \rangle}, \quad \text{and} \quad \beta_4 = \frac{\langle AB 34 \rangle}{\langle AB 13 \rangle}. \quad (3.14.292)$$

With this identification, we can re-write the integrand in terms of the four auxiliary variables in momentum-twistor space as,

$$d\log(\beta_1) \cdots d\log(\beta_4) = d\log\left(\frac{\langle AB 41 \rangle}{\langle AB 13 \rangle}\right) d\log\left(\frac{\langle AB 12 \rangle}{\langle AB 31 \rangle}\right) d\log\left(\frac{\langle AB 23 \rangle}{\langle AB 31 \rangle}\right) d\log\left(\frac{\langle AB 34 \rangle}{\langle AB 13 \rangle}\right).$$

If we recast this expression as an integration measure on the space of lines (AB) in momentum-twistor space, we find that

$$d\log\left(\frac{\langle AB 41 \rangle}{\langle AB 13 \rangle}\right) d\log\left(\frac{\langle AB 12 \rangle}{\langle AB 31 \rangle}\right) d\log\left(\frac{\langle AB 23 \rangle}{\langle AB 31 \rangle}\right) d\log\left(\frac{\langle AB 34 \rangle}{\langle AB 13 \rangle}\right) = \quad (3.14.293)$$

$$\frac{\langle d^2 z_A AB \rangle \langle d^2 z_B AB \rangle \langle 1234 \rangle \langle 2341 \rangle}{\langle AB 12 \rangle \langle AB 23 \rangle \langle AB 34 \rangle \langle AB 41 \rangle},$$

which is precisely the familiar form of the integrand given in reference [65].

Before moving on to the case of the n -particle MHV one-loop integrand, let us go back and understand why only one of the three terms in the 6-particle NMHV tree amplitude survived the forward-limit, as the reason will prove quite instructive. Let us choose to always represent the $(n+2)$ -point tree-amplitude appearing in the forward limit using the BCFW recursion which deforms legs (AB) . Recall that the tree-amplitude recursion can be broken into three parts as in (3.14.278):

1. a k -preserving inverse-soft factor: $\mathcal{A}_{n-1}^{(k)} \otimes \mathcal{A}_3^{(1)}$;
2. a k -increasing inverse-soft factor: $\mathcal{A}_3^{(2)} \otimes \mathcal{A}_{n-1}^{(k-1)}$; (3.14.294)
- and 3. terms for which $n_L, n_R \geq 4$.

Of these, it is not hard to see that if (AB) are the distinguished legs of the bridge, the first two contributions listed above *always* vanish. More precisely, any on-shell form for which A or B is an inverse-soft factor will vanish in the forward-limit. (We should notice that ‘ A or B being an inverse-soft factor’ is a *sufficient* condition for an on-shell form to vanish in the forward limit, but not a *necessary* one.)

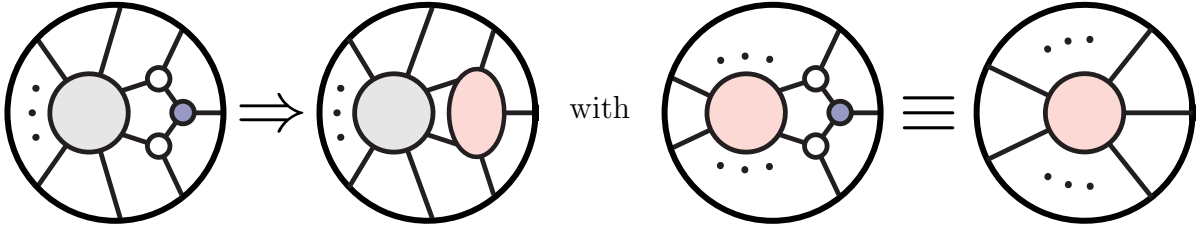
Let us now see why any contributions to the lower-loop amplitude where A or B is an inverse-soft factor will vanish. Consider the forward-limit of a term for which A is a k -preserving inverse-soft factor (the argument is the same in all other cases):

(3.14.295)

Notice that the kinematical constraints associated with the middle—black—vertex requires that λ_A be expandable in terms of λ_B and λ_n ; but in the forward-limit, we identify λ_A with λ_B , which implies that $\lambda_{AB} \propto \lambda_n$. As such, the kinematical constraints do not allow for there to be any unfixed degrees of freedom associated with λ_{AB} (which should represent loop-integration degrees of freedom).

We are now prepared to determine the n -point MHV one-loop integrand in general. The bridge-term always contributes a term $\mathcal{A}_{n-1}^{(2),1} \otimes \mathcal{A}_3^{(1)}$, which is simply a k -preserving inverse-soft factor adding n to the $(n-1)$ -point one-loop amplitude; more interesting are the forward-limit terms. These come from the forward-limit of $\mathcal{A}_{n+2}^{(3),0}$; among the terms that contribute to the higher-point NMHV tree-amplitude, we have seen that only those obtained from bridging $\mathcal{A}_{n_L}^{(2)} \otimes \mathcal{A}_{n_R}^{(2)}$ with $n_L, n_R \geq 4$ contribute.

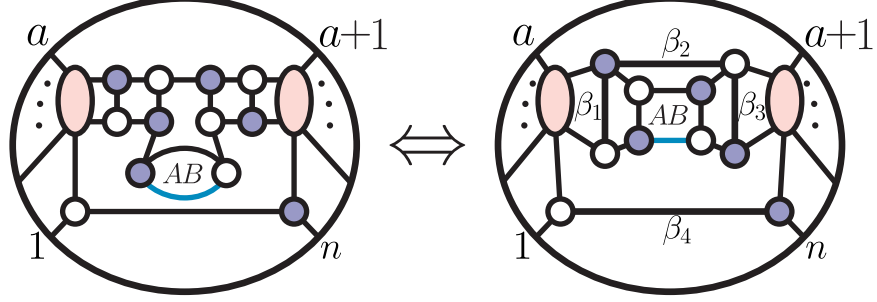
Because k -preserving inverse soft factors act trivially in momentum-twistors, and the left- and right-amplitudes appearing in the NMHV tree-amplitudes are trivially chains of inverse-soft factors, it will be useful to define the notion of an “MHV region” obtained by any number of successive k -preserving inverse-soft factors:



Allowing for such MHV regions in our diagrammatic expansion, we see that the one-loop MHV integrand is given by,

We can rearrange the NMHV forward-limit contributions as we did above in order to make manifest the sequence of BCFW-bridges which parameterize the extra degrees

of freedom:



Proceeding as before, we can identify the shifted momentum-twistors appearing in the box as,

$$(AB) = (\widehat{a}\widehat{n}) \quad \text{with} \quad \left\{ \begin{array}{l} z_{\widehat{a}} = z_a + \beta_1 z_{a+1} + \beta_2 z_1 \\ z_{\widehat{n}} = z_n + \beta_3 z_1 + \beta_4 z_{n-1} \end{array} \right\}, \quad (3.14.296)$$

which allows us to re-cast the BCFW-bridge variables β_i in terms of the line (AB) :

$$\beta_1 = \frac{\langle AB 1 a \rangle}{\langle AB a+1 1 \rangle}, \quad \beta_2 = \frac{\langle AB a a+1 \rangle}{\langle AB a+1 1 \rangle}, \quad \beta_3 = \frac{\langle AB n-1 n \rangle}{\langle AB 1 n-1 \rangle}, \quad \text{and} \quad \beta_4 = \frac{\langle AB n 1 \rangle}{\langle AB 1 n-1 \rangle}.$$

Therefore, we see that the forward-limit terms are given by:

$$\begin{aligned} & \text{Diagram} = d\log(\beta_1) d\log(\beta_2) d\log(\beta_3) d\log(\beta_4) \\ & = d\log\left(\frac{\langle AB 1 a \rangle}{\langle AB 1 a+1 \rangle}\right) d\log\left(\frac{\langle AB a a+1 \rangle}{\langle AB 1 a+1 \rangle}\right) d\log\left(\frac{\langle AB n-1 n \rangle}{\langle AB 1 n-1 \rangle}\right) d\log\left(\frac{\langle AB n 1 \rangle}{\langle AB 1 n-1 \rangle}\right). \end{aligned}$$

Quite amazingly, if we re-cast this integration measure directly in terms of the line (AB) , we see that this is equivalent to,

$$\begin{aligned} & \text{Diagram} = \frac{\langle d^2 z_A AB \rangle \langle d^2 z_B AB \rangle \langle AB (1 a a+1) \cap (1 n-1 n) \rangle^2}{\langle AB 1 a \rangle \langle AB a a+1 \rangle \langle AB a+1 1 \rangle \langle AB 1 n-1 \rangle \langle AB n-1 n \rangle \langle AB n 1 \rangle} \\ & \equiv K[a; n-1]. \end{aligned}$$

We have obtained this result entirely by manipulating pictures of on-shell diagrams; of course the result precisely matches the form obtained by direct computation, using the methods of [65], where all MHV one-loop integrands were given in the form,

$$\mathcal{A}_n^{(2),1} = \sum_{1 < a < b < n} K[a; b]. \quad (3.14.297)$$

Before moving on to multi-loop integrands, it is worth mentioning that for one-loop integrands, so long as the forward-limits are taken of tree-amplitudes obtained by

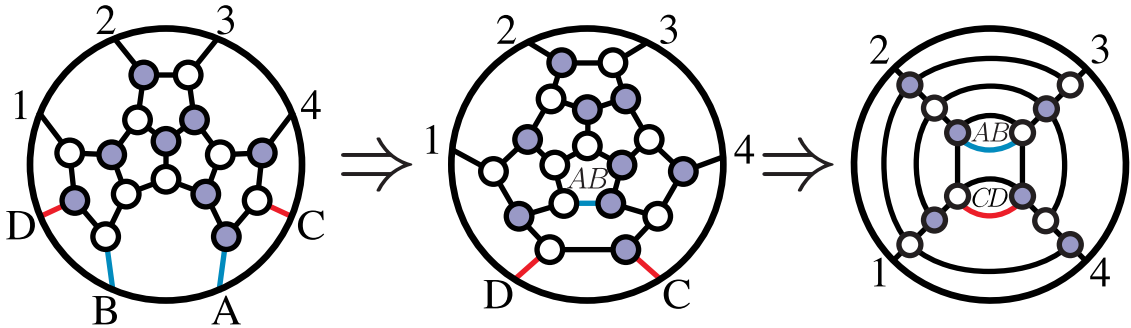
BCFW deforming the identified legs (AB), it turns out that the obvious k -preserving and k -increasing inverse-soft factors are the *only* terms which vanish in the forward limit; this allows us to conclude that,

$$\# \text{ BCFW terms in the one-loop amplitude } \mathcal{A}_n^{(k),1}: \binom{n-2}{k} \binom{n-2}{k-2}. \quad (3.14.298)$$

(It turns out that this counting holds regardless of how the forward-limit terms are recursed—even though it is generally difficult to identify beforehand which terms will vanish if (AB) are not singled-out for the recursion. Beyond one-loop, however, the number of non-vanishing contributions is not invariant, and depends sensitively on how the lower-loop amplitudes are recursed.)

When expressing tree-amplitudes and their forward-limits in terms of canonical coordinates on the auxiliary Grassmannian, it is obvious that all loop integrands can be—and are most naturally—expressed in such a ‘ $d\log$ ’-representation. Although in principle we have all the tools necessary to construct such formulae for all amplitudes—and although the BCFW recursion relations (3.14.277) is *dramatically* more efficient than any representation obtained using ‘traditional’ methods (such as Feynman diagrams)—even the simplest 2-loop integrands would require more space to write completely than would be warranted for the purpose of illustration.

Let us therefore content ourselves to consider one simple example of a contribution to the 4-particle 2-loop integrand which arises as the double forward-limit of a of the contributions to the 8-particle N^2 MHV tree-amplitude, that of $(\mathcal{A}_4^{(2)} \otimes \mathcal{A}_4^{(2)}) \otimes \mathcal{A}_4^{(2)}$:



In the last step, we have made liberal use of square-moves and merge/un-merge operations to bring it in the form which exposes a sequence of recognizable BCFW-bridges which themselves encode the additional degrees of freedom.

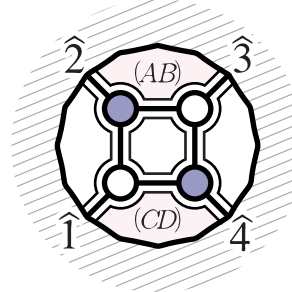
Using the tools described in [65] to compute this contribution directly as a ‘function’ of lines (AB) and (CD) in momentum-twistor space, the following rational

integrand is found:

$$\frac{\langle d^2 z_A AB \rangle \langle d^2 z_B AB \rangle \langle d^2 z_C CD \rangle \langle d^2 z_D CD \rangle \langle 1234 \rangle^3 \langle AB(CD) \cap (341)1 \rangle^2}{\langle AB14 \rangle \langle AB1(123) \cap (CD) \rangle \langle AB1(234) \cap (CD) \rangle \langle AB(((CD(341) \cap (AB)) \cap (12))34) \cap (CD)1 \rangle \langle ABCD \rangle \langle CD34 \rangle}.$$

While the expression above is of course obtained in a straight-forward way, it is obviously rather complicated and not particularly illuminating. Moreover, as written in the form given above—as a rational integrand—it is not at all obvious that there exists *any* change of variables for which it becomes simply the wedge-product of 8 logarithmic factors. But from our present perspective, the existence of such a change of coordinates is an obvious consequence of the Grassmannian formulation of the initial tree-amplitude; and it will be instructive to see how this remarkable connection is realized.

To be extremely concrete, we want to identify the lines (AB) and (CD) as parameterizing the region-momenta according to,



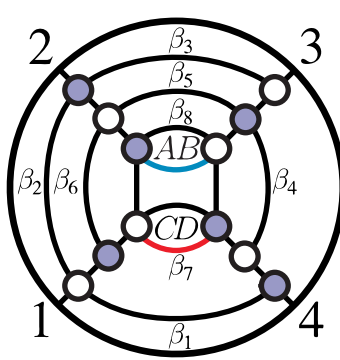
with

$$(AB) = (\widehat{23})$$

$$(CD) = (\widehat{41})$$

$$(3.14.299)$$

We can find the shifted momentum-twistors $z_{\widehat{a}}$ by performing the successive BCFW-shifts obvious from the way the double forward-limit graph is drawn:



| bridge | BCFW shift |
|--------|---------------------------------|
| (1 4) | $z_4 \mapsto z_4 + \beta_1 z_3$ |
| (1 2) | $z_2 \mapsto z_2 + \beta_2 z_3$ |
| (3 2) | $z_2 \mapsto z_2 + \beta_3 z_1$ |
| (4 3) | $z_3 \mapsto z_3 + \beta_4 z_2$ |
| (2 3) | $z_3 \mapsto z_3 + \beta_5 z_4$ |
| (2 1) | $z_1 \mapsto z_1 + \beta_6 z_4$ |
| (1 4) | $z_4 \mapsto z_4 + \beta_7 z_3$ |
| (3 2) | $z_2 \mapsto z_2 + \beta_8 z_1$ |

 \Rightarrow

$$\left\{ \begin{array}{l} z_{\widehat{1}} = z_1 + \beta_5(z_4 + \beta_1 z_3); \\ z_{\widehat{2}} = z_2 + \beta_2 z_3 + \beta_3 z_1 \\ \quad + \beta_8(z_1 + \beta_5(z_4 + \beta_1 z_3)); \\ z_{\widehat{3}} = z_3 + \beta_4(z_2 + \beta_2 z_3 + \beta_3 z_1) \\ \quad + \beta_6(z_4 + \beta_1 z_3); \\ z_{\widehat{4}} = z_4 + \beta_1 z_3 + \beta_7 \beta_6(z_4 + \beta_1 z_3) \\ \quad + \beta_7(z_3 + \beta_4(z_2 + \beta_2 z_3 + \beta_3 z_1)); \end{array} \right.$$

One can readily verify that quite remarkably, with this change of variables, the complicated expression given above becomes simply,

$$d\log(\beta_1) \wedge \cdots \wedge d\log(\beta_8). \tag{3.14.300}$$

IV. The Transcendentality of Loop Amplitudes

The integrand obtained from the BCFW recursion relations allows us to draw some important general conclusions about the structure of the final, integrated expressions for the amplitude. Let us start with MHV amplitudes. As we have seen, all the BCFW terms at L loops can be written in the form,

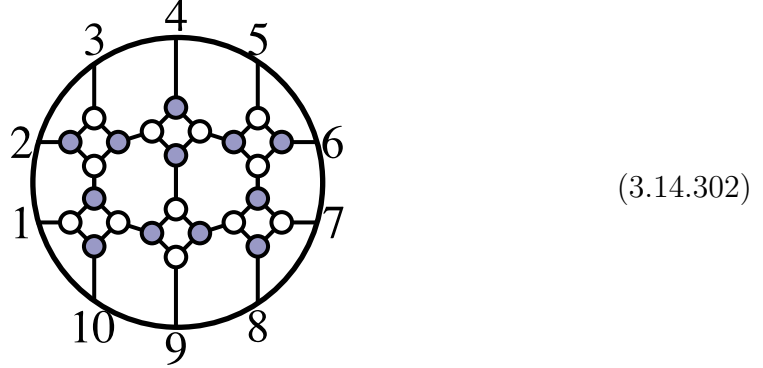
$$\mathcal{A}_{n,L}^{(2)} = \mathcal{A}_{n,0}^{(2)} \times \prod_{j=1}^{4L} d\log(\beta_j). \quad (3.14.301)$$

The first and most obvious point to observe is that the integrand has *only* logarithmic singularities! There are *no* “*sub-leading*” pieces of the integrand with less than the maximal number of logarithmic singularities. At one-loop, this (together with dual conformal invariance) tells us the famous fact that the loop amplitude only depends on “box” integrals, and doesn’t involve any triangles, bubbles, or rational pieces [174, 175].

As we have stressed a number of times, the fact that the integrand has only logarithmic singularities is not at all obvious from inspection of the actual rational functions involved in sufficiently high loop-amplitude integrands, where there don’t seem to be enough “obvious” singularities in cutting propagators, and so singularities must emerge as “composites”. By contrast, the positive Grassmannian story makes this fact completely obvious. Intuitively, this guarantees that after integration, the L -loop MHV amplitudes can always be expressed as a sum of polylogarithms of transcendentality $2L$. The reason is roughly that discontinuities of the amplitude are related to unitarity cuts that put pairs of particles on-shell; thereby computing partial residues of the integrand. Taking $2L$ discontinuities gives the leading singularity “1”, which has no further discontinuities. These amplitudes are thus “pure”—not polluted by lower-transcendentality terms, which would arise from pieces of the integrand without purely logarithmic singularities. This has long been conjectured to be true for MHV amplitudes in connection to the maximal transcendentality principle of [176]. We see that the property needed of the integrand to guarantee this is a trivial consequence of the $d\log$ form.

Beyond MHV amplitudes, we know that the integrated amplitudes can involve more complicated functions than polylogarithms. For instance, as pointed out in ref. [136], the two-loop, 10-point N^3 MHV amplitude includes a contribution from a

function whose seven-fold discontinuity is proportional to the following on-shell form:



$$(3.14.302)$$

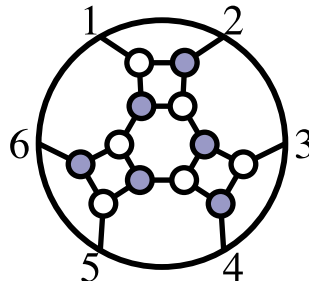
$\{7, 6, 10, 9, 8, 12, 11, 15, 14, 13\}$

This on-shell graph corresponds to a 17-dimensional cell in $G(5, 10)$; the kinematical constraints will fix this to an integral over one degree of freedom (interpreted as the ‘hepta-cut’ of the two-loop integrand). The component amplitude proportional to,

$$(\tilde{\eta}_1^1 \tilde{\eta}_1^2) (\tilde{\eta}_2^1 \tilde{\eta}_2^2) (\tilde{\eta}_3^2 \tilde{\eta}_3^3) (\tilde{\eta}_4^2 \tilde{\eta}_4^3) (\tilde{\eta}_5^2 \tilde{\eta}_5^3) (\tilde{\eta}_6^3 \tilde{\eta}_6^4) (\tilde{\eta}_7^3 \tilde{\eta}_7^4) (\tilde{\eta}_8^4 \tilde{\eta}_8^1) (\tilde{\eta}_9^4 \tilde{\eta}_9^1) (\tilde{\eta}_{10}^4 \tilde{\eta}_{10}^1), \quad (3.14.303)$$

(a component which vanishes exactly at tree-level and one-loop) vanishes on all the positroid cells in the boundary of (3.14.302). Therefore, the only contour integral available must enclose the Jacobian resulting from the kinematical constraints; this Jacobian generically involves the square-root of an irreducible quartic, implying that (at least for this component) the seven-fold discontinuity of the 2-loop integrand is an elliptic integral.

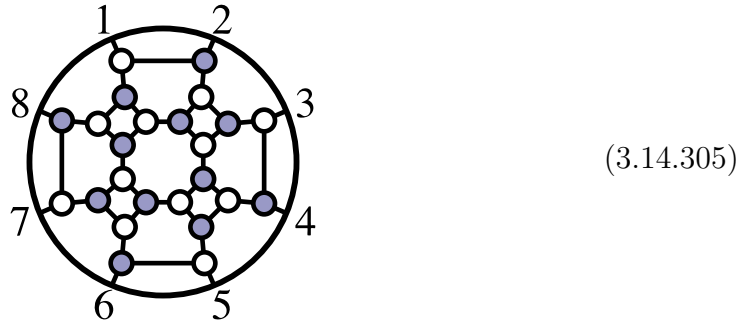
We can understand the difference between MHV and higher- k amplitudes from the Grassmannian. Recall that cells of dimensionality $(2n-4)$ are fully localized by the kinematical constraints. Since for MHV amplitudes, $\dim(G(2, n)) = (2n-4)$, *all* of the unfixed degrees of freedom associated with ‘loop-momenta’ are associated with faces which can always be removed by reduction (as there no irreducible graphs with more faces than that of the top-cell). Beyond MHV, however, the reduction of on-shell diagrams can result in cells of higher dimensionality than $(2n-4)$. For example, consider the top-cell of $G(3, 6)$:



$$(3.14.304)$$

Here, we have chosen a representative graph which makes it clear that it can be associated with a triple-cut of the 6-particle amplitude at 1-loop. The $9 - 8 = 1$ degree of freedom of the top-cell which is not fixed by the kinematical constants can always be interpreted as the single integration variable of a triple-cut integral.

Similarly, the top-cell of $G(4, 8)$ is 16-dimensional, while the kinematical constraints can be used to isolate only $2 \times 8 - 4 = 12$ degrees of freedom; therefore, the top-cell on $G(4, 8)$ can be viewed as an on-shell differential form with *four* unfixed auxiliary degrees of freedom—which can in fact be interpreted as the four-degrees of freedom of a ‘loop-integrand’ at one-loop. Indeed, we can represent the top-cell by,



Therefore beyond MHV, while the integration measures are purely $d\log$'s, some free integration variables are *inside* the Grassmannian, and must be localized by the kinematic constraints. This is the reason why more complicated functions can appear after integration. However, it is clear that for fixed n and k , the functions can't get arbitrarily more complicated at high loop orders. The reason is that at most $\dim(G(k, n)) - (2n - 4)$ of the integration variables can remain ‘entangled’ in the Grassmannian (meaning that they cannot be pulled-off as overall $d\log$ factors in the measure via bubble-reduction); at arbitrarily-high loop order, all but a finite number of these auxiliary degrees of freedom must be associated with the more trivial factors in the measure arising from bubble-reduction.

Actually, it is easy to see that, for NMHV amplitudes, the integrations that are “stuck” in the Grassmannian can easily be removed, preserving the $d\log$ form, and thus that all NMHV amplitudes are also polylogarithms. Let us illustrate with the top cell of $G(3, 6)$; it is convenient to work in momentum-twistor language, where this maps to the top cell of $G(1, 6)$. On the support of the (ordinary) δ -functions, we have a 1-form which we can represent as,

$$[1234(5+\beta6)]d\log(\beta), \tag{3.14.306}$$

However, we can use the identity among the 5-brackets, (??), to rewrite this as

$$\begin{aligned}
& [1\ 2\ 3\ 4\ 5]d\log(\beta) + [2\ 3\ 4\ 5\ 6]d\log\left(\beta - \frac{\langle 2345 \rangle}{\langle 2346 \rangle}\right) + [3\ 4\ 5\ 6\ 1]d\log\left(\beta - \frac{\langle 3451 \rangle}{\langle 3461 \rangle}\right) \\
& + [4\ 5\ 6\ 1\ 2]d\log\left(\beta - \frac{\langle 4512 \rangle}{\langle 4612 \rangle}\right) + [5\ 6\ 1\ 2\ 3]d\log\left(\beta - \frac{\langle 5123 \rangle}{\langle 6123 \rangle}\right) \quad (3.14.307)
\end{aligned}$$

In this way, we have removed the integration variable from inside the Grassmannian and decomposed the result into a sum of terms, each of which is in canonical form. The same thing can be done for the top cell of any NMHV amplitude, since the “internal” variables always occur linearly. Things can start becoming non-trivial at N²MHV, where square-roots first make an appearance, and as we’ve seen concretely above, already for 10-particle N³MHV amplitudes, elliptic integrals do make an appearance.

The on-shell, BCFW-representation of loop-integrands delivers them manifestly in a canonical, $d\log$ -form; but having noted that the integrand can be put in this form, it is natural to wonder if this is a consequence of the BCFW-representation, or a more general result. For instance, in reference [177], extremely compact, *local* forms of many integrands were found; can these also be written in terms of integrands with only logarithmic singularities? The answer yes: the $d\log$ form is a *general* property of “pure” integrands with unit leading singularities. Let us briefly demonstrate this fact with two examples: local forms of the MHV 1- and 2-loop integrands.

In [177], the 1-loop MHV integrand was given in the local form,

$$\begin{aligned}
& \text{Diagram: A circle with a smaller inner circle. The inner circle is shaded and contains the label } \mathcal{A}_n^{(2),1}. \text{ The outer circle has } n \text{ radial lines connecting it to the inner circle. Three dots are placed above the inner circle.} \\
& \text{Diagram} = \sum_{a < b < a} I_X[a; b], \quad (3.14.308)
\end{aligned}$$

where $I_X[a; b]$ denotes the integrand,

$$I_X[a; b] \equiv \frac{\langle AB d^2 z_A \rangle \langle AB d^2 z_B \rangle \langle AB (a-1\ a\ a+1) \cap (b-1\ b\ b+1) \rangle}{\langle AB\ a-1\ a \rangle \langle AB\ a\ a+1 \rangle \langle AB\ b-1\ b \rangle \langle AB\ b\ b+1 \rangle \langle AB\ X \rangle}, \quad (3.14.309)$$

and where X is an arbitrary reference-line in momentum-twistor space (spanned by any pair of twistors). Remarkably, it turns out that $I_X[a; b]$ can be expressed in canonical form:

$$d\log\left(\frac{\langle AB\ a-1\ a \rangle}{\langle AB\ X \rangle}\right) d\log\left(\frac{\langle AB\ a\ a+1 \rangle}{\langle AB\ X \rangle}\right) d\log\left(\frac{\langle AB\ b-1\ b \rangle}{\langle AB (aX) \cap (b-1\ b\ b+1) \rangle}\right) d\log\left(\frac{\langle AB\ b\ b+1 \rangle}{\langle AB (aX) \cap (b-1\ b\ b+1) \rangle}\right).$$

3.15 Outlook

We have explored much of the remarkable physics and mathematics of scattering amplitudes in planar $\mathcal{N} = 4$ SYM, as seen through the lens of on-shell diagrams as the primary objects of study. Let us conclude by making some brief comments on further avenues of research.

One immediate extension of our work is the continued study of theories with $\mathcal{N} < 4$ SUSY, whose most basic features we sketched out in section 3.13. For $\mathcal{N} \geq 1$, all-loop BCFW recursion holds just as for $\mathcal{N} = 4$, together with its realization in terms of on-shell diagrams. For $\mathcal{N} = 0$ SUSY, the forward limit of tree amplitudes are singular, and thus don't directly give us the single-cuts of the loop-integrand [103]. More thought is needed to establish a connection between on-shell diagrams and the full amplitude, though it is likely that fully understanding the on-shell diagrams will continue to play an important role in determining $\mathcal{N} = 0$ amplitudes as well.

The general connection between on-shell diagrams and the Grassmannian has nothing to do with any particular theory, only with the general picture of amalgamating basic three-particle amplitudes, and the connection to the positive Grassmannian in particular holds for any planar theory. Only the form on the Grassmannian changes from theory to theory. As briefly discussed in section 3.13, the essential physical novelty of gauge theories with $\mathcal{N} \leq 2$ supersymmetry is the presence of UV-divergences. The most physical, Wilsonian, way to think about UV-divergences makes critical use of off-shell ideas, and so a major challenge is finding the correct way of thinking about such physics in a directly on-shell language. It is fascinating to see that the UV and IR singularities, together with UV/IR decoupling, is reflected directly in on-shell diagrams through simple structures in the Grassmannian. A clear goal would be to understand the physics of the renormalization group along these lines.

Another obvious extension is to push beyond the planar limit, starting already with $\mathcal{N} = 4$ SYM; in this case, there is no longer an obvious notion of “the loop integrand”, and thus we must learn how to establish a connection between on-shell diagrams and the full scattering amplitude along the lines of the BCFW construction in the planar limit. It is also very likely that on-shell ideas can be used to deter-

mine other observables in gauge theories beyond scattering amplitudes, including all correlation functions. These objects also have discontinuities and cuts, and the on-shell diagrams for leading singularities of form-factors and correlation functions are exactly the same as the (in general non-planar) on-shell diagrams we have been considering. The structure of cuts has already proved to be powerful in determining form-factors, [178]. For scattering amplitudes, we have seen that off-shell notions like virtual loop integration variables can be fully understood in on-shell terms. It is tempting to try and compute completely off-shell objects like correlation functions in the same way.

Moving further afield, the basic mathematical structures we have encountered in scattering amplitudes have also recently made an appearance in apparently completely different physical settings, related to conformal blocks for higher Toda theories [40, 179], wall-crossing [180, 181], various versions of the AGT conjecture [182], scattering amplitudes at strong coupling [183], and soliton solutions of the KP equation [184–186]. The identical graphical structure has also appeared in the construction of $\mathcal{N} = 1$ SCFTs associated with quiver gauge theories (see e.g. [187, 188]). The combinatorial classification of on-shell diagrams and these planar $\mathcal{N} = 1$ SCFTs coincide perfectly. It would be interesting to see if the rest of the structure we have been seeing—especially the connection with the positive Grassmannian—have a natural interpretation as well.

There is a unifying theme running through the physics and mathematics we have been discussing. We have an object—the positive Grassmannian—which is fundamentally defined by global properties, either as a real space, by demanding all ordered minors are positive, or as a complex space, by specifying linear dependencies between consecutive vectors. However quite remarkably, the best way of building-up these objects (albeit in a highly redundant way) is through the amalgamation of elementary building blocks.

For scattering amplitudes, amalgamation representations have a direct physical interpretation as on-shell diagrams. For $\mathcal{N} = 1$ gauge theories, they correspond to gluing together gauge groups with bi-fundamental content to generate more complicated quiver gauge theories. For scattering amplitudes, it is physically clear why we should be interested in complicated on-shell diagrams, since they are ultimately needed to compute the amplitude to all-loop order. But what is physically impor-

tant about complicated quiver gauge theories? One possible answer is that precisely these sort of quiver gauge theories, with an infinite number of sites and links, occur in the deconstruction of the still mysterious $(2,0)$ and little string theories in six dimensions, [189]. It would be fascinating to use the powerful new machinery for studying these quivers to try and learn more about the dynamics of the underlying six-dimensional theories, which would perhaps shed some light on a more direct physical reason for the appearance of the same Grassmannian structure in seemingly vastly different settings.

We have seen that scattering amplitudes in $(1+1)$, $(2+1)$ and $(3+1)$ dimensions are described by various interpretations of permutations and associated structures in the Grassmannian. It is natural to ask whether other variations of these mathematical ideas might have a physical interpretation. There is one natural further specialization of the positive Grassmannian we have not discussed, which in fact goes back to the historical roots of the subject: the study of totally positive matrices. Here, one considers $(n \times n)$ square matrices M with positive determinant, and studies the space where all its $(m \times m)$ -minors are non-negative. This classical problem was studied by Gantmacher and Krein [118] and Schoenberg [119] in the 1930's, where the stratification was found to be determined by *pairs* of permutations σ_1 and σ_2 . This theory is a special case of the positive Grassmannian $G(n, 2n)$. Consider cells where the first n columns of the $(n \times 2n)$ C matrix are linearly independent, and also the second n columns are linearly independent. We can then gauge-fix C to the form

$$C = (1_{n \times n} \mid M_{n \times n}), \quad (3.15.311)$$

where M is a positive matrix. Let us label the first n columns $1, \dots, n$ and the second n columns by $1', \dots, n'$. It is clear that e.g. $\sigma(1) = a'$ for some a' in the second set of columns, since 1 can not be in the span of $\{2, \dots, n\}$, given that the first n columns are linearly independent. This is true for all the other columns in the first set—i.e. $\sigma(a) = b'$. Similarly, $\sigma(a') = b$. Thus, we see that our permutation naturally breaks into two pieces, mapping $(1, \dots, n) \mapsto (1', \dots, n')$ and vice-versa. It would be nice to find a physical interpretation for the subclass of on-shell diagrams associated with these pairs of permutations.

We have also seen a reliable guide to the Grassmannian structure associated with

scattering amplitudes is to find a Grassmannian interpretation of the space of external kinematical data. In four dimensions, the λ - and $\tilde{\lambda}$ -planes are represented by points in $G(2, n)$. In three dimensions, the λ -plane is an element of the null orthogonal Grassmannian. What happens in higher dimensions? The description of the external kinematical data in six dimensions is particularly simple [190]. The complexified Lorentz group can be taken to be $SO(5, 1) \sim SL(4)$, and a null momentum vector can be represented as an antisymmetric (4×4) tensor p^{IJ} of vanishing determinant. The complexified little group is $SL(2) \times SL(2)$. As such, we can express the momentum p_a^{IJ} of particle a as,

$$p_a^{IJ} = \epsilon^{\alpha\beta} \lambda_{a\alpha}^I \lambda_{a\beta}^J (= \epsilon^{\dot{\alpha}\dot{\beta}} \tilde{\lambda}_{a\dot{\alpha}}^I \tilde{\lambda}_{a\dot{\beta}}^J). \quad (3.15.312)$$

Note the similarity to ordinary spinor-helicity variables—except that here, the $\alpha, \dot{\alpha}$ indices aren't Lorentz indices as familiar from four dimensions, but are instead indices of the $SL(2) \times SL(2)$ little group. We can group all the λ 's for the particles $a = 1, \dots, n$ together into a $(4 \times 2n)$ -matrix,

$$\Lambda_A^I = (\lambda_{11}^I \ \lambda_{12}^I \ \lambda_{21}^I \ \lambda_{22}^I \ \cdots \ \lambda_{n1}^I \ \lambda_{n2}^I). \quad (3.15.313)$$

Momentum conservation is then the statement that,

$$\Lambda_A^I \Lambda_B^J J^{AB} = 0 \quad \text{where} \quad J \equiv \begin{pmatrix} 0 & 1 & & & \\ -1 & 0 & & & \\ & & \ddots & & \\ & & & 0 & 1 \\ & & & -1 & 0 \end{pmatrix}. \quad (3.15.314)$$

Thus, in close parallel with $(2+1)$ dimensions, the external data in 6 dimensions is associated with a point in the null symplectic Grassmannian, [191]. It would be interesting to see if this structure has any role to play in six-dimensional physics.

Let us close by returning to a number of concrete open directions of research flowing more directly from the ideas presented here.

In this chapter, we have given a complete classification and understanding of all reduced on-shell diagrams, whose invariant content is captured by the permutation associated with the left-right paths. Amongst other things, all terms occurring in the tree-level BCFW recursion relations are reduced graphs, and indeed, the recursion can be described purely combinatorially as a simple and canonical “bridging” of permutations. We have however also seen that non-reduced on-shell diagrams are

also physically important, directly giving the loop integrand. Of course, the non-reduced graphs for the loop integrand arise from merging adjacent legs of higher-point reduced graphs, which we understand completely. Nonetheless, it would clearly be interesting and important to try and extend the classification of the on-shell diagrams to non-reduced graphs as well; in other words, we would like to understand all the invariants on non-reduced graphs, that can be related by merges and square moves. Obviously the left-right path permutations are still invariants, but there are clearly further invariants as well. For instance, suppose we have two non-reduced graphs with exactly the same permutation, but where the first graph has a bad double-crossing between the two paths starting at a and b , while the second has a bad double-crossing for a different pair of paths starting at c and d . Clearly square moves and merges can't connect these two diagrams. It is plausible that the complete set of invariants involves the permutation together with other labels characterizing the pattern of intersections of the left-right paths. Finding a complete classification will be very important, not least because it would allow us to cast the BCFW construction of all-loop integrand in completely combinatorial terms.

We have seen that the all-loop integrand is naturally presented in a “ $d\log$ ” form. This form begs to be integrated, indeed most naïvely of course, these forms integrate to zero! The integrals don't vanish because of branch cuts in the arguments of the logarithms, on the real contour of integration. This leads to novel ways of performing the loop integrations directly in spacetime, which will be pursued in future work.

Finally, the BCFW construction of scattering amplitudes in the Grassmannian still leaves something to be desired. It is not entirely satisfying to give the scattering amplitude a fundamentally recursive definition. Put another way, we have yet to see locality and unitarity fully emerge from more primitive principles in a completely satisfactory way. We would like to have a direct definition of the amplitude, linked to the Grassmannian, making all the symmetries manifest, and discover their singularities in the form of factorization and forward limits as an emergent property. This is bound to be linked to the “polytope picture” studied in [37, 60]. This line of thought will certainly be taken up again with our vastly improved understanding of the positive Grassmannian in hand.

Chapter 4

Locality and Unitarity from Positivity

4.1 Introduction and summary

We have taken significant steps towards a new understanding of scattering amplitudes in $\mathcal{N} = 4$ SYM. Physically, we have understood that the full amplitude, to all loop orders, can be represented as a sum over on-shell processes; mathematically, these on-shell processes are associated with the simple but deep structure of the positive Grassmannian. However, we have not yet succeeded in our main goal, which is to find an entirely new understanding of "what the amplitudes really are", where the fundamental principles of locality and unitarity can be seen as emergent properties from a more primitive starting point.

Our failure to do so so far can be seen quite vividly by the fact that the most natural objects from our Grassmannian viewpoint are individual on-shell processes, but to get the full amplitude we must combine together these on-shell diagrams in certain combinations, as dictated by the all-loop recursion relations. But why do we add these particular combinations; what is wrong with other combinations? The answer is of course that only the "correct" combination is both local and unitary! Thus, despite the fact that we are describing scattering processes in a new way without Lagrangians and path integrals, with no mention of gauge redundancy and no Feynman diagrams, we are still firmly tethered to the usual formalism of quantum field theory. We have not yet succeeded in seeing locality and unitarity emerge from more basic ideas; quite the contrary, while we have found a new basic set of objects from which to build the amplitude, we are *using* locality and unitarity to define what the amplitude is. In order to realize our goal, we need to "cut the chord" tethering us to the usual language of QFT—concepts like "factorization" and "cuts" and "recursion relations" can not be part of the fundamental definition we are looking for. Instead we need

to find a new question to which "the amplitude" is the answer, and understand how locality and unitarity emerge from this new starting point.

For some time, there has been a vague indication for what this new question should be. The amplitude seems to be "the volume" of "some region" in "some space", with all the different representation of the amplitude simply corresponding to different "triangulations" of this space. This picture was partially realized in some extremely simple examples, for NMHV tree amplitudes and MHV 1-loop amplitudes, but the techniques seemed to rely on special features of these cases and seemed impossible to extend to general amplitudes.

We now finally know how to make this picture precise for all amplitudes, in so doing we have found a first example of the complete reformulation for scattering amplitudes we have been seeking. The relevant object is again associated with the Grassmannian but in a new way. We will here content ourselves with motivating and defining this simple new mathematical structure, and showing how it determines "the amplitude". The way in which locality and unitarity and locality emerge, as well as new computations of amplitudes to all loop orders, will be presented in more detailed future work.

To begin with, let us start with the simplest familiar geometric object of all, a triangle in two dimensions. Thinking projectively, the vertices are Z_1^I, Z_2^I, Z_3^I where $I = 1, \dots, 3$. The interior of the triangle is a collection of points of the form

$$Y^I = c_1 Z_1^I + c_2 Z_2^I + c_3 Z_3^I, \text{ where } c_a > 0 \quad (4.1.1)$$

Indeed, this was how we began our discussion of positive Grassmannian; the interior of the triangle can be thought of as $(c_1, c_2, c_3)/\text{GL}(1)$, with $c_a > 0$. One obvious generalization of the triangle is to a simplex in a general projective space, which then further generalizes to the positive Grassmannian as we have discussed in previous chapters.

But there is another natural generalization we can consider. Instead of considering a triangle, we can think of a more general polygon with n vertices Z_1^I, \dots, Z_n^I . Once again we would like to discuss the interior of this region. However in general this is not canonically defined—if the points Z_a are distributed randomly, they don't obviously

enclose a region of which the Z_a are all vertices. Only if the Z_a form a *convex* polygon do we have a canonical "interior" to talk about.

We know that convexity for the Z_a is a special case of positivity in the sense of the positive Grassmannian. In other words, the points Z_a form a closed polygon only if the $3 \times n$ matrix with columns Z_a has all positive (ordered) minors:

$$\langle Z_{a_1} Z_{a_2} Z_{a_3} \rangle > 0 \quad \text{for} \quad a_1 < a_2 < a_3 \quad (4.1.2)$$

Having arranged for this, the interior of the polygon is given by points of the form

$$Y^I = c_1 Z_1^I + c_2 Z_2^I + \cdots + c_n Z_n^I \quad \text{with} \quad c_a > 0 \quad (4.1.3)$$

Note that this can be thought of as an interesting pairing of two different positive spaces. We have

$$(c_1, \cdots, c_n) \in G^+(1, n), \quad (Z_1, \cdots, Z_n) \in G^+(3, n) \quad (4.1.4)$$

which we are jamming together to produce

$$Y^I = c_a Z_a^I \quad (4.1.5)$$

in $G(1, 3)$.

This object has a natural generalization to higher projective spaces; we can consider n points Z_a^I in $G(1, 1 + m)$, with $I = 1, \cdots, 1 + m$, which are positive

$$\langle Z_{a_1} \cdots Z_{a_{1+m}} \rangle > 0 \quad (4.1.6)$$

Then, the analog of the "inside of the polygon" are points of the form

$$Y^I = c_a Z_a^I, \quad \text{with} \quad c_a > 0 \quad (4.1.7)$$

It is trivial to see that this object is only cyclically invariant if m is even; so the first new case beyond simple polygons is $m = 4$. We can further generalize this structure into the Grassmannian, by considering a region in $G(k, k + m)$ with co-ordinates

$$Y_\alpha^I, \quad \alpha = 1, \cdots, k, \quad I = 1, \cdots, k + m \quad (4.1.8)$$

determined by some positive external data via

$$Y_\alpha^I = C_{\alpha a} Z_a^I \quad (4.1.9)$$

where

$$C_{aa} \subset G^+(k, n), Z_a^I \subset G^+(k + m, n) \quad (4.1.10)$$

Let us call this space

$$P_{n,k;m} \quad (4.1.11)$$

which carves out a part of $G(k, k + m)$. Said in words, we are given a collection of Z_a which are a positive configuration of vectors in $k + m$ dimensions. These determine a region inside $G(k, k + m)$, which is the image of the top-cell of the Grassmannian $G(k, n)$ under the map given above.

Incredibly, for $m = 4$, $P_{n,k;m=4}$ (which we henceforth refer to as $P_{n,k}$ for brevity) actually completely determines all the $N^k MHV$ tree amplitudes! Locality and unitarity for trees follow directly from the positive geometry. Indeed, given the rules for determining the amplitude we will describe in a moment, approaching the singularities of the amplitude corresponds to moving to the boundaries of this region. For $m = 4$, which is the case of direct relevance to amplitudes, it is easy to see that the boundaries correspond to those k planes that pass through the 4-plane made from $Z_i Z_{i+1} Z_j Z_{j+1}$! Not co-incidentally, if we think of the Z 's as momentum-twistor external data, these precisely correspond to the structure of local poles where $\langle ii + 1 jj + 1 \rangle \rightarrow 0$. Furthermore, on this boundary, positivity forces the space to split into "left" and "right" pieces with lower k and n , precisely reproducing the factorization property that reflects unitarity. Locality and unitarity both emerge from positivity.

Before showing how to determine the (super)amplitude from this geometry, let us define the notion of a "volume" associated with this space. We can do this already going all the way back to the triangle or polygon. The usual notion of "area" is obviously not projectively meaningful. However there is a closely related idea that is. For the triangle, we can consider a 2-form in Y -space, which has logarithmic singularities on the boundaries of the triangle. Written invariantly, this 2-form is

$$\omega_{123} = \frac{\langle Y dY dY \rangle \langle 123 \rangle^2}{\langle Y12 \rangle \langle Y23 \rangle \langle Y31 \rangle} \quad (4.1.12)$$

If we pick a particular set of positive co-ordinates e.g. if we expand $Y = Z_3 + c_1 Z_1 +$

$c_2 Z_2$, then

$$\omega_{123} = \frac{dc_1}{c_1} \frac{dc_2}{c_2} \tag{4.1.13}$$

The form for the polygon P can be obtained by first triangulating the polygon in some way, then summing the elementary two-form for each triangle, for instance as $\omega = \sum_i \omega_{1ii+1}$.

In general, given some space P we can try and find a form ω_P with logarithmic singularities on the boundaries of P . If such a form exists, it has all the same additive properties as the intuitive notion of “volume”. And to prove that it exists and also compute it, all we need to do is “triangulate” (better, “cellulate”) the space P , in other words, find a collection of positive co-ordinates which tile the whole space, without overlapping. For each cell, there is a form which is just given wedging together the $d\log$ ’s of the positive co-ordinates.

We’ll now show that the tree amplitude is completely fixed by $\omega_{P_{n,k}}$. But how do we extract a super-amplitude from this completely bosonic object? Also, there is the peculiar feature that the external data are $(4 + k)$ dimensional, while we usually think of the data as 4 bosonic and 4 fermionic variables per particle.

The geometry tells us the right way to think about this. Any specific point Y_0 in $G(k, k + 4)$ breaks the $GL(4 + k)$ symmetry of the projective space down to $GL(4)$ symmetry, that we identify with our familiar conformal symmetry. In other words, suppose

$$Y = (\mathbf{1}_{k \times k} | 0_{k \times 4}) \tag{4.1.14}$$

Then it makes sense to think of the first 4 components of the Z_a as being our usual bosonic momentum-twistors z_a acted on by the unbroken $GL(4)$:

$$Z_a = \begin{pmatrix} z_a \\ *_1 \\ \vdots \\ *_k \end{pmatrix} \tag{4.1.15}$$

but we still have to decide how to interpret the remaining k entries of Z_a . Clearly, if they are normal bosonic variables, we have an infinite number of extra degrees of

freedom. It is therefore natural to try and make the remaining components infinitesimal, by saying that some $\mathcal{N} + 1$ 'st power of them vanishes. This is equivalent to saying that each entry can be written in terms of Grassmann parameters as

$$Z_a = \begin{pmatrix} z_a \\ \phi_1^A \cdot \eta_{1A} \\ \vdots \\ \phi_k^A \cdot \eta_{Ak} \end{pmatrix} \quad (4.1.16)$$

where $\phi_{1,\dots,k}$ and η_a are Grassmann parameters, and $A = 1, \dots, \mathcal{N}$.

Now there is a unique way to extract the amplitude. We simply localize the form $\omega_{P_{n,k}}$ to Y_0 , and integrate over the ϕ 's:

$$M_{n,k}(z_a, \eta_a) = \int d^{\mathcal{N}} \phi_1 \cdots d^{\mathcal{N}} \phi_k \int \omega_{P_{n,k}} \delta^{4k}(Y; Y_0) \quad (4.1.17)$$

Note that there is really no integral to perform in the second step; the delta functions fully fix Y . Indeed, any form ω on the Grassmannian can always be written as

$$\omega_{P_{n,k}}[Y; Z_a] = \langle Y_1 \cdots Y_k d^4 Y_1 \rangle \cdots \langle Y_1 \cdots Y_k d^4 Y_k \rangle f_{n,k}(Y; Z_a) \quad (4.1.18)$$

and our expression just says that

$$M_{n,k}(z_a, \eta_a) = \int d^{\mathcal{N}} \phi_1 \cdots d^{\mathcal{N}} \phi_k f_{n,k}(Y_0; Z_a) \quad (4.1.19)$$

Note that we can define this operation for an \mathcal{N} , however, only for $\mathcal{N} = 4$ does M further have weight zero under the rescaling (z_a, η_a) .

In order to compute $\omega_{P_{n,k}}$ we need to find a cell decomposition of $P_{n,k}$. In turn, this corresponds to finding special $4k$ dimensional cells of $G^+(k, n)$, whose images under the $Y = C \cdot Z$ map give non-overlapping cells that cover all of $P_{n,k}$. Very beautifully, we find that those collection of $4k$ dimensional cells of $G^+(k, n)$ corresponding to the BCFW representation of tree amplitudes provide one class of cellulations of this sort!

Let us move on to loops. Again, we defer the discussion of why even thinking about "loops" is completely natural to future work, and here simply describe what extended positive space determines the form corresponding to the loop integrand. We can already start at $k = 0$ with the MHV loop integrand; the integration variables are just L lines in momentum-twistor space. We can represent each line by a pair of

points A_γ for $\gamma = 1, 2$; modulo $GL(2)$ action. For a single loop, the only notion of positivity we can have is obviously simply that

$$A_\gamma^I = C_{\gamma a} Z_a^I \quad (4.1.20)$$

where all the (2×2) minors of the $G(2, n)$ matrix $C_{\gamma a}$ are positive. For L loops we have this condition for each loop, but we clearly need more, since the loops must interact somehow. The only possible extension is to simply say that not only the 2 minors of all the C 's individually, but all the 4×4 minors built from pairs of C 's, 6×6 minors built from triples and so on, are also all positive! In other words, *all* the $GL(2)^L$ invariant minors obtained by of the $2L \times n$ matrix

$$\begin{pmatrix} C^{(1)} \\ C^{(2)} \\ \dots \\ C^{(L)} \end{pmatrix} \quad (4.1.21)$$

are positive.

For general n, k and loop order L , the relevant space is that of a k plane Y in $(k + 4)$ dimensions, together with the space of L lines $A(1, \dots, L)_\gamma$ living in the 4 dimensional space which is in the complement of Y . Our external data Z_a^I are a positive configuration of vector in $4 + k$ dimensions. We then have the region

$$P_{n,k;L} \quad (4.1.22)$$

defined by

$$Y_\alpha^I = C_\alpha a Z_a^I; A_\gamma^{(i)I} = C_\gamma^{(i)} a Z_a^I \quad (4.1.23)$$

where all the minors of the matrix $(k + 2L) \times n$ matrix

$$\begin{pmatrix} C \\ C^{(1)} \\ \dots \\ C^{(L)} \end{pmatrix} \quad (4.1.24)$$

which contain C , and any number of $GL(2)^L$ invariant blocks from the $C^{(1)}, \dots, C^{(L)}$ are positive.

Once again, we must find a cell-decomposition of this space, which then yields the form $\omega_{P_{n,k;L}}$, and the integrand of the super-amplitude at any loop order is extracted from ω in exactly the same way as described above for trees.

Once again, quite remarkably, the singularity structure of the loop integrand encoding both locality and unitarity is a direct consequence of this new positive structure. All-loop BCFW provides one cell-decomposition of this space. But interestingly, while the BCFW decomposition of the tree amplitude also corresponds to quite canonical triangulations, this does not appear true at loop level. Indeed, to e.g. compute the 4 particle amplitude at 3-loops, the loop BCFW recursion forces us to go to begin with 10 pt N^3 MHV tree amplitudes and take forward limits; it is peculiar that we have to go to this very different space to get the result. By contrast in our final formulation, the loop integrand forms are defined directly by positive conditions in the space where they live.

For instance, consider the 4-particle integrand at all loop orders. We can parametrize each $C^{(i)}$ as

$$C^{(i)} = \begin{pmatrix} 1 & x_i & 0 & -w_i \\ 0 & y_i & 1 & z_i \end{pmatrix} \quad (4.1.25)$$

In this simple case the positivity constraints are just that all the 2×2 and 4×4 minors are positive, translating to

$$x_i, y_i, z_i, w_i > 0, (x_i - x_j)(z_i - z_j) + (y_i - y_j)(w_i - w_j) < 0 \quad (4.1.26)$$

Finding the cell decomposition of this extremely simple-looking space, that can be defined on a single line, would give us the 4-particle amplitude to all-loop order.

It is remarkable that the simple picture, merely moving from “triangles” to “polygons”, suitably generalized to the Grassmannian, leads us to the space $P_{n,kL}$, whose “volume” gives us the scattering amplitudes for a non-trivial interacting quantum field theory in four dimensions, with locality and unitarity seen as emergent consequences of positivity. It is also fascinating that while in the conventional formalism of field theory locality and unitarity are at odds, forcing the introduction of large redundancies to be allowed to co-exist, in this new picture they emerge hand-in-hand from the same principle.

$P_{n,k,L}$ is a large generalization of the positive Grassmannian, the role of $G^+(k, n)$ is to provide all the different "shapes" for the possible cell decompositions, but the fundamental object is $P_{n,k,L}$. Interestingly, while $G^+(k, n)$ was relatively recently studied by mathematicians, the space $P_{n,k,L}$ is as of yet completely un-known in mathematics. We expect it to continue to reveal amazing surprises for both physics and mathematics as we initiate a more systematic exploration of its properties.

4.2 MHV amplitudes at all loop orders

In the MHV case there is no supersymmetric extension of external data and the space is just the momentum twistor space P^3 . Therefore, the positivity of external data is just the positivity of external momentum twistors Z_i^I , $I = 1, \dots, 4$, ie. $Z \in G_+(4, n)$. The point inside the positive region is

$$A^I = C_a Z_a^I, \quad a = 1, \dots, n, \quad I = 1, \dots, 4 \quad (4.2.27)$$

The definition (4.2.27) is not cyclically invariant therefore this is not a case of our interest. Instead of a single point A we can consider two points A, B that form a line $A_\alpha = (A, B)$.

I. One-loop amplitudes

In this case we have just a single line.

$$A_\alpha^I = C_{\alpha a} Z_a^I \quad (4.2.28)$$

where $C_{\alpha a}$ is a positive Grassmannian $G_+(2, 4)$. The boundaries of this region are $\langle AB i i+1 \rangle = 0$. The possible boundaries of the space are $\langle AB i j \rangle = 0$, ie. where the line $Z_A Z_B$ intersects the line $Z_i Z_j$. Plugging (4.2.28) we get

$$\langle AB i j \rangle = \sum_{1 \leq k < \ell \leq n} (k \ell) \langle k \ell i j \rangle \quad (4.2.29)$$

We require $\langle AB i j \rangle$ to be positive inside the positive region and zero on the boundary. However, the sum (4.2.29) does not have the uniform sign for general

indices i, j, k, ℓ . Despite all minors of the C -matrix are positive, $\langle k \ell \rangle > 0$ for $k < \ell$, not all four-brackets of external momentum twistors are positive as well, e.g. if $k < i < \ell < j$ then $\langle k \ell i j \rangle < 0$ while for $k < \ell < i < j$, $\langle k \ell i j \rangle < 0$. This does not happen when $j = i+1$ because $\langle k \ell i i+1 \rangle > 0$. As a result the boundaries of the space are $\langle AB i i+1 \rangle$ for $i = 1, 2, \dots, n$.

The form associated with the positive region has logarithmic singularities on the boundaries of the region which are $\langle AB i i+1 \rangle$. Therefore the general structure of the form is

$$\Omega_n = \frac{\langle AB d^2 A \rangle \langle AB d^2 B \rangle \cdot \mathcal{N}(AB, Z_i)}{\langle AB 12 \rangle \langle AB 23 \rangle \langle AB 34 \rangle \dots \langle AB n 1 \rangle} \quad (4.2.30)$$

where the numerator forces all singularities to be logarithmic. In fact, just demanding this property together with vanishing on all unphysical singularities¹ fixes the numerator $\mathcal{N}(AB, Z_i)$ completely as we will show in []. In the four-point case the numerator is independent on AB and we get

$$\Omega_4 = \frac{\langle AB d^2 A \rangle \langle AB d^2 B \rangle \langle 1234 \rangle^2}{\langle AB 12 \rangle \langle AB 23 \rangle \langle AB 34 \rangle \langle AB 41 \rangle}. \quad (4.2.31)$$

We want to triangulate the positive space P in terms of elementary building blocks, each of them is just the dlog of all variables. BCFW gives such a triangulation as was showed in the chapters 2 and 3 called the *kermit* formula. There is also a local expansion discussed in chapter 1 where the one-loop amplitude is written as linear combination of pentagons and boxes. This is a very different expansion than the kermit formula, note that term-by-term it contains only physical poles. However, this does not correspond to the triangulation of the positive region. The reason is that some of the lower dimensional boundaries are outside the positive region. Let us show it explicitly on the generic pentagon. Let us calculate the residue on the triple cut $\langle AB n 1 \rangle = \langle AB i i+1 \rangle = \langle AB j j+1 \rangle = 0$. It is easy to see that the residue is non-zero but the codimension three boundary representing the geometry of the line $Z_A Z_B$ is not allowed. Look at the double-cut $\langle AB i i+1 \rangle = \langle AB j j+1 \rangle = 0$, then

$$Z_A = Z_i + \alpha Z_{i+1}, \quad Z_B = Z_j + \beta Z_{j+1} \quad (4.2.32)$$

¹We wrote the form Ω_n such that only physical poles $\langle AB i i+1 \rangle$ are present in (4.2.30). However, these are only first boundaries. The numerator must vanish on all unphysical higher boundaries.

and

$$C = \begin{pmatrix} 0 & \dots & 0 & 1 & \alpha & 0 & \dots & 0 & 0 & 0 & 0 & \dots & 0 \\ 0 & \dots & 0 & 0 & 0 & 0 & \dots & 0 & 1 & \beta & 0 & \dots & 0 \end{pmatrix} \quad (4.2.33)$$

Minors of this matrix must be positive, therefore both $\alpha, \beta > 0$. Now we calculate the triple cut $\langle AB1n \rangle = 0$,

$$\langle AB1n \rangle = \langle 1ijn \rangle + \beta \langle 1ij+1n \rangle + \alpha \langle 1i+1jn \rangle + \alpha\beta \langle 1i+1j+1n \rangle \quad (4.2.34)$$

All terms on the right hand side are positive because $\langle 1i+1j+1n \rangle > 0$, all four-brackets are ordered, and there is no way how to set $\langle AB1n \rangle$ to zero. Similar argument applies for all other terms and none of the terms in the sum (??) lies in the positive region only.

II. Two-loop amplitudes

We generalize the picture presented for the one-loop integrands to the integrand at any loop order. We start with the MHV case where the positive data are external momentum twistors living in $G_+(4, n)$. All the issues with extended twistors for $k > 0$ are absent here. We first discuss the two-loop amplitudes and then the generalization to all loop orders.

In the MHV one-loop case the region that defined the integrand was associated with the single line AB in P^3 which was parametrized as

$$\mathcal{A}_\alpha^I = C_{\alpha a} Z_a^I, \quad I = 1, \dots, 4 \quad (4.2.35)$$

where $\mathcal{A}_\alpha = (A, B)$, matrix $C_{\alpha a}$ is the top cell of $G_+(2, n)$ and Z_a are the positive external data living in $G_+(4, n)$. There is a natural generalization to the two-loop case. Instead of a single line we consider two lines $(AB), (CD)$ in P^3 parametrized using positive external data as

$$\mathcal{A}_\alpha^{(1)I} = C_{\alpha a}^{(1)} Z_a^I \quad (4.2.36)$$

$$\mathcal{A}_\alpha^{(2)I} = C_{\alpha a}^{(2)} Z_a^I \quad (4.2.37)$$

with $\mathcal{A}_\alpha^{(1)} = (A, B)$ and $\mathcal{A}_\alpha^{(2)} = (C, D)$. Each line has its own private $G_+(2, n)$ matrix $C_{\alpha\alpha}^{(1)}$, resp. $C_{\alpha\alpha}^{(2)}$. We can choose them to be top cells of $G_+(2, n)$ but that would be a redundant description because we really look just for a union of all four-dimensional cells similar to the one-loop case. Now if we do not impose any additional constraints on matrices $C^{(1)}$, $C^{(2)}$, the region we get is just two copies of the MHV one-loop, and therefore corresponds to the square of MHV one-loop integrand. We have to do something more special to get the region for MHV two-loop integrand. Let us combine $C^{(1)}$ and $C^{(2)}$ into the bigger 4 by n matrix,

$$C = \begin{pmatrix} C^{(1)} \\ C^{(2)} \end{pmatrix} = \begin{pmatrix} * & * & * & * & \dots & * & * \\ * & * & * & * & \dots & * & * \\ * & * & * & * & \dots & * & * \\ * & * & * & * & \dots & * & * \end{pmatrix} \quad (4.2.38)$$

This matrix has positive 2 by 2 minors made out of first two or last two rows. The extra constraint we impose is that: *All 4 by 4 minors of matrix C are positive.* Then the space of all lines (AB) and (CD) built by the collection of all eight-dimensional matrices (4.2.38) under the map (4.2.37) specify the region P that corresponds to the n -pt two-loop integrand.

The integrand form

As in the previous sections there exists an unique form Ω associated with the region that has logarithmic singularities on its boundaries. There is a trivial relation between the form $\Omega_n^{(2)}$ and the integrand for the MHV amplitude $I_n^{(2)}$,

$$\Omega_n^{(2)} = d\omega_{AB} d\omega_{CD} \times I_n^{(2)}(AB, CD, Z_i) \quad (4.2.39)$$

where $d\omega_{AB}$ and $d\omega_{CD}$ are measures for lines (AB) and (CD) ,

$$d\omega_{AB} = \langle AB d^2 A \rangle \langle AB d^2 B \rangle \quad d\omega_{CD} = \langle CD d^2 C \rangle \langle CD d^2 D \rangle. \quad (4.2.40)$$

The integrand $I_n^{(2)}(AB, CD, Z_i)$ is a rational function of two lines (AB) , (CD) and external twistors Z_i . The poles of $I_n^{(2)}$ are associated with the boundaries of the positive region:

$$\langle ABCD \rangle \text{ and } \langle AB_{ii+1} \rangle, \langle CD_{jj+1} \rangle \quad \text{for } i, j = 1, \dots, n \quad (4.2.41)$$

and we can write in the form

$$I_n^{(2)}(AB, CD, Z_i) = \frac{N(AB, CD, Z_i)}{\langle AB_{12} \rangle \dots \langle AB_{n1} \rangle \langle ABCD \rangle \langle CD_{12} \rangle \dots \langle CD_{n1} \rangle} \quad (4.2.42)$$

where the numerator $N(AB, CD, Z_i)$ is a degree $(n - 3)$ function in (AB) , (CD) and degree 4 function in Z_i . Its role is to vanish on all configurations that violate properties of the amplitude, or equivalently ensures that the corresponding region is positive.

BCFW triangulation

The loop BCFW recursion relations gives us the four-point two-loop amplitude written in the form,

$$M_{4,2}^{2-loop} = \text{FL}(M_{6,1}^{1-loop}) \quad (4.2.43)$$

where FL stands for the forward-limit. Six point NMHV 1-loop amplitude includes 16 terms. There are different ways how to perform a forward-limit, also the number of terms is not constant. We use the most natural choice of BCFW shifts which also allows us to do directly the double-forward-limit on eight point N²MHV tree amplitude. As a result we get eight terms and another eight are obtained by symmetrization $AB \leftrightarrow CD$. Each term is fully specified by the C matrix which contains eight parameters $\beta_1, \beta_2, \dots, \beta_8$. The eight matrices are

$$\begin{pmatrix} 1 + \beta_3\beta_8 & \beta_8 & -\beta_1\beta_2 + \beta_8(\beta_4 - \beta_1\beta_2\beta_3) & -\beta_2(1 + \beta_3\beta_8) \\ \beta_3 & 1 & \beta_4 - \beta_1\beta_2\beta_3 & -\beta_2\beta_3 \\ -\beta_6\beta_7 & 0 & 1 + \beta_1\beta_5 + \beta_1\beta_7(1 + \beta_2\beta_6) & \beta_5 + \beta_7(1 + \beta_2\beta_6) \\ -\beta_6 & 0 & \beta_1(1 + \beta_2\beta_6) & 1 + \beta_2\beta_6 \end{pmatrix} \begin{pmatrix} 1 + \beta_8(\beta_3 - \beta_4\beta_5\beta_6) & \beta_8(1 + \beta_2\beta_6) & \beta_6\beta_8(1 + \beta_1\beta_5) & \beta_5\beta_6\beta_8 \\ \beta_3 - \beta_4\beta_5\beta_6 & 1 + \beta_2\beta_6 & \beta_6(1 + \beta_1\beta_5) & \beta_5\beta_6 \\ -\beta_4(\beta_5 + \beta_7) & \beta_2 & 1 + \beta_1(\beta_5 + \beta_7) & \beta_5 + \beta_7 \\ -\beta_4 & 0 & \beta_1 & 1 \end{pmatrix} \\
\begin{pmatrix} 1 + \beta_2\beta_8 & \beta_8 & \beta_4\beta_8(1 + \beta_1\beta_3) & \beta_3\beta_4\beta_8 \\ \beta_2 & 1 & \beta_4(1 + \beta_1\beta_3) & \beta_3\beta_4 \\ -\beta_6\beta_7 & 0 & 1 + \beta_1(\beta_3 + \beta_5 + \beta_7) & \beta_3 + \beta_5 + \beta_7 \\ -\beta_6 & 0 & \beta_1 & 1 \end{pmatrix} \begin{pmatrix} 1 - \beta_4\beta_5\beta_6\beta_8 & \beta_8 & \beta_8(\beta_2 + \beta_6(1 + \beta_1\beta_3 + \beta_1\beta_5)) & \beta_6\beta_8(\beta_3 + \beta_5) \\ -\beta_4\beta_5\beta_6 & 1 & \beta_2 + \beta_6(1 + \beta_1\beta_3 + \beta_1\beta_5) & \beta_6(\beta_3 + \beta_5) \\ -\beta_4(\beta_5 + \beta_7) & 0 & 1 + \beta_1(\beta_3 + \beta_5 + \beta_7) & \beta_3 + \beta_5\beta_7 \\ -\beta_4 & 0 & \beta_1 & 1 \end{pmatrix} \\
\begin{pmatrix} 1 + \beta_8(\beta_2 - \beta_4\beta_5\beta_6) & \beta_8 & \beta_6\beta_8(1 + \beta_1\beta_3 + \beta_1\beta_5) & \beta_6\beta_8(\beta_3 + \beta_5) \\ \beta_2 - \beta_4\beta_5\beta_6 & 1 & \beta_6(1 + \beta_1\beta_3 + \beta_1\beta_5) & \beta_6(\beta_3 + \beta_5) \\ -\beta_4(\beta_5 + \beta_7) & 0 & 1 + \beta_1(\beta_3 + \beta_5 + \beta_7) & \beta_3 + \beta_5 + \beta_7 \\ -\beta_4 & 0 & \beta_1 & 1 \end{pmatrix} \begin{pmatrix} 1 & \beta_1 & \beta_2 & 0 \\ -1 & 0 & \beta_3 & \beta_4 \\ 0 & \beta_1\beta_4 & \beta_2\beta_4 + \beta_5 + \beta_1\beta_3\beta_6 & \beta_1\beta_4\beta_6 \\ -\beta_8 & -\beta_1\beta_4 & -\beta_2\beta_4 + \beta_1\beta_3\beta_7 + \beta_3\beta_8 & \beta_1\beta_4\beta_7 + \beta_4\beta_8 \end{pmatrix} \\
\begin{pmatrix} 1 & \beta_1 & \beta_2 & 0 \\ -1 & 0 & \beta_3 & \beta_4 \\ \beta_1 + \beta_5 & \beta_6 & -\beta_1\beta_3 & -\beta_1\beta_4 \\ -\beta_1 & \beta_7 + \beta_1\beta_4\beta_8 & \beta_1\beta_3 + \beta_2\beta_4\beta_8 & \beta_1\beta_4 \end{pmatrix} \begin{pmatrix} 1 + \beta_4\beta_8 & \beta_8(1 + \beta_3\beta_6) & -\beta_1\beta_2 + \beta_8(\beta_6 - \beta_1\beta_2\beta_4) & -\beta_2(1 + \beta_4\beta_8) \\ \beta_4 & 1 + \beta_3\beta_6 & \beta_6 - \beta_1\beta_2\beta_4 & -\beta_2\beta_4 \\ -\beta_5\beta_7 & \beta_3 & 1 + \beta_1\beta_7(1 + \beta_2\beta_5) & \beta_7(1 + \beta_2\beta_5) \\ -\beta_5 & 0 & \beta_1(1 + \beta_2\beta_5) & 1 + \beta_2\beta_5 \end{pmatrix}$$

and other eight are obtained just by flipping first two and last two rows. The form Ω_i for each term is just the dlog of all eight parameters,

$$\Omega_i = \text{dlog}\beta_1 \text{dlog}\beta_2 \dots \text{dlog}\beta_8 \quad (4.2.44)$$

Now we have to solve for β_i in terms of bi-twistors AB, CD and external momentum twistors Z_1, Z_2, Z_3, Z_4 . Of course, the result is guaranteed to be dual conformal invariant and therefore written in terms of four-brackets.

The form Ω_P for the whole positive region is then written as

$$\Omega_P = \sum_{i=1}^{16} \Omega_i(AB, CD, Z_i) \quad (4.2.45)$$

with $\Omega_{8+i}(AB, CD, Z_i) = \Omega_i(CD, AB, Z_i)$, therefore only eight matrices are really independent and these we present above.

From matrix to the form

Let us show on the explicit example of the seventh matrix how to solve for β_i and rewrite (4.2.44) as $\Omega_i(AB, CD, Z_i)$.

$$\begin{pmatrix} 1 & \beta_1 & \beta_2 & 0 \\ -1 & 0 & \beta_3 & \beta_4 \\ \beta_1 + \beta_5 & \beta_6 & -\beta_1\beta_3 & -\beta_1\beta_4 \\ -\beta_1 & \beta_7 + \beta_1\beta_4\beta_8 & \beta_1\beta_3 + \beta_2\beta_4\beta_8 & \beta_1\beta_4 \end{pmatrix} \quad (4.2.46)$$

It is easy to solve for coefficients $\beta_1, \beta_2, \beta_3, \beta_4$ because these are the only parameters of first two rows. We know that the line AB has four degrees of freedom so the solution must be independent on CD . The four-brackets with AB only are

$$\begin{aligned} \langle AB12 \rangle &= \beta_2\beta_4, & \langle AB23 \rangle &= \beta_4, & \langle AB34 \rangle &= \beta_1, & \langle AB14 \rangle &= \beta_1\beta_3, \\ \langle AB31 \rangle &= \beta_1\beta_4, & \langle AB42 \rangle &= \beta_2 + \beta_3 \end{aligned} \quad (4.2.47)$$

where we suppressed $\langle 1234 \rangle$ which is always present on the right hand side. We can easily construct the ratios that are projective in AB ,

$$\beta_1 = \frac{\langle AB31 \rangle}{\langle AB23 \rangle}, \quad \beta_2 = \frac{\langle AB12 \rangle}{\langle AB23 \rangle}, \quad \beta_3 = \frac{\langle AB14 \rangle}{\langle AB34 \rangle}, \quad \beta_4 = \frac{\langle AB31 \rangle}{\langle AB34 \rangle} \quad (4.2.48)$$

Solving for $\beta_5, \beta_6, \beta_7, \beta_8$ is a little more complicated but still the solutions are very easy to find

$$\begin{aligned} \beta_5 &= \frac{\langle AB(CD2) \cap (341) \rangle \langle AB13 \rangle}{\langle CD12 \rangle \langle AB23 \rangle \langle AB34 \rangle}, & \beta_6 &= \frac{\langle 34(AB1) \cap (CD1) \rangle \langle AB13 \rangle}{\langle CD12 \rangle \langle AB23 \rangle \langle AB34 \rangle} \\ \beta_7 &= \frac{\langle CD(AB) \cap (341)(23) \cap (AB1) \rangle \langle AB13 \rangle}{\langle CD23 \rangle \langle AB12 \rangle \langle AB23 \rangle \langle AB34 \rangle}, & \beta_8 &= \frac{\langle AB(CD2) \cap (341) \rangle}{\langle AB12 \rangle \langle CD23 \rangle} \end{aligned}$$

Once we have all β_i , the form is trivial (4.2.44). We can also rewrite (4.2.44) in the more standard way as

$$\Omega_7 = \langle AB d^2 A \rangle \langle AB d^2 B \rangle \times \mathcal{I}_7(AB, CD, Z_i) \quad (4.2.49)$$

where

$$\mathcal{I}_7(AB, CD, Z_i) = \frac{\langle AB13 \rangle^2 \langle 1234 \rangle^4}{\langle AB23 \rangle \langle AB34 \rangle \langle AB14 \rangle \langle CD12 \rangle \langle CD23 \rangle \langle 34(AB1) \cap (CD1) \rangle \langle CD(23) \cap (AB1) \rangle \langle AB \cap (341) \rangle} \quad (4.2.50)$$

Note that the expression contains three spurious poles. We can do this exercise for remaining seven matrices (and get other eight just by flipping $AB \leftrightarrow CD$). The sum of all sixteen terms is then equal to the sum of four double boxes.

III. Generalization to all loop orders

The picture we presented at two-loops has a natural generalization to all loop orders. At L loops we consider L lines $(AB)_1, \dots, (AB)_L$ in P^3 parametrized as usual

$$\begin{aligned} \mathcal{A}_\alpha^{(1)I} &= C_{\alpha a}^{(1)} Z_a^I \\ \mathcal{A}_\alpha^{(2)I} &= C_{\alpha a}^{(2)} Z_a^I \\ &\vdots \\ \mathcal{A}_\alpha^{(L)I} &= C_{\alpha a}^{(L)} Z_a^I \end{aligned} \tag{4.2.51}$$

where all $C^{(i)}$ are top cells of $G_+(2, n)$, resp. the collection of all four-dimensional cells of $G_+(2, n)$. Without any other constrain this would correspond to n^{th} power of one-loop amplitude. Let us combine all $G_+(2, n)$ matrices into the big $2L$ by n matrix C ,

$$C = \begin{pmatrix} C^{(1)} \\ C^{(2)} \\ \vdots \\ C^{(L)} \end{pmatrix} = \left(\begin{array}{ccccccc} * & * & * & \dots & * & * & * \\ * & * & * & \dots & * & * & * \\ \hline * & * & * & \dots & * & * & * \\ * & * & * & \dots & * & * & * \\ \hline \vdots & \vdots & \vdots & & \vdots & \vdots & \vdots \\ \hline * & * & * & \dots & * & * & * \\ * & * & * & \dots & * & * & * \end{array} \right) \Bigg\} 2L \tag{4.2.52}$$

To get the n -point L -loop MHV amplitude we demand the positivity of all 2ℓ by 2ℓ minors of the matrix C for $\ell = 1, 2, \dots, L$. The minors always include both or none of the rows of the given block from $C^{(i)}$. So we never consider minors that involve just one row of any $C^{(i)}$. This is an obvious assumption because the single row does not have any meaning due to the $GL(2)$ transformation acting on $C^{(i)}$.

The integrand form

As in the previous sections there exists an unique form Ω_P associated with the region that has logarithmic singularities on its boundaries. There is a trivial relation between the form $\Omega_{P_n}^{(L)}$ and the integrand for the MHV amplitude $I_n^{(L)}$,

$$\Omega_{P_n}^{(L)} = d\omega_1 d\omega_2 \dots d\omega_L \times I_n^{(L)}(A_1 B_1, \dots, A_L B_L, Z_i) \quad (4.2.53)$$

where $d\omega_j$ is a measure for a line $(AB)_j$,

$$d\omega_j = \langle A_j B_j d^2 A_j \rangle \langle A_j B_j d^2 B_j \rangle. \quad (4.2.54)$$

The integrand $I_n^{(L)}$ is a dual conformal invariant rational function of L bi-twistors $A_j B_j$ and n external momentum twistors Z_i .

Collinear region

Let us consider n -pt ℓ -loop MHV amplitude and calculate the residue where $(AB)_\ell$ lies in the plane $(Z_{i-1} Z_i Z_{i+1})$ and passes the point Z_i . This is an allowed cut because it does not violate the positivity condition. Furthermore, it does not impose any constraint on the part $(AB)_i$, $i = 1, 2, \dots, \ell-1$ therefore the residuum must be proportional to lower loop amplitude with loop momenta $(AB)_1 \dots (AB)_{\ell-1}$ (with no shifts). In this region we parametrize

$$A_\ell = Z_i \quad B_\ell = \alpha Z_{i-1} + \beta Z_{i+1}$$

where we do not fix $GL(1)$ of α, β (i.e. we are free to fix one of them to 1). As we will see in the next subsection if $\alpha = 0$ or $\beta = 0$, the residuum is directly the lower loop amplitude. Therefore, on this cut

$$\text{Cut} A_n^{(\ell)}(1, 2, \dots, n) = \frac{1}{\alpha\beta} \cdot A_n^{(\ell-1)}(1, 2, \dots, n)$$

This relation has a critical consequence on the integrand of the logarithm of the amplitude. It is very easy to prove that the above expression implies that the logarithm of the amplitude vanishes on this cut.

The other consequence is that if $(AB)_\ell$ is already placed in this special position, i.e. in a plane $(Z_{i-1}Z_iZ_{i+1})$ passing through the point Z_i , there are only two different quadrupole cuts we can get from this triple cut, i.e. $\alpha = 0$ or $\beta = 0$. It is also evident from the expression above, that there are no other choices. Obviously we can not cut some random $\langle AB j j+1 \rangle$ because the corresponding leading singularity does not have a location $(AB)_\ell = Z_i Z_j$ as it should. The only choice would be to cut $\langle (AB)_\ell (AB)_k \rangle$. However, let us look at the minors of the $(4 \times n)$ matrix $(A_\ell B_\ell A_k B_k)$. Most of them are vanishing, the interesting one is $(i-1 i i+1, j)$ for some j ,

$$(i \pm 1 i i+1 j) = (i i \pm 1)_\ell (i+1 j)_k + (i i+1)_\ell (i-1 j)_k$$

Cutting $\langle (AB)_\ell (AB)_k \rangle = 0$ we also set this minor to zero. However, this is a sum of two numbers, both of them non-negative. Therefore setting it to zero would mean to set both terms to zero independently which is not possible, we can not have $(i i+1)_\ell = (i-1 i)_\ell = 0$ – then all minors of $(AB)_\ell$ would be zero.

Loop factorization

There is one additional property which is obvious from positivity: loop factorization. Let us take n -pt ℓ -loop MHV amplitude and calculate the residue $(AB)_\ell = ij$,

$$\text{Cut } A_n^{(\ell)}(1, 2, \dots, n) = \sum_{\ell_1 + \ell_2 = \ell - 1} A_{n_1}^{(\ell_1)}(i, i+1, \dots, j) \cdot A_{n_2}^{(\ell_2)}(j, j+1, \dots, i)$$

This is a consequence of the positivity of $(n \times 2\ell)$ matrix $A_1 B_1 \dots A_\ell B_\ell$.

4.3 N^k MHV one-loop amplitudes

The extension to the general N^k MHV one-loop amplitude must combine both features we saw in previous sections: the special k -plane Y living in $(k+4)$ dimensions and a line AB in \mathbb{P}^3 . There is a natural geometry that unifies both these objects: We consider the $k+4$ dimensional space, the k -plane Y inside this space and the 4-dimensional complement T . The line AB lives in this complement. This means that the space T (the letter T obviously stands for twistor space) is not a fixed \mathbb{P}^3 but it changes depending on the choice of Y .

We have two objects Y_α^I and A_γ^I which can be parametrized

$$Y_\alpha^I = C_{\alpha a} Z_a^I \quad A_\gamma^I = \mathcal{L}_{\gamma a} Z_a^I \quad (4.3.55)$$

where C matrix is $G_+(k, n)$ and the \mathcal{L} matrix is $G_+(2, n)$ as before. But this is not quite correct. The line $A_\alpha^I \sim (AB)$ is defined with respect to the k -plane Y , therefore the invariant objects is the $(k+2)$ -dimensional plane (YAB) rather than the 2-plane (AB) . Let us combine Y and AB into

$$W_\alpha^I = (Y_1^I, Y_2^I, \dots, Y_k^I, A_1^I, A_2^I) \quad (4.3.56)$$

then we expand

$$W_\alpha^I = C_{\alpha a} Z_a^I \quad (4.3.57)$$

where

$$C = \left(\begin{array}{c} \uparrow \\ \leftarrow C^{(Y)} \rightarrow \\ \downarrow \\ \hline \uparrow \\ \leftarrow C^{(A)} \rightarrow \\ \downarrow \end{array} \right) = \left(\begin{array}{cccccc} * & * & * & \dots & * & * \\ \vdots & \vdots & \vdots & \vdots & \vdots & \vdots \\ * & * & * & \dots & * & * \\ \hline * & * & * & \dots & * & * \\ * & * & * & \dots & * & * \end{array} \right) \quad (4.3.58)$$

The condition we impose is that all minors of matrices $C^{(Y)}$ and C are positive.

I. NMHV amplitudes

In the special case of $k = 1$ we can formulate the problem purely geometrically. The matrix $C^{(Y)}$ consists just of one row and the matrix C is $(3 \times n)$,

$$C = \left(\begin{array}{cccccc} * & * & * & \dots & * & * \\ \hline * & * & * & \dots & * & * \\ * & * & * & \dots & * & * \end{array} \right) \quad (4.3.59)$$

All entries in the first row must be positive as well as all (3×3) minors. It is interesting to see what is the symmetry of this matrix. Note that it is NOT a

$GL(3)$ because we treat the first row as being special and it has only positive entries. Therefore the actual symmetry of the matrix is smaller. Let us parametrize C as

$$C = \begin{pmatrix} y_1 & y_2 & y_3 & \cdots & y_{n-1} & y_n \\ y_1 \vec{v}_1 & y_2 \vec{v}_2 & y_3 \vec{v}_3 & \cdots & y_{n-1} \vec{v}_{n-1} & y_n \vec{v}_n \end{pmatrix} \quad (4.3.60)$$

where \vec{v}_j are two-dimensional vectors. Writing C in that form requires the positivity of all (3×3) minors of the matrix

$$\tilde{C} = \begin{pmatrix} 1 & 1 & 1 & \cdots & 1 \\ \vec{v}_1 & \vec{v}_2 & \vec{v}_3 & \cdots & \vec{v}_n \end{pmatrix} \quad (4.3.61)$$

Matrices C and \tilde{C} differ just by re-scaling of columns by y_i which are all positive numbers. The matrix \tilde{C} represents a polygon in \mathbb{P}^2 . There are two different symmetries of \tilde{C} :

1. $GL(2)$ symmetry responsible for the choice of origin of two-dimensional space \vec{v}_i .

$$\vec{v}_j \rightarrow L \cdot \vec{v}_j$$

2. Translation T^2 of all vectors,

$$\vec{v}_j \rightarrow \vec{v}_j + \vec{d}$$

The total symmetry is then $GL(2) \times T^2 \times GL(1)$. This has a very nice geometric interpretation. It represents a convex polygon where three of the points are fixed. This is also the case for the polygon with $GL(3)$ symmetry but there we can fix the three points to arbitrary positions and they are all identified. In the case of $GL(2) \times T^2 \times GL(1)$ the angle between two of the lines connecting these three points is fixed, e.g. the right angle.

The task is to add $n-3$ other points $4, 5, \dots, n$ into the positive quadrant such that the resulting polygon is convex. The fourth point can be obviously added to any position in the first quadrant above the line 13. However, starting with five point we have to consider more cases.

Note that the positive region for four-point $P_{4,1}^{(1)}$ is spanned by a single matrix only. This is an analogue of the top cell of the positive Grassmannian. However, the

corresponding form vanishes. Therefore, we concentrate on the five point case as the first non-trivial.

BCFW triangulation

First we provide the result obtained by the loop BCFW recursion relations. In this case there is just one terms in the expansion which is the forward limit of 7pt N²MHV amplitude,

$$A_{5,1}^{1-loop} = FL(A_{7,2}^{tree}) \quad (4.3.62)$$

While $A_{7,2}^{tree}$ contains six terms in the BCFW expansion, only three of them do survive the forward limit. The matrices C are

$$C_1 = \begin{pmatrix} b_2(1+t_1) & b_1 & t_2 & a_2 t_2 + t_3 & 1+t_1+t_4 \\ 0 & a_1 & 1 & a_2 & 0 \\ -b_2 & -b_1 & 0 & 0 & -1 \end{pmatrix}$$

$$C_2 = \begin{pmatrix} 1+t_1 & t_2 & t_3+a_1 t_4 & b_1+a_2 t_4 & b_2 \\ 1 & 0 & -a_1 & -a_2 & 0 \\ -1 & 0 & 0 & -b_1 & -b_2 \end{pmatrix}$$

$$C_3 = \begin{pmatrix} t_1 & t_2 & t_3 & t_4 & 1 \\ 0 & t_2 & t_3+a_1+b_1 a_2 & a_2 & 0 \\ 0 & 0 & b_2 a_2 & t_4+b_2 & 1 \end{pmatrix}$$

We solve for eight parameters t_1, t_2, t_3, t_4 and a_1, a_2, b_1, b_2 from equations

$$Y^I = C_{1a} Z_a^I \quad W_\alpha^I = C_{\alpha a} Z_a^I \quad (4.3.63)$$

where W_α is the three-plane (YAB) . The result is

$$\Omega_1 = \frac{\langle 12345 \rangle^4}{\langle Y2345 \rangle \langle Y3451 \rangle \langle YAB51 \rangle \langle YAB12 \rangle \langle YAB23 \rangle \langle AB(Y145) \cap (Y234) \rangle} \quad (4.3.64)$$

$$\Omega_2 = \frac{\langle 12345 \rangle^4 \langle YAB14 \rangle^2}{\langle Y1234 \rangle \langle YAB12 \rangle \langle YAB34 \rangle \langle YAB45 \rangle \langle YAB41 \rangle \langle AB(Y123) \cap (Y145) \rangle \langle AB(Y145) \cap (Y234) \rangle} \quad (4.3.65)$$

$$\Omega_3 = \frac{\langle 12345 \rangle^4}{\langle Y4512 \rangle \langle Y5123 \rangle \langle YAB23 \rangle \langle YAB34 \rangle \langle YAB45 \rangle \langle AB(Y123) \cap (Y145) \rangle} \quad (4.3.66)$$

We see the interesting pattern of spurious poles cancelation. The first and the third terms contain spurious poles $\langle AB(Y145) \cap (Y234) \rangle$ and $\langle AB(Y123) \cap (Y145) \rangle$ which are canceled by the second term that contains both of them.

For this special case of 5pt NMHV we also know the local triangulation. It is a parity conjugate of 5pt MHV one-loop amplitude which has the local expansion

$$\Omega = \frac{\langle AB(512) \cap (234) \rangle \langle 3451 \rangle - \langle AB51 \rangle \langle 1234 \rangle \langle 2345 \rangle - \langle AB34 \rangle \langle 4512 \rangle \langle 5123 \rangle}{\langle AB12 \rangle \langle AB23 \rangle \langle AB34 \rangle \langle AB45 \rangle \langle AB51 \rangle} \quad (4.3.67)$$

The parity conjugation replaces $\langle AB(512) \cap (234) \rangle \rightarrow \langle AB13 \rangle$ and adds Y to any four-bracket. Also we multiply the result by the R-invariant $[12345]$,

$$\Omega = \frac{\langle 12345 \rangle^4}{\langle Y1234 \rangle \langle Y2345 \rangle \langle Y3451 \rangle \langle Y4512 \rangle \langle Y5123 \rangle} \times \frac{\langle YAB13 \rangle \langle Y2345 \rangle \langle Y4512 \rangle - \langle YAB51 \rangle \langle Y1234 \rangle \langle Y2345 \rangle - \langle YAB34 \rangle \langle Y4512 \rangle \langle Y5123 \rangle}{\langle YAB12 \rangle \langle YAB23 \rangle \langle YAB34 \rangle \langle YAB45 \rangle \langle YAB51 \rangle} \quad (4.3.68)$$

It is easy to show that (4.3.68) is equal to the sum of three BCFW terms.

4.4 General conjecture for the integrand

In the case of N^k MHV ℓ -loop integrand we have a natural $(k+4)$ -dimensional space with a positive k -plane Y defined via

$$Y_\alpha^I = C_{\alpha a} Z_a^I \quad (4.4.69)$$

where C is the top cell, respectively union of $4k$ -dimensional cells of $G_+(k, n)$. This k -plane has a natural complement which is P^3 . We consider ℓ lines $(AB)_i$, $i = 1, \dots, \ell$ in this space,

$$A_\sigma^{I(j)} = C_{\sigma a}^{(j)} Z_a^I, \quad j = 1, \dots, \ell. \quad (4.4.70)$$

The index I runs from 1 to $k+4$ but each line $(AB)_i$ is defined with respect the k -plane Y . Therefore only four directions of $(AB)_i$ that are orthogonal to Y are

relevant. Also there is no invariant meaning of matrices $C^{(j)}$ if we do not specify C which defines the k -plane Y . Therefore it is natural to build the $k+2$ by n matrices $\tilde{C}^{(j)}$,

$$\tilde{C}^{(j)} = \begin{pmatrix} C \\ C^{(1)} \end{pmatrix} \quad (4.4.71)$$

and we demand them to be positive, ie. all their $k+2$ by $k+2$ minors are positive and $\tilde{C}^{(j)} = G_+(k+2, n)$. Furthermore, we define a big $k+2\ell$ by n matrix \tilde{C} ,

$$\tilde{C} = \begin{pmatrix} C \\ C^{(1)} \\ C^{(2)} \\ \vdots \\ C^{(\ell)} \end{pmatrix} \quad (4.4.72)$$

and demand all relevant $k+2j$ by $k+2j$ minors to be positive. By relevant we mean all minors that contain k rows from C together with j pairs of rows from $C^{(j)}$. We call this structure *generalized Grassmannian* $G_+(k, n, \ell)$.

We associate a form Ω_P which has logarithmic singularities on the boundaries of this space. The boundaries correspond to setting $(k+4)$ -brackets to zero,

$$\langle Y \ i \ i+1 \ j \ j+1 \rangle = 0 \quad \text{or} \quad \langle Y \ A \ B \ i \ i+1 \rangle = 0 \quad (4.4.73)$$

In fact, the form Ω_P depends on external momentum twistors Z_i , the k -plane Y and the $k+2$ -planes $Y(AB)_j$ rather than lines $(AB)_j$.

Chapter A

All 2-Loop NMHV Amplitude Integrands

In this appendix, we will provide all the details that go into the formula for the n -point 2-loop NMHV amplitude, which can be graphically represented as follows:

$$\mathcal{A}_{\text{NMHV}}^{2\text{-loop}} = \sum_{\substack{i < j < l < m \leq k < i \\ i < j < k < l < m \leq i \\ i \leq l < m \leq j < k < i}} \text{Diagram 1} + \frac{1}{2} \sum_{i < j < k < l < i} \text{Diagram 2} \times \left\{ \begin{array}{l} \mathcal{A}_{\text{NMHV}}^{\text{tree}}(j, \dots, k; l, \dots, i) \\ + \mathcal{A}_{\text{NMHV}}^{\text{tree}}(i, \dots, j) \\ + \mathcal{A}_{\text{NMHV}}^{\text{tree}}(k, \dots, l) \end{array} \right\}$$

$\times [i, j, j+1, k, k+1]$

Of these two terms, only the first requires any comment, because the second summand involves only the familiar double-pentagons which generate the MHV two-loop amplitude's integrand.

As indicated by the ranges of the summation, the first sum actually represents a sum over three distinct cyclic orderings of the labels (i, j, k, l, m) , corresponding to each of the following cyclically-ordered integrands,

| | | | |
|------------------|--|--|--|
| Integrand: | | | |
| Range: | $i < j < l < m \leq k < i$ | $i \leq l < m \leq j < k < i$ | $i < j < k < l < m \leq i$ |
| Boundary terms : | $\left\{ \begin{array}{l} \mathbf{A} \quad i+1 = j \\ \mathbf{B} \quad i-1 = k+1 \end{array} \right\}$ | $\left\{ \begin{array}{l} \mathbf{A} \quad i = l \\ \mathbf{B} \quad i-1 = k+1 \end{array} \right\}$ | $\left\{ \begin{array}{l} \mathbf{A} \quad i+1 = j \\ \mathbf{B} \quad i = m \end{array} \right\}$ |

For each range of indices, there are *boundary-terms* for which the general integrand's numerator must change slightly; these have been indicated in the table above. Given the ranges and boundaries indicated above, the numerators for these contributions to the 2-loop NMHV amplitude are given by,

| term | numerator |
|-------------------------|---|
| non-boundary | $\langle AB (i-1 i i+1) \cap (\Sigma_{i,j,k}) \rangle$ |
| A boundary | $\langle AB i+1(i-1 i) \cap (\Sigma_{i,j,k}) \rangle$ |
| B boundary | $\langle AB i-1(i i+1) \cap (\Sigma_{i,j,k}) \rangle$ |
| A&B boundary | $\langle AB i+1 i-1 \rangle \langle i \Sigma_{i,j,k} \rangle$ |

where in all these cases the special plane $\Sigma_{i,j,k}$ is given by the same object encountered at one-loop, but with the arbitrary bitwistor X replaced by (lm) ,

$$\Sigma_{i,j,k} \equiv \frac{1}{2} \left[(j j+1) \left((i k k+1) \cap (lm) \right) - (k k+1) \left((i j j+1) \cap (lm) \right) \right].$$

Chapter B

All 3-Loop MHV Amplitude Integrands

In this appendix, we present the explicit form of the n -point 3-loop MHV amplitude, which we represent graphically graphically represented as follows:

$$\mathcal{A}_{\text{MHV}}^{3\text{-loop}} = \frac{1}{3} \sum_{\substack{i_1 \leq i_2 < j_1 \leq \\ \leq j_2 < k_1 \leq k_2 < i_1}} \text{Diagram 1} + \frac{1}{2} \sum_{\substack{i_1 \leq j_1 < k_1 < \\ < k_2 \leq j_2 < i_2 < i_1}} \text{Diagram 2}$$

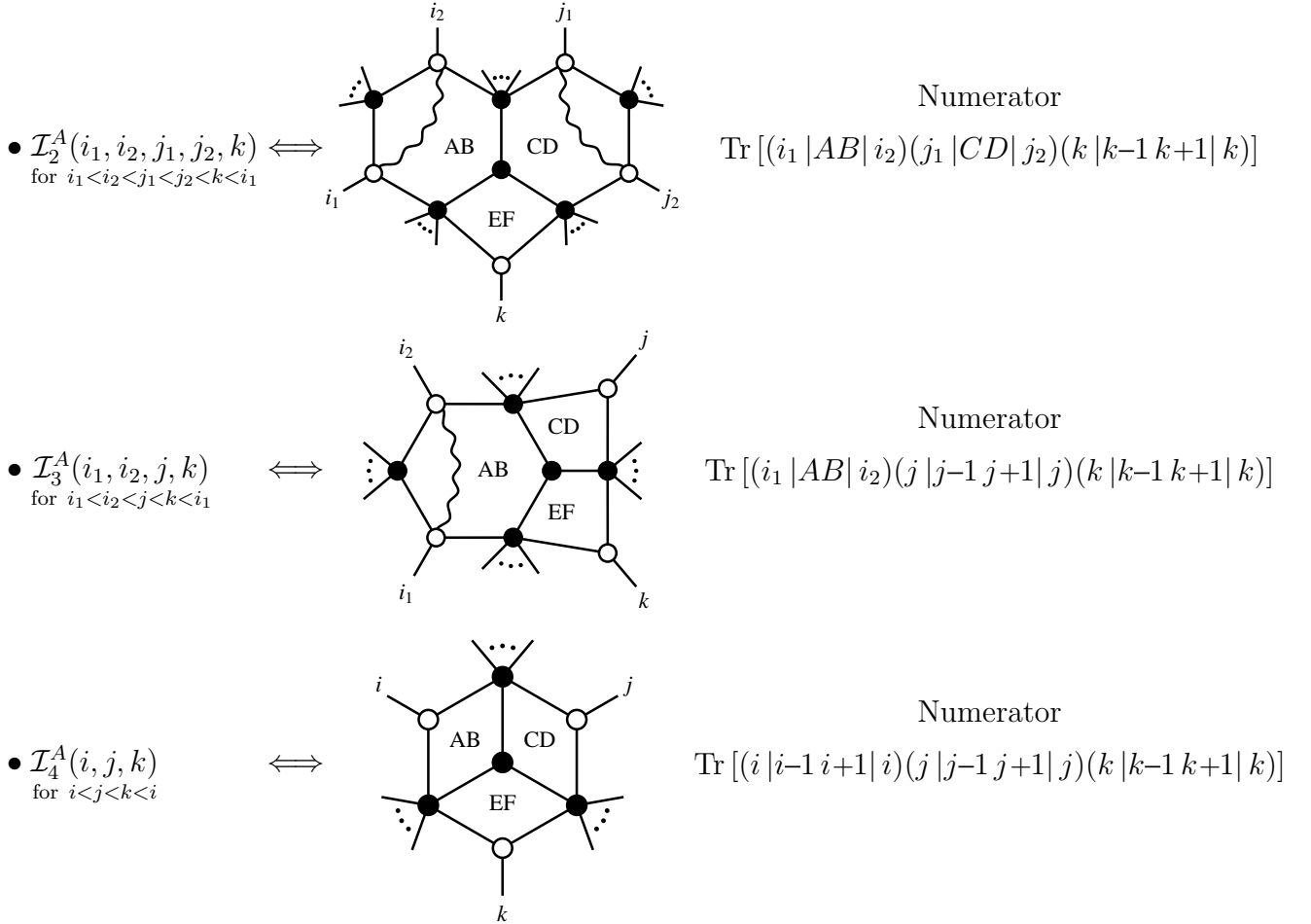
As described in the body of this Chapter, the ‘boundary terms’ of the summands above require some comment. We will discuss the two topologies separately, starting with with the first summand in the equation above. Because when any two of the indices become identified in the first graph the wavy-line numerators become ill-defined, special consideration must be made for each of the degenerations allowed in the range of the summand—that is, all the cases where two or more of the indices are identified. Separating each type of such degeneration that is allowed in the first summand,

$$\frac{1}{3} \sum_{\substack{i_1 \leq i_2 < j_1 \leq \\ \leq j_2 < k_1 \leq k_2 < i_1}} \text{Diagram 1} = \left\{ \begin{array}{l} 1 \times \frac{1}{3} \sum_{\substack{i_1 < i_2 < j_1 < \\ < j_2 < k_1 < k_2 < i_1}} \mathcal{I}_1^A(i_1, i_2, j_1, j_2, k_1, k_2) \quad \left(\begin{array}{l} \text{all indices} \\ \text{distinct} \end{array} \right) \\ 3 \times \frac{1}{3} \sum_{\substack{i_1 < i_2 < j_1 < \\ < j_2 < k < i_1}} \mathcal{I}_2^A(i_1, i_2, j_1, j_2, k) \quad (k_1 = k_2 \equiv k) \\ 3 \times \frac{1}{3} \sum_{i_1 < i_2 < j < k < i_1} \mathcal{I}_3^A(i_1, i_2, j, k) \quad \left(\begin{array}{l} k_1 = k_2 \equiv k \\ j_1 = j_2 \equiv j \end{array} \right) \\ 1 \times \frac{1}{3} \sum_{i < j < k < i} \mathcal{I}_4^A(i, j, k) \quad \left(\begin{array}{l} k_1 = k_2 \equiv k \\ j_1 = j_2 \equiv j \\ i_1 = i_2 \equiv i \end{array} \right) \end{array} \right.$$

forms (the equality of which offering further justification for calling this a ‘trace’):

$$\begin{aligned}
& \text{Tr} [(i_1 | AB | i_2)(j_1 | CD | j_2)(k_1 | EF | k_2)] \\
& \equiv \langle i_2 j_1 \left[\left(j_2 k_1 \left((k_2 i_1 A) \cap (FE) \right) \right) \cap (DC) \right] B \rangle - (A \leftrightarrow B); \\
& = \langle j_2 k_1 \left[\left(k_2 i_1 \left((i_2 j_1 C) \cap (BA) \right) \right) \cap (FE) \right] D \rangle - (C \leftrightarrow D); \\
& = \langle k_2 i_1 \left[\left(i_2 j_1 \left((j_2 k_1 E) \cap (DC) \right) \right) \cap (BA) \right] F \rangle - (E \leftrightarrow F).
\end{aligned}$$

As we will see presently, this numerator will change only very slightly for the boundary terms in the summand. Always leaving the propagators and wavy-line implicit from the the corresponding figures, the remaining integrands are defined according to the following:

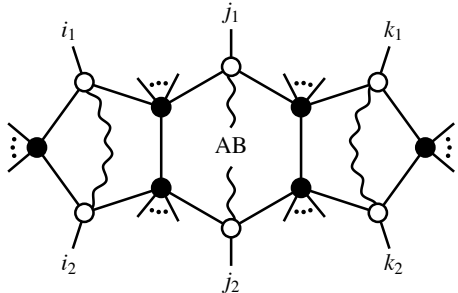
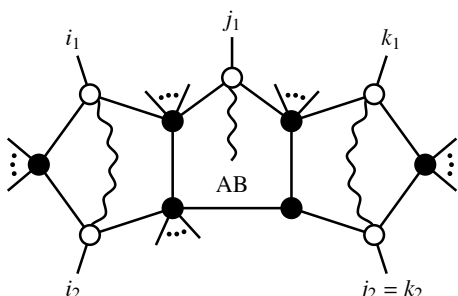
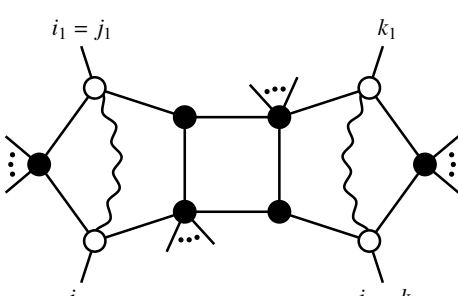


For the second topology, the boundary terms in the summand lead to just three separate contributions that must be specifically addressed.

$$\frac{1}{2} \sum_{\substack{i_1 \leq j_1 < k_1 < \\ < k_2 \leq j_2 < i_2 < i_1}} \text{Diagram} = \begin{cases} 1 \times \frac{1}{2} \sum_{\substack{i_1 < j_1 < k_1 < \\ < k_2 < j_2 < i_2 < i_1}} \mathcal{I}_1^B(i_1, j_1, k_1, k_2, j_2, i_2) & \begin{pmatrix} \text{all indices} \\ \text{distinct} \end{pmatrix} \\ 2 \times \frac{1}{2} \sum_{\substack{i_1 < j_1 < k_1 < \\ < k_2 < i_2 < i_1}} \mathcal{I}_2^B(i_1, j_1, k_1, k_2, i_2) & (k_2 = j_2 \equiv k_2) \\ 1 \times \frac{1}{2} \sum_{\substack{i_1 < k_1 < \\ < k_2 < i_2 < i_1}} \mathcal{I}_3^B(i_1, k_1, k_2, i_2) & \begin{pmatrix} i_1 = j_1 \equiv i_1 \\ k_2 = j_2 \equiv k_2 \end{pmatrix} \end{cases}$$

As above, the overall factor of $\frac{1}{2}$ reflects the \mathbb{Z}_2 -symmetry of the integrand (we remind the reader that each term in the summand is to be fully-symmetrized with respect to the $3!$ permutations of the loop variables). As before, we have exploited the symmetry of the integrand to identify various boundary terms: the degenerations $i_1 = j_1$ and $k_2 = j_2$, being equivalent in the cyclic sum, they can be combined into the single summand \mathcal{I}_2^B —which explains its relative factor of 2.

With this, we can directly present the three classes of integrands of the second topology which contribute to the 3-loop MHV amplitude:

| | | |
|--|---|--|
| $\bullet \mathcal{I}_1^B(i_1, j_1, k_1, k_2, j_2, i_2)$ for $i_1 < j_1 < k_1 < k_2 < j_2 < i_2 < i_1$ | \iff  | <p style="text-align: center;">Numerator</p> $\langle AB(i_2 i_1 j_2) \cap (j_1 - 1 j_1 j_1 + 1) \rangle$ $\times \langle AB(j_2 - 1 j_2 j_2 + 1) \cap (j_1 k_1 k_2) \rangle$ |
| $\bullet \mathcal{I}_2^B(i_1, j_1, k_1, k_2, i_2)$ for $i_1 < j_1 < k_1 < k_2 < i_2 < i_1$ | \iff  | <p style="text-align: center;">Numerator</p> $\langle AB(i_2 i_1 k_2) \cap (j_1 - 1 j_1 j_1 + 1) \rangle$ $\times \langle k_2 + 1 j_1 k_1 k_2 \rangle$ |
| $\bullet \mathcal{I}_3^B(i_1, k_1, k_2, i_2)$ for $i_1 < k_1 < k_2 < i_2 < i_1$ | \iff  | <p style="text-align: center;">Numerator</p> $\langle k_2 i_2 i_1 i_1 + 1 \rangle$ $\times \langle k_2 + 1 i_1 k_1 k_2 \rangle$ |

Bibliography

- [1] S. Weinberg, *The Quantum theory of fields. Vol. 1: Foundations*. Cambridge University Press, 1995. 1, 8
- [2] N. Seiberg and E. Witten, “Electric-Magnetic Duality, Monopole Condensation, and Confinement in $\mathcal{N} = 2$ Supersymmetric Yang-Mills Theory,” *Nucl. Phys.* **B426** (1994) 19–52, [arXiv:hep-th/9407087](#). 1
- [3] N. Seiberg, “Electric-Magnetic Duality in Supersymmetric non-Abelian Gauge Theories,” *Nucl. Phys.* **B435** (1995) 129–146, [arXiv:hep-th/9411149](#). 1
- [4] A. Kapustin and E. Witten, “Electric-Magnetic Duality And The Geometric Langlands Program,” *Commun. Num. Theor. Phys.* **1** (2007) 1–236, [arXiv:hep-th/0604151](#). 1
- [5] J. M. Maldacena, “The Large- N Limit of Superconformal Field Theories and Supergravity,” *Adv. Theor. Math. Phys.* **2** (1998) 231–252, [arXiv:hep-th/9711200](#). 1
- [6] M. L. Mangano and S. J. Parke, “Multiparton Amplitudes in Gauge Theories,” *Phys. Rept.* **200** (1991) 301–367, [arXiv:hep-th/0509223](#). 1
- [7] L. J. Dixon, “Calculating Scattering Amplitudes Efficiently,” [arXiv:hep-ph/9601359](#). 1, 18
- [8] F. Cachazo and P. Svrcek, “Lectures on Twistor Strings and Perturbative Yang-Mills Theory,” *PoS RTN2005* (2005) 004, [arXiv:hep-th/0504194](#). 1
- [9] Z. Bern, L. J. Dixon, and D. A. Kosower, “On-Shell Methods in Perturbative QCD,” *Annals Phys.* **322** (2007) 1587–1634, [arXiv:0704.2798 \[hep-ph\]](#). 1
- [10] B. Feng and M. Luo, “An Introduction to On-Shell Recursion Relations,” [arXiv:1111.5759 \[hep-th\]](#). 1, 225
- [11] R. Roiban, M. Spradlin, and A. Volovich, “Scattering Amplitudes in Gauge Theories: Progress and Outlook,” *J. Phys.* **A44** (2011) no. 45, 1. 1, 2, 3, 107

- [12] Z. Bern, L. J. Dixon, D. C. Dunbar, and D. A. Kosower, “One-Loop n -Point Gauge Theory Amplitudes, Unitarity and Collinear Limits,” *Nucl. Phys.* **B425** (1994) 217–260, [arXiv:hep-ph/9403226](#). 2, 21, 49, 149
- [13] E. Witten, “Perturbative Gauge Theory as a String Theory in Twistor Space,” *Commun. Math. Phys.* **252** (2004) 189–258, [arXiv:hep-th/0312171](#). 2, 8, 76, 183
- [14] R. Britto, F. Cachazo, B. Feng, and E. Witten, “Direct Proof of Tree-Level Recursion Relation in Yang- Mills Theory,” *Phys. Rev. Lett.* **94** (2005) 181602, [arXiv:hep-th/0501052](#). 2, 5, 70, 109, 225
- [15] N. Beisert, C. Ahn, L. F. Alday, Z. Bajnok, J. M. Drummond, *et al.*, “Review of AdS/CFT Integrability: An Overview,” *Lett. Math. Phys.* **99** (2012) 3–32, [arXiv:1012.3982 \[hep-th\]](#). 2, 3
- [16] N. Arkani-Hamed, F. Cachazo, C. Cheung, and J. Kaplan, “A Duality For The S -Matrix,” *JHEP* **1003** (2010) 020, [arXiv:0907.5418 \[hep-th\]](#). 2, 29, 32, 33, 70, 71, 72, 80, 102, 131, 177, 181, 201
- [17] L. Mason and D. Skinner, “Dual Superconformal Invariance, Momentum Twistors and Grassmannians,” *JHEP* **0911** (2009) 045, [arXiv:0909.0250 \[hep-th\]](#). 2, 33, 71, 136, 187
- [18] N. Arkani-Hamed, F. Cachazo, and C. Cheung, “The Grassmannian Origin Of Dual Superconformal Invariance,” *JHEP* **1003** (2010) 036, [arXiv:0909.0483 \[hep-th\]](#). 2, 33, 71, 184
- [19] J. L. Bourjaily, J. Trnka, A. Volovich, and C. Wen, “The Grassmannian and the Twistor String: Connecting All Trees in $\mathcal{N}=4$ SYM,” *JHEP* **1101** (2011) 038, [arXiv:1006.1899 \[hep-th\]](#). 2, 4, 72, 76
- [20] J. Drummond, “Review of AdS/CFT Integrability, Chapter V.2: Dual Superconformal Symmetry,” *Lett. Math. Phys.* **99** (2012) 481–505, [arXiv:1012.4002 \[hep-th\]](#). 2

- [21] A. B. Goncharov, “A Simple Construction of Grassmannian Polylogarithms,” [arXiv:0908.2238 \[math.AG\]](#). 3
- [22] A. B. Goncharov, M. Spradlin, C. Vergu, and A. Volovich, “Classical Polylogarithms for Amplitudes and Wilson Loops,” *Phys. Rev. Lett.* **105** (2010) 151605, [arXiv:1006.5703 \[hep-th\]](#). 3, 98
- [23] S. Caron-Huot, “Superconformal Symmetry and Two-Loop Amplitudes in Planar $\mathcal{N}=4$ Super Yang-Mills,” *JHEP* **1112** (2011) 066, [arXiv:1105.5606 \[hep-th\]](#). 3
- [24] L. F. Alday, “Some Analytic Results for Two-Loop Scattering Amplitudes,” *JHEP* **1107** (2011) 080, [arXiv:1009.1110 \[hep-th\]](#). 3
- [25] L. J. Dixon, J. M. Drummond, and J. M. Henn, “Bootstrapping the Three-Loop Hexagon,” *JHEP* **1111** (2011) 023, [arXiv:1108.4461 \[hep-th\]](#). 3
- [26] P. Heslop and V. V. Khoze, “Wilson Loops @ 3-Loops in Special Kinematics,” *JHEP* **1111** (2011) 152, [arXiv:1109.0058 \[hep-th\]](#). 3
- [27] L. J. Dixon, J. M. Drummond, and J. M. Henn, “Analytic Result for the Two-Loop Six-Point NMHV Amplitude in $\mathcal{N} = 4$ Super Yang-Mills Theory,” *JHEP* **1201** (2012) 024, [arXiv:1111.1704 \[hep-th\]](#). 3
- [28] J. L. Bourjaily, A. DiRe, A. Shaikh, M. Spradlin, and A. Volovich, “The Soft-Collinear Bootstrap: $\mathcal{N}=4$ Yang-Mills Amplitudes at Six and Seven Loops,” *JHEP* **1203** (2012) 032, [arXiv:1112.6432 \[hep-th\]](#). 3
- [29] B. Eden, P. Heslop, G. P. Korchemsky, and E. Sokatchev, “Constructing the Correlation Function of Four Stress-Tensor Multiplets and the Four-Particle Amplitude in $\mathcal{N} = 4$ SYM,” *Nucl. Phys.* **B862** (2012) 450–503, [arXiv:1201.5329 \[hep-th\]](#). 3
- [30] S. Caron-Huot and S. He, “Jumpstarting the All-Loop S -Matrix of Planar $\mathcal{N}=4$ Super Yang-Mills,” *JHEP* **1207** (2012) 174, [arXiv:1112.1060 \[hep-th\]](#). 3
- [31] A. Sever, P. Vieira, and T. Wang, “OPE for Super Loops,” *JHEP* **1111** (2011) 051, [arXiv:1108.1575 \[hep-th\]](#). 3

- [32] A. Sever, P. Vieira, and T. Wang, “From Polygon Wilson Loops to Spin Chains and Back,” *JHEP* **1212** (2012) 065, [arXiv:1208.0841 \[hep-th\]](#). 3
- [33] N. Gromov, V. Kazakov, and P. Vieira, “Exact Spectrum of Anomalous Dimensions of Planar $\mathcal{N} = 4$ Supersymmetric Yang-Mills Theory,” *Phys. Rev. Lett.* **103** (2009) 131601, [arXiv:0901.3753 \[hep-th\]](#). 3
- [34] N. Arkani-Hamed, J. Bourjaily, F. Cachazo, and J. Trnka, “Local Spacetime Physics from the Grassmannian,” *JHEP* **1101** (2011) 108, [arXiv:0912.3249 \[hep-th\]](#). 4, 72
- [35] N. Arkani-Hamed, J. Bourjaily, F. Cachazo, and J. Trnka, “Unification of Residues and Grassmannian Dualities,” *JHEP* **1101** (2011) 049, [arXiv:0912.4912 \[hep-th\]](#). 4, 72, 76
- [36] J. M. Drummond, J. M. Henn, and J. Trnka, “New Differential Equations for On-Shell Loop Integrals,” *JHEP* **1104** (2011) 083, [arXiv:1010.3679 \[hep-th\]](#). 4
- [37] N. Arkani-Hamed, J. L. Bourjaily, F. Cachazo, A. Hodges, and J. Trnka, “A Note on Polytopes for Scattering Amplitudes,” *JHEP* **1204** (2012) 081, [arXiv:1012.6030 \[hep-th\]](#). 4, 6, 11, 56, 57, 69, 248
- [38] G. Lusztig, “Total Positivity in Reductive Groups,” in *Lie Theory and Geometry, In Honor of B. Kostant*, vol. 123 of *Prog. in Math.*, pp. 531–569. Birkhauser, Boston, 1994. 6, 102, 152
- [39] S. Fomin and A. Zelevinsky, “Cluster Algebras. I. Foundations,” *J. Amer. Math. Soc.* **15** (2002) no. 2, 497–529, [arXiv:math/0104151](#). 6
- [40] V. V. Fock and A. B. Goncharov, “Moduli Spaces of Local Systems and Higher Teichmüller Theory,” *Publ. Math. IHES* (2006) no. 103, 1–212, [arXiv:math.AG/0311149](#). 6, 245
- [41] V. V. Fock and A. B. Goncharov, “Cluster Ensembles, Quantization and the Dilogarithm,” *Ann. Sci. L’Ecole Norm. Sup.* (2009) , [arXiv:math.AG/0311245](#). 6

- [42] V. V. Fock and A. B. Goncharov, “Cluster \mathcal{X} -Varieties, Amalgamation and Poisson-Lie Groups,” in *Algebraic Geometry and Number Theory, Dedicated to Drinfeld’s 50th birthday*, pp. 27–68. Birkhauser, Boston, 2006.
[arXiv:math.RT/0508408](#). 6, 136
- [43] A. Postnikov, “Total Positivity, Grassmannians, and Networks,”
[arXiv:math/0609764](#). 6, 102, 120, 123, 152, 156
- [44] A. Knutson, T. Lam, and D. Speyer, “Positroid Varieties: Juggling and Geometry,” [arXiv:1111.3660 \[math.AG\]](#). 6, 152, 155, 195
- [45] A. B. Goncharov and R. Kenyon, “Dimers and Cluster Integrable Systems,”
[arXiv:1107.5588 \[math.AG\]](#). 6, 209
- [46] D. Thurston, “From Dominoes to Hexagons,” [arXiv:math/0405482](#). 6, 120, 123
- [47] P. De Causmaecker, R. Gastmans, W. Troost, and T. T. Wu, “Multiple Bremsstrahlung in Gauge Theories at High-Energies. 1. General Formalism for Quantum Electrodynamics,” *Nucl. Phys.* **B206** (1982) 53. 8, 12
- [48] J. F. Gunion and Z. Kunszt, “Improved Analytic Techniques for Tree Graph Calculations and the $G g q \bar{q}$ Lepton anti-Lepton Subprocess,” *Phys. Lett.* **B161** (1985) 333. 8, 12
- [49] R. Kleiss and W. J. Stirling, “Spinor Techniques for Calculating $p\bar{p} \rightarrow W^\pm Z^0 + \text{Jets}$,” *Nucl. Phys.* **B262** (1985) 235–262. 8, 12
- [50] N. Arkani-Hamed, F. Cachazo, and J. Kaplan, “What is the Simplest Quantum Field Theory?,” *JHEP* **1009** (2010) 016, [arXiv:0808.1446 \[hep-th\]](#). 8, 27, 70
- [51] V. P. Nair, “A Current Algebra for Some Gauge Theory Amplitudes,” *Phys. Lett.* **B214** (1988) 215. 8, 107, 181
- [52] M. Bianchi, H. Elvang, and D. Z. Freedman, “Generating Tree Amplitudes in $\mathcal{N} = 4$ SYM and $\mathcal{N} = 8$ SG,” *JHEP* **0809** (2008) 063, [arXiv:0805.0757 \[hep-th\]](#). 8

- [53] J. Drummond, J. Henn, G. Korchemsky, and E. Sokatchev, “Generalized Unitarity for $\mathcal{N} = 4$ Super-Amplitudes,” *Nucl. Phys.* **B869** (2013) 452–492, [arXiv:0808.0491 \[hep-th\]](#). 8, 53
- [54] L. F. Alday, J. Maldacena, A. Sever, and P. Vieira, “Y-System for Scattering Amplitudes,” *J. Phys.* **A43** (2010) 485401, [arXiv:1002.2459 \[hep-th\]](#). 11, 98
- [55] L. F. Alday, D. Gaiotto, J. Maldacena, A. Sever, and P. Vieira, “An Operator Product Expansion for Polygonal Null Wilson Loops,” [arXiv:1006.2788 \[hep-th\]](#). 11, 98
- [56] D. Gaiotto, J. Maldacena, A. Sever, and P. Vieira, “Bootstrapping Null Polygon Wilson Loops,” *JHEP* **1103** (2011) 092, [arXiv:1010.5009 \[hep-th\]](#). 11
- [57] J. Drummond, J. Henn, G. Korchemsky, and E. Sokatchev, “Dual Superconformal Symmetry of Scattering Amplitudes in $\mathcal{N} = 4$ super Yang-Mills Theory,” *Nucl. Phys.* **B828** (2010) 317–374, [arXiv:0807.1095 \[hep-th\]](#). 11, 53, 70, 77, 202
- [58] F. A. Berends, R. Kleiss, P. De Causmaecker, R. Gastmans, and T. T. Wu, “Single Bremsstrahlung Processes in Gauge Theories,” *Phys. Lett.* **B103** (1981) 124. 12
- [59] J. Drummond, J. Henn, V. Smirnov, and E. Sokatchev, “Magic Identities for Conformal Four-Point Integrals,” *JHEP* **0701** (2007) 064, [arXiv:hep-th/0607160](#). 12, 16, 70, 73, 185
- [60] A. Hodges, “Eliminating Spurious Poles from Gauge-Theoretic Amplitudes,” [arXiv:0905.1473 \[hep-th\]](#). 13, 15, 71, 185, 248
- [61] R. Penrose, “Twistor Algebra,” *J. Math. Phys.* **8** (1967) 345. 13, 182
- [62] A. Hodges, “The Box Integrals in Momentum-Twistor Geometry,” [arXiv:1004.3323 \[hep-th\]](#). 15, 19, 74
- [63] L. Mason and D. Skinner, “Amplitudes at Weak Coupling as Polytopes in AdS_5 ,” *J. Phys.* **A44** (2011) 135401, [arXiv:1004.3498 \[hep-th\]](#). 19, 74

- [64] W. L. van Neerven and J. A. M. Vermaseren, “Large Loop Integrals,” *Phys. Lett.* **B137** (1984) 241. 20, 149
- [65] N. Arkani-Hamed, J. L. Bourjaily, F. Cachazo, S. Caron-Huot, and J. Trnka, “The All-Loop Integrand For Scattering Amplitudes in Planar $\mathcal{N}=4$ SYM,” *JHEP* **1101** (2011) 041, [arXiv:1008.2958 \[hep-th\]](#). 22, 23, 57, 62, 64, 109, 111, 221, 225, 230, 234, 236, 237
- [66] J. M. Drummond and J. M. Henn, “Simple Loop Integrals and Amplitudes in $\mathcal{N} = 4$ SYM,” *JHEP* **1105** (2011) 105, [arXiv:1008.2965 \[hep-th\]](#). 22, 65
- [67] L. F. Alday, J. M. Henn, J. Plefka, and T. Schuster, “Scattering into the Fifth Dimension of $\mathcal{N} = 4$ super Yang-Mills,” *JHEP* **1001** (2010) 077, [arXiv:0908.0684 \[hep-th\]](#). 23, 74, 99
- [68] R. J. Eden, P. V. Landshoff, D. I. Olive, and J. C. Polkinghorne, *The Analytic S-Matrix*. Cambridge University Press, 1966. 26, 107
- [69] R. Britto, F. Cachazo, and B. Feng, “Generalized Unitarity and One-Loop Amplitudes in $\mathcal{N} = 4$ Super-Yang-Mills,” *Nucl. Phys.* **B725** (2005) 275–305, [arXiv:hep-th/0412103](#). 26, 31, 149
- [70] F. Cachazo, “Sharpening The Leading Singularity,” [arXiv:0803.1988 \[hep-th\]](#). 27, 29, 147
- [71] P. Griffiths and J. Harris, *Principles of Algebraic Geometry*. Wiley Classics Library. John Wiley & Sons Inc., New York, 1978. 28, 30, 72, 83, 128, 195
- [72] E. I. Buchbinder and F. Cachazo, “Two-Loop Amplitudes of Gluons and Octa-Cuts in $\mathcal{N} = 4$ super Yang-Mills,” *JHEP* **0511** (2005) 036, [arXiv:hep-th/0506126](#). 29, 146, 147
- [73] N. Arkani-Hamed, F. Cachazo, C. Cheung, and J. Kaplan, “The S -Matrix in Twistor Space,” *JHEP* **1003** (2010) 110, [arXiv:0903.2110 \[hep-th\]](#). 33, 80, 97, 232

- [74] J. Drummond and L. Ferro, “The Yangian Origin of the Grassmannian Integral,” *JHEP* **1012** (2010) 010, [arXiv:1002.4622 \[hep-th\]](#). 33, 72, 185, 190, 191, 192
- [75] H. Schubert, *Kalkül der Abzählenden Geometrie*. Verlag von B. G. Teubner, 1879. 34
- [76] W. Burau and B. Renschuch, *Ergänzungen zur Biographie von Hermann Schubert*. Mitt. Math. Ges. Hamb. 13, pp. 63-65, ISSN 0340-4358, 1993. 34
- [77] A. Brandhuber, P. Heslop, and G. Travaglini, “Proof of the Dual Conformal Anomaly of One-Loop Amplitudes in $\mathcal{N} = 4$ SYM,” *JHEP* **10** (2009) 063, [arXiv:0906.3552 \[hep-th\]](#). 53, 70
- [78] H. Elvang, D. Z. Freedman, and M. Kiermaier, “Dual Conformal Symmetry of 1-Loop NMHV Amplitudes in $\mathcal{N} = 4$ SYM Theory,” *JHEP* **1003** (2010) 075, [arXiv:0905.4379 \[hep-th\]](#). 53, 70
- [79] S. Caron-Huot, “Notes on the Scattering Amplitude / Wilson Loop Duality,” *JHEP* **1107** (2011) 058, [arXiv:1010.1167 \[hep-th\]](#). 58, 221
- [80] Z. Bern, L. J. Dixon, and V. A. Smirnov, “Iteration of Planar Amplitudes in Maximally Supersymmetric Yang-Mills Theory at Three Loops and Beyond,” *Phys. Rev.* **D72** (2005) 085001, [arXiv:hep-th/0505205](#). 68, 149
- [81] M. Spradlin, A. Volovich, and C. Wen, “Three-Loop Leading Singularities and BDS Ansatz for Five Particles,” *Phys. Rev.* **D78** (2008) 085025, [arXiv:0808.1054 \[hep-th\]](#). 68
- [82] R. Britto, F. Cachazo, and B. Feng, “New Recursion Relations for Tree Amplitudes of Gluons,” *Nucl. Phys.* **B715** (2005) 499–522, [arXiv:hep-th/0412308](#). 70, 109, 225
- [83] A. Brandhuber, P. Heslop, and G. Travaglini, “A Note on Dual Superconformal Symmetry of the $\mathcal{N} = 4$ Super Yang-Mills S-Matrix,” *Phys. Rev.* **D78** (2008) 125005, [arXiv:0807.4097 \[hep-th\]](#). 70, 80

- [84] L. F. Alday and J. M. Maldacena, “Gluon Scattering Amplitudes at Strong Coupling,” *JHEP* **06** (2007) 064, [arXiv:0705.0303 \[hep-th\]](#). 70, 185
- [85] L. F. Alday and J. Maldacena, “Comments on Gluon Scattering Amplitudes via AdS/CFT,” *JHEP* **11** (2007) 068, [arXiv:0710.1060 \[hep-th\]](#). 70, 185
- [86] A. Brandhuber, P. Heslop, and G. Travaglini, “MHV Amplitudes in $\mathcal{N} = 4$ Super Yang-Mills and Wilson Loops,” *Nucl. Phys.* **B794** (2008) 231–243, [arXiv:0707.1153 \[hep-th\]](#). 70, 185
- [87] J. M. Drummond, G. P. Korchemsky, and E. Sokatchev, “Conformal Properties of Four-Gluon Planar Amplitudes and Wilson loops,” *Nucl. Phys.* **B795** (2008) 385–408, [arXiv:0707.0243 \[hep-th\]](#). 70, 185
- [88] J. M. Drummond, J. Henn, G. P. Korchemsky, and E. Sokatchev, “On Planar Gluon Amplitudes/Wilson Loops Duality,” *Nucl. Phys.* **B795** (2008) 52–68, [arXiv:0709.2368 \[hep-th\]](#). 70, 185
- [89] J. M. Drummond, J. Henn, G. P. Korchemsky, and E. Sokatchev, “The Hexagon Wilson Loop and the BDS Ansatz for the Six-Gluon Amplitude,” *Phys. Lett.* **B662** (2008) 456–460, [arXiv:0712.4138 \[hep-th\]](#). 70, 185
- [90] J. M. Drummond, J. Henn, G. P. Korchemsky, and E. Sokatchev, “Hexagon Wilson Loop = Six-Gluon MHV Amplitude,” *Nucl. Phys.* **B815** (2009) 142–173, [arXiv:0803.1466 \[hep-th\]](#). 70, 185
- [91] Z. Bern *et al.*, “The Two-Loop Six-Gluon MHV Amplitude in Maximally Supersymmetric Yang-Mills Theory,” *Phys. Rev.* **D78** (2008) 045007, [arXiv:0803.1465 \[hep-th\]](#). 70, 185
- [92] L. F. Alday and J. Maldacena, “Null Polygonal Wilson Loops and Minimal Surfaces in Anti- de-Sitter Space,” *JHEP* **11** (2009) 082, [arXiv:0904.0663 \[hep-th\]](#). 70, 185
- [93] J. M. Drummond, J. M. Henn, and J. Plefka, “Yangian Symmetry of Scattering Amplitudes in $\mathcal{N} = 4$ Super Yang-Mills Theory,” *JHEP* **05** (2009) 046, [arXiv:0902.2987 \[hep-th\]](#). 70, 185, 190

- [94] J. M. Drummond, J. Henn, G. P. Korchemsky, and E. Sokatchev, “Conformal Ward Identities for Wilson Loops and a Test of the Duality with Gluon Amplitudes,” *Nucl. Phys.* **B826** (2010) 337–364, [arXiv:0712.1223 \[hep-th\]](#). 70
- [95] A. Brandhuber, P. Heslop, and G. Travaglini, “One-Loop Amplitudes in $\mathcal{N} = 4$ Super Yang-Mills and Anomalous Dual Conformal Symmetry,” *JHEP* **08** (2009) 095, [arXiv:0905.4377 \[hep-th\]](#). 70
- [96] J. Drummond and L. Ferro, “Yangians, Grassmannians and T-duality,” *JHEP* **1007** (2010) 027, [arXiv:1001.3348 \[hep-th\]](#). 72, 185, 190
- [97] N. Beisert, J. Henn, T. McLoughlin, and J. Plefka, “One-Loop Superconformal and Yangian Symmetries of Scattering Amplitudes in $\mathcal{N} = 4$ Super Yang-Mills,” *JHEP* **04** (2010) 085, [arXiv:1002.1733 \[hep-th\]](#). 72, 185, 190
- [98] T. Bargheer, N. Beisert, W. Galleas, F. Loebbert, and T. McLoughlin, “Exacting $\mathcal{N} = 4$ Superconformal Symmetry,” *JHEP* **11** (2009) 056, [arXiv:0905.3738 \[hep-th\]](#). 72
- [99] G. Korchemsky and E. Sokatchev, “Superconformal Invariants for Scattering Amplitudes in $\mathcal{N} = 4$ SYM Theory,” *Nucl. Phys.* **B839** (2010) 377–419, [arXiv:1002.4625 \[hep-th\]](#). 72, 190
- [100] J. M. Drummond and J. M. Henn, “All Tree-Level Amplitudes in $\mathcal{N} = 4$ SYM,” *JHEP* **04** (2009) 018, [arXiv:0808.2475 \[hep-th\]](#). 72, 96, 225
- [101] D. Nandan, A. Volovich, and C. Wen, “A Grassmannian Étude in NMHV Minors,” *JHEP* **1007** (2010) 061, [arXiv:0912.3705 \[hep-th\]](#). 72, 76
- [102] A. Sever and P. Vieira, “Symmetries of the $\mathcal{N} = 4$ SYM S -Matrix,” [arXiv:0908.2437 \[hep-th\]](#). 73
- [103] S. Caron-Huot, “Loops and Trees,” *JHEP* **1105** (2011) 080, [arXiv:1007.3224 \[hep-ph\]](#). 73, 88, 100, 111, 244
- [104] R. Roiban, M. Spradlin, and A. Volovich, “On the Tree-Level S -Matrix of Yang-Mills Theory,” *Phys. Rev.* **D70** (2004) 026009, [arXiv:hep-th/0403190](#). 76

- [105] L. Dolan and P. Goddard, “Tree and Loop Amplitudes in Open Twistor String Theory,” *JHEP* **06** (2007) 005, [arXiv:hep-th/0703054](#). 76
- [106] M. Bullimore, L. Mason, and D. Skinner, “Twistor-Strings, Grassmannians and Leading Singularities,” *JHEP* **1003** (2010) 070, [arXiv:0912.0539 \[hep-th\]](#). 79
- [107] J. Kaplan, “Unraveling $\mathcal{L}_{n,k}$: Grassmannian Kinematics,” *JHEP* **1003** (2010) 025, [arXiv:0912.0957 \[hep-th\]](#). 79, 136
- [108] N. Arkani-Hamed and J. Kaplan, “On Tree Amplitudes in Gauge Theory and Gravity,” *JHEP* **0804** (2008) 076, [arXiv:0801.2385 \[hep-th\]](#). 80, 82
- [109] L. Mason and D. Skinner, “Scattering Amplitudes and BCFW Recursion in Twistor Space,” *JHEP* **1001** (2010) 064, [arXiv:0903.2083 \[hep-th\]](#). 80
- [110] D. Skinner, “A Direct Proof of BCFW Recursion for Twistor-Strings,” *JHEP* **1101** (2011) 072, [arXiv:1007.0195 \[hep-th\]](#). 80
- [111] Z. Bern and G. Chalmers, “Factorization in One-Loop Gauge Theory,” *Nucl. Phys.* **B447** (1995) 465–518, [arXiv:hep-ph/9503236](#). 89
- [112] A. P. Hodges, “Twistor Diagrams for All Tree Amplitudes in Gauge Theory: A Helicity-Independent Formalism,” [arXiv:hep-th/0512336](#). 97, 113
- [113] L. F. Alday, D. Gaiotto, and J. Maldacena, “Thermodynamic Bubble Ansatz,” *JHEP* **1109** (2011) 032, [arXiv:0911.4708 \[hep-th\]](#). 98
- [114] L. F. Alday, B. Eden, G. P. Korchemsky, J. Maldacena, and E. Sokatchev, “From Correlation Functions to Wilson Loops,” *JHEP* **1109** (2011) 123, [arXiv:1007.3243 \[hep-th\]](#). 98, 221
- [115] B. Eden, G. P. Korchemsky, and E. Sokatchev, “From Correlation Functions to Scattering Amplitudes,” *JHEP* **1112** (2011) 002, [arXiv:1007.3246 \[hep-th\]](#). 98, 221
- [116] J. M. Henn, S. G. Naculich, H. J. Schnitzer, and M. Spradlin, “Higgs-Regularized Three-Loop Four-Gluon Amplitude in $\mathcal{N} = 4$ SYM:

- Exponentiation and Regge Limits,” *JHEP* **04** (2010) 038, [arXiv:1001.1358 \[hep-th\]](#). 99
- [117] J. M. Henn, S. G. Naculich, H. J. Schnitzer, and M. Spradlin, “More Loops and Legs in Higgs-Regulated $\mathcal{N} = 4$ SYM Amplitudes,” *JHEP* **08** (2010) 002, [arXiv:1004.5381 \[hep-th\]](#). 99
- [118] F. Gantmacher and M. Krein, “Sur les Matrices Oscillatoires,” *CR Acad. Sci. Paris* **201** (1935) . 102, 246
- [119] I. J. Schoenberg, “Über Variationsvermindernde Lineare Transformationen,” *Math. Z.* **32** (1930) 321–322. 102, 246
- [120] O. Aharony, O. Bergman, D. L. Jafferis, and J. Maldacena, “ $\mathcal{N} = 6$ Superconformal Chern-Simons-Matter Theories, $M2$ -Branes and Their Gravity Duals,” *JHEP* **0810** (2008) 091, [arXiv:0806.1218 \[hep-th\]](#). 103, 206
- [121] V. Pestun, “Localization of Gauge Theory on a Four-Sphere and Supersymmetric Wilson Loops,” *Commun. Math. Phys.* **313** (2012) 71–129, [arXiv:0712.2824 \[hep-th\]](#). 104
- [122] D. Gaiotto and E. Witten, “S-Duality of Boundary Conditions In $\mathcal{N} = 4$ Super Yang-Mills Theory,” *Adv. Theor. Math. Phys.* **13** (2009) , [arXiv:0807.3720 \[hep-th\]](#). 104
- [123] P. Benincasa and F. Cachazo, “Consistency Conditions on the S -Matrix of Massless Particles,” [arXiv:0705.4305 \[hep-th\]](#). 105, 106
- [124] G. ’t Hooft, “A Planar Diagram Theory for Strong Interactions,” *Nucl. Phys.* **B72** (1974) 461. 106
- [125] Z. Bern, L. J. Dixon, and D. A. Kosower, “On-Shell Recurrence Relations for One-Loop QCD Amplitudes,” *Phys. Rev.* **D71** (2005) 105013, [arXiv:hep-th/0501240](#). 109
- [126] D. C. Dunbar, J. H. Eittle, and W. B. Perkins, “Augmented Recursion For One-loop Amplitudes,” *Nucl. Phys. Proc. Suppl.* **205-206** (2010) 74–79, [arXiv:1011.0559 \[hep-th\]](#). 109

- [127] R. H. Boels, “On BCFW Shifts of Integrands and Integrals,” *JHEP* **1011** (2010) 113, [arXiv:1008.3101 \[hep-th\]](#). 109
- [128] S. D. Alston, D. C. Dunbar, and W. B. Perkins, “Complex Factorisation and Recursion for One-Loop Amplitudes,” *Phys. Rev.* **D86** (2012) 085022, [arXiv:1208.0190 \[hep-th\]](#). 109
- [129] R. Britto, F. Cachazo, and B. Feng, “Computing One-Loop Amplitudes from the Holomorphic Anomaly of Unitarity Cuts,” *Phys. Rev.* **D71** (2005) 025012, [arXiv:hep-th/0410179](#). 109
- [130] M. B. Green, J. H. Schwarz, and L. Brink, “ $\mathcal{N} = 4$ Yang-Mills and $\mathcal{N} = 8$ Supergravity as Limits of String Theories,” *Nucl. Phys.* **B198** (1982) 474–492. 115
- [131] C.-N. Yang, “Some Exact Results for the Many Body Problems in One Dimension with Repulsive Delta Function Interaction,” *Phys. Rev. Lett.* **19** (1967) 1312–1314. 118, 119
- [132] R. J. Baxter, “Partition Function of the Eight Vertex Lattice Model,” *Annals Phys.* **70** (1972) 193–228. 118, 119
- [133] F. Cachazo and D. Skinner, “On the Structure of Scattering Amplitudes in $\mathcal{N} = 4$ Super Yang-Mills and $\mathcal{N} = 8$ Supergravity,” [arXiv:0801.4574 \[hep-th\]](#). 146, 147
- [134] F. Cachazo, M. Spradlin, and A. Volovich, “Leading Singularities of the Two-Loop Six-Particle MHV Amplitude,” *Phys. Rev.* **D78** (2008) 105022, [arXiv:0805.4832 \[hep-th\]](#). 147
- [135] D. A. Kosower and K. J. Larsen, “Maximal Unitarity at Two Loops,” *Phys. Rev.* **D85** (2012) 045017, [arXiv:1108.1180 \[hep-th\]](#). 147
- [136] S. Caron-Huot and K. J. Larsen, “Uniqueness of Two-Loop Master Contours,” *JHEP* **1210** (2012) 026, [arXiv:1205.0801 \[hep-ph\]](#). 147, 239

- [137] P. Mastrolia, E. Mirabella, and T. Peraro, “Integrand Reduction of One-Loop Scattering Amplitudes Through Laurent Series Expansion,” *JHEP* **1206** (2012) 095, [arXiv:1203.0291 \[hep-ph\]](#). 147, 149
- [138] Z. Bern, L. J. Dixon, D. C. Dunbar, and D. A. Kosower, “Fusing Gauge Theory Tree Amplitudes into Loop Amplitudes,” *Nucl. Phys.* **B435** (1995) 59–101, [arXiv:hep-ph/9409265](#). 149
- [139] Z. Bern, J. Rozowsky, and B. Yan, “Two-Loop Four-Gluon Amplitudes in $\mathcal{N} = 4$ SuperYang-Mills,” *Phys. Lett.* **B401** (1997) 273–282, [arXiv:hep-ph/9702424](#). 149
- [140] Z. Bern, J. Carrasco, H. Johansson, and D. Kosower, “Maximally Supersymmetric Planar Yang-Mills Amplitudes at Five Loops,” *Phys. Rev.* **D76** (2007) 125020, [arXiv:0705.1864 \[hep-th\]](#). 149
- [141] G. Ossola, C. G. Papadopoulos, and R. Pittau, “CutTools: A Program Implementing the OPP Reduction Method to Compute One-Loop Amplitudes,” *JHEP* **0803** (2008) 042, [arXiv:0711.3596 \[hep-ph\]](#). 149
- [142] I. M. Gelfand, R. M. Goresky, R. D. MacPherson, and V. V. Serganova, “Combinatorial Geometries, Convex Polyhedra, and Schubert Cells,” *Adv. in Math.* **63** (1987) no. 3, 301–316. 151
- [143] N. E. Mnëv, “The Universality Theorems on the Classification Problem of Configuration Varieties and Convex Polytope Varieties,” in *Topology and Geometry—Rohlin Seminar*, vol. 1346 of *Lecture Notes in Math.*, pp. 527–543. Springer, Berlin, 1988. 151
- [144] K. Rietsch, “An Algebraic Cell Decomposition of the Nonnegative Part of a Flag Variety,” *J. Algebra* **213** (1999) no. 1, 144–154, [arXiv:alg-geom/9709035](#). 152
- [145] L. K. Williams, “Shelling Totally Nonnegative Flag Varieties,” *J. Reine Angew. Math.* **609** (2007) 1–21, [arXiv:math/0509129 \[math.CO\]](#). 172

- [146] L. K. Williams, “Enumeration of Totally Positive Grassmann Cells,” *Adv. Math.* **190** (2005) no. 2, 319–342, [arXiv:math/0307271 \[math.CO\]](#). 173
- [147] S. J. Parke and T. R. Taylor, “An Amplitude for n -Gluon Scattering,” *Phys. Rev. Lett.* **56** (1986) 2459. 181
- [148] R. Penrose and M. A. H. MacCallum, “Twistor Theory: An Approach to the Quantization of Fields and Space-Time,” *Phys. Rept.* **6** (1972) 241–316. 182
- [149] R. Penrose, “Twistor Quantization and Curved Space-Time,” *Int. J. Theor. Phys.* **1** (1968) 61–99. 182
- [150] E. H. Kronheimer and R. Penrose, “On the Structure of Causal Spaces,” *Proc. Cambridge Phil. Soc.* **63** (1967) 481–501. 182
- [151] R. Penrose, “The Central Programme of Twistor Theory,” *Chaos Solitons Fractals* **10** (1999) 581–611. 182
- [152] A. Ferber, “Supertwistors and Conformal Supersymmetry,” *Nucl. Phys.* **B132** (1978) 55. 183
- [153] M. Staudacher, “Review of AdS/CFT Integrability, Chapter III.1: Bethe Ansatz and the R-Matrix Formalism,” *Lett. Math. Phys.* **99** (2012) 191–208, [arXiv:1012.3990 \[hep-th\]](#). 206
- [154] M. S. Bianchi, M. Leoni, and S. Penati, “An All Order Identity between ABJM and $\mathcal{N} = 4$ SYM Four-Point Amplitudes,” *JHEP* **1204** (2012) 045, [arXiv:1112.3649 \[hep-th\]](#). 206
- [155] M. S. Bianchi, M. Leoni, A. Mauri, S. Penati, and A. Santambrogio, “Scattering Amplitudes/Wilson Loop Duality In ABJM Theory,” *JHEP* **1201** (2012) 056, [arXiv:1107.3139 \[hep-th\]](#). 206
- [156] M. S. Bianchi, M. Leoni, A. Mauri, S. Penati, and A. Santambrogio, “Scattering in ABJ theories,” *JHEP* **1112** (2011) 073, [arXiv:1110.0738 \[hep-th\]](#). 206

- [157] M. S. Bianchi, M. Leoni, A. Mauri, S. Penati, and A. Santambrogio, “One Loop Amplitudes In ABJM,” *JHEP* **1207** (2012) 029, [arXiv:1204.4407 \[hep-th\]](#). 206
- [158] T. Bargheer, F. Loebbert, and C. Meneghelli, “Symmetries of Tree-Level Scattering Amplitudes in $\mathcal{N} = 6$ Superconformal Chern-Simons Theory,” *Phys. Rev.* **D82** (2010) 045016, [arXiv:1003.6120 \[hep-th\]](#). 209
- [159] S. Lee, “Yangian Invariant Scattering Amplitudes in Supersymmetric Chern-Simons Theory,” *Phys. Rev. Lett.* **105** (2010) 151603, [arXiv:1007.4772 \[hep-th\]](#). 209, 212
- [160] Y.-t. Huang and A. E. Lipstein, “Dual Superconformal Symmetry of $\mathcal{N} = 6$ Chern-Simons Theory,” *JHEP* **1011** (2010) 076, [arXiv:1008.0041 \[hep-th\]](#). 209
- [161] D. Gang, Y.-t. Huang, E. Koh, S. Lee, and A. E. Lipstein, “Tree-level Recursion Relation and Dual Superconformal Symmetry of the ABJM Theory,” *JHEP* **1103** (2011) 116, [arXiv:1012.5032 \[hep-th\]](#). 209
- [162] A. Agarwal, N. Beisert, and T. McLoughlin, “Scattering in Mass-Deformed $\mathcal{N} \geq 4$ Chern-Simons Models,” *JHEP* **0906** (2009) 045, [arXiv:0812.3367 \[hep-th\]](#). 212
- [163] T. Bargheer, N. Beisert, F. Loebbert, T. McLoughlin, N. Beisert, *et al.*, “Conformal Anomaly for Amplitudes in $\mathcal{N} = 6$ Superconformal Chern-Simons Theory,” *J. Phys.* **A45** (2012) 475402, [arXiv:1204.4406 \[hep-th\]](#). 212
- [164] A. Brandhuber, G. Travaglini, and C. Wen, “A Note on Amplitudes in $\mathcal{N} = 6$ Superconformal Chern-Simons Theory,” *JHEP* **1207** (2012) 160, [arXiv:1205.6705 \[hep-th\]](#). 212
- [165] A. Brandhuber, G. Travaglini, and C. Wen, “All One-Loop Amplitudes in $\mathcal{N} = 6$ Superconformal Chern-Simons Theory,” *JHEP* **1210** (2012) 145, [arXiv:1207.6908 \[hep-th\]](#). 212

- [166] L. Mason and D. Skinner, “The Complete Planar S -Matrix of $\mathcal{N} = 4$ SYM as a Wilson Loop in Twistor Space,” *JHEP* **12** (2010) 018, [arXiv:1009.2225 \[hep-th\]](#). 221
- [167] M. Bullimore and D. Skinner, “Holomorphic Linking, Loop Equations and Scattering Amplitudes in Twistor Space,” [arXiv:1101.1329 \[hep-th\]](#). 221
- [168] B. Eden, G. P. Korchemsky, and E. Sokatchev, “More on the Duality Correlators/Amplitudes,” *Phys. Lett.* **B709** (2012) 247–253, [arXiv:1009.2488 \[hep-th\]](#). 221
- [169] B. Eden, P. Heslop, G. P. Korchemsky, and E. Sokatchev, “The Super-Correlator/Super-Amplitude Duality: Part I,” [arXiv:1103.3714 \[hep-th\]](#). 221
- [170] B. Eden, P. Heslop, G. P. Korchemsky, and E. Sokatchev, “The Super-Correlator/Super-Amplitude Duality: Part II,” [arXiv:1103.4353 \[hep-th\]](#). 221
- [171] P. C. Schuster and N. Toro, “Constructing the Tree-Level Yang-Mills S -Matrix Using Complex Factorization,” *JHEP* **0906** (2009) 079, [arXiv:0811.3207 \[hep-th\]](#). 221, 225
- [172] S. He and H.-b. Zhang, “Consistency Conditions on S -Matrix of Spin 1 Massless Particles,” *JHEP* **1007** (2010) 015, [arXiv:0811.3210 \[hep-th\]](#). 221
- [173] J. L. Bourjaily, “Efficient Tree-Amplitudes in $\mathcal{N}=4$: Automatic BCFW Recursion in MATHEMATICA,” [arXiv:1011.2447 \[hep-ph\]](#). 228
- [174] Z. Bern, “String Based Perturbative Methods for Gauge Theories,” [arXiv:hep-ph/9304249](#). 239
- [175] Z. Bern and A. Morgan, “Supersymmetry Relations Between Contributions to One-Loop Gauge Boson Amplitudes,” *Phys. Rev.* **D49** (1994) 6155–6163, [arXiv:hep-ph/9312218](#). 239

- [176] A. Kotikov and L. Lipatov, “DGLAP and BFKL Equations in the $\mathcal{N} = 4$ Supersymmetric Gauge Theory,” *Nucl. Phys.* **B661** (2003) 19–61, [arXiv:hep-ph/0208220](#). 239
- [177] N. Arkani-Hamed, J. L. Bourjaily, F. Cachazo, and J. Trnka, “Local Integrals for Planar Scattering Amplitudes,” *JHEP* **1206** (2012) 125, [arXiv:1012.6032](#) [[hep-th](#)]. 242, 243
- [178] A. Brandhuber, O. Gurdogan, R. Mooney, G. Travaglini, and G. Yang, “Harmony of Super Form Factors,” *JHEP* **1110** (2011) 046, [arXiv:1107.5067](#) [[hep-th](#)]. 245
- [179] V. V. Fock and A. B. Goncharov, “The Quantum Dilogarithm and Quantisation of Cluster Varieties,” *Inventiones Math.* **175** (2009) 223–286, [arXiv:math.QA/0702397](#). 245
- [180] M. Kontsevich and Y. Soibelman, “Stability Structures, Motivic Donaldson-Thomas Invariants and Cluster Transformations,” [arXiv:0811.2435](#) [[math.AG](#)]. 245
- [181] D. Gaiotto, G. W. Moore, and A. Neitzke, “Wall-Crossing in Coupled $2d-4d$ Systems,” [arXiv:1103.2598](#) [[hep-th](#)]. 245
- [182] L. F. Alday, D. Gaiotto, and Y. Tachikawa, “Liouville Correlation Functions from Four-Dimensional Gauge Theories,” *Lett. Math. Phys.* **91** (2010) 167–197, [arXiv:0906.3219](#) [[hep-th](#)]. 245
- [183] L. F. Alday, “Review of AdS/CFT Integrability, Chapter V.3: Scattering Amplitudes at Strong Coupling,” *Lett. Math. Phys.* **99** (2012) 507–528, [arXiv:1012.4003](#) [[hep-th](#)]. 245
- [184] Y. Kodama and L. Williams, “KP Solitons, Total Positivity, and Cluster Algebras,” *Proc. Natl. Acad. Sci. USA* **108** (2011) no. 22, 8984–8989, [arXiv:1105.4170](#) [[math.CO](#)]. 245
- [185] Y. Kodama and L. Williams, “KP Solitons and Total Positivity for the Grassmannian,” [arXiv:1106.0023](#) [[math.CO](#)]. 245

- [186] Y. Kodama and L. Williams, “A Deodhar Decomposition of the Grassmannian and the regularity of KP solitons,” [arXiv:1204.6446 \[math.CO\]](#). 245
- [187] J. J. Heckman, C. Vafa, D. Xie, and M. Yamazaki, “String Theory Origin of Bipartite SCFTs,” [arXiv:1211.4587 \[hep-th\]](#). 245
- [188] S. Franco, D. Galloni, and R.-K. Seong, “New Directions in Bipartite Field Theories,” [arXiv:1211.5139 \[hep-th\]](#). 245
- [189] N. Arkani-Hamed, A. G. Cohen, D. B. Kaplan, A. Karch, and L. Motl, “Deconstructing $(2, 0)$ and Little String Theories,” *JHEP* **0301** (2003) 083, [arXiv:hep-th/0110146](#). 246
- [190] C. Cheung and D. O’Connell, “Amplitudes and Spinor-Helicity in Six Dimensions,” *JHEP* **0907** (2009) 075, [arXiv:0902.0981 \[hep-th\]](#). 247
- [191] We thank Yu-tin Huang for discussions on this point. 247